Engineering an inducible NO pathway to facilitate cell-electronics communication

Orr Yarkoni

This thesis is submitted towards the qualification of Doctor of Philosophy.

Newcastle University, School of Chemical Engineering and Advanced Materials.

10/2011

I Acknowledgements

For this work I would like to thank my supervisor, Dr. Daniel Frankel. Additional, thanks go to Dr. Lynn Donlon for her guidance in writing and Darman Nordin for his help in the laboratory. I would also like to thank Dr. Mark Birch for access to Tissue Culture facilities, Dr. Anil Wipat for access to Microbial culture facilities and Dr. Chris Voigt for his insight and guidance in synthetic biology. Special thanks go to Dr. Wendy Smith for Primer acquisition and equipment troubleshooting, Brian Calliando and Felix Moser for assistance in microbial culture techniques. This body of work was made possible by the EPSRC, grant number EP/H019081/1.

II Table of Contents

III Table of Figures

IV Abbreviations

- Ach: Acetylcholine
- BH4: Tetrahydrobiopterin
- CAM: Calmodullin
- Cfu: Colony Forming Units
- cGMP: Cyclic Guanosine Monophosphate
- CWE: Coated Wire Electrodes
- DAF-2 DA: 4,5 Diaminofluorescein Diacetate
- DAPI: 4',6-diamidino-2-phenylindole
- DHFR: Dihydrofolate reductase
- EB: Elution Buffer
- EDRF: Endothelial Derived Relaxing Factor
- eNOS: Endothelial Nitric Oxide Synthase
- ET : Electron Transfer
- FAD: Flavin Adenine Dinucleotide
- FCS: Fetal Calf Serum
- FET: Field Effect Transistors
- FMN: Flavin Mononucleotide
- FRAP: FKBP12-Rapamycin Associated Protein
- HCl: Hydrochloric Acid
- iNOS: Inducible Nitric Oxide Synthase
- LAPS: Light Addressable Potentiometric Sensors
- LB: Lysogeny Broth
- LED: Light Emitting Diode
- L-NMMA: N^g-methyl-L-arginine
- L-NNA: N^w-nitro-L-arginine
- LOC: Lab on a Chip
- LOV: Light Oxygen Voltage domain
- MEA: Micro Electrode Array
- NAD: Nicotinamide Adenine Dinucleotide
- NADPH: Nicotinamide Adenine Dinucleotide Phosphate
- 7-NI: 7-Nitroindazole
- NiTSPc: Tetrasulphonated Nickel Phthalocyanine

- nNOS: Neuronal Nitric Oxide Synthase
- NO: Nitric Oxide
- NOS: Nitric Oxide Synthase
- PCR: Polymerase Chain Reaction
- QCM: Quartz Crystal Microbalance
- SNAP: S-Nitroso-N-acetyl-D,L-penicillamine
- SOB: Super Optimal Broth
- TAE: Tris-acetate-EDTA
- Taq: Thermus aquaticus (referring to polymerase)
- YPD: Abbreviation of YEPD (Yeast Extract Peptone Dextrose)
- YPDS: YPD with the addition of sorbitol

V Abstract

Turning cells into useful devices to perform unnatural functions creates the potential to permit the interface between biological organisms and electronics. In this thesis cell-based devices were designed and constructed to respond to either light or a specific chemical stimulus. Design constraints were defined by the eventual application of the device, a biohybrid robot.

The enzyme endothelial nitric oxide synthase (eNOS) was chosen as a target for genetic engineering. Prior to constructing the device a suitable host for the engineered construct was selected. CHO-K1 cells were transfected with nitric oxide synthase and expression levels were characterized *via* flow cytometry and inhibitor studies. A novel method for the effective delivery of inhibitors was developed and applied to demonstrate that transfected eNOS was sufficiently expressed to produce a measurable output. In addition, a balance between the native nitric oxide production machinery of the cells and the transfected endothelial nitric oxide synthase was observed.

Two systems were designed and constructed for stimuli responsive nitric oxide production. The first system was designed to produce nitric oxide in response to the presence of the antibiotic rapamycin. Chemical induced dimerization would bring the two separated domains of endothelial nitric oxide synthase into close enough proximity to re-establish protein function. The separate oxygenase and reductase domains were successfully amplified and subsequently fused with components of the chemically induced dimerization system.

The second system involved fusing a domain from the plant gene Nhp1 (Light Oxygen Voltage domain - LOV) capable of harvesting a photon, with mouse endothelial nitric oxide synthase. This strategy aimed to hijack the wild type protein's native electron transfer pathway. Manipulation was carried out in bacteria with subsequent transfection into CHO-K1 cells.

Subsequent testing of nitric oxide production the mutant cells confirmed the optical sensitivity of the mutant eNOS. Moreover both LOV mutant cell lines were capable of fast response times and switching behaviour.

The findings of this thesis demonstrate that genetic engineering of endothelial nitric oxide synthase is a suitable strategy for the controlled release of nitric oxide upon optical stimulation. Moreover the potential of an engineered cell to respond quickly to stimuli has been realized, comparing favourably to genetically engineered systems that rely on gene expression to elicit an output.

Chapter 1 Introduction and Literature Review

In recent years the application of genetic engineering to the construction of biological devices has received considerable attention. The majority of biological strategies for device construction focus on *biomolecule-based* applications such as protein immobilisation on solid state devices. Although more complex, the *cell engineering* approach yields numerous advantages. By turning cells into signal transduction agents, a variety of unique applications can be devised, which harness the power of the cellular machinery. The first part of this review will focus on the current state of the art in sensors and cell based biosensors.

The successful design of a genetically engineered sensor system requires detection of an environmental stimulus by the cell and subsequent response to produce a detectable output. A potential cell derived output signal is the signalling molecule nitric oxide (NO) which will be reviewed in detail along with its production *in vivo via* nitric oxide synthase (NOS).

Biosensors that rely upon signals generated *via* a chemical stimulus, have received considerable attention. A novel approach to this transduction route, chemical induced dimerization (CID) will be discussed. However, one of the most exciting areas of biological device construction relates to the generation of a detectable output in response to an optical stimulus. Early applications focused on the use of photoactive proteins whilst the emerging field of optogenetics aims to harness the power of genetic engineering to create cellular responses to light.(Deisseroth, 2011) In the final section of this chapter the areas of photoactive sensors, proteins and optogenetics will be reviewed with respect to device applications.

1.1 Cyberplasm - the construction of a semi autonomous biohybrid robot

Synthetic biology can be described as the use of engineering principles to build useful devices from biological building blocks or using unnatural building components in biological systems. This definition can be taken one step further to include the complete design and construction of artificial organisms.

Recent advances in robotics design using nature as an inspiration include the biomimetic variety pioneered by Ayers *et al.*(J. Ayers & Witting, 2007)' (J. Ayers & Rulkov, 2010). This approach has been successful in imitating some of the behavioural advantages of marine animals such as the lobster and lamprey. The Cyberplasm project

aims to harness the power of synthetic biology at the cellular level by exploiting bacteria and mammalian cells to carry out device like functions. In addition this exploitation aims to allow the cells to communicate with the robot electronics thus addressing the integration between bio and robot components. Furthermore synthetic biology is attempted at a larger scale by interfacing multiple cellular devices together, connecting to an electronic nervous system and in effect creating a multi-cellular biohybrid robot. Motile function will be achieved by engineering muscle cells to contract upon light stimuli allowing movement of the robot to be powered by mitochondrial conversion of glucose to ATP.

The Cyberplasm project aims to build a biohybrid microrobot capable of autonomous behaviour. This robot will be a hybrid of both synthetic parts and biologically engineered cellular components. Interfacing the biological and synthetic components is one of the key challenges in building such a machine that will be achieved by transforming mammalian cells into sensors and actuators, respectively. The overall design is presented in Figure 1.

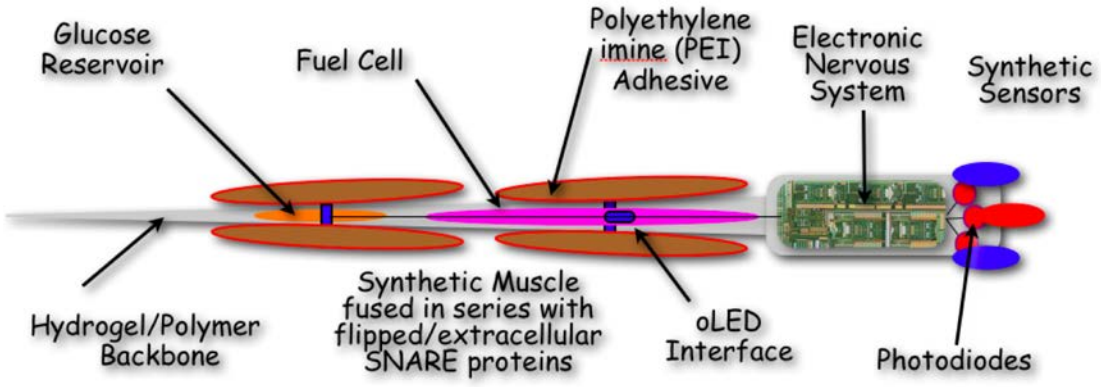

Figure 1 Schematic representation of the Cyberplasm micro-robot. Synthetic muscle propels the robot through liquid. Synthetic sensors, either photoreceptive or chemoreceptive, will report signals from the immediate environment. These signals will in turn be processed via the electronic components. An electronic brain will control signal impulses to drive the muscle cells by causing a biomimetic neurotransmission. Power for the muscle units will be derived from the mitochondrial conversion of glucose to energy. The source of glucose will be

constructed within the hydrogel/polymer body and delivered to the muscle cells in a controlled fashion.

Modification of myoblasts (muscle cells) will be attempted in order to produce actuators capable of propelling the robot through fluid. Firstly a controllable assembly of myotubes will be performed by harnessing flipped SNAREs (soluble N-ethylmaleimide-sensitive fusion protein attachment protein receptors) and a Tet-Off gene expression system. The miniaturization of Cyberplasm cannot accommodate a power supply with sufficient power for electrical stimulation of myotubes. Therefore a controlled iontophoresis of acetylcholine (Ach) to simulate myotubes will generate contraction. Another option for the electronic controlled stimulation of muscle will be attempted by the activation of channelrhodopin-2 whereby shining blue light onto muscle causes an increase in intracellular Ca^{2+} and drives contractions.

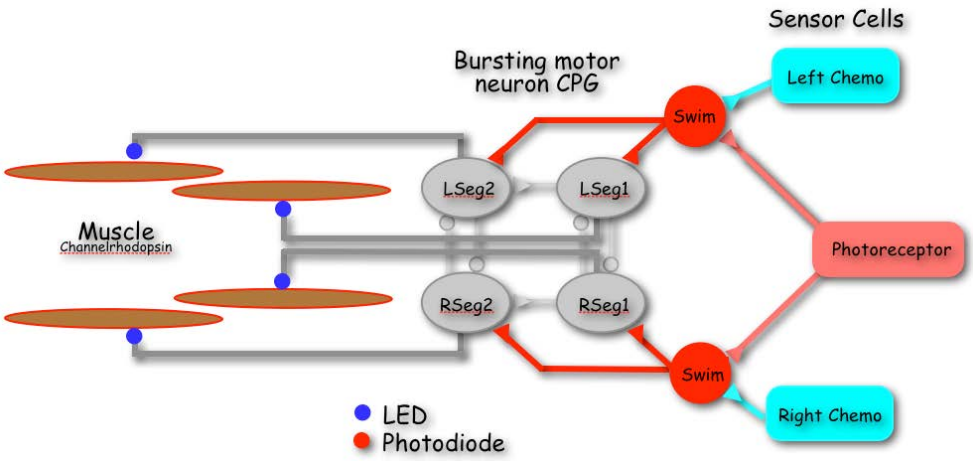

Figure 2 Block diagram of the control system linking the various components of Cyberplasm.

Response of the sensor cells will be used to activate a central pattern generator (CPG) for swimming through bilaterally paired CPG neurons, Figure 2. The CPGs will be connected through inhibitory synapses and excitatory synapses to generate a swim motor program that alternates on the two sides and propagates from the anterior muscle to the posterior muscle. This pattern will generate propagating waves of muscle contraction that will underlie forward swimming. The CPG neurons will be activated by synaptic input from commands that receive inputs directly from the bioengineered sensor cells *via* the electrochemical nitric oxide sensor described in this thesis. Key to control of adaptive behaviour of the robot is rapid response of the sensors to changing

environmental conditions. Achievement of this goal requires that the reporter operates with a short time-constant. The sensors are in effect the "eyes" and "nose" of the robot and the development of these sensors is the subject of this thesis.

Cyberplasm integration will be accomplished *via* a combination of nano/microscale fabrication and matching the synthetic biology with materials development. The body of Cyberplasm will have several functions. Its core will consist of a hydrogel with tuneable mechanical properties and a polydimethylsiloxane (PDMS) based microbial fuel cell. The hydrogel will be modified using microscale patterning of PEI to allow for adhesion of myotubes. Additionally, mechanical properties of the hydrogel will be tuned *via* crosslinking to allow maximum motile propulsion of myotubes. Electronic connections will be fabricated using evaporated gold on a PDMS skeleton frame. This frame will be the basis of a highly novel microbial fuel cell to power the electronic brain, photodiodes and LEDs. The work undertaken in this thesis aims to create Cyberplasm's sensory mechanisms using a cell-based biosensor capable of generating a chemical signal upon stimulation which will be converted to electrical current *via* the use of an electrode.

1.2 Current technology for measuring biologically derived signals

The majority of biosensors harness naturally occurring reactions to create a measurable output, often with an intermediate signal transduction step. Sensor systems exhibiting quantitative measurements rely on the scalability of the reaction being measured. There are various criteria that must be addressed in the design of new sensor systems. They include sensitivity, selectivity, stability, artefact minimization, power consumption, analytical capabilities, reliability and cost.(Hanrahan, Patil, & Joseph Wang, 2004)

1.2.1 Micro electrode arrays

Micro Electrode Arrays (MEAs) originated in the 1980's, when progress in microelectronic technology made it possible to accurately measure low currents and produce very small electrodes. Using this principle, electrodes have been modified to detect the presence of penicillin(Nishizawa, Matsue, & Uchida, 1992) and to simultaneously detect O_2, H_2O_2 and Glucose. In addition MEAs have been developed

to measure electrical activity in cultured neurons at both the network and single cell level.(Ben-Jacob & Hanein, 2008)

Micro-Electrode arrays come in a variety of designs, Figure 3. The type of design is usually dependant on the application in question, as an example, design A from Figure 3 would be appropriate for detection of a single reaction from a sample, design C would be appropriate for the detection of multiple analytes from a single sample and design D would be appropriate for detecting a single reaction from multiple samples. Electrodes in the array can be made selective towards a variety of compounds by either applying a different potential per electrode or by chemical surface modification.

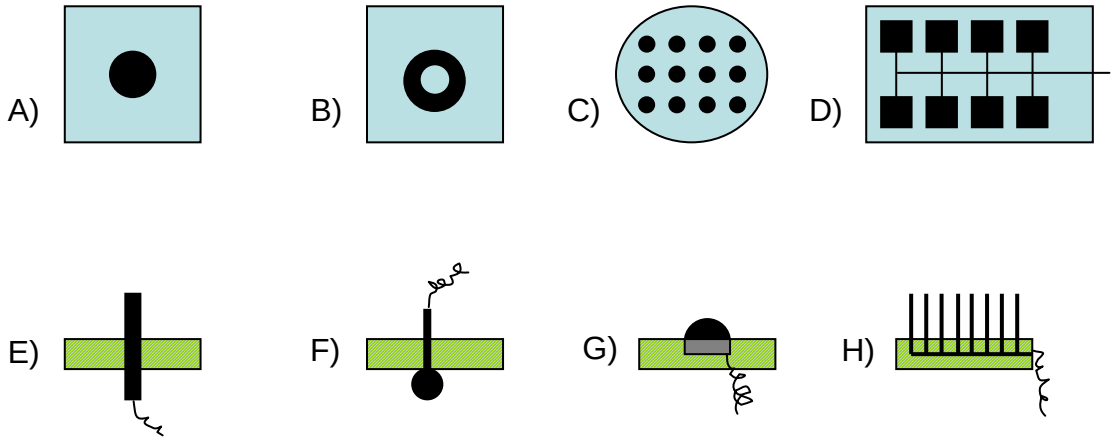

Figure 3 Diagram showing a variety of microelectrode arrays. A) Microdisk B) Microring C) Microdisk array D) Nanolithographically produced microband array E) Microcylinder F) Microsphere G) Microhemisphere H) Fiber array. Adapted from (Amatore, Holub, & Marecek, 2000)**.**

1.2.2 Light addressable potentiometric sensor (LAPS)

An example of a solid-state sensor suitable for measurements in biological systems is the Light-addressable Potentiometric Sensor (LAPS). When light of an appropriate wavelength is applied to the sensor, electron-hole pairs are formed. These subsequently become separated in the depletion layer as electrons move towards the silicon and holes accumulate at the insulator-silicon interface. This leads to a separation of charge which moves in the external circuit such that can it be detected by an ammeter. Surface charge is pH dependent and that any change in pH can be measured by determining the shift in the photoresponse curve from its starting position at any pH value. The change in pH is

only measured at the locations that are illuminated, Figure 4. Each LED can be turned on independently allowing for a local pH measurement due to the discrete chemistries present at the sensor surface.(John C Owicki et al., 1994)

LAPS systems were initially used to measure the electric properties of phospholipid bilayer membranes. In this instance, membrane capacitance, conductance and transmembrane potential were measured.(Sigal, D. H. Hafeman, J. W. Parce, & McConnel, 1989) A major limitation is that it can only measure processes which produce a change in pH. Fortunately there are many such processes including those mediated by T cell receptors, G-coupled receptors, Haematopoietic-family of receptors and ligand gated ion channels.(Nag, H. G. Wada, Fok, Green, & S. D. Sharma, 1992)'(Nag, H. G. Wada, Deshpande, Passmore, & Kendrick, 1993)'(J.C. Owicki, J. W. Parce, Kercso, Sigal, & Muir, 1992)'(Raley-Susman, Miller, J.C. Owicki, & Sapolsky, 1992)'(H. G. Wada, Indelicato, Meyer, Kitamura, & Miyajima, 1993)

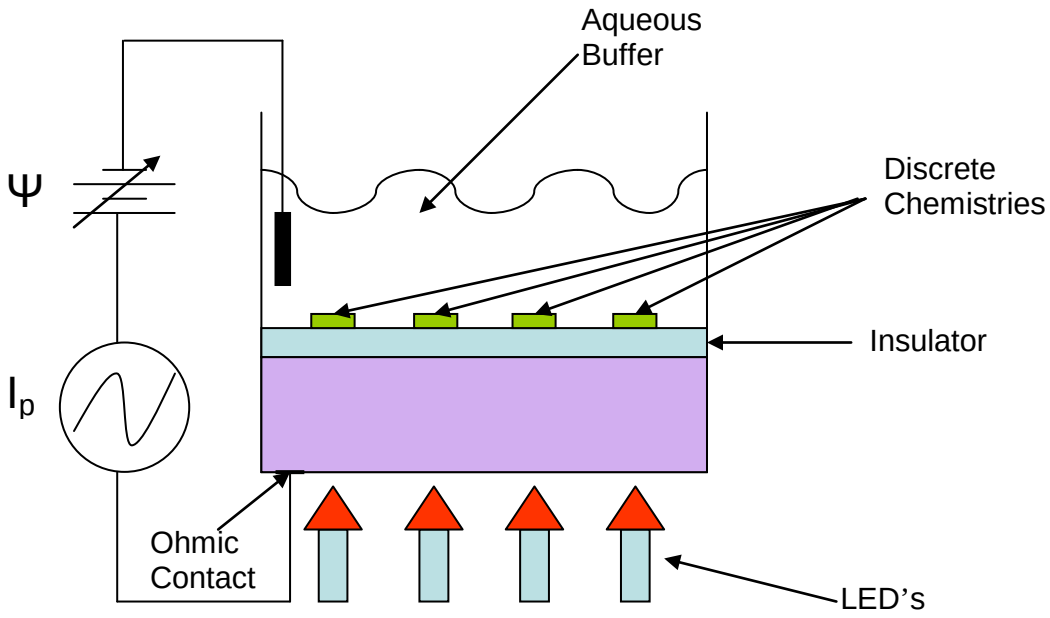

Figure 4 Schematic representation of the LAPS sensor (adapted from Owicki *et al*).(John C Owicki et al., 1994) **An electrode in the aqueous buffer works as both a controlling and a reference electrode. Ground potential is selected as the potential of the non-insulated area. Potential is then altered using a potentiostat (depicted by Ψ) so that the solution is negative in comparison with the potential of the silicon. The potential remains relatively constant up to a few nanometres of the insulator surface. The LAPS therefore measures Ip (alternating photo-current)**

1.2.3 Amperometric sensors

Electrochemical sensors can also function amperometrically, in which case the potential difference caused between the working and reference electrodes is used to induce a change in oxidation state of the target chemical compound. This is nearly always an electroactive species and the resulting change in current caused by this reaction is measured.(Stradiotto, Yamanaka, & Zanoni, 2003) In the case of solid state electrodes, surface modification has allowed for the design and construction of sensors for a variety of applications. This modification is usually achieved by altering surface chemistries. Bioactive reagents can be placed onto the electrode as a coating which will cause a redox reaction when in contact with the appropriate analyte, which will in turn produce a detectable amperometric response (in other words, a change in current).(Stradiotto *et al*., 2003) The immobilization of the bioactive reagent can be achieved by a variety of processes, such as chemisorption, polymer coating, chemical reactions or composite formation.(Murray, Ewing, & Durst, 1987) Examples of this include the modification of carbon electrodes with tetraruthenated cobalt porphyrin for the detection of nitrites/nitrates,(J. R. C. Rocha, Angnes, Bertotti, Araki, & Toma, 2002) modification of carbon electrodes with cellulose acetate and uricase for the detection of uric acid(Markas, Gilmartin, & J. P. Hart, 1994) and the modification of a platinum electrode with nickel tetrasulphonated phtalocyanine for the detection of nitric oxide.(Guo, Murohara, Buerke, Scalia, & Lefer, 1996) The use of pre-concentrating agents to achieve a higher degree of selectivity has been well documented. These are usually ion-exchange polymers which confer increased selectivity towards the specific analyte, and act by either conferring size exclusion properties, charge exclusion properties or state exclusion properties (i.e. permeability to gases but not liquids). This is advantageous as it eliminates contact of unwanted reagents with the electrode and by doing so increase the concentration of the desired analyte near the electrode surface. Examples of this include Nafion, poly(vinyl sulphate), poly(L-lysine), deprotonated poly(acrylic acid) and cellulose acetate.(Stradiotto *et al*., 2003)

Amperometric electrodes have been modified to function as biosensors by using enzymes as the oxidising/reducing agent. This allows for the detection of a variety of biological entities such as metabolites or drugs within a biological fluid. These types of sensors are particularly successful if the enzyme in question is an oxygenase or a dehydrogenase as these produce a very noticeable change in current at the electrode surface.(Joseph Wang, 1999)

Simple deposition of enzymes on to the electrode surface would lead to the creation of a barrier for detection of the redox reaction, thus enzymes are immobilized at a discrete distance from the electrode. Strategies to achieve this immobilization include tethering of the enzyme using redox relay units, the use of diffusional mediators and immobilization of the protein using redox polymers.(Joseph Wang, 1999)[25]

Examples of this type of sensor modification include a lactate dehydrogenase based sensor, capable of measuring lactate concentrations in blood samples. Irregularities of lactate levels have been linked to medical conditions such as hypoxia and lactic acidosis. In order to achieve this, NAD^+ dependent lactate dehydrogenase was immobilized onto an electrode using the ferricyanide ion as a mediator.(N. Sato & Okuma, 2006)

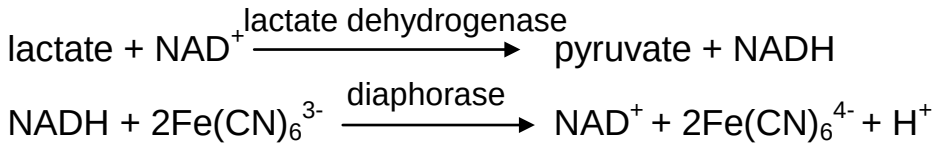

Figure 5 representation of the reaction occurring at the electrode interface for the lactate sensor developed by (N. Sato & Okuma, 2006)**.**

1.2.4 Field Effect Transistors

Ion selective field effect transistors (ISFET) are based on normal FETs where the solid state device is capable of both high-input and low out-put impedance. By this principle, the device becomes able to measure charge build-up across the ion-selective membrane. FETs were the first fully miniaturised silicon sensors, having been invented in the 1970's, and have been used to create a variety of sensors.(Schoning & Poghossian, 2002) FETs are made using micro-fabrication techniques, which while substantially increasing their manufacturing cost does make them very small and so makes it possible to create a full array capable of sensing a variety of analytes which can be incorporated into an *in vivo* application.(Stradiotto *et al.*, 2003) FET's were originally designed to work at relatively low end applications (unlike silicon technology) and as such were not expected to run processes such as computer memory, and instead became components of lower end technology such as ID tags and Smart Cards.(H. E. Katz & Bao, 2000) Due to its chemical tuneability and ease of construction, the FET sensor has been adapted for a variety of uses.

The FET works by measuring the current between a source and drain electrodes which occurs when a voltage is applied to the gate. When there is no current flowing between source and drain, the gate is "off" and when voltage is applied to the semi-conductor, a charge forms between the semiconductor and dielectric layer causing a subsequent increase in current between source and drain electrodes, effectively turning the gate "on". For a representation of this, refer to Figure 6.(H. E. Katz & Bao, 2000)

The principle behind the employment of FET's as biosensors is relatively straightforward. Cells are grown on a silicon chip composed of many FET gates, Figure 6. When the gate is "open", the bioelectric potential can be measured as FET's were shown to function when detecting electrolytes. The challenge has been to find a way to couple the cell's electric signal into the FET electronic circuit.(Neher, 2001)

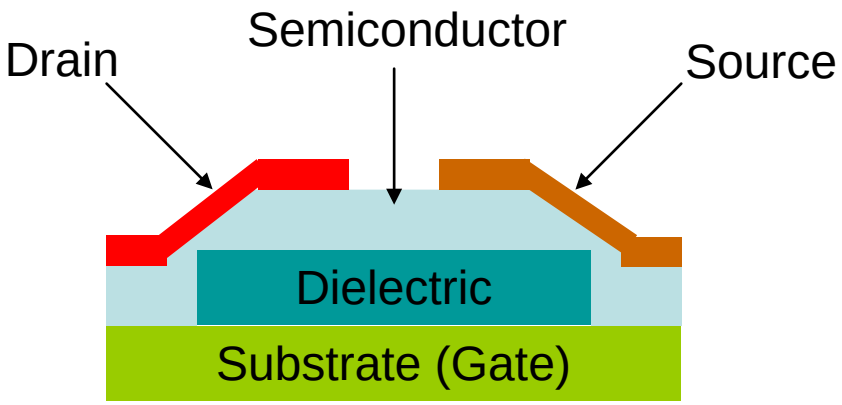

Figure 6 Representation of the FET system, where gate logic is employed. Adapted from (H. E. Katz & Bao, 2000)**.**

1.2.5 Lab on a Chip sensors

The lab on a chip (LOC) concept is an extremely popular one due to its many theoretical advantages. These largely rely on the fact that the system can be tuned to allow genomic, proteomic or cellular analysis.(Weigum, Floriano, Christodoulides, & Mcdevitt, 2007)(Ali et al., 2003). In theory, it is possible to compile enough data running a single sample in experiment to determine a diagnosis. The aim of the LOC is to be able to run a small scale sample through a single or battery of tests (depending on the required amount of data) run on a chip (a microfluidic network which exposes the sample to a variety of conditions including the presence of proteins, nucleotides,

antibodies or antigens) which can then be assessed *via* either an optical or electrical signal, depending on the method of detection employed in the design.(Weigum et al., 2007)

The work of Mehnaaz *et al* shows a successful design for a LOC application with the function of sorting DNA sequences as well as detecting point mutations using fluorescence marking.(Ali et al., 2003) Aldehyde-terminated agarose microspheres were bound to avidin docking sites *via* amination. Subsequently, biotinylated sequences complementary to the target sequences are bound to the bead, which is immobilized on a silicon chip. The sample is then pumped through the environment containing the bead and the target sequence binds to the bead. This was proven using fluorescently marked target sequences. This shows much promise to this system which has the potential of significantly increasing the efficiency of current DNA sequence detection methods due to its higher probing surface area which leads to higher detection rates.(Ali et al., 2003) The avidin-biotin interaction can also be harvested for many other applications, providing further directions of research using the principles demonstrated by the above mentioned sensor design.

An example of another such LOC application can be found in the work of Shannon *et al*.(Weigum et al., 2007) In this example, the application works *via* production of a fluorescent signal in the presence of epidermal growth factor receptor (EGRF), a marker for oral cancer. Using a fluorescently labelled EGRF biomarker, the system produces a fluorescent signal which can be detected by harnessing the design of the LOC. In this case, cells are immobilized on a membrane from culture by the filter capture method of membrane use and can subsequently be used for expression monitoring and fluorescence labelling. The system designed by the group shows some of the required steps for many such systems and is also limited in the same way that many such systems are. It contains microfluidic channels which lead to the membrane to trap the cells and dispose of waste. The immobilization of cells allows their imaging and the acquisition of data using fluorescence cytometry.(Weigum et al., 2007)

1.3 *In Situ* vs. *In vitro* sensors

In Situ sensors require additional operational characteristics in order to be viable. The sensor has to be small, resistant to bio-fouling, present an appropriate degree of selectivity (low noise generated by co-existing compounds) and be resistant to a variety of changes in natural conditions. Biofouling is one of the major causes of *in vivo* sensor

failure. It is caused by accumulation of compounds, proteins and cells on the sensor/membrane surface and causes a rapid deterioration in sensor function.(Wisniewski & Reichert, 2000) *In vitro*, sensors can be more delicate and the conditions for detection can be perfected but this comes at a cost. *In vitro* experiments not only fall short of in situ experiments in as much as the conditions do not represent what is actually happening in the system being examined, but in addition the sample must be processed prior to examination adding time and cost to the application of the sensor particularly in the healthcare sector.

In situ sensors have stringent biocompatibility requirements. The insertion of foreign material into the human body brings about immediate physiological responses which vary in accordance to the environment they are introduced to, i.e. blood, tissue or bone. These responses can ultimately lead to a wide variety of possible interactions with the sensor, affecting its performance.(Shin & Schoenfisch, 2006) Examples of this include biofouling in blood *via* adhesion of platelets or protein deposition in intravascular sensors which causes a subsequent drop in sensor quality, be it in sensitivity or longevity.(Frost, Rudich, H. Zhang, Maraschio, & Meyerhoff, 2002) Strategies towards improving sensor survivability in these conditions include selection of materials known to not cause an immune response (such as those developed for the prosthetics industry) and the localized attenuation of host response using co-factors known to alleviate the sensor integration procedure. An example of this is mentioned in the work of Frost *et al*(Frost, Rudich, H. Zhang, Maraschio, & Meyerhoff, 2002) where the use of nitric oxide is employed to improve sensor lifetime by discouraging cell/platelet adhesion to the sensor. This study showed that when an NO releasing membrane was added to the sensor, bacterial adhesion was drastically reduced when compared to the control.(Frost, Rudich, H. Zhang, Maraschio, & Meyerhoff, 2002) However, limitations as to the longevity of NO releasing polymers/substrates make it so that long term activity of NO release *in situ* around the electrode is not currently possible using this approach.(Shin & Schoenfisch, 2006)

Sensors implanted sub-cutaneously face a different set of challenges as the main responses causing sensor degradation include cell-adhesion and sensor encapsulation by fibrous tissue. The implantation procedure in these cases initiates the body's healing mechanism by damaging capillaries or simply displacing tissue. This triggers a series of responses starting with the inflammatory response, which causes the adsorption of proteins and inflammatory cells onto the sensor. Phagocytic cells then surround the sensor, attempting to destroy it. These events are detrimental to the sensor in as much as

they cause the accumulation of matter on the sensor surface restricting the functional area designed for analyte/sensor interaction. Phagocytic cell binding also causes the consumption of some analytes such as glucose and oxygen whilst producing highly active free radicals (peroxygen, superoxide, nitric oxide, etc) which can interact either with the sensor directly causing background noise or with the analyte, reducing detected analyte concentration and so dampening the signal perceived by the sensor.(Shin & Schoenfisch, 2006) As the body's healing mechanism continues to take action, the tissue surrounding the foreign material becomes increasingly constricting and avascular, cutting off the potential sensor from the analyte it should be measuring.(Shin & Schoenfisch, 2006)

In addition to the effect of the sensor itself on the organism it is inserted to, there is also contamination to consider. The introduction of foreign organisms such as bacteria during sensor implantation or even the concentration of such species at the sensor/host interface can lead to complications. Sterilization techniques exist to prevent this from happening, however, this process can many times damage the sensor particularly membrane containing sensors. In these cases, temperature/chemical sterilisation can lead to polymer degradation and so cause sensor damage, whilst not even guaranteeing complete sensor sterilization. Common cases of implant associated infections occur from bacterial biofilm formation on the sensor surface. This implies that bacteria have formed colonies capable of creating these biofilm protective layers of exopolysaccharides which provides the colonies with immunity from the host immune system as they can neither be phagocytosed nor attacked by antibodies. Unfortunately, this biofilm formation also renders them immune to antibiotics as it acts as a chemical barrier, resulting in a necessity to remove the implanted sensor.(Shin & Schoenfisch, 2006)

A variety of metal contaminant sensitive electrodes have been designed and constructed seeing as they have a variety of applications and their miniaturization is less of a critical factor as they can be used to detect large volumes of sample. One such sensor, described in the work of Wang *et al*,(Joseph Wang *et al*., 1997) focused on the detection of uranium and nickel using a potentiometric glass carbon disk electrode system. To this effect, the electrode surface was modified with propyl-gallate (for uranium detection) and dimethylglyoxime (for nickel detection) and the sensor showed a good amount of selectivity towards these analytes. However, the necessary accumulation period for the analyte meant that the sensor was only effective after at least a two minute accumulation period of the sample. Although the degassing step

necessary for many other equivalent systems had been neutralized in this instance as the system was capable of detecting mg/mL concentrations of the analyte without the degassing step. Sensitivity of the sensor depended on the analyte flow rate, with nickel sensitivity increased by increasing flow rate to above 10 μL/min and uranium sensitivity decreasing above said rate. A further limitation of this system is that it relies on the continuous delivery of the sensing ligand to the receptor as well as the analyte in question, thus limiting its *in situ* application.(Joseph Wang *et al*., 1997)

1.4 Cell-based Biosensors

Cells are equipped with a variety of receptors capable of transducing chemical signals into electrical ones. It is suggested that by coupling these cellular properties with an electrical readout it is possible to effectively use cells as biosensors for a variety of applications such as pharmaceutical screening and environmental monitoring.(Neher, 2001) The main advantages of cell-based biosensors are as follows:

Self-replicating - as cells divide the sensor is perpetuated.
Specificity - cells are highly specific through receptor based activation of signalling cascades
Complexity - cells are capable of performing simultaneous tasks
Stability - biochemical reactions within the cell are enclosed within the protective cell membrane, preventing biofouling of internal components.

The disadvantages of cell-based biosensors include:

Limited operating environment - cells require environments with varied but specific conditions. Although a type of cell can be found to survive virtually every naturally existing environment (including within another organism), each cell is restricted to its own specific operating conditions.

Complexity - With multiple events occurring simultaneously and with interrelated processes it can be difficult to focus on one pathway without interfering with/affecting another.

Cells can create signals of varied natures, including chemical, optical and electrical. Currently, there are several existing methods for extracellular potential measurement,

including microelectrode arrays (MEA)(Valderrama *et al*., 1995)'(Amatore et al., 2000)'(Bakker & Telting-diaz, 2002), field effect transistors (FET)(H. E. Katz & Bao, 2000)'(Schoning & Poghossian, 2002)'(Neher, 2001), light-addressable potentiometric sensors (LAPS)(John C Owicki et al., 1994)'(G. Xu et al., 2005) and patch-clamp.(G. Xu et al., 2005) These methods, particularly microelectrode arrays and field effect transistors, allow for monitoring of cell potential over a prolonged periods of time (days or weeks) and are non invasive. Their major limitation comes from only being able to record data from electrically active cells such as neurones.(C. K. Young, Ingebrandt, Krause, Offenhauser, & Knoll, 2001) In addition, sensor construction relies on the use of microelectronic-fabrication techniques which have limited resolution of feature separation of 50-200 μm.(G. Xu et al., 2005)'(George, Parak, & Gaub, 2000)

Cells have inherent limitations when used as sensors. In biological tissues cells are separated from each other by gaps of 10-20 nm. When grown on artificial surfaces, these gaps are at a minimum of 40 nm which limits cell density in artificial devices.(Neher, 2001) Cell adhesion also poses a difficulty in the construction of cell-based biosensors. If the gap between the cells and the silicon chip is too large (usually due to the thickness of the electrolyte layer), the contact resistance is increased, which leads to current leakage through the electrolytes. Reducing the gaps between cells and the gaps between cell and chip is necessary to improve the sensitivity of the system.(Fan, 2001)

Rainina *et al* (Rainina, Efremenco, & Varfolomeyev, 1996) produced a cell-based sensor utilizing cryoimmobilized *E. coli* cells capable of hydrolyzing organophosphate neurotoxins. Its *Modus operandi* relied on cell produced organophosphate hydrolase cleaving P-O, P-S, P-F and P-CN bonds, generating two protons per cleavage event. Quantity of protons released was directly proportional to the amount of hydrolyzed organophosphate. A sensitivity of 0.001 mM to 1 mM was achieved with a response time of between ten and twenty minutes. The immobilized cells were found to be hydrolytically active for over two months when placed at 4 °C in a potassium phosphate buffer.(Rainina et al., 1996)

Further examples of the application of cell based sensor technology in the medical field can be found in the work of Rider *et al*.(Rider *et al*., 2003) They have developed a pathogen sensor based on B-cell recognition with a detection limit as low as 20 colony forming units (cfu) for the chosen pathogen.(Rider *et al*., 2003) The work shown by this group exemplifies an existing sensor type called CANARY (cellular analysis and notification of antigen risks and yields). It relies on the genetic modification of B cells,

causing the secretion of aequorin in the cytosol and the introduction of specific antibodies into the cell membrane. Aequorin is a bioluminescent calcium sensitive protein. When the appropriate pathogen binds to the antibody mesh on the cell membrane the interaction causes an influx of calcium. This can be detected *via* its reaction with aequorin which produces a luminescent photo signal.(Rider *et al.*, 2003)

Creation of novel cell-based biosensors can take place using one of two routes, utilizing pre-existing cellular machinery, or the insertion of foreign genetic material to create the bio-sensing properties. Special consideration must be given when inserting foreign genetic material to avoid undesirable protein-protein interactions, the inactivation of the target protein due to misfolding, or interference caused by inappropriate insertion site selection. In addition, the full range of insertion effects, primary and secondary, cannot be accurately predicted prior to experimentation.

1.5 Nitric Oxide

Discovered by Joseph Priestley in 1772, nitric oxide is a gaseous molecule that has generated considerable scientific interest. The 1998 Nobel Prize in physiology was awarded to Robert F. Furchgott, Louis J. Ignarro and Ferid Murad for the implication of NO in cellular signalling (Murad, 2005). Nitric oxide is now known to perform a number of intra and extracellular functions including lysis within macrophages,(J S Beckman & W H Koppenol, 1996) acting as a signalling molecule in both animals and plants (Wendehenne, Pugin, & Klessig, 2001) and demonstrating cytotoxic activity (both within the producing cell and towards foreign pathogens).(Borutaite & Brown, 2005) The diffusivity of NO is extremely high (over 3300 $\mu m^2/s$) and the molecule can easily cross the cell membrane making it an ideal messenger.(Xiaoping Liu et al., 2008) As such, NO is a ubiquitous mediator of cellular signalling throughout every system of complex organisms.(Llorens, Jordán, & Nava, 2002)

Early *in vitro* experiments suggested that the molecule is extremely cytotoxic however more recently the observed toxicity has been shown to be mostly caused by interaction of NO with superoxide, and the subsequent production of peroxynitrite. Superoxide may be produced at low concentrations under specific conditions *in vivo* by nitric oxide synthase (NOS) proteins (discussed in section 1.6) facilitating the formation of peroxynitrile and wrongly attributing the observed toxicity to the NO molecule.(Alderton, Cooper, & Knowles, 2001) Although termed a free radical, NO has limited reactivity due to its structure. The molecule is a 15 electron system resulting

in a single unpaired electron. However, as most biologically active compounds contain paired electrons in their highest occupied molecular orbital, their binding to NO is unlikely, preventing high levels of reactivity and toxicity.(J S Beckman & W H Koppenol, 1996) NO does however readily bind to other systems possessing unpaired electrons such as other free radicals, transition metals and transition metal complexes such as haem.(J S Beckman & W H Koppenol, 1996) Due to its free radical nature, NO can easily gain or lose an electron so as to gain a more favourable electron structure. It can hence exist as either a radical ($NO^{\bullet}$), a nitrosonium cation (NO^{+}) or the anionic nitroxyl radical NO^{-}.(Neill, Desikan, & Hancock, 2003)

Despite its expected low reactivity, NO is involved in many physiological processes. The earliest reported use for the molecule as a signalling agent was for gastro-intestinal relaxation.(Moncada & Higgs, 2006) In this case, NO was found to be present mainly in neurones (being produced by type I NOS). Firing of the neurone leads to the creation of action potentials which in turn creates an uptake of calcium. This calcium surge activates calmodulin and thus enhances NO production. Nitric oxide would then travel to smooth muscle cells in the vicinity, binding to guanylyl cyclase, causing an increase in intracellular cGMP. The result of this change would be muscular relaxation. The first evidence of NO being used as a signalling molecule was reported during investigations into a molecule termed EDRF (endothelium-derived relaxation factor). EDRF was first discovered in 1980 and was shown to promote muscular relaxation through neuronal activation of endothelial cells.(Furchgott & Zawadzki, 1980) Subsequent experiments demonstrated that the action of EDRF was inhibited by the presence of the superoxide anion and haemoglobin. In 1987 it was proposed that EDRF might in fact be NO. This was a revolutionary suggestion as NO had not been thought to be produced in mammals, much less suspected of being produced as a response to a biological signal. Further testing comparing the action of laboratory obtained NO to that of EDRF proved that the two were one and the same.(Palmer, Ferrige, & Moncada, 1987) This has also been demonstrated using genetic knock-out mice. Mice without the type I NOS gene have largely distended stomachs similar to the human condition hypertrophic pyloric stenosis, a condition in which the pylorus leading from the stomach to the small intestine is narrowed and prevents normal digestion.(Mungrue, D S Bredt, Stewart, & Husain, 2003)

Nitric oxide has also been implicated in regulation of blood flow, with evidence pointing towards it having a particular role in vasodilator nerves. It has also been associated with migraines, erectile dysfunction and the vascular reflex in hypercapnia

(increased carbon dioxide levels in blood), as evidenced by NO inhibition studies.(Iadecola, F. Zhang, & X. Xu, 1993) However the use of knock-out mice suggests that there are also alternative pathways to the hypercapnia vascular reflex.(Estevez & Phillis, 1997) Although there is some evidence that points towards the relationship between decreased NO and erectile dysfunction, it is not conclusive as such problems are also claimed to be age related. Type I NOS production in the penis has also been found to be dependent on androgens such as testosterone, which grants more credibility towards the functionality of NO in the erection of the penis, but less in regards to its direct connection with impotence which could stem from a lack of the androgenic hormones due to the ageing process.(Iadecola et al., 1993)'(Lue, 2000)

There are several methods of measuring NO concentration in a sample. The simplest approach involves measuring the amount of more stable NO by-products. This method has the disadvantage of being an indirect measurement. Moreover environmental conditions may affect the formation of the by-products making the estimation process less reliable. Another technique, discussed more detail in chapter 4 is direct electrochemical measurement. This relies on a surface modified electrode conducting a real-time measurement of NO by measuring the amount of redox reactions carried out by the molecule at the electrode surface. With correct calibration procedures, the amount of NO in the sample can be determined. Finally NO can be "fluorescently labelled". This is not actual labelling of the NO molecule itself but using of a compound that upon reaction with NO produces a fluorescent output. The most commonly used compounds are diaminofluoresceins (DAF's). They react with NO to form triazolofluoresceins producing fluorescence in the green light spectrum.(H Kojima *et al*., 1998)'(N Nakatsubo, 1998)

1.5.1 Nitric Oxide as a Messenger

In contrast to acetylcholine, which is secreted by a transporter and travels to a receptor on an adjacent cell's membrane, nitric oxide relies on its uniquely high diffusivity to act as a messenger, and its chemical interactions to cause a signalling cascade. NO has been shown to act on processes such as the inhibition of platelet aggregation, relaxation of smooth muscle, immune regulation and neural communication.(H. H. Schmidt & Walter, 1994)

NO mostly reacts with molecules with unpaired electrons, such as O_2, superoxide and metal ions/complexes. When it reacts with oxygen, which is present intracellularly

at concentrations varying between 20-200 μM it usually forms N_2O_3 which subsequently has the capability of interacting with thiols and amides in the cell, creating a potentially cytotoxic effect when present at high concentrations.(Coddington, Hurst, & Lymar, 1999)'(Mayer & Hernmens, 1997) N_2O_3 is an intermediary in the reaction of NO with oxygen in aqueous solution which is as follows:

$$4NO + O_2 + 2H_2O \rightarrow [\ 2N_2O_3 + 2H_2O\ ] \rightarrow 4NO_2^- + 4H^+$$

NO also reacts with superoxide at diffusion controlled rates to form peroxynitrite, ONO_2^-. This molecule is fairly stable but is readily protonated to form ONO_2H^+, which is extremely reactive. However, a competing reaction between peroxynitrite, glutathione and CO_2 within the cell is usually preferred. This reaction either oxidises glutathione or forms nitrosoperoxycarbonate $ONO_2CO_2^-$, respectively.(Coddington *et al*., 1999) Due to its inherent reactivity, peroxynitrite has a half life of approximately one second. NO also binds at diffusion controlled rates to the haem group of guanylate cyclase, which is one of the supposed targets of NO. This reaction increases intracellular production of cGMP by a second order of magnitude using nanomolar concentrations of NO. The reactivity of glutathione with NO can be explained as a result of its his-bound haem which can form a pentacoordinate ferrous nitrosyl complex under aerobic conditions.(Stone, Sands, Dunham, & M. A. Marletta, 1995)

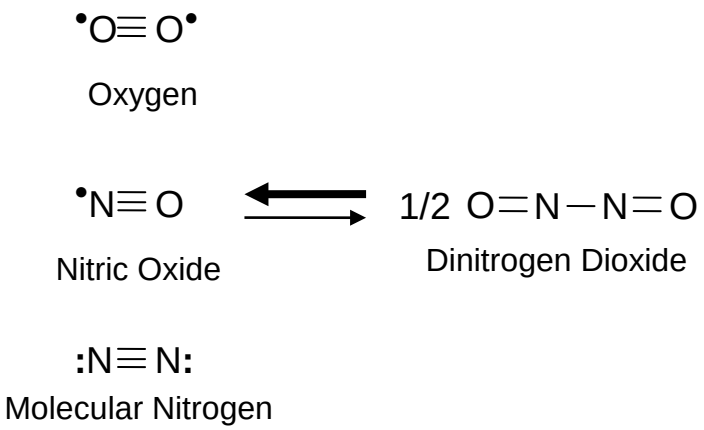

Figure 7 Diagram of the reaction of Nitric Oxide with Oxygen. Nitric Oxide does not dimerize at room temperatures due to unfavourable kinetics. The two unpaired electrons of oxygen allow the formation of bonds with nitric oxide molecules. The lack of formation of net bonds results in it being more energy

favourable for nitric oxide to exist as a monomer as opposed to dinitrogen dioxide. Adapted from Beckman *et al*. (J S Beckman & W H Koppenol, 1996)

Nitric oxide reacts most readily with haem proteins such as haemogloblin, which have been found to scavenge NO almost immediately as shown in Beckman *et al*,(J S Beckman & W H Koppenol, 1996) whilst superoxide dismutase has been shown to nearly double the half life of NO.(Palmer, Ferrige, & Moncada, 1987) *In vivo*, NO levels are constantly being reduced due to its contact with the bloodstream, where erythrocytes are widely available containing haemoglobin, and the presence of superoxide which is a relatively common molecule within cells.

NO has been found to be capable of inducing apoptosis at high concentrations. However, this is mostly due to the formation of reactive nitrogen species such as RNS's. Inversely, the role of NO in shear stress induced apoptosis demonstrates an inverse effect, the inhibition of apoptosis.(Dimmeler, Hermann, Galle, & Zeiher, 1999)

1.5.2 Nitric Oxide in Phagocytosis

In phagocytosis, as in many other processes that are carried out within the cell, there is a delicate balance between NO and O_2^{-}.(Fang, 1997) Although the NOS and NADPH oxidase pathways are regulated independently and in different ways, it has been shown that they are co-stimulated by inflammatory signals and that the presence of both free radicals allows for the production of several RNS thought to play a part in phagocytosis.(Fang, 1997) The presence and potency of intermediates produced by the interaction of O_2^{-} and NO provides a molecular basis for the relationship between the oxidative burst and NOS activity inherent in phagocytosis.(Fang, 1997) NO produced is also thought to be valuable for its ability to protect cells from excessive oxidative bursts by reducing the level of available prooxidant iron in the cell. This maintains a tolerable level of hydrogen peroxide (H_2O_2) as well as potentially protecting the membrane from oxidative damage by reducing rates of lipid peroxidation.(Fang, 1997) It has been found that addition of compounds which stimulate NO production *via* type II NOS reduced the efficiency of phagocytosis, whilst inhibiting production of NO enhance it.(Kopec & Carroll, 2000) Other findings have revealed the inverse relationship, and the increase of NOS II produced NO caused potentiated phagocytosis whilst inhibition using N^G-nitro-L-arginine methyl ester (L-NAME) impaired it.(Fang, 1997) In the former case where samples were taken prior to addition of NO generating compounds, it was found that

only types I and III NOS were being expressed and thus phagocytosis occurred normally, whilst activation of type II NOS impaired phagocytosis.(Kopec & Carroll, 2000) iNOS or type II NOS are primarily if not solely used to produce NO at levels high enough to be toxic, given that the purpose of most cells presenting type II NOS is to eliminate foreign organisms such as bacteria, though the phagocytosis of some types of bacteria does not seem to elicit an NO response.(Gross *et al*., 1998)'(Weikert, Lopez, Abdolrasulnia, Chroneos, & Shepherd, 2000)'(B. Zhang, Cao, Cross, Domachowske, & Rosen, 2002) Thus, type II NOS produces much higher levels than types I and III which are constituently active and so may be implicated in a variety of conditions such as chronic inflammation and autoimmune diseases, rheumatoid arthritis and even asthma.(Fang, 1997)'(Kopec & Carroll, 2000)'(Alderton et al., 2001)'(Thomassen *et al*., 1997) *In vitro* studies using NO donor compounds have also shown that NO itself has antimicrobial activity, inhibiting and even killing bacteria such as *Salmonella*. NO has also been attributed anti-viral, fungal and anti-parasitical properties as well as being involved in the destruction of tumour cells. (Fang, 1997)'(Tsai et al., 1997)'(Nascimento, Ribeiro-Dias, & Russo, 1998) In fact, the presence of NO in host cells/blood may at least in part, contribute to bacterial symptom suppression in latent asymptomatic infection. It has also been found that reducing levels of NO causes reactivation of diseases such as Tuberculosis, Epstein-Barr virus and Leishmaniasis.(Fang, 1997) It is possible that the function of nitric oxide in T Lymphocyte activation is responsible for some of the occurrences described.(Clark, Gorman, & Cope, 2007)

1.6 Nitric Oxide Synthases

Nitric oxide synthases (NOS) consist of a family of proteins responsible for cellular production of NO. Functional NOS consists of a NOS dimer bound to two calmodulin (CAM) proteins and several co-factors. These include (6R)-5,6,7,8-tetrahydrobiopterin (BH4), FAD, FMN and iron protoporphyrin IX (haem). In combination with the co-factors, the NOS complex catalyses the conversion of oxygen, NADPH and L-arginine into nitric oxide, citrulline and NADP.(Alderton et al., 2001)

Mammalian NOS exist in three isoforms, neuronal (nNOS), inducible (iNOS) and endothelial (eNOS). All NOS isoforms exist as haploids in the human genome and homology between the isoforms is thought to be between 50-60%. Although there are several differences between the proteins, such as dependence on co-factors, production

type (constitutive or inducible) and the type of cells in which the isoform is present, these are not sufficiently well understood to provide a conclusive reason for the variation between isoforms.(Alderton et al., 2001)

nNOS stands out from the other isoforms genetically as it contains a PDZ domain (which stands for a region of PSD-95 Disc large/ ZO-1 homology, PSD being post synaptic density protein) upstream of the rest of the sequence, which is homologous to the other NOS isoforms.(Brenman *et al*., 1996) The eNOS gene also stands out for having a myristoylation and palmytoylation site in its 5' region, a feature which has not yet been reported for the other isoforms of the protein.(Thomas Michel, 1999) All of the mammalian NOS proteins exhibit a bidomain structure consisting of an oxidase and a reductase region, which contain binding sites for the previously mentioned co-factors (Figure 8). More detailed information regarding electron flow through co-factors is given in Figure 9.

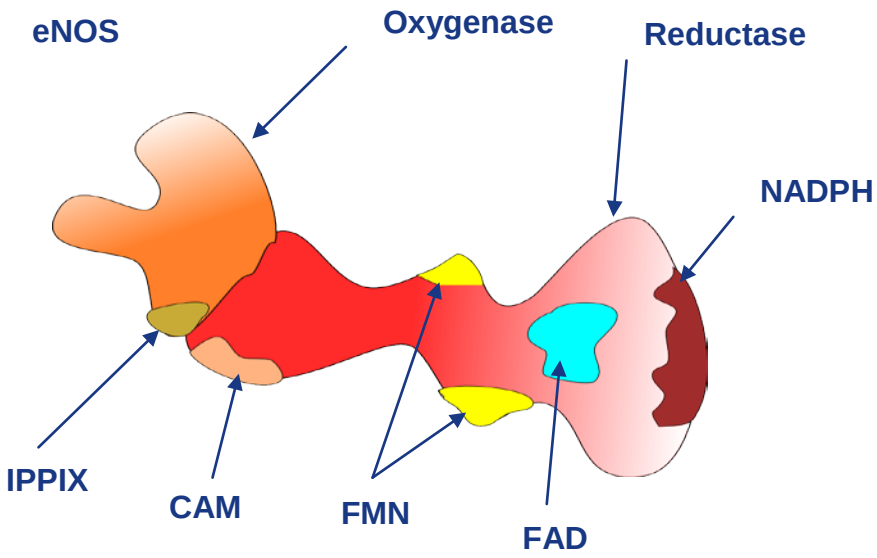

Figure 8 eNOS functional domains and Co-factors. Illustration of the functional domains of NOS and binding locations respective to domain of co-factors. Electrons donated from the conversion of NADPH to $NADP^+$ and H^+ proceeds along the reductase domain with FMN and FAD acting as electron carriers. The electron flow is facilitated by the calcium bound CAM and proceed to the iron haem and BH4 co-factors which then catalyse the conversion of L-arginine and oxygen into nitric oxide. Figure adapted from Alderton *et al.* (Alderton et al., 2001)

With the exception of the oxygenase domain of nNOS, the 3D structures for all three NOS isoforms have been resolved, including the structure of the protein dimer when

bound to co-factors, (Figure 10). This structural information is vital for the purpose of designed site-directed mutagenesis as it allows scientists to target areas to modify with a significant reasoning towards predicted site function. The three isoforms differ in several aspects, including protein size. eNOS contains 1203 amino acids (133 kDa), iNOS 1153 amino acids (131 kDa) and nNOS 1403 amino acids (161 kDa). The location in the genome is also different with eNOS, iNOS and nNOS being found in chromosomes 7, 17 and 12, respectively.(Geller *et al*., n d)(P. A. Marsden *et al*., 1992)

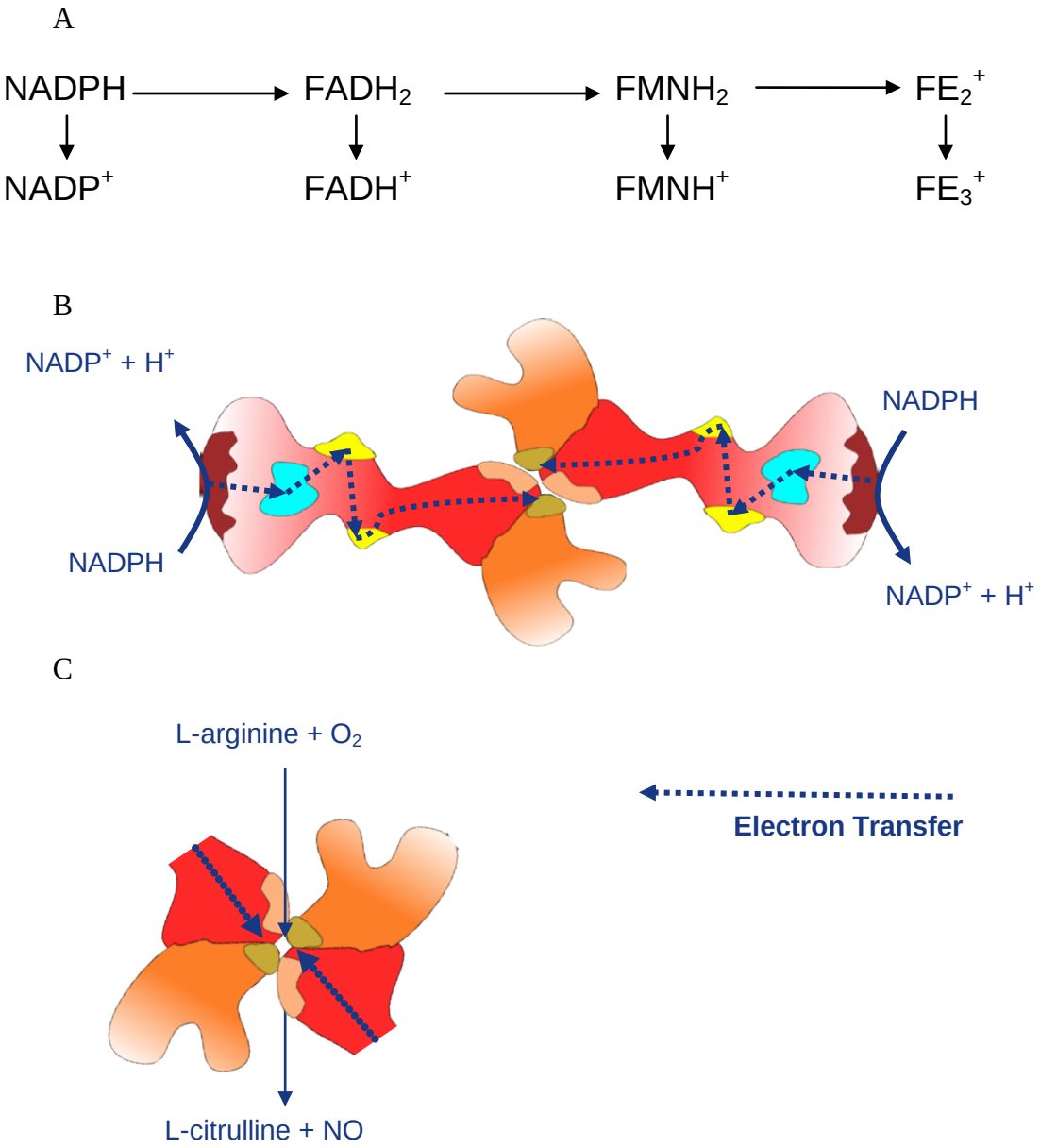

Figure 9 Schematic representing the electron flow from NADPH to the iron haem site which is thought to be responsible for facilitation of the transition of L-arginine to L-citrulline (adapted from Alderton et al,(Alderton et al., 2001)**) A) A diagram demonstrating the flow of electrons in eNOS. B) An illustration of the**

flow of electrons in an eNOS dimer as described in A. C) The catalytic core where L-arginine and O_2 are converted to citrulline and NO.

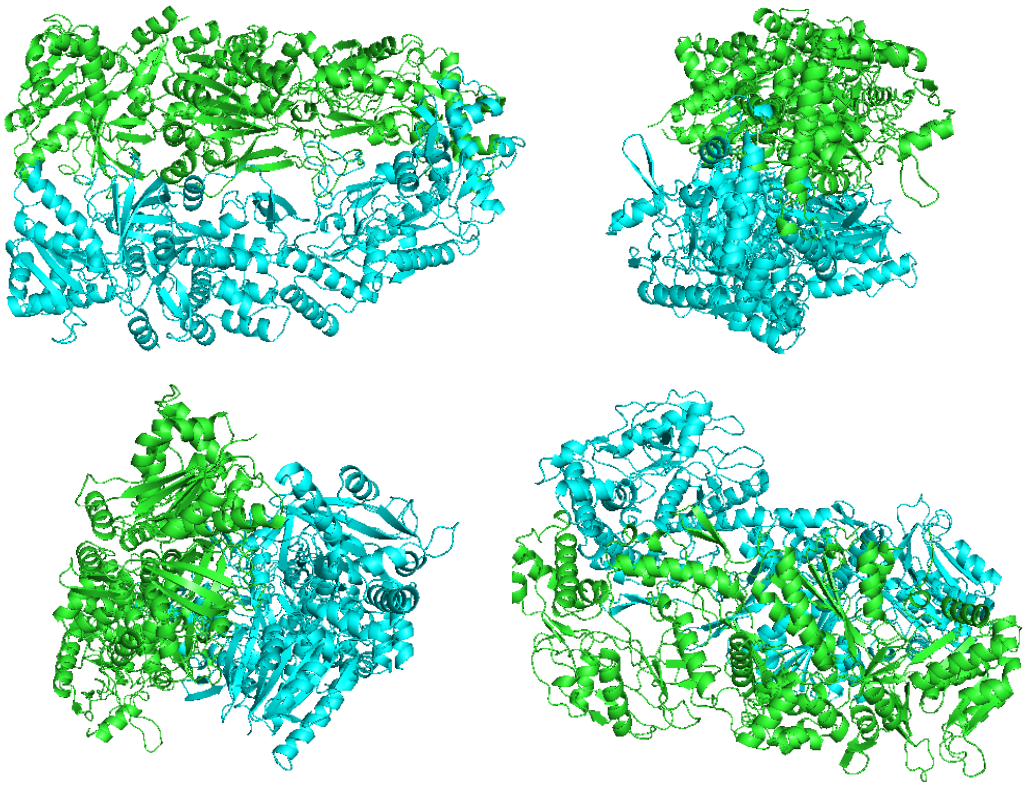

Figure 10 Image depicting the structure of the type III NOS dimer when bound to L-arginine and BH4. Dimer formation is necessary in order to render the protein functional, therefore a dimer is represented. This image is a result of the fusion of the C terminus of 1FOP to the N terminus of 1TLL - both obtained from PDB (a protein structure database known as Protein Data Bank provided by the Research Collaboratory for Structural Bioinformatics). 1FOP corresponds to the oxygenase domain of eNOS. 1TLL corresponds to the reductase domain of nNOS. As homology between the two isoforms (nNOS and eNOS) is >50%, this was considered to be sufficient to construct the model. Green/Blue shows individual AA chains of the dimer.

A schematic representation of the NOS genes is given in Figure 11. The dimerization of NOS is thought to occur in a similar fashion, irrespective of isoform. It is suggested that the dimerization occurs *via* the oxygenase domain of the proteins, creating the reaction pocket containing the haem molecule, the BH4 binding site and the L-arginine binding site. This is further stabilized by a zinc tetrathiolate which is located at an equidistant point between the two iron haems. Binding of the zinc molecule is thought to occur at a highly conserved site within the protein (eNOS Cys99, iNOS Cys115) and has been shown to stabilize the dimer formation by forming an additional eight hydrogen bonds.(H. Li *et al*., 1999) The bonds are located four residues distant from the BH4 binding site in iNOS, suggesting that the zinc is necessary for stabilizing the reaction pocket formed by dimerization and promoting BH4 binding, without directly affecting enzyme function. Further dimerization is thought to occur *via* the reductase domains of nNOS and eNOS, but since the crystal structures for these have not been elucidated these remain as assumptions. In addition, dimerization appears to be stabilized by the binding of BH4 and L-arginine, which suggests that enzyme activity is dependent on the presence of both the substrate and co-factors. This was shown by the conversion of a nNOS dimer which was found to be superior in resistance to SDS once bound to BH4 and L-arginine, though this observation has not been confirmed for the other two isoforms.(Klatt *et al*., 1995) BH4 has been found to bind to the haem containing domain of NOS, interacting with the haem molecule in such a way that its binding location is immediately adjacent to the L-arginine binding site where the catalytic reaction occurs.(Raman *et al*., 1998)

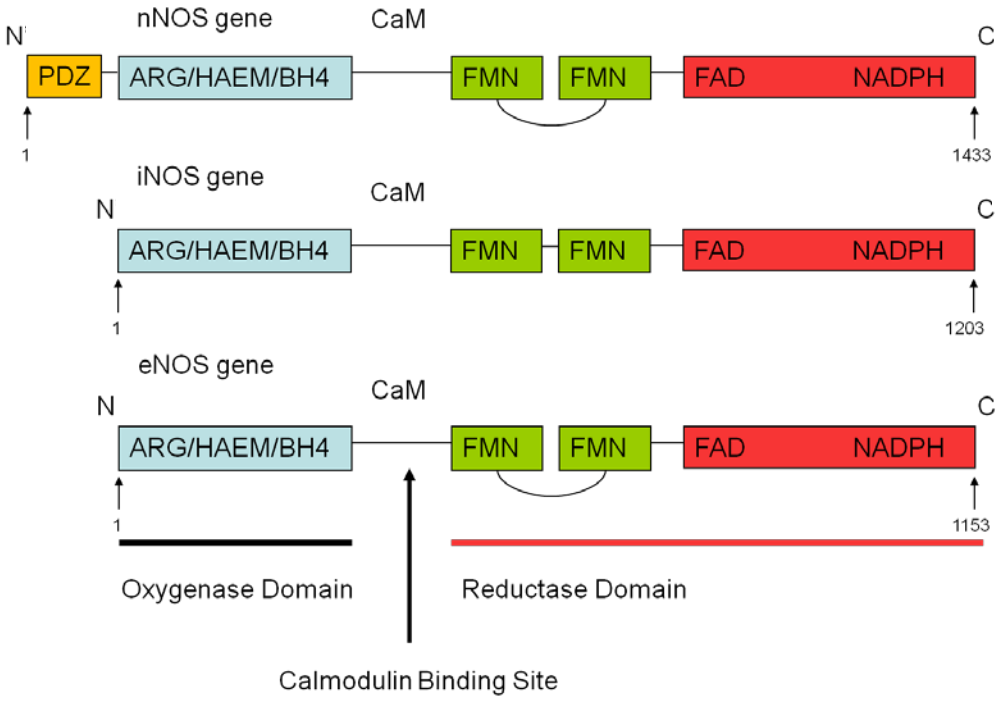

Figure 11 Schematic of the genes of the three NOS isoforms, showing the proposed binding sites for various co-factors and other elements required for the formation of NO. As can be seen from the figure, nNOS contains an additional domain and the proposed dimer formation domains in the reductase domain of the protein (the loop between FMN binding domains) is only present in nNOS and eNOS. Dimer formation in iNOS is thought to occur within proximal and distal regions of the oxygenase domain. ARG: arginine, HAEM (iron protoporphyrin IX haem), FMN: flavin mononucleotide, FAD: flavin adenine dinucleotide, NADPH: nicotinamide adenine dinucleotide phosphate.(Alderton et al., 2001)

iNOS appears to be less dependent on the reductase domain for dimerization and thus is thought to be more dependent on BH4 binding to stabilize dimers than the other two isoforms.(R. C. Venema, Hong Ju, Ryan, & V. J. Venema, 1997) This was illustrated by Marletta *et al* where the isoforms were expressed in a BH4 free environment using bacteria. Dimerization occurred more readily with nNOS and eNOS than with iNOS. This has been investigated and confirmed using limited proteolysis(Lowe et al., 1996) and yeast two-hybrid systems.(R. C. Venema *et al.*, 1997)

NOS's produce NO *via* the conversion of L-arginine to L-citrulline. This reaction requires NADPH, L-arginine and O_2. The reaction occurs at the L-arginine binding site of the NOS dimer and forms one molecule of NO per molecule of L-arginine used. A

diagram of this reaction is given in Figure 12. It has been found using fluorescence studies that eNOS produces NO at a rate of 50 nM/hour.(N Nakatsubo, 1998) Production of NO from iNOS does not depend upon the concentration of calcium unlike for nNOS/eNOS, where in the absence of calcium the enzyme also produces superoxide (O^-). This tends to react readily with NO, due to the fact that both molecules are super radicals resulting in the production of peroxynitrite, a highly cytotoxic compound.(W.H. Koppenol, Moreno, Pryor, Ischiropoulos, & J.S. Beckman, 1992)

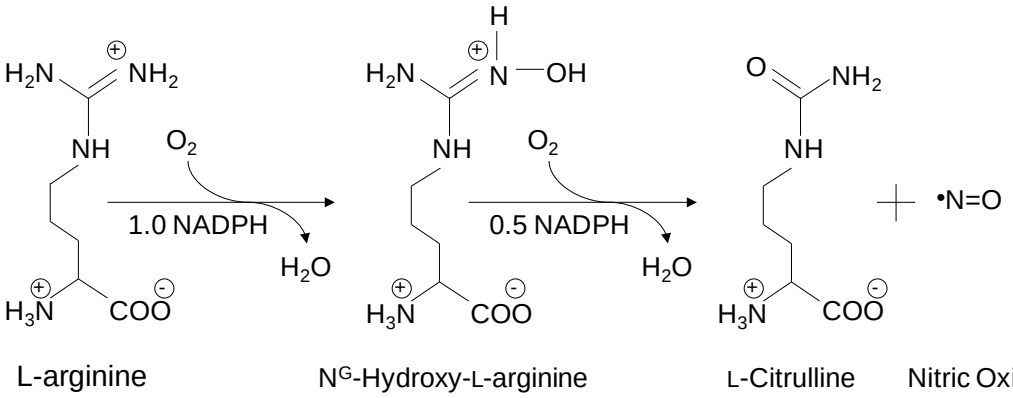

Figure 12 Diagram of the NO producing reactions catalyzed by NOS's. As can be seen in the diagram, NOS catalyzes the formation of NO *via* the conversion of L-arginine to L-citrulline, using NADPH as an electron donor and oxygen as a proton carrier through a condensation reaction. Overall, the reaction requires 1.5 NADPH molecules, 2 O_2 molecules and L-arginine to form one molecule of NO.

On rare occasions NOS have also been found to produce superoxide from NADPH oxidation. Of the three isoforms, nNOS appears to allow this reaction more readily than either eNOS or iNOS. Superoxide production transpires with a higher frequency when the level of BH4 or L-arginine is lower than the K_m value or in the presence of NO inhibitors such as N^G-methyl-L-arginine (L-NMMA).(Sroes *et al.*, 1998)(Xia, L. J. Roman, Masters, & J.L. Zweier, 1998) All three isoforms can produce superoxide under certain conditions such as those detailed above, and it is proposed that when both free radicals are produced they form peroxynitrite from their highly favourable interaction, reducing the levels of both molecules in the system. This has only been shown under *in vitro* conditions.(J.S. Beckman, T. W. Beckman, J. Chen, Marshall, & Freeman, 1990) eNOS, the endothelial NOS, has been found to be implicated in several areas of physiology, mostly pertaining to the formation of smooth muscle tissue and the process of angiogenesis.(Mungrue, D S Bredt, Stewart, & Husain, 2003)(Amano, 2002)

1.6.1 Regulation of NOS activity

NOS is heavily regulated due to the nature of its products. This regulation is mediated by NO self inhibition of NOS, the presence of co-factors and the level of Ca^{2+} ions. The relevance of Ca^{2+} is explained by the action of calmodulin. Calmodulin, the first identified co-factor for NOS only binds to NOS at high concentrations of Ca^{2+} and is responsible for the facilitation of electron transfer from the reductase domain to the haem domain in the protein. This is required for the catalytic conversion of L-arginine to L-citrulline. As was previously mentioned, the necessary levels of Ca^{2+} vary between isoforms, with iNOS requiring the least amount of Ca^{2+} to produce NO as a by-product of the aforementioned reaction.(D.S. Bredt & Snyder, n d)'(Gachhui *et al*., 1996) eNOS is highly sensitive to Ca^{2+} and is in fact transiently activated by a large variety of cellular signals such as receptor binding, cell-wall stress and even blood pressure.(Amano, 2002) NO is also responsible for NOS regulation as part of a feedback loop. NO has been found to block the site of catalytic conversion by reacting with the surrounding area to form one of its many highly reactive by-products.(Boucher, Moali, & Tenu, 1999)

1.6.2 Genetic engineering of Nitric Oxide Synthases

The genetic modification of NOS for research purposes has received surprising little attention. To date, several point mutations have been induced to further elucidate its function and determine which amino acid groups are vital to its function. Using these methods, it has been found that mutation of the serine 1177 residue of eNOS attenuates phosphorylation of the protein and reduces its activity.(Dimmeler, Fleming, *et al*., 1999) Another example can be found in the work of Robinson and Michel whereby the involvement of cysteines 15 and 26 were found to be vital in the palmitoylation of eNOS.(Robinson & T. Michel, 1995) Other approaches involve altering the level of NOS expression and thus raising the production of NO to higher levels. Kader *et al* (Kader et al., 2000) studied the effect of NOS overexpression on platelet aggregation and smooth muscle cell proliferation.

To date however, chimeric forms of NOS have not been created. The potential application for novel NOS proteins are varied, with the possibility of commercial and medical uses, as NO plays a vital role in various physiological processes in numerous

organisms. See section 1.5 of the literature review for the role of NO in physiological processes.

In order to create functional chimeric NOS, it is vital to preserve the oxygenase domain where the catalytic conversion of L-arginine to L-citrulline takes place. This phenomenon is observed in bacterial NOS which have been found to contain only an oxygenase domain. It is hypothesized that the reduction function is carried out by other proteins found in bacteria and therefore the reductase domain becomes obsolete.(Gosh & Salerno, 2003) It is further hypothesized that the reduction events of the redox chain necessary to form eNOS in these life forms are carried out by other proteins, such as flavodoxins or ferredoxins.(Gosh & Salerno, 2003) Due to this, the majority of genetic alterations proposed towards the creation of chimeric NOS will focus on the reductase domain of the protein.

One of the few transgenic NOS cell lines created was developed by Kaur *et al*.(Kaur *et al*., 2009) The group transfected human endothelial progenitor cells with eNOS accompanied by a reporter system. The cell line was transfected using a lipofectamine method of mammalian transfection. This method relies on encasing plasmids in liposomes to facilitate their uptake by cells. The resulting strain was shown to produce higher levels of NO, demonstrated by increased nitrite concentration in the solution. The strategy included a GFP reporter, which was used to estimate transfection efficiency. Cells were plated at equal densities in plates containing fibronectin (an extracellular matrix protein) to promote adhesion. Transfected cells showed a 35-40% increase in eNOS expression compared to untransfected cells. The ability of cells to form spindle like structures was then assessed and the eNOS transfected cells were shown to exhibit a marked increase in cells displaying the mature morphology. Cells containing transfected eNOS but lacking the GFP marker proved to be the faster developing strain as demonstrated by confocal microscopy, with both samples showing an increase in maturation over the control untransfected cells. This elegant experiment served to establish the hypothesis that transgenic forms of eNOS can be used to treat certain ailments such as CAD (coronary heart disease).(Kaur *et al*., 2009) Patients with CAD exhibited reduced endothelial progenitor cell maturation and the cellular transplantation which could be possible with cells such as those developed by the Kartha group may work to attenuate damage caused by myocardial ischaemia (Kaur *et al*., 2009). Endothelial progenitor cells have recently been implicated in the reparation of the endothelial monolayer.

Another field in NO research has been the creation of transgenic mice for the purpose of studying NO function in physiology. The majority of these involve the creation of knock out mice which either lack an NOS altogether or contain a loss of function mutation. The findings presented in such studies are invaluable as they demonstrate the ubiquity of NO signalling as well as determining physiological roles of the NOS's and NO itself. An example of such research can be found in the work of Mrowka *et al* where the effect of NO on arterial blood pressure was studied.(Stauss, Nafz, Mrowka, & Persson, 2000)

It is important to note that not all work directly pertaining to the study of NOS involves genetic engineering. In one chemical approach, a compound containing a chromophore analogous to NADPH was developed to replace NADPH binding, creating a photosensitive NOS.(Beaumont *et al*., 2008) This compound named Nanotrigger was designed so that only when light of a specific wavelength shines on the proteins, nitric oxide is released which can subsequently be detected by an electrode. In the absence of light incidence, the Nanotriggers block NADPH binding sites without undergoing reduction. However upon subsequent incidence of light the reduction reaction is initiated. Slama-Schwok *et al* have verified that the compound causes eNOS to produce NO in response to light.(Lambry, Beaumont, Tarus, Blanchard-Desce, & Slama-Schwok, 2009) This work could be used as a novel, dependable method to test NO inhibitors or as a tool for researchers working on processes involving NO and its by-products.

1.6.3 Cellular NOS

Nitric Oxide Synthases are present in a large variety of cell types as NO is a highly versatile intra and inter-cellular messenger. More than one isoform may be present in a cell type and information regarding the presence/absence of NOS isoforms in a cell line is crucial when attempting cell-engineered NO strategies.

The work of Tullio *et al* demonstrated that CHO-K1 cells are capable of expressing the nNOS and eNOS isoforms of NOS.(Florio *et al*., 2003) This result was obtained *via* northern blot, a technique demonstrating the presence of specific RNA sequences in cells which are demonstrative of active protein expression.

The body of work depicted in the literature demonstrates that the insertion of eNOS to various cell lines is possible, with non-lethal effects and detectable by a large variety

of methods. The findings show that insertion of the eNOS gene has been used for characterization of the protein, elucidation of some of its interactions and many of its effects.

eNOS has been transfected into various cell lines. These include muscle cells, COS-7 and CHO-K1. COS-7 (CV-1(Simian) in Origin SV-40+) cells were transfected with eNOS using a DEAE-dextran-chloroquine protocol with the purpose of further characterizing eNOS and a transient cell line was obtained. In this work, transfected cells were combined with the A23187 calcium ionophore to demonstrate enhanced eNOS activity in cells. This provided evidence as to the dependence of eNOS on calcium concentrations for protein activity (S Lamas, P. a Marsden, G. K. Li, Tempst, & T Michel, 1992). The study utilised cGMP measurements as a method of quantifying NO production.

The transfection of smooth muscle cells with eNOS has been described in the work of Sato *et al.*(J. Sato *et al.*, 2000) In this work, cells were transfected using a Lipofectamine protocol and the effect of transfection was monitored and analyzed. The findings from the study demonstrated a decrease in cell proliferation combined with an increase in p17 and p21. It was also found that the expression of the constitutively active NOS isoform eNOS did not cause an increase in cellular apoptosis over a time-frame of 72 hours. Another example involves the transfection of vascular smooth muscle cells. This can be found in the work of Gurjar *et al.*(Gurjar, R. V. Sharma, & Bhalla, 1999) The study demonstrated the inhibitory effect of eNOS produced NO on the metalloproteases MMP-2 and MMP-9, which are relevant towards cellular migration after injury. In this work, a wild type cell line was used as a control and an additional control involving transfection of cells with GFP was used to verify that it was not the transfection procedure which elicited a response. The involvement of NO was conclusively demonstrated by rescuing the wild type phenotype by use of an eNOS inhibitor and thereby restoring cellular migratory capability.

An example where CHO-K1 cells were transfected with eNOS can be found in the work of Noiri *et al.*(Noiri, 2002) In this case, the intent was to characterize a missense mutation in eNOS (Glu298Asp) and its association with Renal disease. The reason behind the group's interest in this mutation was due to its frequent occurrence in patients exhibiting end-stage renal disease. Cells were transfected with mutant and wild type eNOS. The method used to detect NO was an indirect one, measuring Nitrite accumulation *via* the fluorescent interaction of 2,3-diaminonaphtalene with nitrite. The data demonstrated a dramatic decrease in cellular nitrite production in the mutant cell

line, indicating that a deficiency in eNOS produced NO is in fact linked to end-stage renal disease.

In some cases, eNOS transfections were utilized to re-introduce the protein to knock-out organisms. One such example can be found in the work of Feron *et al*, where this approach was taken to elucidate the interaction between Caveolin-1 and eNOS.(Feron & Balligand, 2006) In this case, neonatal cardiomyocites were used and cells were transfected with both wild type eNOS and a variation containing a mutation which removes its myristoylation site. The findings support a strong interaction between the two proteins and propose Caveolin-1 to be a strong antagonist to NO production as eNOS activity was shown to dramatically increase in the absence of Caveolin-1.

1.7 Chemical Inducers of Dimerization

Chemical inducers of dimerization (CIDs) are a relatively recent development in the field of biomolecular engineering. It involves the use of an agent to trigger binding of two targets, bringing the targets within functional distance of each other. The principle of this system requires compounds that have the ability to bind to two different protein domains. By tagging proteins with the domains that bind to the compound, the proteins come within close enough proximity to bind to each other and thereby create a dimer. Several proteins function as homo/heterodimers and this technique allows inducible dimerization. In addition CID can also be used to catalyze protein activity for proteins that require dimer formation.

An example of a CID system can be found in the work of Crabtree *et al*.(Belshaw, Spencer, Crabtree, & S L Schreiber, 1996) In this study the group used the immunosuppressant cyclosporin A to create a CID system which would bind a chimeric protein containing a cyclophilin domain and a cytoplasmic signalling domain of FAS. To achieve this, $(CSA)_2$ was synthesized from cyclosporin and the signalling domain of FAS was fused to a cyclophilin. This allowed the creation of homodimers upon introduction of CSA to the system. When CSA is introduced, two cyclophylin molecules bind to CSA, bringing the fused FAS domains close together and thereby creating a functional homodimer. The design resulted in the induction of apoptosis upon dimer formation.

An alternate approach was taken by Hu *et al*.(Kopytek, Standaert, Dyer, & Hu, 2000) In this work, the group focused on the immunosuppressant *bis*-methroxate and its

ability to dimerize dihydrofolate reductase (DHFR). To construct this CID system, the group synthesized *bis*-methroxate and assayed its ability to dimerize DHFR *via* gel-filtration analysis of the purified protein. They found a complex corresponding to double the molecular weight of the monomer (suggesting dimer formation) and discovered that the off-rate of the complex was approximately one hundred times slower than the wild type dimer. This suggested that the *bis*MTX/DHFR2 complex is capable of creating more energy favourable conditions for protein interaction than the wild type dimer.

Many CID systems rely on compounds which are known to have immunosuppressant qualities. In both the described examples, the chemical responsible for the formation of dimers is a type of immunosuppressant. Another example of CID systems is that based on rapamycin/Frb/FKBP12. Unlike the two systems mentioned previously, the rapamycin utilizes three components rather than two. The system works by sequential binding of the two protein domains to rapamycin. FKBP12 (part of the mTOR gene) is known to interact directly with Rapamycin, whereas Frb (the FKBP12 binding domain of the FRAP protein) only binds to the Rapamycin/FKBP12 complex, Figure 13. (Drenan, Xiangyu Liu, Bertram, & Zheng, 2004)

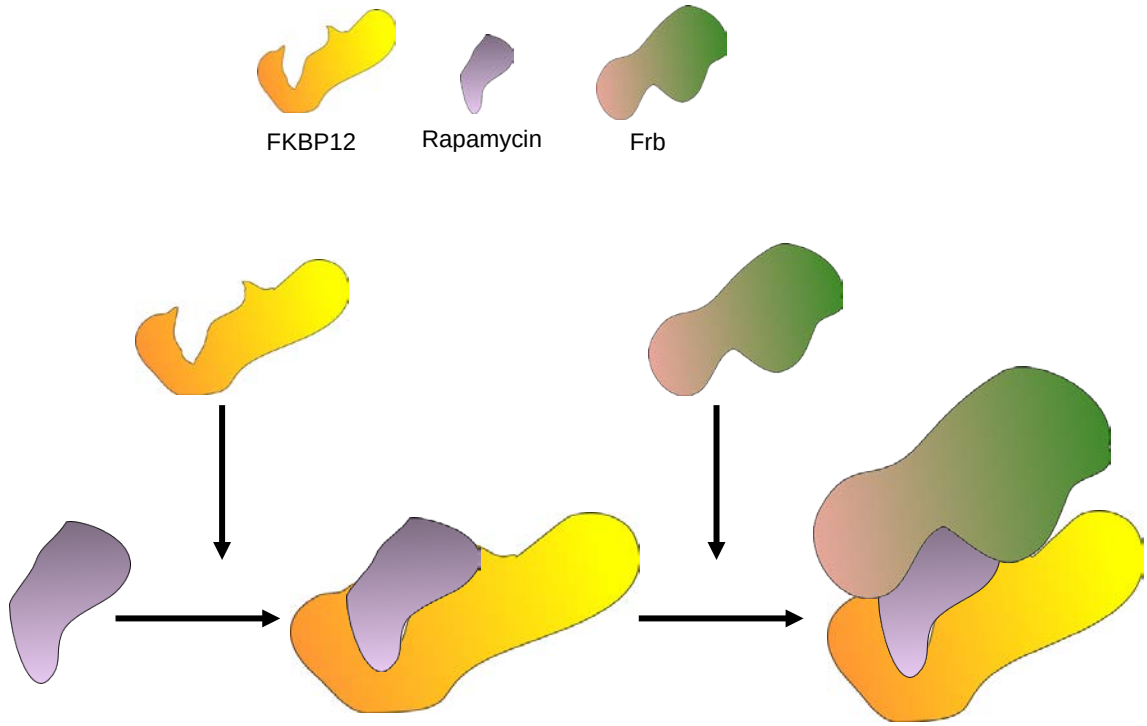

Figure 13 An illustration of the Rapamycin CID system and the sequential binding between Rapamycin 0.91 kDa, FKBP12 12.6 kDa and Frb 11 kDa.

The cytotoxicity of many of the compounds used for the creation of CID systems limits their application to mutants where the cytotoxic activity of the compound is abolished. For example, rapamycin is known to arrest yeast cells in G_1 of the cell cycle.(Heitman, Movva, & Hall, 1991) Alternatively construction of analogues of these cytotoxic compounds could reduce or remove their inherent toxicity.

1.8 Photoactive Sensors

Recent and continuous advances in both ability to detect/process light-based signals and genetic engineering have lead to the creation of the emerging field of photoactive sensors. Such sensors generally emit or absorb light so as to create a signal to be detected in response to the target analyte. Unlike previously described sensors such as the LAPS system, these utilize naturally occurring proteins or chemically derived polymers which can either emit light when they come in contact with the analyte or alternatively absorb light to excite a component and create a chemical or electrical signal.

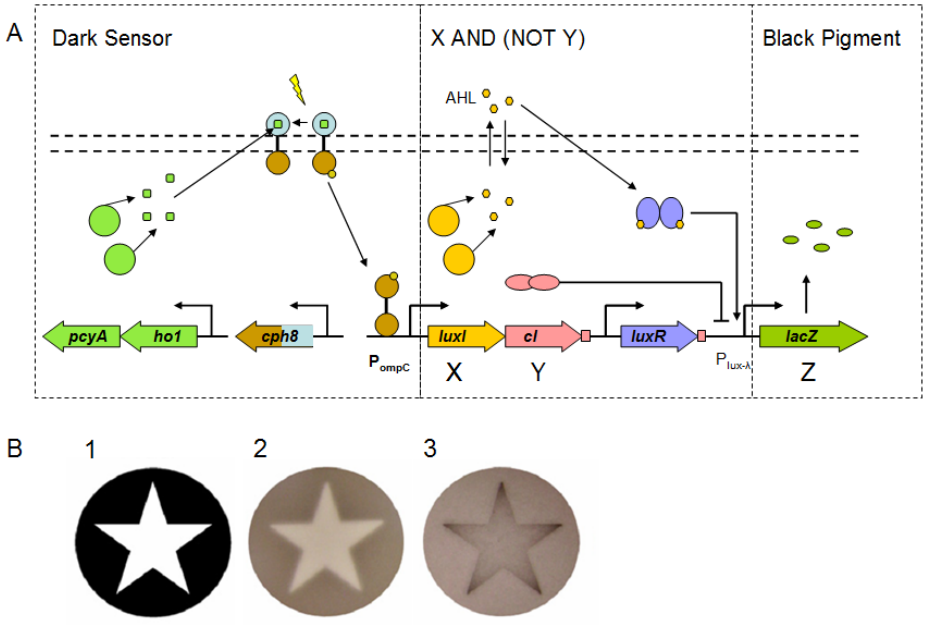

Figure 14 The genetic circuit for edge detection Adapted from Tabor *et al* (Tabor *et al*., 2009)**. A: The Dark Sensor component works by incorporating a chimeric cph8 gene which requires the interaction of pcyA and ho1 gene product (PCB) to phosphorylate the response regulator OmpR, which in turn binds to the PompC promoter and continues the circuit to the X AND (NOT Y) gate. The light sensitive switch is within the cph8 chimeric protein, which is sensitive to red light in a**

manner which prevents the phosphorylation reaction when light is present. If light is not present, the circuit is continued and allows the expression of luxL (a quorum sensing gene from *V. fischeri* responsible for the production of AHL) and cI (a repressor of transcription) are expressed (Egland & Greenberg, 1999)**. The product of luxL activates transcription under the P-luxλ promoter whilst the product of cI represses this transcription event. Due to this, when X is present and Y is absent higher transcription levels of the subsequent gene in the circuit - lacZ would be expected. This in turn would lead to the production of pigment by the cleaving action of lacZ on the sugar β-galactosidase. B: 1) Mask. 2) Cell culture expressing lacZ directly under a light sensitive promoter. 3) Cell culture with the edge detection gene circuit. C shows darker pigment on the edge of light detection rather than on the parts which are not illuminated.**(Tabor *et al*., 2009)

One of the most commonly utilized light emitting proteins in research is GFP. Isolated from *Aequorea victoria*, this protein fluoresces at a wavelength of 398 nm and is often used as a reporter in experiments relating to protein expression.(Gorokhovatsky *et al*., 2004)(Motoike *et al*., 2000) In such studies, the GFP protein is fused to the protein being expressed so as to form a direct relationship between the levels of expressed protein and intensity of fluorescence.(Motoike *et al*., 2000) This simple and efficient method has led to a better understanding of promoters and terminators leading to the optimization of expression systems.

An elegant example of genetic engineering to create a cellular photo-detector was pioneered by Voigt(Levskaya *et al*., 2005) and Ellington.(Tabor *et al*., 2009) By creating cells which repress pigment production upon light incidence, and using simple masks it was possible to replicate an image onto a bacterial plate, Figure 14. However as the system is reliant on photoactivation of transcription machinery, it takes several hours for the cells to produce the pigment with continuous exposure to light. In addition, the process is irreversible meaning that only one image may be formed on a bacterial plate. Therefore the system, although innovative, is still inferior to conventional methods of photography and must be further adapted to become anything more than proof of concept.In order to truly harness the potential of cellular photo-detectors, the photon detecting system must be incorporated into protein activation rather than transcription coupled. By using this method, the reporting of light incidence can be reduced in time from hours to seconds or potentially milliseconds, depending on the activity of the target protein. To achieve this, the system must be designed so as to

produce a molecule detectable by the electrode specifications (*i.e.* size, charge, necessary concentration) whilst keeping in mind the effect the signalling molecule would have on the cell. There are many proteins which are light sensitive, as previously described, but the cascade these proteins trigger is not necessarily one which is optimal for electrode detection. To circumvent this, many approaches can be taken, each with its set of benefits and disadvantages. A down-stream element in the cascade of protein activation may be detectable. However, whilst preserving the integrity of the system this causes a delay in the signal and depending on the detector system involved may not be feasible. Approaches such as the creation of AND, OR or NOR gates so as to link expression of one gene to the activation of another shares the advantages/disadvantages previously delineated. Creating a chimeric fusion protein which will act as both detector and imitator of signal would lead to the highest rate of signal delivery, but could severely compromise protein function, reducing or even abolishing protein activity.

1.9 Optogenetics

Optogenetics is an area of genetic engineering which focuses on creating cellular responses to light.(Deisseroth, 2011) A large proportion of these approaches rely on opto-activated gene transcription/translation through various mechanisms such as the use of light-activated ligands, light-triggered cascade events and the use of chimeric fusion proteins involving light-activated domains.

One major family of light-sensitive switch proteins used in this field are opsins. Members of this family include bacteriorhodopsin and channel rhodopsin. The advantage of using light dependent activation for cellular processes is the ease with which the system can be activated/inactivated and the specificity which can be conferred. Practical applications of optogenetics have quickly developed to the stage where the degree of complexity is high. This is due to the possibility of targeting specific cell types, activation with light of a specific wavelength and a possible response time in the order of milliseconds.

Peng *et al* have developed a system that achieves insulin expression as a result of blue light stimuli.(H. Ye, Daoud-El Baba, Peng, & Fussenegger, 2011) This was accomplished by introducing melanopsin into a cell line, which when combined with a G-protein coupled receptor caused a signalling cascade in turn activating an inserted trans-gene expression. The system was tested *in vivo* and the chosen trans-gene was an insulin encoding one. Mice were treated with encapsulated mutant cells and exposed

intra-corporeally to blue light for a period of 48 hours. This invasive procedure was achieved using optical fibres to deliver light at the correct wavelength with sufficient intensity. The results showed that mice with the micro-encapsulated cells, both those suffering from diabetes and wild type, showed an increased level of insulin in the blood, signifying successful trans-gene activation.(H. Ye et al., 2011) By replacing the insulin gene with any other product, it would theoretically be possible to express any protein in a similar fashion.

Gene level optogenetic systems, suffer time-lapse related issues. As the majority of optogenetic systems rely on light-dependent gene transcription, the response rate is limited by the native cell-machinery in as far as producing the target protein. This causes a time lag between stimuli and response in the order of several hours. For some applications, *i.e.* insulin production in diabetics this would probably be a favourable trait, but for many other systems it would be detrimental. One method of bridging this gap would be to create photo-activable proteins which would become directly photo-stimulated, or designing a signalling cascade that would have an effect on a protein level rather than a gene level. A possible method of achieving this would be *via* protein phosphorylation. By initiating a cascade that would cause the activation of a kinase or phosphorylase which could target the protein of interest it would be possible to severely decrease the response-time and thus improve the efficacy of the desired effect.

Another innovative application derived from optogenetic engineering is described in the work of Erica Pastrana.[93] The system described was designed so as to modulate neuronal activation *via* a light-dependant change of membrane potential. To achieve this effect, channelrhodopsin2 was used in conjunction with NpHR and Arch to control the flow of ions through the cell membrane. Illumination of Chr2 with blue light (470 nm) causes an influx of Na^+ and Ca^{2+} ions and an outflow of K^+ ions. Illumination of NpHR with orange light (589 nm) would lead to an influx of Cl^- whereas light at 575nm would activate Arch so as to cause an efflux of H^+. By using all three in conjunction it is possible to modulate membrane potential behaviour. Shining blue light would result in a rapid accumulation of positively charged ions whilst yellow or orange light would result in the induction of a negative charge *via* the influx of Cl^- ions (NpHR) and an outflow of H^+ ions (Arch) respectively. By not allowing the cell to accumulate sufficient positive potential to permit a trigger event, the activating potential threshold is never reached and therefore response is attenuated. Thus exposure to all light wavelengths would result in no effect caused by the system and the presence of an isolated wavelength of light (470 nm) the system is activated.(Pastrana, 2010)

The two systems described above demonstrate both the transcription/translation use of optogenetics and the photoactivated protein approach to create malleable, responsive and selective systems with potential technological applications. Although there are several advantages to the photoactivated protein approach of optogenetics, its major drawback is that it is severely limited in potential applications. This limitation is derived from the fact that photoactive proteins only produce limited functions such as ion channel activation in the case of opsins and electron transfer to a flavin mononucleotide in the case of LOV (Light Oxygen Voltage domains). Although these can be harnessed to produce a desirable function, there is an issue of the compatibility of these mechanisms with the target operation. The gene transcription/translation method offers much more varied application possibilities as the system can be tailored to act on different target genes. In essence, the protein tool-kits available to construct optogenetic systems are far more limited than the genetic equivalent.

As a follow up to the previously described optogenically controlled neurone activation/inactivation strategy, Deisseroth *et al* also constructed a rhodopsin-GPCR chimera (OptoXR) that responded to green light.(Deisseroth, 2011) GPRCs are capable of producing protein cascades therefore they have potential applications in more complex systems. An exemplary application of the OptoXR system involves neuronal biochemical pathways. Neurones are as a family capable of using GPCR activation as a form of intracellular communication *via* the serotonergic, dopaminergic and adrenergic pathways as well as *via* a downstream cascade of neurotransmitters such as Gaba and glutamate. It is therefore thought that by integrating Opto-XRs it will be possible to manipulate neuronal signalling in a spatio-temporal controlled manner. These light-activated proteins work on an extremely fast time-scale which varies between proteins ranging from approximately 4 milliseconds to almost 30 minutes. It is noteworthy that the majority of these proteins work on a millisecond scale.

1.10 LOV

LOV (Light Oxygen Voltage) domains are a part of the phototropin family of proteins. These proteins are thought to be vital for the common process found in many plants denominated phototropism, the bending of the plant stem so as to maximize light exposure. This occurs by the de-synchronized growth of cells, with cells growing faster on the side exposed to light and slower on the side exposed to darkness, causing a bend in the stem and increasing the plant surface area exposed to sunlight. This class of

photoactive protein has absorption ranges in the UV-A/blue light range and is involved in a large variety of plant cell behaviours, among them leaf positioning.(Iino, 2006)'(Inoue, T. Kinoshita, Takemiya, M. Doi, & K. Shimazaki, 2008) The protein autophosphorylates under light incidence and is involved in other processes such as stomatal opening and chloroplast migration. Phototropins are vital for plant life and the appropriate physiological responses allowing natural cycles such as photosynthesis and the Krebs cycle to occur.(Toshinori Kinoshita et al., 2001)'(Volkov & Ranatunga, 2006)

LOV domains were originally discovered in the 120 kDa protein NPH1 bBlue light receptor phototropin) which is an autophosphorylating kinase which depends on UVA/blue light as its inducer. The phototropin sub-group family LOV contains two members: LOV-1 and LOV-2, each with an approximate molecular weight of 12 kDa.(Volkov & Ranatunga, 2006) Both proteins bind to the same chromophore and both bind to flavin mononucleotides (FMN). The binding process can occur in darkness and has a maximal absorption peak of 447 nm whilst when occurring in light it has an absorption peak of 385 nm.(Cho *et al*., 2007) The interaction between LOV proteins and FMN is thought to be derived from the proximity of a reactive cysteine from LOV (cys 62) to the isoalloxazine ring moiety of the flavin molecule. The covalent chemical bond formed by the cysteinyl-flavinoid complex occurs within microseconds of light exposure.(Winslow R. Briggs et al., 2007)(Möglich, R. Ayers, & Moffat, 2009)In effect, this means that in dark conditions, LOV binds to FMN non-covalently, but upon light incidence a covalent bond is formed.(Michael Salomon *et al*., 2001) The dark state shows an absorption peak at 447 nm and upon incidence of blue light the LOV-Flavin complex forms an intermediate state with an adsorption peak of 715 nm and transitions to the signalling state with an adsorption peak of 385 nm. The protein therefore cycles between an inactive state (447 nm) and an active one (385 nm) depending on the absence/presence of light. This effect is presumed to be due to the interaction between the C(4a) carbon in FMN and the cysteine 39 residue from LOV.(Zenichowski, Gothe, & Saalfrank, 2007) Mutation of the LOV cysteine 39 residue into alanine or serine results in a loss of protein photoactivity, further proving its involvement in the photochemical process described.(Michael Salomon, John M Christie, Knieb, Lempert, & Winslow R Briggs, 2000)

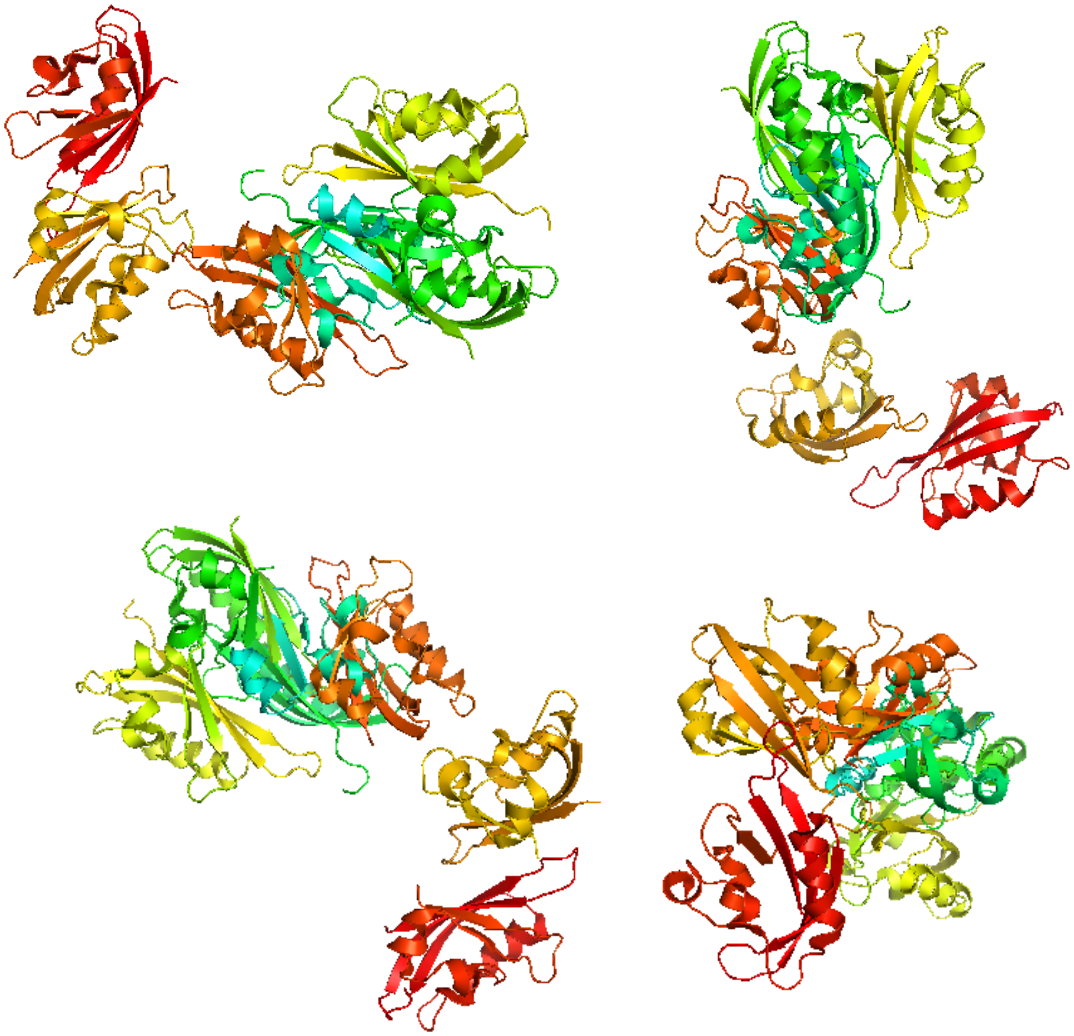

Figure 15 The structure of LOV1/2 domains. Obtained by fusing PDB files 2Z6D (LOV1) and 1JNU (LOV2) as the complete protein structure has not yet been elucidated. Fusion was performed by attaching N terminus of 2Z6D to the C terminus of 1JNU. The selected colourscheme corresponds to location of the structure in relation to N or C terminus. The colourscheme goes from blue (N terminus) to red (C terminus).

In nature, the LOV-2 gene is thought to act as a photoactivable switch used to turn on a kinase pathway found in phototropin. *In vitro* studies of LOV-2 activation in the phototropin gene *phot2* have indeed shown LOV-2 to act in a manner showing a dark-state repressor of *phot2* PKA kinase of the PAS family.(Matsuoka, Iwata, Zikihara, Kandori, & Tokutomi, 2007)

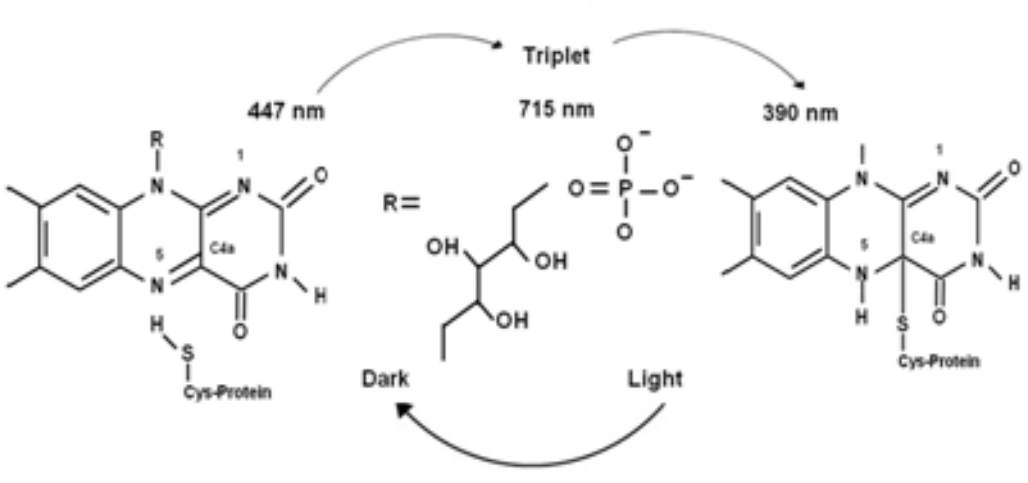

Figure 16 The LOV1-FMN interaction cycle upon blue light incidence. Shown are the dark stage (educt) and light stage (adduct) with the transitory triplet stage in between. Adapted from Zenichowski *et al* (Zenichowski *et al*., 2007)

LOV has attracted much attention due to its relatively small size and its inducible functions. The roles of analogues of the LOV proteins found in bacteria are currently unknown. It is proposed that they may act as photoreceptors involved in phototaxis, regulation of DNA expression and in some cases play a part in photosynthetic machinery.(Crosson, Rajagopal, & Moffat, 2003) LOV domains are recognized as targets for optogenetics, the engineering of genetic systems so as to render them light activable/inducible and therefore create systems which will alter the cellular behaviour upon incidence of light. (Pastrana, 2010)

LOV is becoming prominent in the realm of light activable proteins. Its affinity to FMN has been further studied by the work of Briggs *et al* whereby using LOV fused to CBP (calmodulin binding protein) to enhance purification of the protein using a calmodulin resin affinity chromatography.(J M Christie, M Salomon, Nozue, M Wada, & W R Briggs, 1999) The mutant exhibited a slightly shifted absorption spectrum, thought to be caused by the fused CBP domain. This finding demonstrates the fact that proteins may behave differently when fused to other domains. Although in this case the shift in absorption spectrum is a minor issue, in other systems this could prove problematic depending on the intended application of the fusion protein.

The exploitation of the photo-activable mechanism of LOV is in its emerging stages. Work by Moffat *et al* allowed the creation of a LOV/Kinase fusion protein which became light inactivated.(Möglich et al., 2009) This was demonstrated by measuring

levels of phosphorylated FixJ, a target of the Ytva kinase. In this work it was demonstrated that, in effect, it was possible to abolish Ytva activity upon light incidence by using a fused Ytva-LOV construct. It is important to note that Ytva is naturally inactivated by the its signalling molecule, meaning that the abolishment of protein activity demonstrates a successful signalling event. The vast majority of proteins which are light sensitive show increased protein activity upon light incidence, rendering this study useful for specific applications regarding protein inactivation.(Möglich et al., 2009) Unfortunately, as in the case of nature, most applications involving photo-activable sensors desire the opposite result.

1.11 Aims and Objectives:

Research within this thesis aims to design and construct a cell based device capable of converting an external stimulus (either chemical or optical) into a measurable output for the eventual integration with electronics. This system involves mutating the NO producing gene eNOS to output NO in response to a specified stimulus. Signal transduction will be achieved *via* the use of an amperometric sensor capable of detecting nitric oxide and thereby creating a suitable bio-electro interface. In this way it will be possible to create an artificial signal transduction pathway (opto-chemi-electro) as well as a reporter/detector system capable of producing an electrical output in response to a selected chemical input. To implement the chemically responsive strategy, the FKBP12/FRAP/rapamycin system is proposed, whereby the eNOS protein is separated according to domain and attached by a linker to the relevant region of the FKBP12 gene and the FRB domain of the FRAP protein. In the presence of rapamycin, these proteins should bind and bring the chimeric eNOS fragments close enough together to bring the domains within functional distance, allowing the production of NO.. This system can potentially be modified to respond to a variety of stimuli and allows detection within seconds of exposure, providing a real time quantitative signal regarding the presence of an agent. This can in turn be developed into an array capable of detecting the presence of a variety of analytes from a single population of cells. Photoactivation of eNOS will be attempted *via* appropriate genetic modification of the eNOS gene *via* insertion of the LOV domains. The LOV strategy will require the insertion of single or multiple copies of the LOV gene into the eNOS protein. The LOV will bind to FMN within the protein and upon incidence of light at 385 nm wavelength, electron transfer will occur between the photoactivated LOV to the FMN molecule.

Using the naturally occurring electron transfer pathway of eNOS, the electron should travel across the co-factors in the ET pathway and finally be used to reduce citrulline and produce the NO as a by-product. Ultimately, the NADPH binding site of eNOS will be mutated to create a loss of function mutation. Without the NADPH binding event to generate electron transfer, the protein will depend on photoactivation to produce NO, removing the necessity of a chemical substrate and reducing signal interference.

Chapter 2 Materials and Methods

2.1 Materials and apparatus

Sigma-Aldrich: DAF-2 DA, DAPI, Rhodamine Phalloidin, Nafion 117, NiTSPc, NaOH, $CuCl_2$, Kanamycin,

NaCl, Bacto Peptone, EDTA, L-NNA, L-NMMA, 7NI

Syngene: UV-Transilluminator

Riedel de Haen: HCl

Nanodrop: Spectrophotometer for DNA sample concentration detection

Labconco: Refrigerated Centrivap Concentrator

Jennway: pH meter

ATCC: CHO-K1 cell line, pEX_EF1_CFP-NOS3 plasmid

Addgene: pBABE-TetCMV-puro-mVenus-LOV plasmid

Ascent Scientific: SNAP

Promega: DNTP's

Fermentas: EcoRI, Buffer B Pink

Epicenter: T5 exonuclease

NEB: Phusion Polymerase, Phusion buffer, Taq Polymerase, Taq buffer, HpaI, NheI, AccI, NotI. T4 DNA ligase

Invitrogen: Opti-MEM media, Lipofectamine LTX with Plus Reagent

Fisherbrand: Pipettes, Pipette Boy, Gloves.

Eppendorf: Universal tubes (1.5 mL)

Greiner Bio-One: 50 mL Falcon tubes.

ITDNA: Primers

Major Science: Potentiostat for electrophoresis.

Biometra: Tanks used for electrophoresis.

BD Biosciences: FACSCANTO II flow cytometer

Leica: Fluorescence Microscope

BASi: Platinum Electrode, Aluminium oxide slurry, Silver/Silver Chloride electrode, microcloth polishing pad

Ivium: Ivium Compactstat potentiostat

Gibco: HBSS, PBS, DMEM, Penicillin Streptomycin, Glutamate, Trypsin

2.2 Cell Handling

2.2.1 Medium

In order to ensure replication and survival cells require specific nutrients within the growth environment, however the exact requirements for favourable growth and division differ between organisms and cell types. For mammalian cells such as *CHO-K1*, commercially available DMEM medium supplemented with 10% FCS, 1% glutamate and 1% penicillin streptomycin was used.

To obtain an agar gel for bacterial plates, 2% agar is added to the mixture prior to the autoclaving step. It is important not to let the gel set before plating occurs. When adding antibiotics to screen for resistance (selective markers), these should be added after the solution has reached a temperature of less than 60 °C. SOB medium is a nutrient rich broth used to grow bacteria after cell damaging processes such as electroporation. 1 L of SOB is prepared from bacto-tryptone (30 g), bacterial yeast extract (5 g), NaCl (0.5 g) and KCl (2.5 mL, 1M) with the remaining volume (up to 1L) composed of ultrapure water.(S. J. Lee et al., 2000) The media is autoclaved prior to use. LB medium is widely used to culture bacteria such as *E.coli* and is composed of tryptone (10 g), yeast extract (5 g) and NaCl (10 g) to which water (800 mL) is added and the volume topped up to 1 L. The solution must be autoclaved before use.(Anderson, 1946)

2.2.2 Strains and Cell Lines

Mammalian cells (Chinese Hamster Ovary cell, K1 strain) were purchased from ATCC, USA. For the purposes of this project, only two strains of micro-organism were required:

- *E.coli* TOP 10, a strain of *E.coli* with reduced infectivity (generously donated by the Chris Voigt Laboratory, UCSF, USA).
- JM109 cells, a strain of *E.coli* with reduced infectivity and high transformation efficiency. Obtained from promega.

2.2.3 Master Colonies

Plate grown bacterial cells were selected and removed using a toothpick. The toothpick was placed in a vial containing growth medium (10 mL, LB) and cells left to

grow overnight to an OD600 of 3-6 followed by centrifugation at 3700 rpm for 10 minutes. Supernatant was removed and fresh medium added along with glycerol to a total concentration of 20-30% of solution. The sample was then placed in a cryotube and stored in a freezer at -80 °C.

Mammalian *CHO-K1* cells were grown in DMEM supplemented with 10% FCS and 1% penicillin streptomycin and 1% Glutamate and incubated at 37 °C and 5% CO_2 to a confluency of approximately 80%. Cells were washed in PBS/HBSS (2 mL) to remove serum and phenol red and then underwent trypsin treatment to detach adhered cells. This was achieved using a 1:1 ratio of trypsin and PBS/HBSS and centrifuged (1400 rpm) to form a pellet which was resuspended in DMEM supplemented with 20% FCS and 7.5% DMSO. The cell suspension was then placed into appropriate cryotubes which were inserted to an isopropanol "nest" and stored at -80 °C for 2-3 days followed by subsequent storage in liquid nitrogen until required.

2.2.4 Transfection of CHO-K1 Cells

Mammalian cells cannot undergo the transformation procedures endured by bacterial or yeast cells due to their intricate nature, therefore a different method must be undertaken to successfully transfect these cell lines with the plasmid of interest. One of the more efficient methods of transfecting mammalian cells is Lipofection, whereby the plasmid of interest is encased in liposomes which then fuse to the cell membrane encouraging uptake of the plasmid DNA by the cells. Transfection was carried out according to the following protocol. The day prior to transfection, cells were trypsinized, counted and plated in a 24-well plate at a concentration of 4×10^4 cells per 0.5 mL of growth medium. Cell density at the time of transfection was targeted at 50-80% confluency. A solution of plasmid DNA (0.5 μg, 100 ng/μL per well) was prepared in Opti-MEM reduced Serum media (100 μL, Invitrogen, UK) with no extra serum added. The solution was then treated with Lipofectamine LTX (1.5 μL) per well and the resulting mixture incubated for 25 minutes at room temperature to allow the formation of DNA-Lipofectamine LTX complexes. Old media was removed from the cells and replaced with fresh growth medium. Each well containing cells was then treated directly with the DNA-Lipofectamine LTX complex solution (100 μL) and mixed by gentle rocking of the plate back and forth. Cells were then incubated for 24 hours at 37 ºC at 5% CO_2 prior to addition of marker antibiotic.

The incubation period described in the final step is necessary to allow expression of the antibiotic resistance conferred by the plasmid of interest, which is essential to the formation of "stable" expression lines. In the majority of cases the plasmid of interest will be non-essential and display transient expression with the plasmid dropping out of cell culture over time, with subsequent loss of gene expression. It is therefore desirable for plasmids to contain antibiotic resistance to ensure their continued presence within transfected cell lines.

2.2.5 CHO-K1 Geneticin Kill Curve

In order to confirm the presence of the correct DNA sequences in transformed cells, transformed cell lines were subjected to a geneticin (G418) kill curve. Transformed and untransformed cells were grown in a 24 well plate with 1 mL medium containing the following G418 concentrations: 5 mg/mL, 1 mg/mL, 0.8 mg/mL and 0.4 mg/mL. Due to the highly variable concentrations demonstrated in literature for the G418 dosage of cells and the acting mechanism of G418, it was necessary to construct a kill curve specific to the cell line of interest. Cells were then left to grow for 1 week, medium changed every 3 days (maintaining the antibiotic concentration between changes) and following this course of antibiotics the wells were observed under a microscope. The aim of these experiments was to determine the concentration of G418 necessary to kill untransfected cells whilst maintaining the viability of transformed cells.

2.2.6 Staining with DAF-2 DA

DAF-2 DA allows for fluorescent staining of nitric oxide in cells. The staining agent is cell-wall permeable and allows visualization of localized nitric oxide production within the cell using fluorescent microscopy. Like many fluorescent staining agents, DAF-2 DA is extremely light sensitive and all work with DAF-2 DA was conducted in low-light environments. Cell staining was carried out according to the following protocol. The day prior to staining, cells were trypsinized and counted. Cells were plated in a 6-well plate containing a coverslip at a concentration of 4×10^4 cells per 0.5 mL of growth medium. Cells were then incubated at 37 ºC at 5% CO_2 overnight. Cells were washed with PBS prior to staining to remove BSA, phenol red or any such compounds present in media which could interfere with the fluorescent dye. A working solution of DAF-2 DA was achieved *via* dilution. PBS was removed and 1 mL of the

diluted DAF-2 DA solution added. Cells in the staining solution were then incubated at room temperature for 30-40 minutes. The solution was then aspirated and the sample washed with PBS to remove excess fluorophore. Samples were kept in PBS after the wash in the previous step until required for imaging which was performed immediately after staining due to the lack of the paraformaldehyde fixing step. The coverslip was removed using tweezers and then placed on a microscope slide, sample side facing downwards and imaged under a fluorescent microscope.

2.2.7 Staining with Rhodamine Phalloidin/DAPI

Rhodamine phalloidin is a fluorescent compound which binds to the actin cytoskeleton in cells. This allows visualization of the cell structure and facilitates observation of factors such as differentiation and adhesion. DAPI is a fluorescent staining agent which binds to the nucleus of cells, allowing visualization of the nucleus including such events as mitosis. Staining with fluorescent compounds was carried out according to the following protocol. The day prior to staining, cells were trypsinized and counted. Cells were plated in a 6-well plate containing a coverslip at a concentration of 4×10^4 cells per 0.5 mL of growth medium. Cells were then incubated at 37 ºC at 5% CO_2 overnight. Cells were washed with PBS prior to fixing to remove BSA, phenol red or any such compounds present in media which could interfere with the fluorescent dye. 4% paraformaldehyde (1 mL) was then added to the cells and left to incubate at room temperature for 15 minutes. The sample was then washed three times using PBS to remove any excess paraformaldehyde. After the final PBS washings were removed, fresh PBS (1 mL) was added to each well. To this, 2 μL of rhodamine phalloidin (2.5 mg/mL in MeOH) was added and the cells incubated in darkness for 25 minutes. The sample was again washed with PBS to remove any excess staining agent and therefore reduce potential noise levels. The coverslip was removed using tweezers and a drop of DAPI staining agent was placed on the surface of the coverslip containing cells. The coverslip was then placed on a microscope slide, sample side facing downwards and imaged under a fluorescent microscope.

2.3 Flow Cytometry

For the purposes of fluorescence intensity measurements, Flow Cytometry was chosen as the most efficient form of data gathering. Flow cytometry measurements were

taken using an FCS CANTO II cytometer and analysed using the BD FACS DIVA software.

2.3.1 Flow Cytometry Sample Preparation

The day prior to measurement, cells were cultured on a 24 well plate at 1 x 10^5 concentration. Following culture, a 10 μL aliquot of 500 μM inhibitor was added to the cells. Alternatively, for inhibitor/LPF complexes, the same concentration of inhibitors was diluted in 100 μL Opti-MEM medium followed by the addition of 1 μL LPF. The complexes were allowed to form by incubating the sample at room temperature for 20 minutes and then added dropwise to the wells containing cells. Cells were then allowed to grow overnight. Just prior to Flow Cytometry measurement, cells were re-exposed to inhibitors or inhibitor/LPF complexes as described previously. Cells were then allowed to incubate for 20 minutes at 37 °C. Medium was subsequently removed and cells were washed with HBSS buffer. Cells were then trypsonized for 4 minutes at 37 °C in a solution consisting of 10X Trypsin in a 1/1 dilution with HBSS. Fresh DMEM media was then added to the cells to halt the Trypsin reaction and samples were placed in centrifuge tubes. The samples were then spun at 500g for 7 minutes after which media was removed and cells were resuspended in HBSS. Cells were then stained with either DAPI or DAF-2 DA as described in 2.2.6. For some samples, DAPI staining was also used for live/dead screening. To achieve this, 2 μL DAPI dye was added simultaneously to DAF-2 DA to 0.5 mL of cells in HBSS at a concentration of 200 μg,

After a 20 minute incubation period with the fluorescent compounds, cells were centrifuged once again and resuspended in HBSS. Samples were then taken for measurement using Flow Cytometry.

2.4 Mutagenesis and eNOS chimera

In order to create the eNOS reporter for the biosensor, various relevant DNA sequences were obtained and combined so as to create two individual systems capable of producing nitric oxide in response to stimuli. The DNA used in engineering experiments was obtained from commercially available plasmids.

2.4.1 Plasmids, Sequences and Primers.

Primers are short sequences of single stranded DNA. These are used in the polymerase chain reaction to select the region of augmented amplification. Many points must be addressed when designing primers. Sequence length should be in multiples of 3 and have a melting point low enough to allow successful PCR. Possible secondary structure melting point must also be addressed when planning the annealing cycle of PCR. These sequences share a high homology with the target sequence and thereby create a point of origin for the sequential addition of bases to the daughter strand of DNA.

Plasmids used in this study include:

- pEX_EF1_NOS3-CFP - Purchased from ATCC
- FKBP-(GGGGS)x2-N-TEV - Generously donated by Chris Voigt Group
- Frb-C-TEV - Generously donated by Chris Voigt Group
- pBABE-TetCMV-puro-mVenus-LOV - Purchased from Addgene Inc.

Plasmid pEX_EF1_NOS3-CFP contains the NOS3 (endothelial nitric oxide synthase) gene and was used throughout this work relating to the genetic engineering of eNOS. Plasmid FKBP-(GGGGS)x2-N-TEV contains the FKBP12 fragment used to form the rapamycin CID system used for chemical activation of eNOS. Plasmid Frb-C-TEV contains the Frb region of the FRAP protein used in conjunction with FKBP12 as part of the rapamycin CID system for chemical activation of eNOS. Plasmid pBABE-TetCMV-puro-mVenus-LOV contains both LOV1 and LOV2 domains, used to create the light-sensitive eNOS.

Plasmid pEX_EF1_NOS3-CFP contains the eNOS gene, the sequence for which is given in Sequence 1. The sequence is divided into the oxygenase and reductase domains of the protein. The two domains were separated into two different fragments using PCR and the primers used are also given in Sequence 1.

Sequence 1 Sequence of the eNOS gene and primers used to separate the oxygenase and reductase domains.

Oxygenase:

5' Primer: CAACAAGTTTGTACAAAAAAGCAGGCTCCG

3' Primer: GACCTTTAAGGAAGTAGCCAATGCAGTGAA

Reductase:

5' Primer: AAGGGGGCAGGCATCACCAGGAAG

3' Primer: GATCAACCACTTTGTACAAGAAAGCTGGGT

Forward FUB NEW: TTCAAGGGAAGGGGGCAGGCATCACCA

Reverse FUB NEW: TGCCCCCTTCCCTTGAAAAGGCTCTCG

For the FKBP12 fragment, the FKBP-(GGGGS)x2-N-TEV plasmid was used. The Sequence of the fragment and the primers used to extract and amplify it are given in Sequence 2

Sequence 2 Sequence of the FKBP12 fragment and primers used in amplification. Blue: FKBP12. Green: Gly/Ser linker.

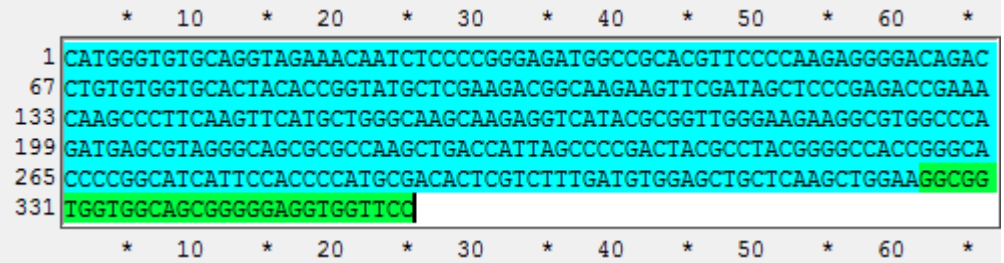

5' Primer: GCCACCATGGGTGTGCAGGTAGAAACAATC

3' Primer: CCACCACCGTCGCCCCCTCCACCAAGGCCG

The Frb-CTEV plasmid was used to obtain the second protein involved in the Rapamycin CID system. The Frb fragment and the primers used in PCR are given in Sequence 3.

Sequence 3 Sequence of the Frb fragment and primers used in amplification. Blue: FKBP12. Green: Gly/Ser linker.

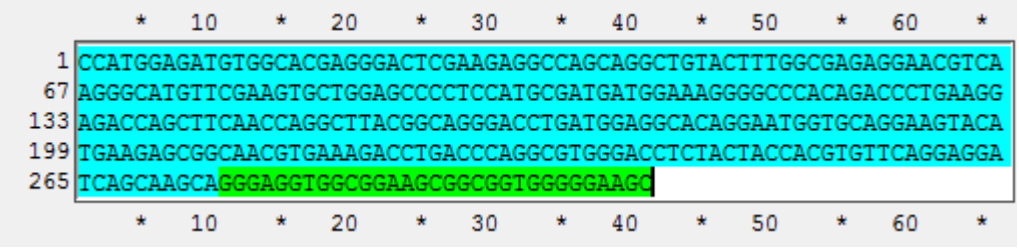

5' Primer: GCCCACCATGGAGATGTGGCACGA

3' Primer: GGTATCAGAGACCATGCTGCTCATGGA

To produce the fragment necessary for fusion into the novel chimeric eNOS, fragments must be prepared for Gibson ligation protocol. The fragments must undergo PCR with primers that elongate the sequence so as to create a region of homology approximately 20 base pairs in length. This is necessary as the T5 exonuclease activity will then digest the sequences and a region of complementary homogeneity is necessary for the T4 ligase to re-ligate digested sequences. Primary (eNOS) fragments were obtained from plasmid pEX_EF1_NOS3-CFP. Secondary fragments (FKBP12 and Frb) were obtained from plasmids FKBP-(GGGGS)x2-N-TEV and Frb-C-TEV. The primers used in PCR are given in Sequence 4 along with the expected sequence for oxygenase/Frb and reductase/FKBP12 domains. Green represents the eNOS sequence and red the Frb sequence. Theoretically, in the presence of rapamycin the protein resulting from the chimeric sequences described in Sequence 4 would be brought within sufficient proximity to each other to allow the oxygenase/reductase domains to interact and therefore restore function to the inactive protein. Primers used in oxygenase/Frb and reductase/FKBP12 fusion and expected resulting sequences:

Sequence 4 Sequence of the oxygenase/Frb fragment and primers used. Blue: FKBP12, Green: Gly/Ser linker Orange: eNOS gene.

For Oxygenase/Frb fusion:
5' Primer: TAGCCAATGCAGTGAAGCCCAATGCCATGGAGA
3' Primer: TCGTGCCACATCTCCATGGCATTGGGCTTCACT

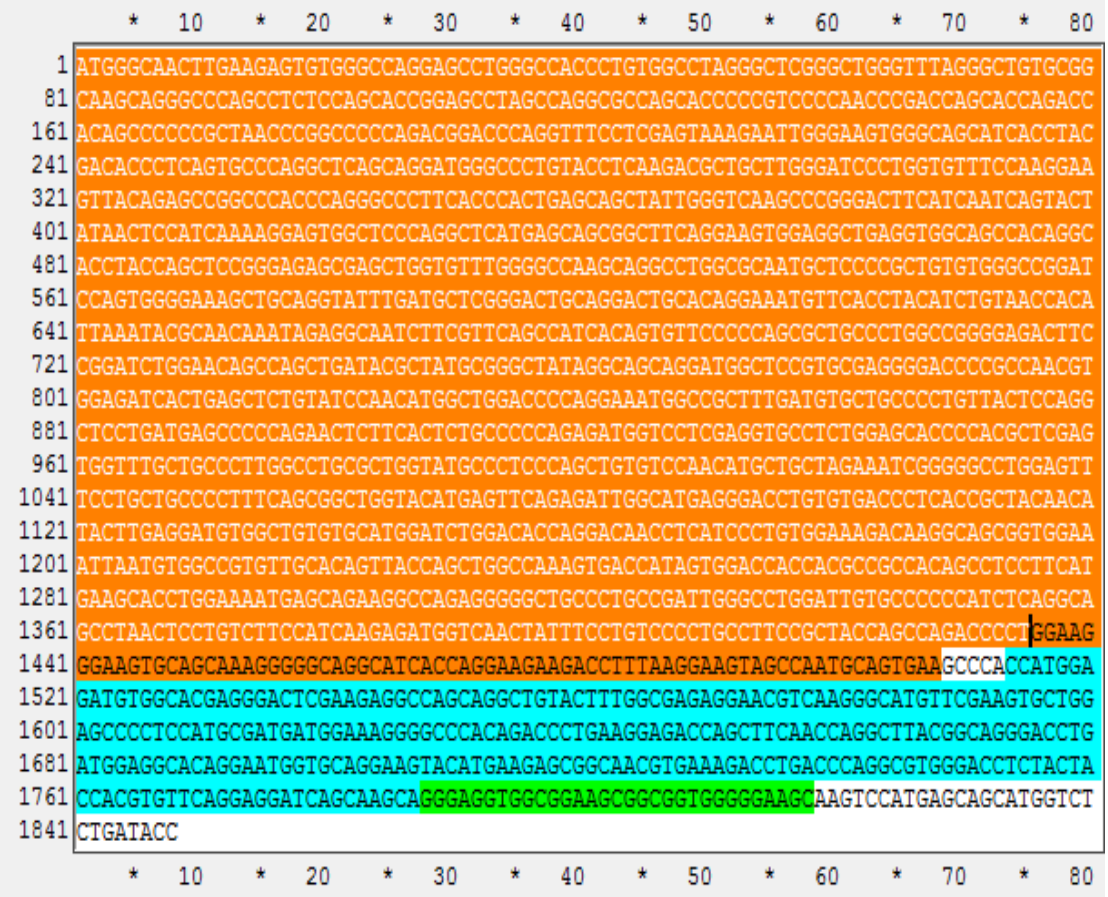

Sequence 5 Sequence of the reductase/FKBP12 fragment and primers used. Blue: FKBP12, Green: Gly/Ser linker Orange: eNOS gene.

For Reductase/FKBP12 fusion:

5' Primer: TTCAAGGGAAGGGGGCAGGCATCACCA

3' Primer: TGCCCCCTTCCCTTGAAAAGGCTCTCG

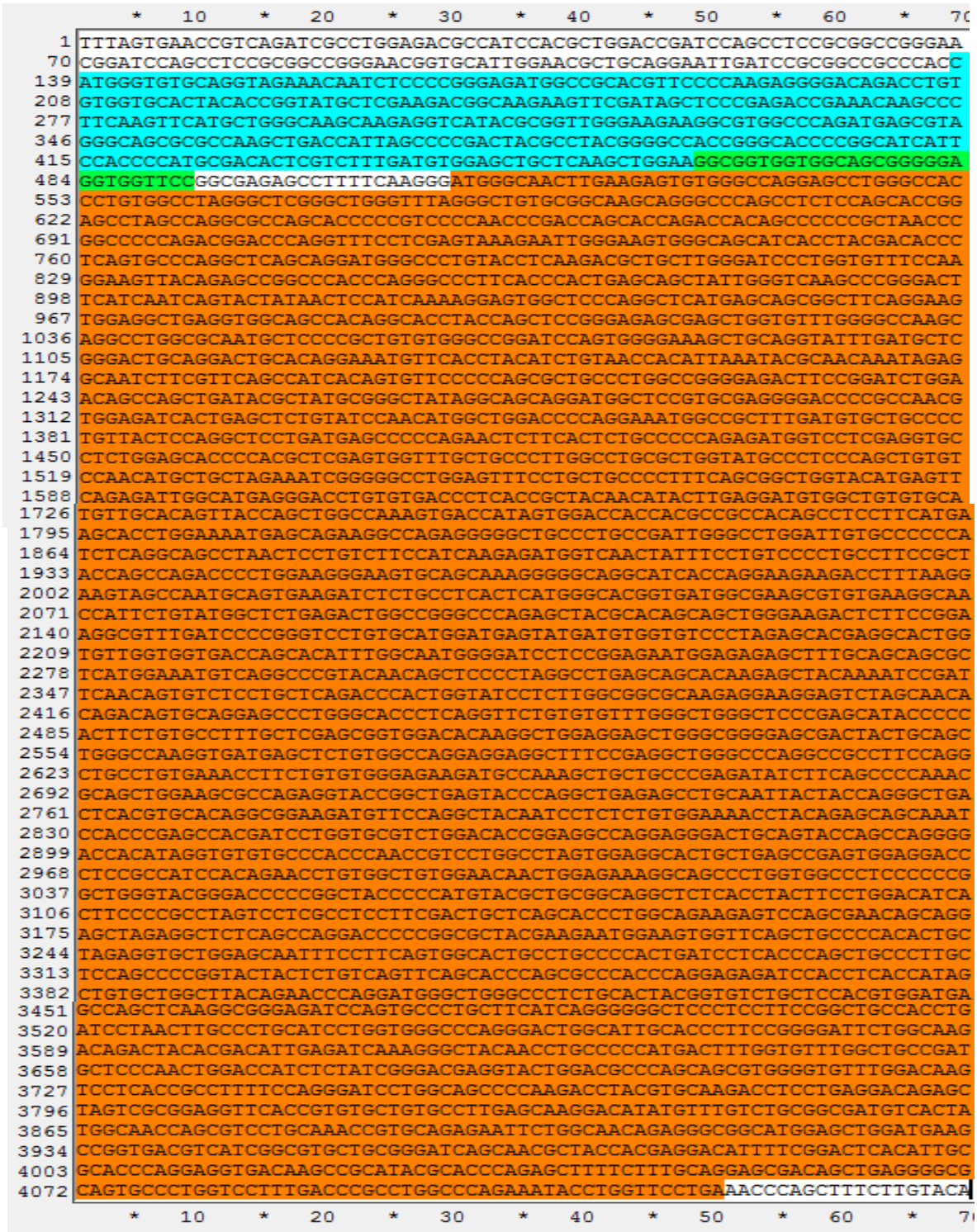

To produce the light sensitive mutant strain of eNOS, the eNOS protein was separated at three different points close to FMN binding domains. The region of the eNOS gene that binds eNOS is given in Sequence 6.

Sequence 6 The FMN binding region of eNOS.

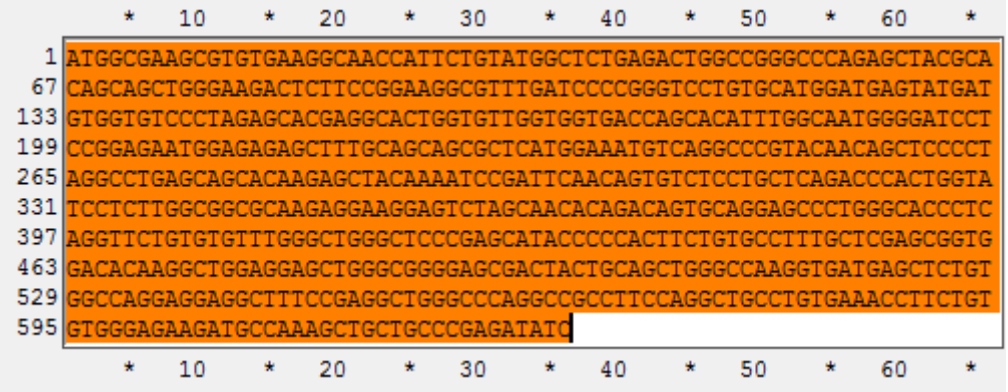

Three segments were obtained using the 5' primer of the oxygenase domain of eNOS and the 3' primers a, b and c, resulting in sequences 7 a, b and c, respectively.

Sequence 7 Primers used to construct sequences a, b and c.

a. 3' - ATACAGAATGGTTGCCTTCACACGCTT
b. 3' - GCCAAGAGGATACCAGTGGGTCTGAGC
c. 3' - CAGCTTTGGCATCTTCTCCCACACAGA

a:

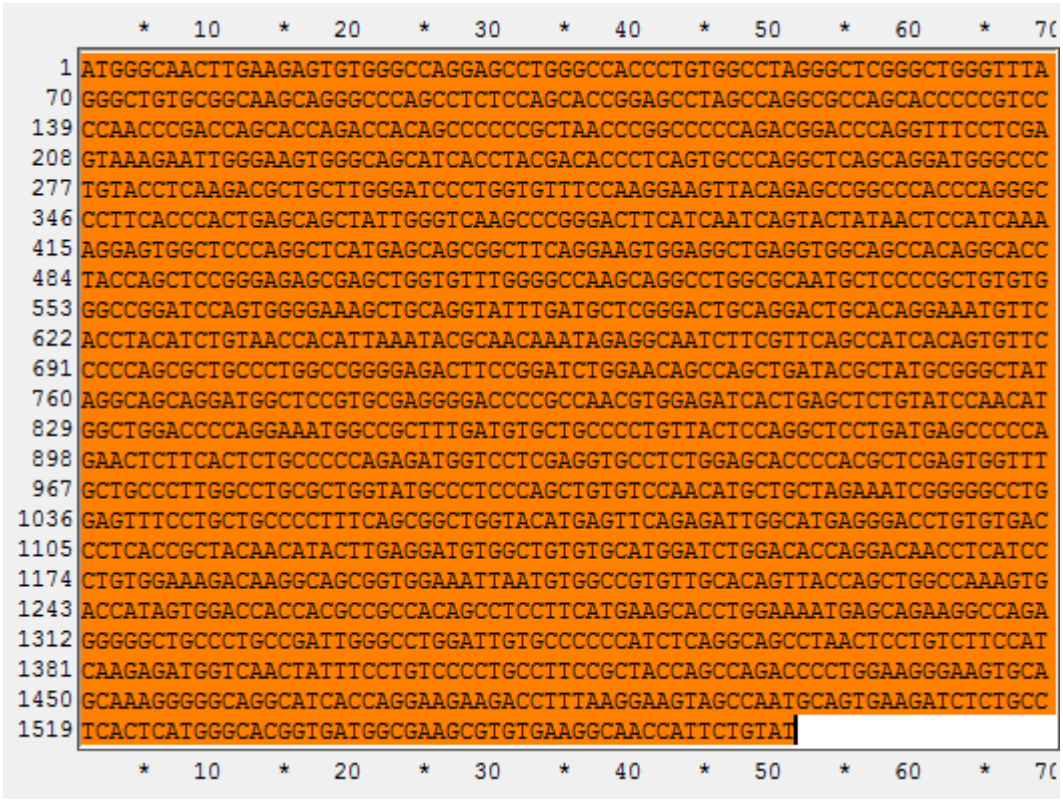
* 10 * 20 * 30 * 40 * 50 * 60 * 70
1 ATGGGCAACTTGAAGAGTGTGGGCCAGGAGCCTGGGCCACCCTGTGGCCTAGGGCTCGGGCTGGGTTTA
70 GGGCTGTGCGGCAAGCAGGGCCCAGCCTCTCCAGCACCGGAGCCTAGCCAGGCGCCAGCACCCCCGTCC
139 CCAACCCGACCAGCACCAGACCACAGCCCCCCGCTAACCCGGCCCCCAGACGGACCCAGGTTTCCTCGA
208 GTAAAGAATTGGGAAGTGGGCAGCATCACCTACGACACCCTCAGTGCCCAGGCTCAGCAGGATGGGCCC
277 TGTACCTCAAGACGCTGCTTGGGATCCCTGGTGTTTCCAAGGAAGTTACAGAGCCGGCCCACCCAGGGC
346 CCTTCACCCACTGAGCAGCTATTGGGTCAAGCCCGGGACTTCATCAATCAGTACTATAACTCCATCAAA
415 AGGAGTGGCTCCCAGGCTCATGAGCAGCGGCTTCAGGAAGTGGAGGCTGAGGTGGCAGCCACAGGCACC
484 TACCAGCTCCGGGAGAGCGAGCTGGTGTTTGGGGCCAAGCAGGCCTGGCGCAATGCTCCCCGCTGTGTG
553 GGCCGGATCCAGTGGGGAAAGCTGCAGGTATTTGATGCTCGGGACTGCAGGACTGCACAGGAAATGTTC
622 ACCTACATCTGTAACCACATTAAATACGCAACAAATAGAGGCAATCTTCGTTCAGCCATCACAGTGTTC
691 CCCCAGCGCTGCCCTGGCCGGGGAGACTTCCGGATCTGGAACAGCCAGCTGATACGCTATGCGGGCTAT
760 AGGCAGCAGGATGGCTCCGTGCGAGGGGACCCCGCCAACGTGGAGATCACTGAGCTCTGTATCCAACAT
829 GGCTGGACCCCAGGAAATGGCCGCTTTGATGTGCTGCCCCTGTTACTCCAGGCTCCTGATGAGCCCCCA
898 GAACTCTTCACTCTGCCCCCAGAGATGGTCCTCGAGGTGCCTCTGGAGCACCCCACGCTCGAGTGGTTT
967 GCTGCCCTTGGCCTGCGCTGGTATGCCCTCCCAGCTGTGTCCAACATGCTGCTAGAAATCGGGGGCCTG
1036 GAGTTTCCTGCTGCCCCTTTCAGCGGCTGGTACATGAGTTCAGAGATTGGCATGAGGGACCTGTGTGAC
1105 CCTCACCGCTACAACATACTTGAGGATGTGGCTGTGTGCATGGATCTGGACACCAGGACAACCTCATCC
1174 CTGTGGAAAGACAAGGCAGCGGTGGAAATTAATGTGGCCGTGTTGCACAGTTACCAGCTGGCCAAAGTG
1243 ACCATAGTGGACCACCACGCCGCCACAGCCTCCTTCATGAAGCACCTGGAAAATGAGCAGAAGGCCAGA
1312 GGGGGCTGCCCTGCCGATTGGGCCTGGATTGTGCCCCCCATCTCAGGCAGCCTAACTCCTGTCTTCCAT
1381 CAAGAGATGGTCAACTATTTCCTGTCCCCTGCCTTCCGCTACCAGCCAGACCCCTGGAAGGGAAGTGCA
1450 GCAAAGGGGGCAGGCATCACCAGGAAGAAGACCTTTAAGGAAGTAGCCAATGCAGTGAAGATCTCTGCC
1519 TCACTCATGGGCACGGTGATGGCGAAGCGTGTGAAGGCAACCATTCTGTAT
* 10 * 20 * 30 * 40 * 50 * 60 * 70

b:

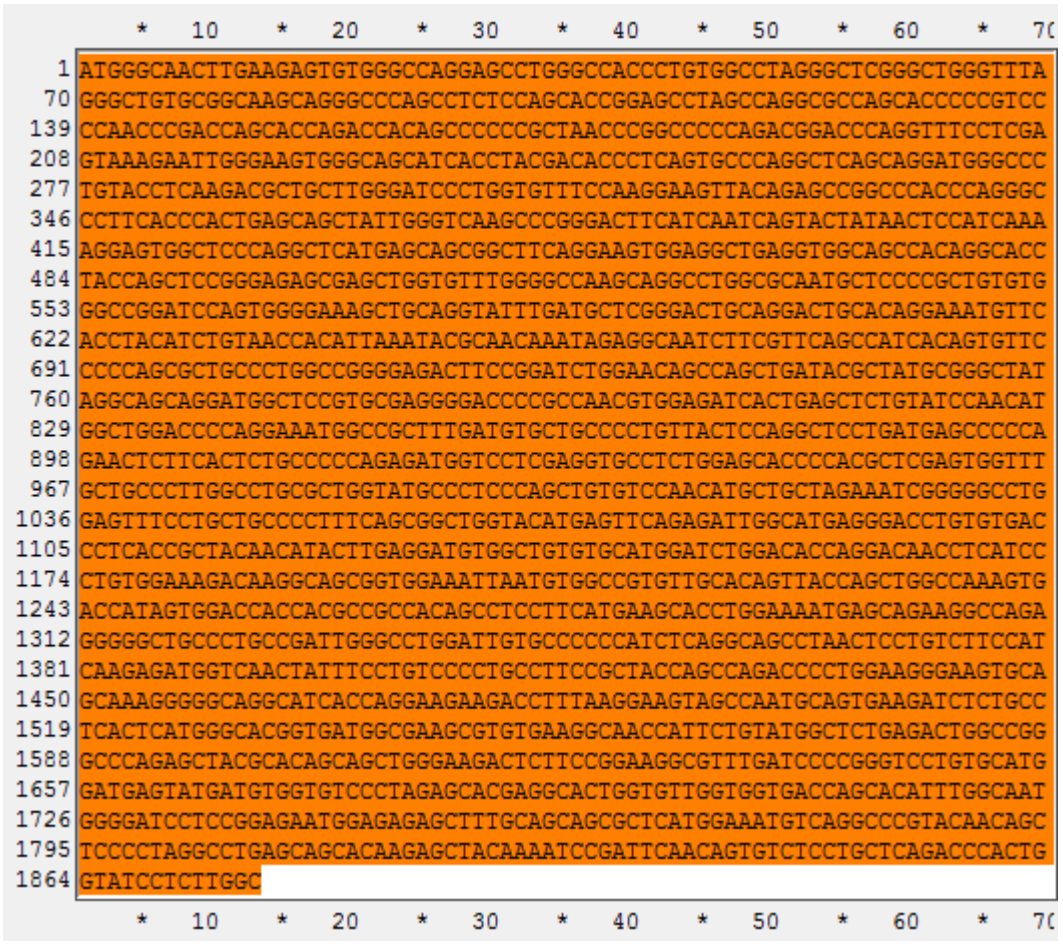
* 10 * 20 * 30 * 40 * 50 * 60 * 70
1 ATGGGCAACTTGAAGAGTGTGGGCCAGGAGCCTGGGCCACCCTGTGGCCTAGGGCTCGGGCTGGGTTTA
70 GGGCTGTGCGGCAAGCAGGGCCCAGCCTCTCCAGCACCGGAGCCTAGCCAGGCGCCAGCACCCCCGTCC
139 CCAACCCGACCAGCACCAGACCACAGCCCCCCGCTAACCCGGCCCCCAGACGGACCCAGGTTTCCTCGA
208 GTAAAGAATTGGGAAGTGGGCAGCATCACCTACGACACCCTCAGTGCCCAGGCTCAGCAGGATGGGCCC
277 TGTACCTCAAGACGCTGCTTGGGATCCCTGGTGTTTCCAAGGAAGTTACAGAGCCGGCCCACCCAGGGC
346 CCTTCACCCACTGAGCAGCTATTGGGTCAAGCCCGGGACTTCATCAATCAGTACTATAACTCCATCAAA
415 AGGAGTGGCTCCCAGGCTCATGAGCAGCGGCTTCAGGAAGTGGAGGCTGAGGTGGCAGCCACAGGCACC
484 TACCAGCTCCGGGAGAGCGAGCTGGTGTTTGGGGCCAAGCAGGCCTGGCGCAATGCTCCCCGCTGTGTG
553 GGCCGGATCCAGTGGGGAAAGCTGCAGGTATTTGATGCTCGGGACTGCAGGACTGCACAGGAAATGTTC
622 ACCTACATCTGTAACCACATTAAATACGCAACAAATAGAGGCAATCTTCGTTCAGCCATCACAGTGTTC
691 CCCCAGCGCTGCCCTGGCCGGGGAGACTTCCGGATCTGGAACAGCCAGCTGATACGCTATGCGGGCTAT
760 AGGCAGCAGGATGGCTCCGTGCGAGGGGACCCCGCCAACGTGGAGATCACTGAGCTCTGTATCCAACAT
829 GGCTGGACCCCAGGAAATGGCCGCTTTGATGTGCTGCCCCTGTTACTCCAGGCTCCTGATGAGCCCCCA
898 GAACTCTTCACTCTGCCCCCAGAGATGGTCCTCGAGGTGCCTCTGGAGCACCCCACGCTCGAGTGGTTT
967 GCTGCCCTTGGCCTGCGCTGGTATGCCCTCCCAGCTGTGTCCAACATGCTGCTAGAAATCGGGGGCCTG
1036 GAGTTTCCTGCTGCCCCTTTCAGCGGCTGGTACATGAGTTCAGAGATTGGCATGAGGGACCTGTGTGAC
1105 CCTCACCGCTACAACATACTTGAGGATGTGGCTGTGTGCATGGATCTGGACACCAGGACAACCTCATCC
1174 CTGTGGAAAGACAAGGCAGCGGTGGAAATTAATGTGGCCGTGTTGCACAGTTACCAGCTGGCCAAAGTG
1243 ACCATAGTGGACCACCACGCCGCCACAGCCTCCTTCATGAAGCACCTGGAAAATGAGCAGAAGGCCAGA
1312 GGGGGCTGCCCTGCCGATTGGGCCTGGATTGTGCCCCCCATCTCAGGCAGCCTAACTCCTGTCTTCCAT
1381 CAAGAGATGGTCAACTATTTCCTGTCCCCTGCCTTCCGCTACCAGCCAGACCCCTGGAAGGGAAGTGCA
1450 GCAAAGGGGGCAGGCATCACCAGGAAGAAGACCTTTAAGGAAGTAGCCAATGCAGTGAAGATCTCTGCC
1519 TCACTCATGGGCACGGTGATGGCGAAGCGTGTGAAGGCAACCATTCTGTATGGCTCTGAGACTGGCCGG
1588 GCCCAGAGCTACGCACAGCAGCTGGGAAGACTCTTCCGGAAGGCGTTTGATCCCCGGGTCCTGTGCATG
1657 GATGAGTATGATGTGGTGTCCCTAGAGCACGAGGCACTGGTGTTGGTGGTGACCAGCACATTTGGCAAT
1726 GGGGATCCTCCGGAGAATGGAGAGAGCTTTGCAGCAGCGCTCATGGAAATGTCAGGCCCGTACAACAGC
1795 TCCCCTAGGCCTGAGCAGCACAAGAGCTACAAAATCCGATTCAACAGTGTCTCCTGCTCAGACCCACTG
1864 GTATCCTCTTGGC
* 10 * 20 * 30 * 40 * 50 * 60 * 70

c:

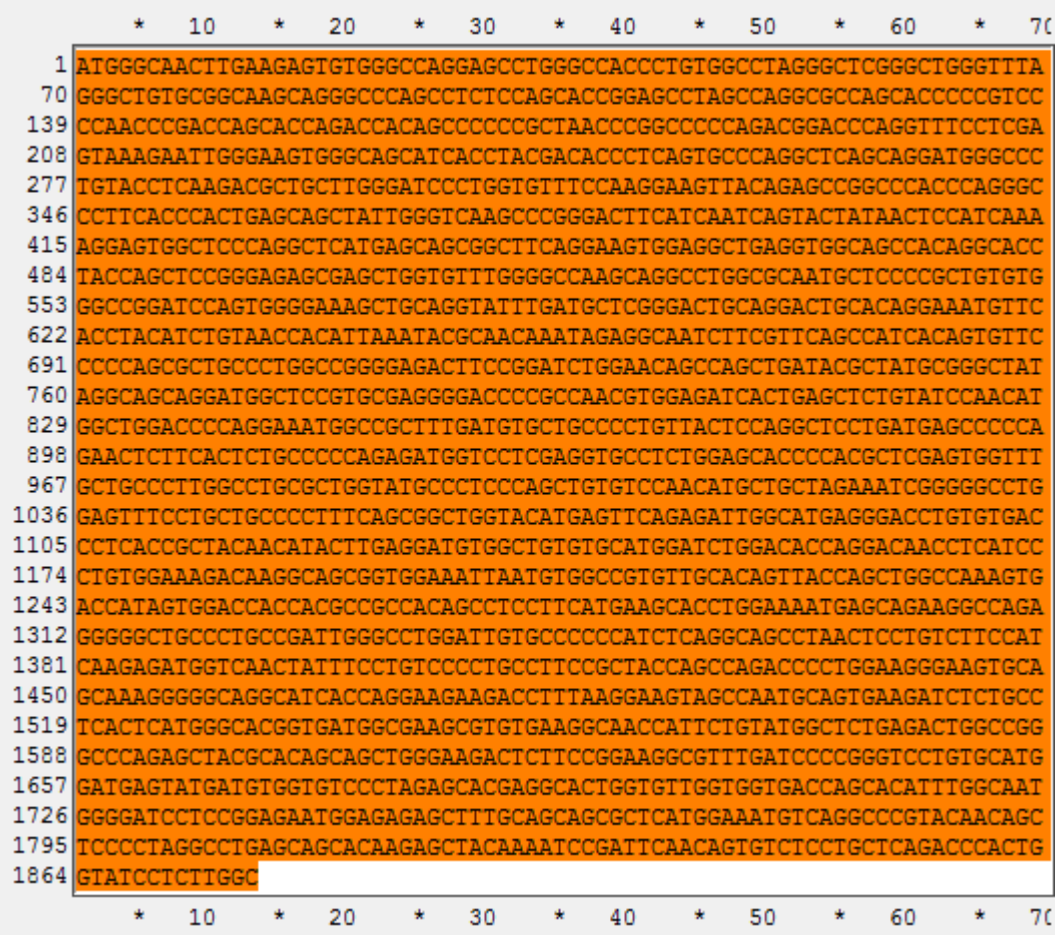

To construct the complementary fusion fragment, the plasmid pBABE-TetCMV-puro-mVenus-LOV was used to obtain the DNA for the LOV domain, the sequence for which is given in Sequence 8. The aim was to then fuse the created segments which terminate in different areas of the FMN binding domain of eNOS to LOV1/2 domains to create the light sensitive mutant.

Sequence 8 Sequence of the LOV domain.

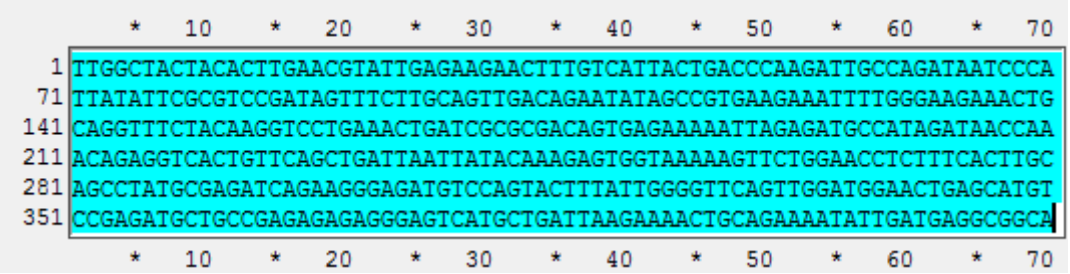

2.4.2 Electroporation

Electroporation is an effective method of transforming competent cells using appropriate plasmids in bacteria. It uses sonication to induce an increase in membrane porosity which increases transformation efficiency. The technique requires placing all the reagents on ice to achieve isothermal conditions. Cells are made competent by growing a colony to OD600 0.6 (+/- 0.2) and then stopping growth by placing the cells on ice for 1-2 minutes. Cells are then spun at 5000 rpm for 3 minutes and supernatant is removed. The cells are then resuspended in 10% glycerol and the spin/resuspend cycle is repeated twice. The sample is centrifuged one last time and the pellet is transferred to a falcon tube at 4 °C. The cells are then aliquoted for immediate use or placed in a freezer at -80 °C for storage. To transform these competent cells, electroporation was used. The competent cells are placed on ice together with the other reagents. After isothermal conditions have been achieved, 70 μL of cells are added to a cuvette along with 2-10 μL DNA (*i.e.* plasmid DNA). The lower the amount of DNA the safer the outcome as if there is too much salt in the solution (originating from the DNA buffer) the cells will die during electroporation, an event termed “sparking”. The cuvette is placed in the electroporator and the device turned on. The time constant value should be higher than 3.5 as a value lower than 2 signifies a sparking event. After electroporation is complete, SOB medium (1 mL) is added to the cuvette and the cells are incubated for 1 hour at optimum temperature (which varies according to the cells/genes used) for recovery. The incubation step is only necessary when the cells are to be grown in/on antibiotic medium, as it takes the cells time from plasmid takeup to express the necessary proteins to confer antibiotic resistance. After the incubation step, cells are plated on appropriate medium. The protocol described is applicable to bacteria such as *E.coli*.

2.4.3 Miniprep

The purpose of this technique is to extract plasmid DNA from bacteria. As the plasmid is a small piece of circular DNA, when the cells are lyzed in steps, the plasmid DNA remains in supernatant. This is cleaned and extracted and the resulting plasmid DNA can be cut by restriction enzymes and run on a gel to check whether the correct DNA was extracted using the miniprep.

The technique was performed using the Qiagen Miniprep Kit. Cells were spun down from a culture at 4000 rpm and the supernatant was removed. The resulting pellet was

resuspended in P1 buffer (250 μL). This was mixed by pippetting and transferred to a 1.5 mL eppendorf tube, followed by the addition of P2 buffer (250 μL). The solution was gently mixed by inversion until no clumps remain visible. Up to a maximum time of 5 minutes is allowed for lysis to occur, otherwise DNA damage is possible. N3 buffer (350 μL) was then added to the solution and this was mixed by gentle inversion, whereupon large amounts of precipitate are generated.

The resulting mixture was centrifuged at 13,200 rpm for 10 minutes and the supernatant was gently captured and placed in a flow column. The column was centrifuged at 13,200 rpm for 30 seconds and the flow-through was discarded. This was followed by the addition of PB (500 μL) and a repeat of the previous spin cycle. After discarding flow-through, PE buffer (750 μL) was added, followed by a repeat of the 13,200 rpm 30 second spin cycle. Flow-through was discarded and the sample was then allowed to run dry at 13,200 rpm for 2 minutes. The column was transferred to a 1.5 mL eppendorf tube and dH_2O (50 μL) was added and the column spun at 13,200 rpm for 30 seconds. The flow-through was reloaded and the previous step repeated to ensure maximum DNA capture. DNA concentration was then verified using NanoDrop spectrophotometry.

2.4.4 Restriction Digest

Restriction Digests are an important technique in molecular biology. These utilize enzymes that recognize specific sites in DNA and cleave the sequence in a specific manner, generating sticky or blunt ends. This allows the construction of recombinant proteins by matching cutting sites in different sequences so that the sticky overhangs match.

For a 50 μL reaction volume, 1 μL of each restriction enzyme is added, as well as 2 μg DNA and 5 μL of appropriate 10 x buffer. The type of buffer used depends on the enzyme, for example AccI requires buffer 4. Ultrapure water is used to raise the volume to 50 μL and the sample is placed in a heating block or water bath at the desired temperature (enzyme specific) for 2-3 hours. The sample is then brought to inactivation temperature (whereby the enzymes are permanently denatured, halting the restriction digest), which varies depending on the proteins used. Some enzymes are not heat inactivated (meaning the temperature required to inactivate the enzyme is high enough to destabilize the DNA). In these cases the sample is run on an agarose gel and subsequently gel extracted to separate the proteins from DNA in solution. The sample

can then be stored at -4 °C until it is needed. It is always recommended to run the results of a restriction digest on a gel to confirm that the obtained fragment number and sizes match those expected.(Stocks, Thorn, & Galton, 1992) It is advisable to use the digested DNA as soon as possible for ligations as the DNA is made substantially more susceptible to damage after digestion.

2.4.5 PCR

PCR is a technique which amplifies desired sections of DNA. It requires the use of forward and reverse primers (small sequences of DNA which are homologous to flanking regions of the DNA of interest) that will selectively amplify DNA. The procedure requires placing all reagents on ice to achieve isothermal conditions. In a 100 μL tube, buffer HF (5 μL) is added, along with each primer (1 μL) and DNA (1-2 μL). To this 10 mM DNTP (1 μL) is added in a 7.5 mM magnesium chloride buffer. Subsequently, Taq polymerase protein (0.5 μL) is then added followed by water to bring the reaction volume to 50 μL. The solution then undergoes a series of thermal cycles leading to denaturation, annealing and extension. Temperature values vary with the type of PCR and the primer sequence. Primers with high GC content tend to have higher melting temperatures, requiring adjustment. PCR with an extended initial 95 °C period can be used to break up cells. A small mixture of cells is added instead of the sample DNA and cells are lyzed by using high temperature and thus release DNA. Primers can then amplify specific regions. This technique is termed "Colony PCR" and is useful as a quick method to confirm the existence of DNA of interest in the bacterial sample.

For PCR containing primers of different melting temperatures, touchdown PCR is applied. This procedure involves cycling of temperatures for primer melting. For example, with primers of melting temperatures 60 and 65 °C, touchdown PCR will entail thirty seconds at 66 °C, thirty seconds at 64 °C, thirty seconds at 62 °C and thirty seconds at 60 °C. This ensures that both primers have melted and annealed to their respective sequences.

2.4.6 Gels

Agarose gels were prepared to differentiate fragments of DNA according to size. A plasmid or section of DNA is selected and then cut with restriction enzymes. If the observed fragment sizes match predicted ones then the correct reactions have occurred.

The agarose concentration of the gel depends on the size of expected fragments of interest. For fragments smaller than 1 Kb a concentration of 2% agarose is used. For fragments between 1 Kb and 5 Kb a varying concentration range of between 1 and 2% is available. Fragments larger than 5 Kb require a gel containing a lower percentage of agarose gel (0.8%). If the concentration is too low, then the gel may melt during electrophoresis.

Gels were prepared in 1 x TAE buffer containing the desired concentration of agarose. This was then microwaved until there were no visible particles and the gel was poured into the mold. After evaporation had ceased, ethidium bromide was added to the setting gel. This hybridizes with DNA and fluoresces under UV light, allowing visualization of DNA fragments which are then compared with a DNA ladder to determine fragment size. Combs are then placed in the gel and it is allowed to cool. The teeth of the comb form the wells into which DNA is introduced. Alternatively, Safeview was used as a replacement for ethidium bromide due to its increased safety. However, Safeview is heat inactivated therefore it must be added when the gel is cooled to below 65 °C. Once the gel had hardened it was placed in an electrophoresis tank containing TAE buffer. Electricity is subsequently run through the tank (70-130 mV) which causes DNA to translocate based on size/charge separation.(Helling, Goodman, & Boyer, 1974) Once the gel has run through, the desired DNA band can be excised from the gel using a scalpel and the DNA can be removed from the agarose using gel extraction.

2.4.7 Gel Extraction

This procedure consists of initial physical removal of DNA from the gel using a scalpel. A UV lamp should be used to visualize DNA aggregation locations and the cut should be made so as to include the minimum amount of agarose gel possible. The gel is then liquefied by the addition of 1.5 μL of diffusion buffer per 1 mg of gel and exposure of the sample for 30 minutes to a temperature of 50 °C. The sample is then spun at 13,200 rpm for 1 minute and transferred to a filter column. The mixture volume is then determined and 3:1 volume of QG buffer is then added upon which the mixture should turn yellow in colour. The column is placed in an appropriate collector and further spun at 13,200 rpm for 30 seconds. The collector is changed and EB buffer (50 μL) is added to the column, followed by a further 30 second spin at 13,200 rpm. Flow-through is added to the column and left to stand for 1 minute, after which the sample is spun again for 30 seconds and DNA is obtained from the collector.

2.4.8 Conventional Ligation

The aim of ligations is to fuse two sources of DNA which have been digested with the same restriction enzymes. These are commonly carried out using a double digest to allow for control of the orientation of the fragments being ligated. The standard protocol for ligations is:

1 μL DNA (concentration >250 ng/μL)
1 μL T4 ligase
1 μL Ligase Buffer
7 μL dH2O

There are several temperatures at which ligation is permissible, with varied protocols. The approach taken was 22 °C for four hours followed by 4 °C for two hours. DNA which has been ligated to a vector such as a plasmid can subsequently be used directly for host transformation.

Ligations performed for the pTARGET^{TM} system use settings similar to the ones above described, however a different source of T4 ligase and ligase buffer are used as some T4 ligases contain exonuclease activity. In addition, pTARGET^{TM} ligations involved placing the ligation sample at 4°C for twelve to eighteen hours as opposed to the protocol for standard ligations described above.

2.4.9 Gibson Ligation

The aim of the Gibson Ligation is to fuse two different sequences of DNA together. To achieve this, both DNA fragments must be pre-modified to contain overlapping ends complimentary to each other. To prepare the sequences for Gibson Ligation of fragments A and B, primers must be designed so as to create an overlap between the two sequences. The primers should be designed so that PCR of fragment A will result in an end product containing at the 3' end the first 20 bases of fragment B. The PCR of fragment B should result in a sequence containing the last 20 bases of fragment A at the 5' end of the sequence. The PCR of the two fragments thus creates a 40 bp region of overlap between the two genes.(Gibson *et al*., 2009)

Gibson Ligation one step isothermal reaction master mix (giving a final volume of 6 mL):

3 mL 1 M Tris-HCL pH 7.5
150 µL 2 M $MgCl_2$
60 µL 100 mM dGTP
60 µL 100 mM dCTP
60 µL 100 mM dATP
60 µL 100 mM dTTP
300 µL 1 M DTT
1.5 g PEG 8000
300 µL 100 mM NAD

Final reaction mix with final volume of 1.2 mL:

320 µL of master mix
0.64 µL T5 exonuclease
20 µL 2U phusion polymerase
160 µL 40U Taq DNA ligase
699.46 µL of dH2O

For the reaction carried out, the DNA to be assembled (5 µL) was added in equimolar amounts to 15 µL of the final reaction mix and incubated for sixty minutes at 50 °C. This reaction results in the formation of a novel sequence combining the fragments in question to create a chimeric gene, which when expressed in the appropriate vector will create the designed protein.

2.5 Measurement System Setup

Once mutant strains of *CHO-K1* were achieved, an electrode setup was prepared to measure NO output from chimeric eNOS. Amperometric measurements were performed using a modified Pt working electrode and an Ag/AgCl combined reference and counter electrode.

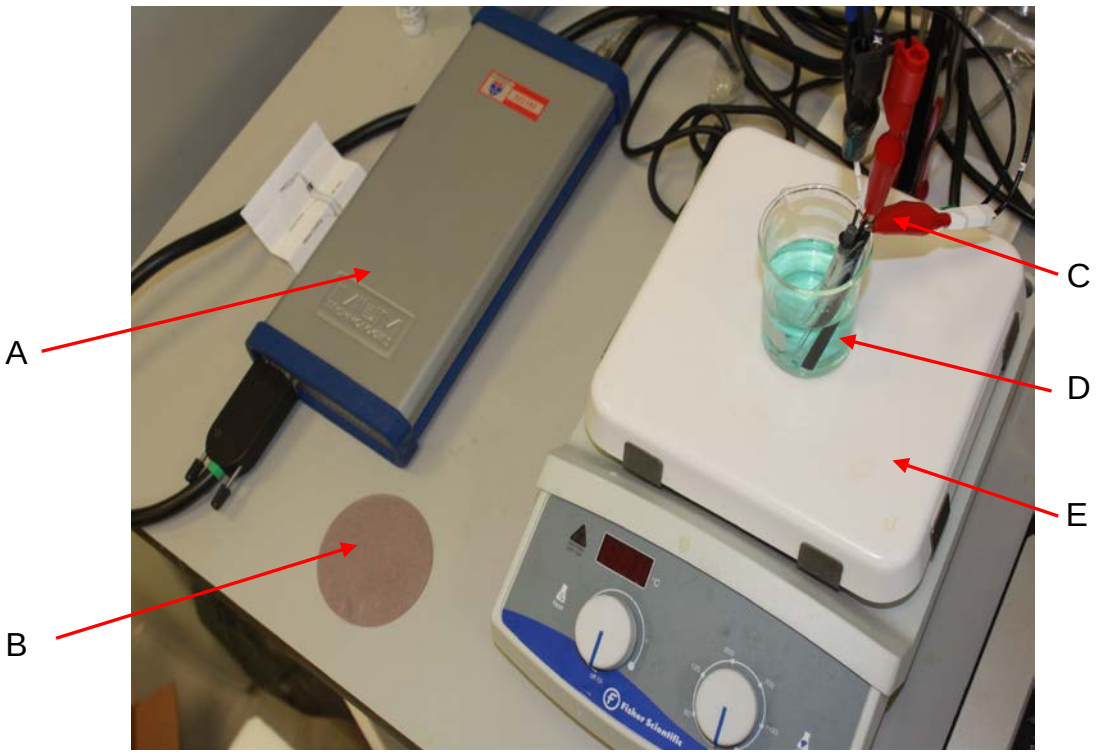

Figure 17 Electrode setup used for measurements. A) Potentiostat, B) micro-cloth polishing pad, C) gator clips, D) electrodes immersed in solution, E) magnetic stirrer.

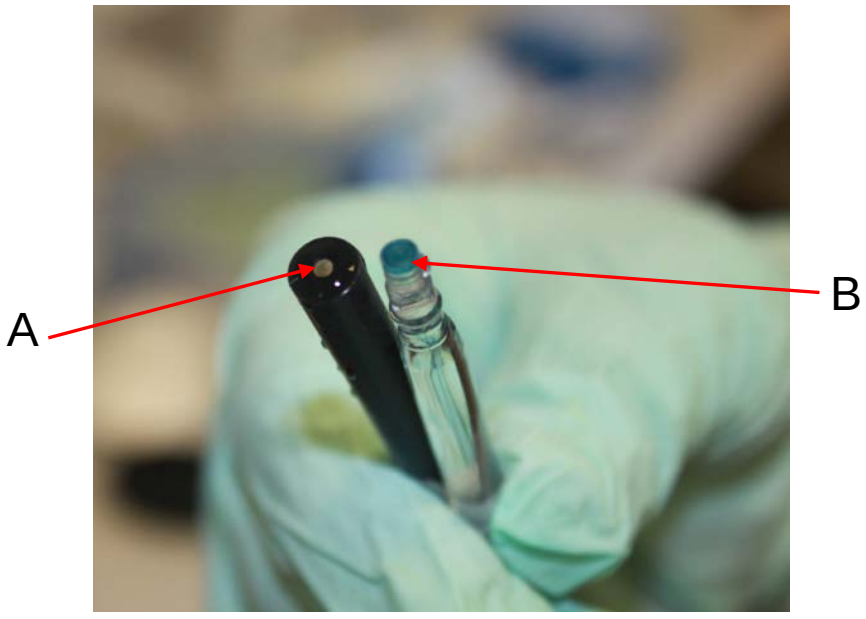

Figure 18 The electrodes used for measurement. A) Modified platinum working electrode and B) the Ag/AgCl reference/counter electrode.

2.5.1 Electrode Preparation

A Pt Electrode was cleaned with aluminium silicate 2 μm bead slurry and a microcloth polishing pad. The electrode was connected to a potentiostat from Iviumstat and then immersed in a 0.1 M NaOH, pH 13 solution containing 2 mM NiTSP. Fifteen cycles of cyclic voltammetry were then applied to the electrode using settings of 0-1.2 V(+) and a scan rate 100 mV/s. This step is necessary to achieve NiTSPc electrodeposition on the electrode surface. The electrode was then removed from solution and allowed to dry at ambient temperature (approximately 10 minutes). The surface of the electrode is further modified by the addition of 5 μL Nafion 117 solution followed by adequate drying time (10-15 minutes). These procedures modify the electrode surface allowing interaction with NO, whilst excluding other agents. In the absence of the Nafion layer, the electrode would be more susceptible to interaction with compounds similar to NO.

2.5.2 Electrode Measurements

Mammalian Cells were grown overnight in 24 well plates with appropriate medium and eNOS. Medium was then aspirated and the cells were washed in PBS. Following this step, cells underwent Trypsin treatment before being resuspended in PBS and washed twice. Final cellular resuspension was done in PBS at 37 °C. This step was necessary to remove free-floating proteins and cellular detritus, which could potentially interfere with the experiment. Other components in DMEM medium such as phenol red and FBS may also interfere with measurements. A pre-prepared electrode is then immersed in the well so as to be in contact with the cell-suspension solution. Cells were in suspension to maximize exposure of the electrode to NO. The electrode was then placed at a constant potential of +750 mV and a background current reading of NO was taken for a period of ten minutes. Stimulus in the form of white light was then introduced using a Dinotte Lighting high intensity lamp and a continuous reading of the release of NO in the form of current was taken.

Chapter 3 The activity of eNOS in CHO-K1 cells

In chapter 1 a detailed discussion of nitric oxide synthase proteins was presented and a strategy towards creation of a chimeric eNOS protein described. It was hoped that the eNOS analogue can be incorporated into mammalian cells, with the CHO-K1 line selected as a prime candidate due to its robust nature and enhanced ability to expressed proteins. However, prior to transfection a detailed characterisation of the wild type cells was required.

3.1 Assessing Cellular NO production using diaminofluoresceins

In order to quantitatively assess NO production in the chosen cell line, a series of experiments were designed in which cells were fluorescently labelled and their fluorescence intensity measured as a marker for NO production. Fluorescent stains provide a vital tool to visualise specific areas within cells, for example, phalloidin-based compounds bind to the actin cytoskeleton, whilst DAPI selectively stains cell nuclei and also acts as a live/dead assay. Such fluorescent compounds can also be used to selectively stain small molecules, such as nitric oxide, produced within cells. 4,5-diaminofluorescein diacetate (1) is a cell permeable dye.(Hirotatsu Kojima et al., 1998)' (Hirotatsu Kojima, Naoki Nakatsubo, et al., 1998) Once inside the cell the acetate groups undergo hydrolysis by intracellular esterase activity to generate the more reactive DAF2 parent compound (2). Rapid reaction with NO produced within the cell yields the highly fluorescent triazolofluorescein (DAF-2T) (3) which can be visualised under a fluorescence microscope equipped with a fluorescein filter set or the fluorescence intensity quantised *via* flow cytometry using an excitation filter of 492 nm and an emission filter of 515 nm.

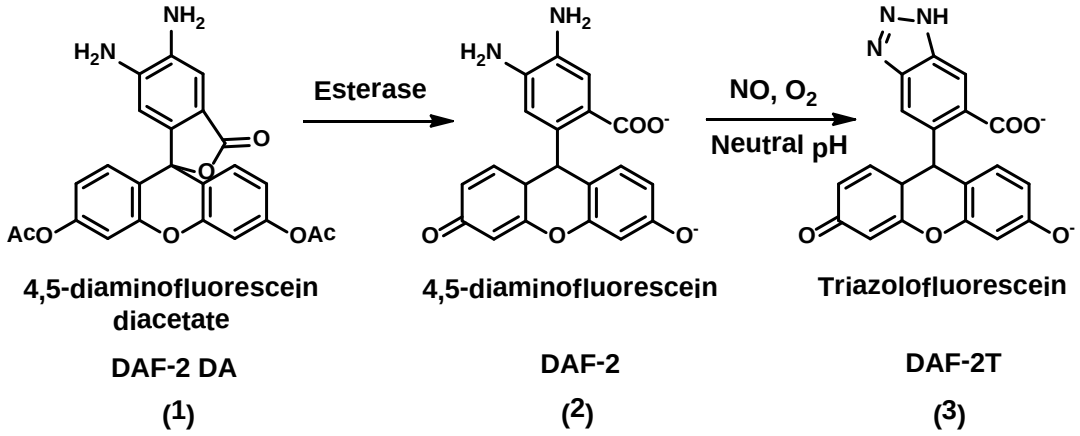

Figure 19 Reaction between DAF-2 DA and Nitric Oxide *in vitro* (taken from www.sigmaaldrich.com).

3.1.1 Inhibition of NOS

The study of NO expression in CHO cells also provides a novel opportunity to examine eNOS inhibition *in vitro*. NO has been implicated in a wide variety of processes *in vivo* giving the molecule, and in particular its inhibition enormous pharmacological significance. A wide variety of compounds have been shown to inhibit NOS activity, ranging from mimics of L-arginine to substituted citrulline deriviatives such as thio- and alkylthiocitrullines and hererocyclics such as nitroindazole or imidazole derivatives.(P K Moore & R. L. Handy, 1997) The first reported case of NOS inhibition used a methylated analogue of L-arginine, known as L-NMMA (Figure 20).(Olken & M. a Marletta, 1993) Inhibition of NOS by arginine mimics (of which L-NNA is also an example)(Furfine, Harmon, Paith, & Garvey, 1993) is thought to occur to *via* a competitive binding mechanism however the precise nature varies according to both the substrate and NOS isoform. The process is highly stereospecific with D analogues demonstrating little or no inhibitory effect. Generally amino acid based inhibitors show little selectivity between NOS isoforms *in vitro*).(P K Moore & R. L. Handy, 1997)

In contrast, hererocyclics such as the nitroindozole 7-NI are believed to bind to the haem domain of NOS and consequently disrupt electron transfer through the protein, preventing NO formation.(Babbedge, Bland-Ward, S. L. Hart, & P K Moore, 1993) Interestingly, interaction between 7-NI and haem also interferes with the binding of L-arginine and BH4, which may explain the apparent inhibitory nature of this compound at alternative sites.(R. L. C. Handy *et al*., 1996)(Klatt et al., 1994)

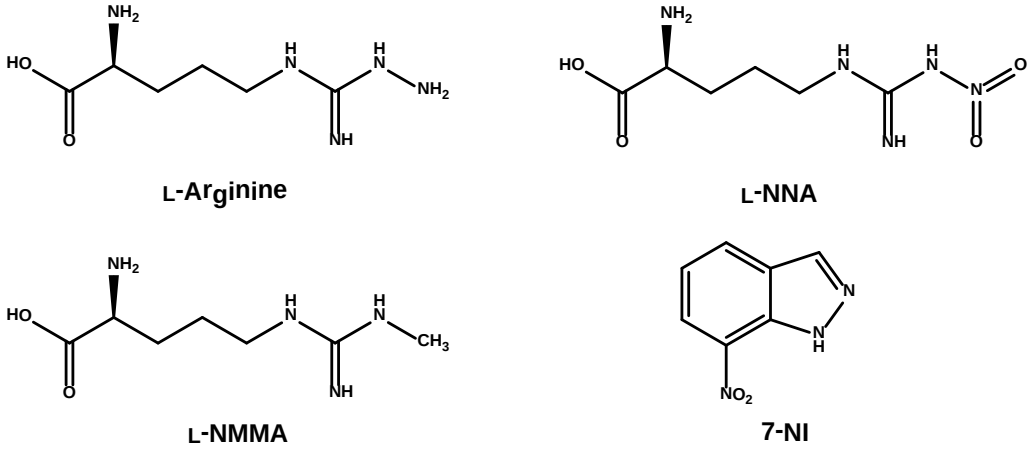

Figure 20 Structures L-arginine and of the NOS inhibitors L-NNA, LNMMA and 7-NI.

For the purpose of this study three commonly used NOS inhibitors, L-NNA, L-NMMA and 7NI were selected and introduced to the cell culture in order to evaluate their activity on cellular NO production. A working concentration of 50 μM was used for each inhibitor. This value was derived so as to be several times higher than the IC50 value of the inhibitors' action on eNOS. The IC values for the purified protein were obtained from the work of Alderton *et al* and are quoted as 0.35 μM, 3.5 μM and 11.8 μM for L-NNA, L-NMMA and 7-NI, respectively.(Alderton et al., 2001) By using a concentration several times higher than the IC50 value it is expected that that the inhibitory effect would be sufficient to be observed *via* flow cytometry methods. However, these concentrations are deliberately somewhat lower than those used in previous studies in order to evaluate whether such concentrations were sufficient to inhibit eNOS production in CHO cells.(Zhan, D. Li, & Johns, 2003), (Navarro-antolin & Santiago Lamas, 2001)

3.1.2 Lipofectamine-based delivery

Despite the extensive study of NO inhibitors over the past two decades, the cell permeability of these compounds has not been thoroughly investigated. In order to probe the uptake of inhibitors into CHO cells, a liposomal delivery method was devised comprising pre-incubation of the inhibitors with Lipofectamine LTX. These

commercially available liposomes are routinely used in the Lipofection route of Eukaryotic cell transfection,(Herrera, Hong, & Garvin, 2006) as shown in Figure 21. Although the exact nature of Lipofectamine has not been disclosed, the system is known to be cationic and provides an efficient means to deliver DNA into cells. It was therefore thought that use of these liposomes which are known to be compatible with mammalian cell membranes would increase intracellular inhibitor concentration providing an interesting comparison with natural uptake of NO inhibitors.

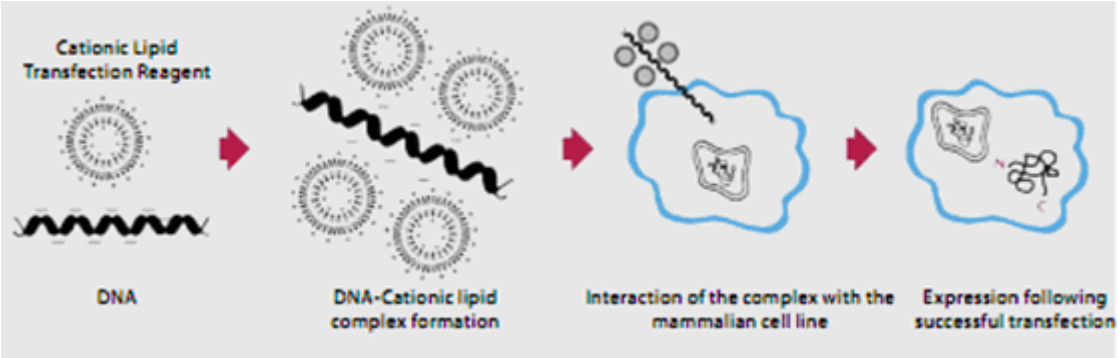

Figure 21 Transfection of DNA into cells using Lipofectamine (taken from invitrogen.com).

3.2 Inhibition of NO production in CHO-K1 cells – effect of inhibitor type and lipofectamine delivery

In order to probe the production of NO within CHO-K1 cells, a series of experiments were designed using DAF-2 DA as a selective stain for nitric oxide. In the first instance the production of NO was assessed in native cells and compared to those treated with known inhibitors of NO. In an analogous experiment, cells were treated with identical concentration of inhibitors in the presence of lipofectamine in an attempt to increase the proportion of inhibitor incorporated into the cell. An initial qualitative analysis of NO production was carried out using a fluorescence microscope prior to quantitative measurement of fluorescence levels using flow cytometry.

3.2.1 Fluorescence microscopy

Prior to flow cytometry analysis, cells were imaged using fluorescent microscopy to verify the activity of the used Fluorescein and whether any qualitative/quantitative information could be gathered from this type of data.

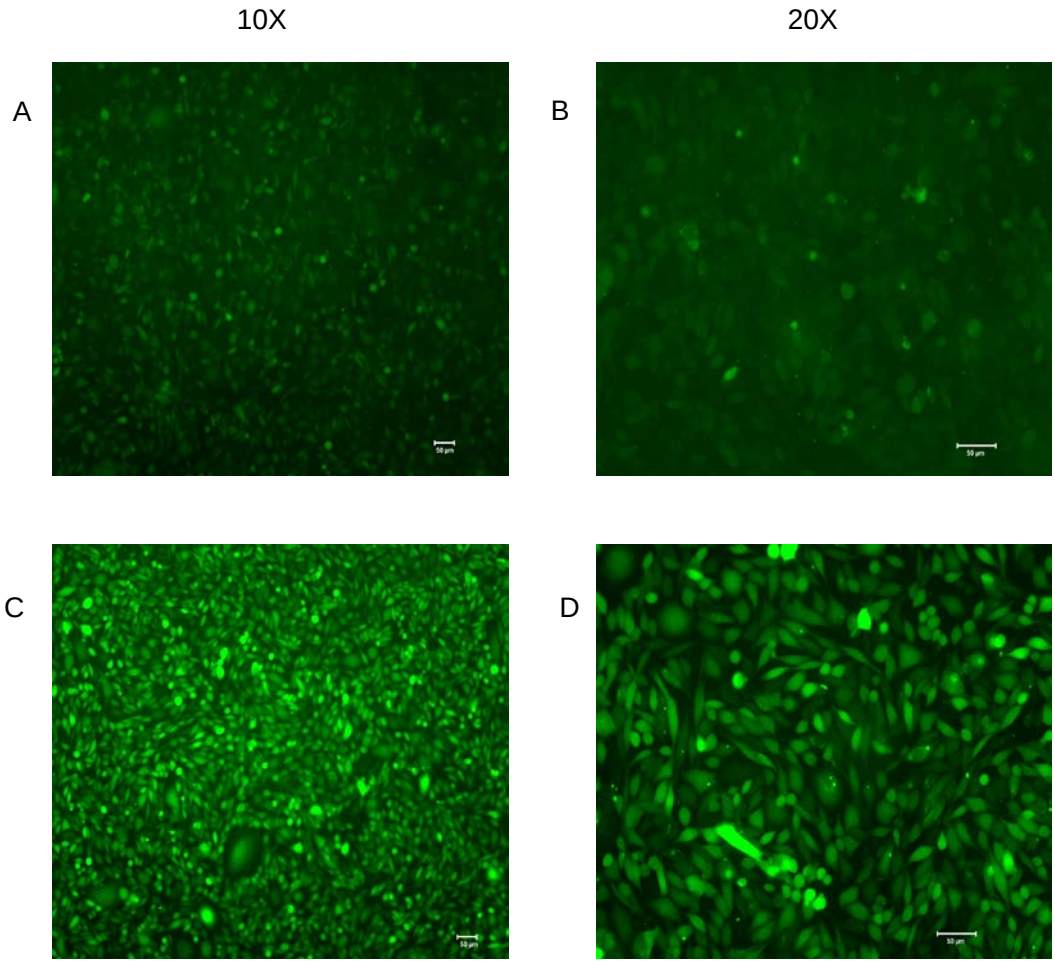

Figure 22 DAF-2 DA staining of CHO-K1 cells. Images A and B are of control samples, untransfected cells, at 10x and 20x magnification respectively. Images C and D are of cells transfected with the PEX_EF1-CFP_NOS3 plasmid at 10x and 20x respectively. Images on each column were taken with the same exposure time at the same magnification. Image modification was also regulated for all images to undergo the same change in histogram. Exposure time for each column was set using the PEX_EF1-CFP_NOS3 mutant cell line and the control image was subsequently taken using the exposure time automatically calculated for the mutant cell line.

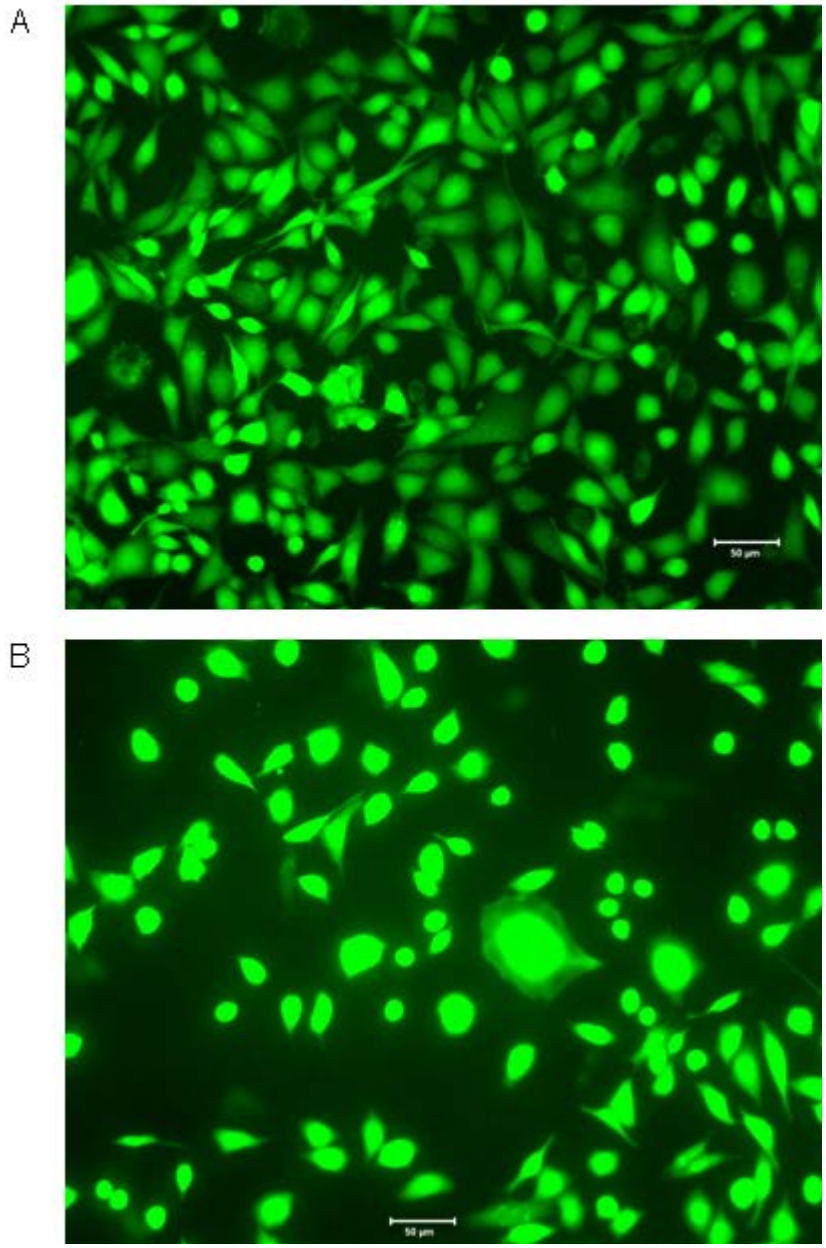

Figure 23 Fluorescent imaging using DAF-2 DA of control and the PEX_EF1-CFP_NOS3 mutant line. A) Control cell line. B) the PEX_EF1-CFP_NOS3 mutant cell line. These images were taken using the same method as the images in the previous figure, with the exception that the exposure time calculation was done inversely. Exposure time was set using the control cell line and subsequently the PEX_EF1-CFP_NOS3 mutant cell line was imaged using the exposure time calculated for the control image. Both images were taken at 20x magnification. All image processing was constant for both images.

As can be seen in Figures 22 and 23 transfected cells showed a higher fluorescence intensity than untransfected cells. This suggests that the mutant cell line is in fact

producing NO at abnormally high quantities. At a higher magnification, as illustrated in Figure 24, it can be seen that NO production is localized within the cell.

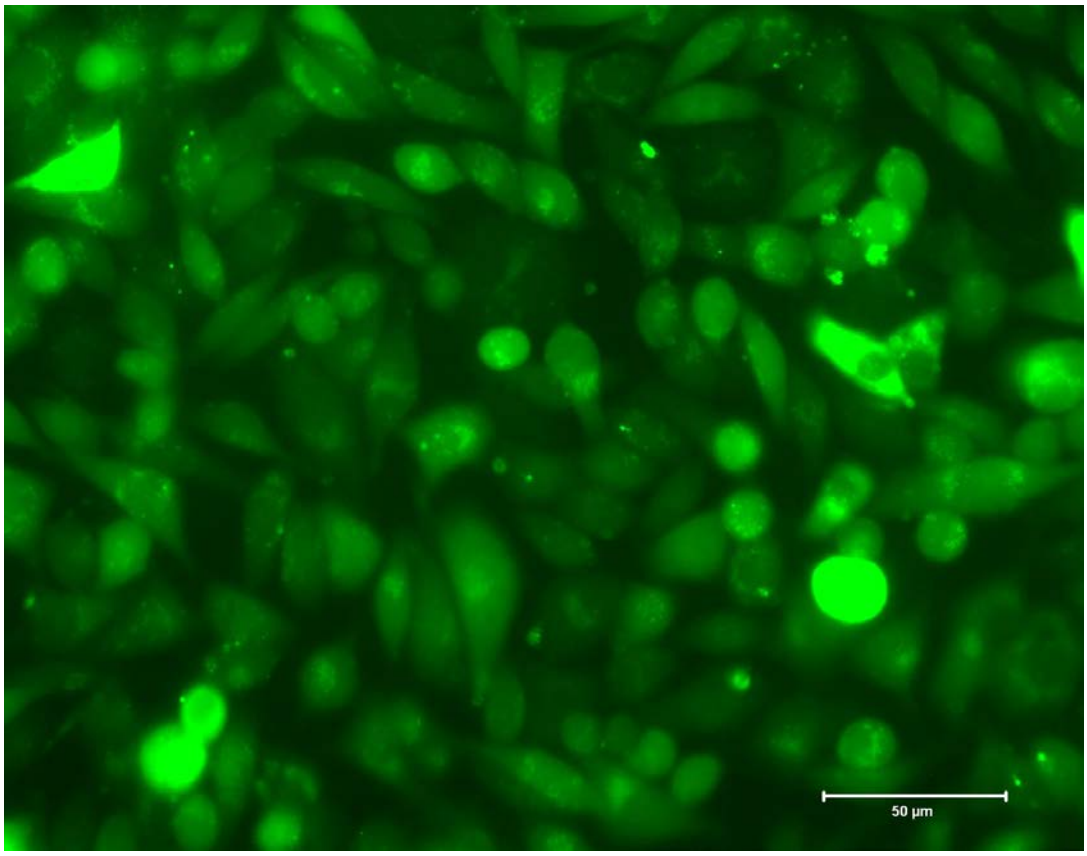

Figure 24 A 40x Magnification of the CHO-K1 mutant cell line transfected with the PEX_EF1-CFP_NOS3 plasmid. NO detection shows higher concentrations around the nucleus, whilst some cells appear to contain substantially higher levels of NO.

A proportion of the cells exhibit significantly higher fluorescence intensity than the majority of the sample, which can be attributed to higher intracellular NO concentrations. There are a number of possible explanations for the observed fluorescence. These include variation of expression rates of the eNOS gene within the cell, the availability of co-factors in solution (competitive binding) and the position of the cells within the growth cycle, with initiation of the apoptotic cycle leading to production of NO *via* non-NOS pathways.

3.2.2 Flow Cytometry Analysis

Flow cytometry is a powerful technique used in the analysis of micron-sized particles and cells. A beam of monochromatic light (usually from a laser) is directed on to the sample stream, whilst detectors placed in line with (forward scatter) and perpendicular to (side scatter) analyse the scattered light. If the particle or cell is fluorescently labelled, emission may occur at a different wavelength from the incident light source. A combination of scattered and fluorescent light is identified by the detectors and by analysing fluctuations in the brightness of each emission peak it is possible to derive a myriad of useful information about each individual particle or cell. For example, forward scatter correlates well with cell volume, whilst side scatter can give an insight into internal components of a particle, such as the shape of cell nuclei.

In many flow cytometry experiments a combination of fluorescent dyes are employed which each have characteristic emission wavelengths. For this reason there are numerous methods of data analysis and interpretation, depending upon the information sought from the experiment. Therefore, prior to delving into experimental results an overview of the analytical method must be given. As each type of experiment conducted using flow cytometry uses different parameters and each type of sample can behave differently, these must be standardized as much as possible throughout experiments whilst preserving the integrity of the data being collected.

In the first instance a plot of side scatter (SSC-A) vs forward scatter (FSC-A) allows the sample gate to be selected. The chosen "sample" gate must encompass the entirety of the cell population being observed whilst filtering out other compounds such as cellular debris (shown in black). As living cells from a cell line will exhibit similar morphology it is reasonable to assign the large population (shown in purple and blue) to a living cell population.

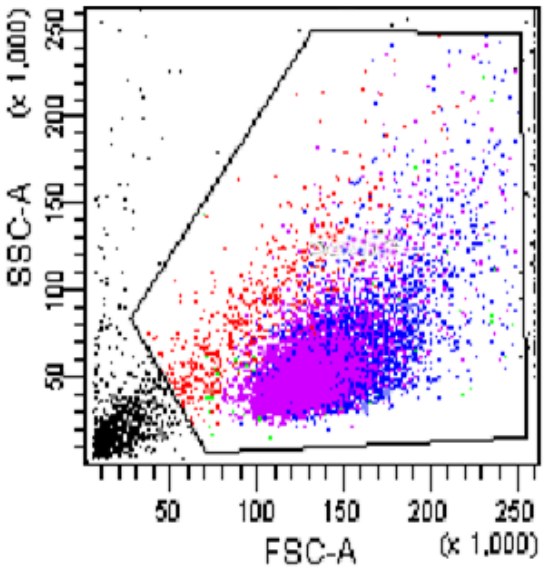

Figure 25 A flow cytometry sample exhibiting the "sample" gate chosen. The population of interest can easily be distinguished using Side Scatter[2] vs Forward Scatter[2]. As living cells from a cell line will exhibit a similar morphology to each other it is safe to assume that the large population (shown in purple and blue) contains a living cell population.

Once the sample gate has been established a more detailed analysis of the data is required. Cells which are positive for DAF-2DA indicate the production of NO, however as NO is an active player in cellular apoptosis, it was also necessary to assess whether apoptotic cells are contributing to the NO measurements obtained. To achieve this, cells were co-stained with DAPI as an indicator of cell death. DAPI demonstrates greater permeability to dead cells than their live counterparts resulting in higher fluorescence intensity. This allows removal of DAPI positive cells from the overall cell population as well as a providing a method of verifying whether apoptotic cells contribute to the measured NO. A plot of DAPI fluorescence intensity vs forward scatter shows two populations, which are attributed to live (blue/purple) and dead (red) cells, respectively.

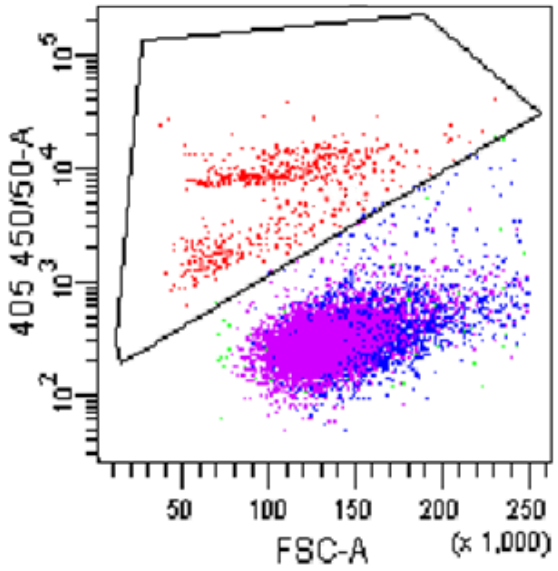

Figure 26 A flow cytometry sample demonstrating the "Dead" population gate. All cells portrayed in this figure are within the "Sample" gate mentioned in Figure 24. Dead cells have a higher fluorescence in the 405 450/50-A measurement due to DAPI staining. DAPI is excited using an Ultraviolet laser with an excitation of 405nm and emission of 450nm. As can be observed, DAPI positive cells occupy a different area to the cell population of interest in respect to their 405 450/50-A fluorescence and can therefore easily be excluded.

Once the dead cells are excluded from the analysis, the remaining live population can be considered which is achieved *via* inversion of the "dead" gate. A plot of DAF-2 DA emission fluorescence intensity vs forward scatter illustrates two distinct populations which are termed “negative” and “positive”. The positive population displays significantly higher fluorescence, suggesting that cells within this population are actively producing NO, whilst those in the negative population display production of NO at a substantially lower level. It can be noted that in Figures 26 and 27 the axes are inverted; the axes on which each parameter is displayed is arbitrary in both cases and are assigned to give the best definition between the two populations in order for them to be separated. Once the populations of interest have been assigned, a histogram of cell count vs fluorescence intensity can be constructed, clearly indicating the proportion of cells in the “negative” and “positive” populations Figure 28.

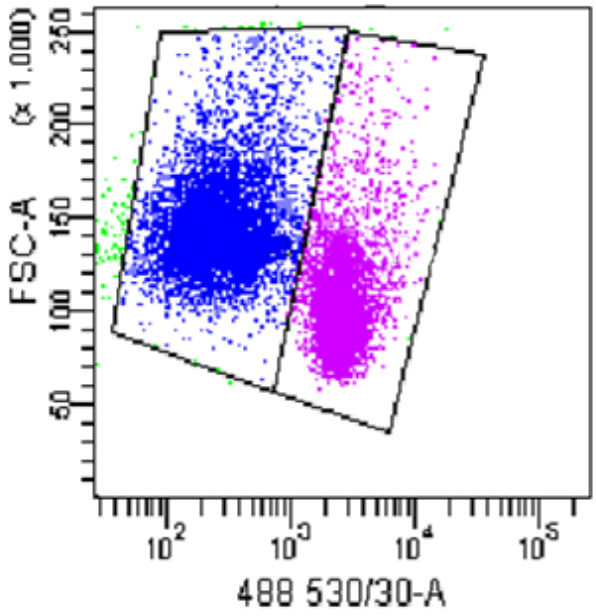

Figure 27 A flow cytometry sample showing the "Live" population of cells under 488 530/30-A fluorescence, the emission spectrum of DAF-2 DA. It was noted that two distinct populations were observed. These were termed "Negative" (Blue) and "Positive" (Pink) as one has a distinctively lower fluorescence than the other. It was therefore assumed that one population is actively producing NO whilst the other has a substantially lower level of NO production.

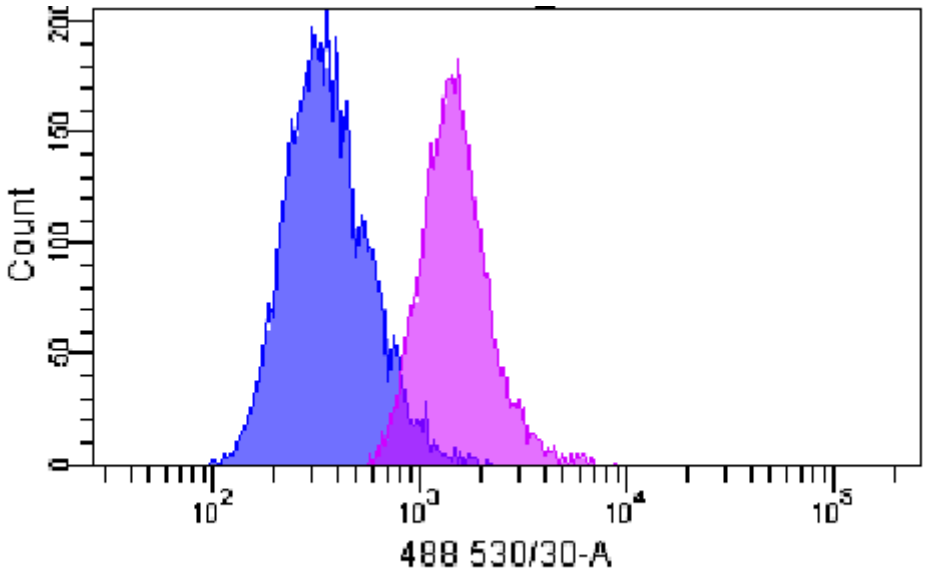

Figure 28 A flow cytometry histogram produced from data which has been processed as delineated in Figures 25-27. The histogram depicts cell count vs

fluorescence intensity on a 488 530/30-A (DAF-2 DA) emission spectrum. The two populations, "Negative" (Blue) and "Positive" (Pink) can be observed.

In order to probe whether apoptotic cells contribute to the positive or negative populations, the DAF-2 DA fluorescence of DAPI positive cells was investigated. Figure 29 shows that DAPI positive cells only contribute to the fluorescence of the negative population and therefore are not actively producing NO. This would indicate that for the purposes of this experiment, dead/dying cells do not contribute to shifts in the positive population.

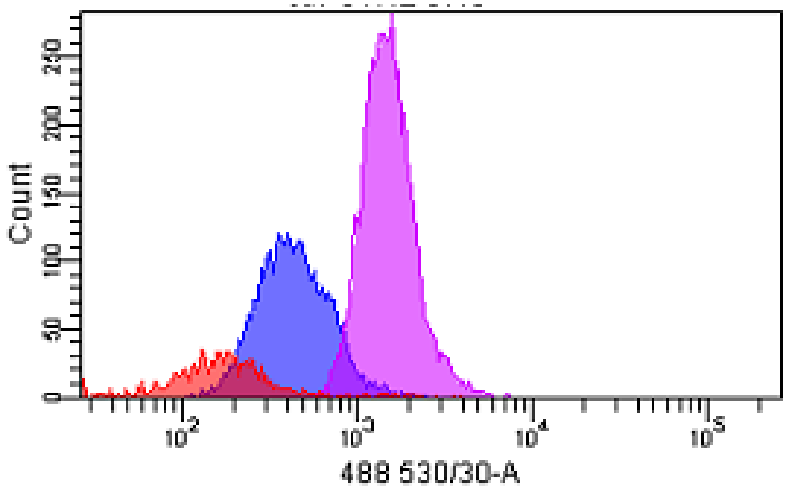

Figure 29 Population histogram from 488 530/30-A (DAF-2 DA fluorescence) data. Blue) Negative Population, Pink) Positive Population, Red) DAPI positive population.

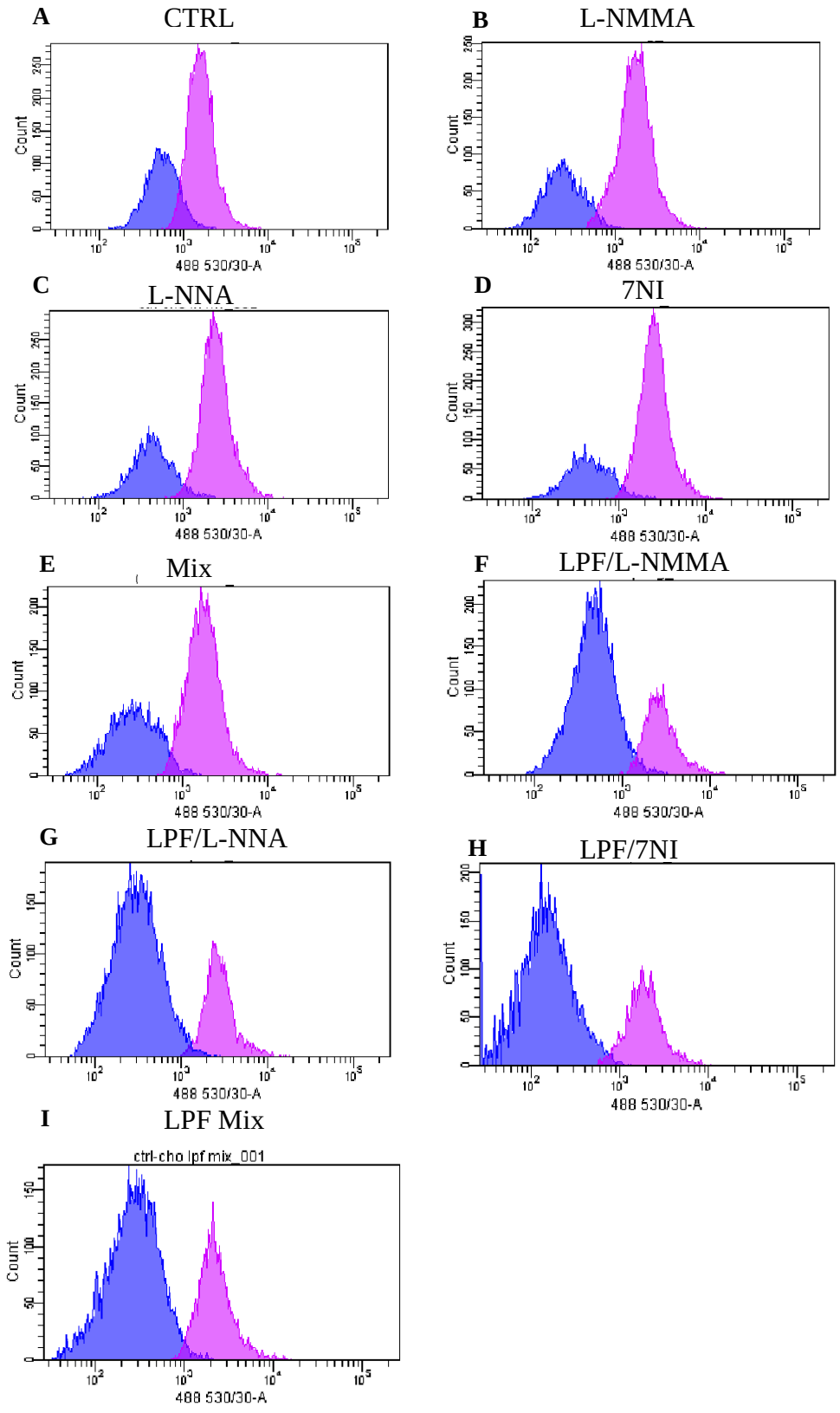

Figure 30 Flow cytometry histogram results. This figure depicts the data gathered from the flow cytometry experiment. Only one representational histogram for each sample shown. A) Control B) With inhibitor L-NMMA C) With inhibitor L-NNA D) With inhibitor 7NI E) With inhibitor mix F) With LPF/L-NMMA G) With LPF/L-NNA H) With LPF/7NI I) With LPF/inhibitor mix.

The analysis discussed in section 3.2.2 was applied to each sample in turn and examples of the fluorescence histograms obtained are shown in Figure 30. Addition of inhibitors in the absence of lipofectamine appears to have little impact upon cellular NO production. This suggests that the concentrations used (50 μM) are insufficient to cause effective inhibition, in contrast to those reported to inhibit NO production in a purified protein. However, in the presence of the liposomes/inhibitor complexes, production of NO is attenuated to a significant extent.

In order to quantify changes in the populations relative to the control sample a statistical analysis of the data was performed. The results are illustrated in Figures 31 and 32 and correlate well with initial observations based upon visual inspection of the histograms. Introduction of the lipofectamine reagent in the absence of inhibitors had no effect on NO production, Figure 31. Within the error limits of the experiment none of the inhibitors tested showed significant changes in the positive and negative populations, appearing very similar to the control, Figure 32. In contrast, many of the inhibitor/lipofectamine complexes did lead to substantial changes, which are also illustrated as percentage changes relative to the control in Figure 32.

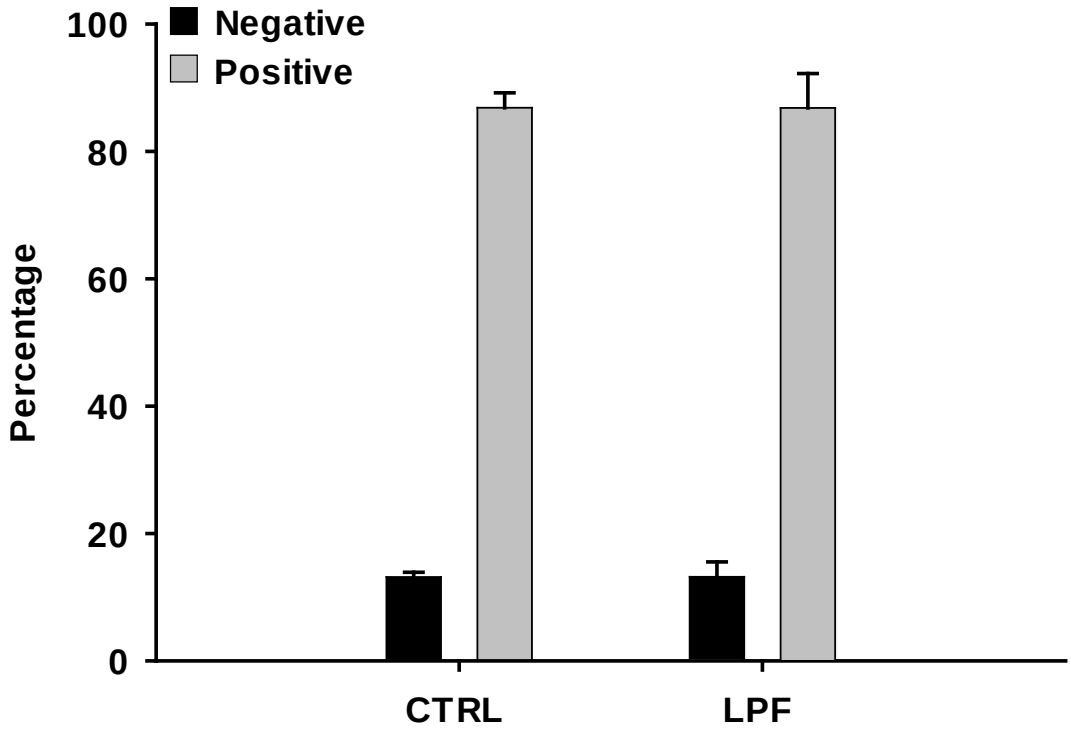

Figure 31 The effect of lipofectamine on the cellular production of NO. It can be observed from the figure that there is no significant difference in the positive and negative populations of the two samples (N=6).

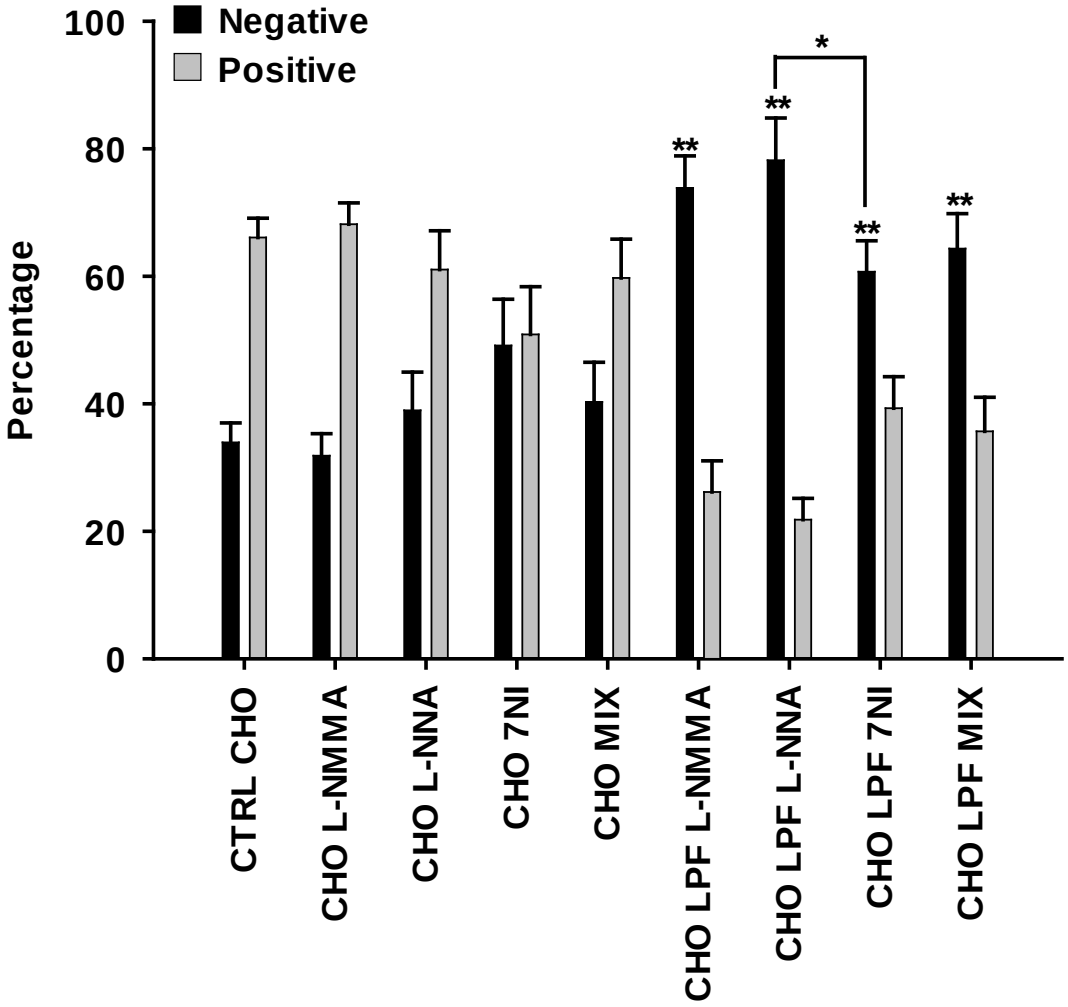

Figure 32 Statistical representation of the positive and negative populations in each group of samples. For each sample approximately 10,000 datapoints were gathered and for all samples N=6. Samples marked ** show $p<0.01$ relative to the control and * $p<0.05$, relative to sample indicated.

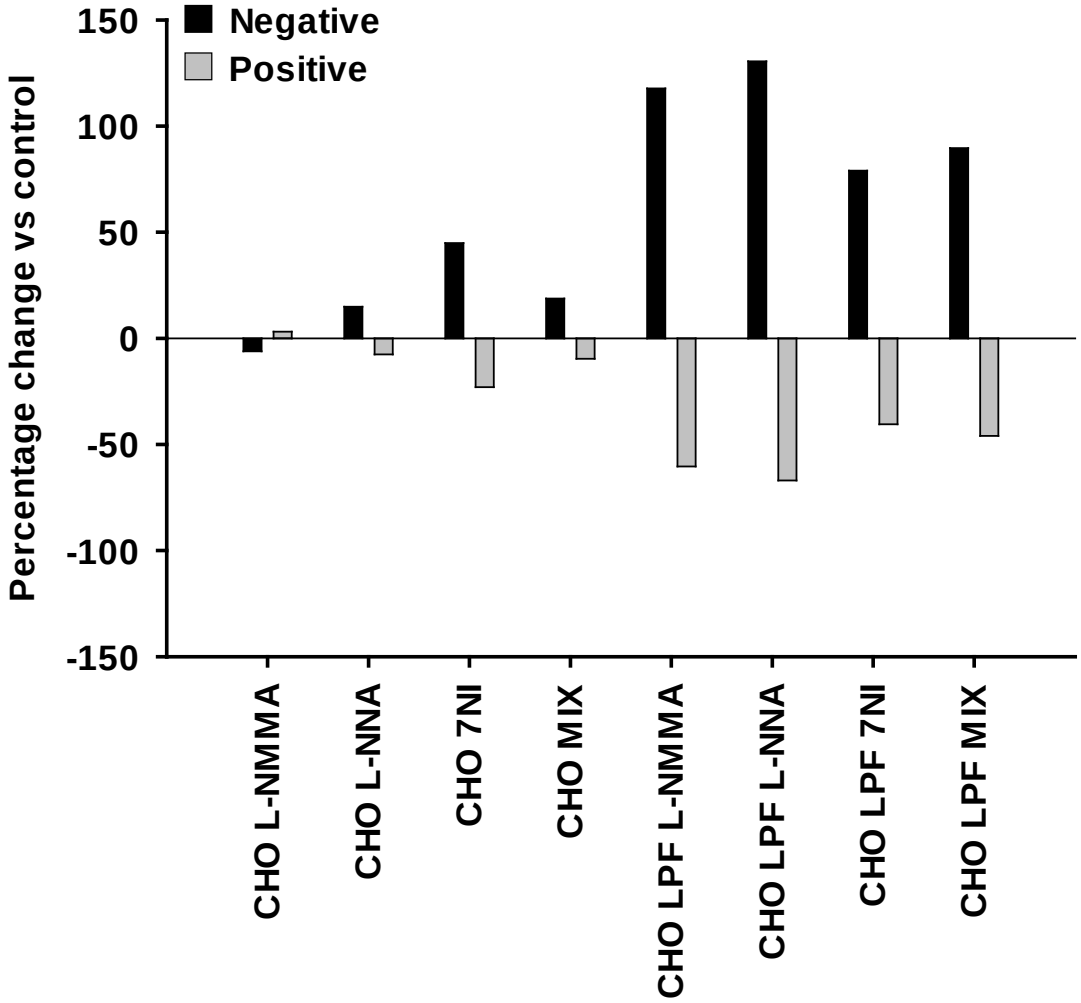

Figure 33 A representation of the change in populations of samples with inhibitors and LPF/inhibitor complexes. All population data was compared to the Control sample shown in Figure 31 to generate a change in percentage from the control. (N=6)

It is interesting to note that LPF-inhibitor complexes containing mimics or L-arginine, in particular the nitro analogue L-NNA, are significantly more effective in attenuating NO production than those containing the heterocyclic 7-NI. This is likely due to the inhibition mechanism which differs between the two inhibitor systems as discussed in section 3.1.1.

These experiments also confirmed that cell permeability presents a major barrier to incorporation of the inhibitors and that liposomal delivery of these compounds proved an effective method of overcoming this barrier. Therefore, although LPF-inhibitor complexes provide a poor comparison for uptake of inhibitors *in vivo*, effective transport of the inhibitor into the cells permits differences in intracellular activity to be

observed which are not apparent using the inhibitors alone. Again this finding is interesting as L-arginine is expected to be readily available in the intercellular environment whereas related mimics appear to be less readily incorporated. It is also noteworthy that in the presence of lipofectamine low concentrations of inhibitor are sufficient to be effective.

3.3 Inhibition of NO production in mutant vs wild type CHO-K1 cells

In order to investigate how the insertion of the eNOS gene into the wild type cell population affects NO production, an experiment was designed using the LPF/inhibitor complexes discussed in sections 3.1-3.2. Cells were transfected using the PEX_NOS3-CFP plasmid and both the wild type and mutant population were subjected to LPF/inhibitor complexes. LPF/inhibitor complexes were chosen due their enhanced inhibitory effect in comparison with the inhibitors in isolation. An assessment of the live/dead cells *via DAPI* staining was not included as results in section 3.2.2 confirmed that DAPI positive cells only effect the negative population.

3.3.1 Flow Cytometry Analysis

Mutant and wild type cells were treated with inhibitor/lipofectamine complexes as described in section 3.2. The flow cytometry data was then analysed as described previously, and the resultant histograms are given in Figure 34. Positive populations are shown in green and negative in blue. A statistical analysis of the data is given in Figure 35, whilst changes in the percentage populations relative to the control are given in Figure 36.

It is interesting to note that that within the error limits of the experiment, baseline NO production is similar in both cell lines. This is not entirely unexpected and one possible explanation may be that in the mutant cell line, native cell machinery responsible for NO production is suppressed in favour of NO production *via* the incorporated eNOS gene. This is most likely due to the type of promoter being used for eNOS expression, EF1. As cells cannot actively repress EF1 for fear of losing cell line integrity, cells may be suppressing other sources of NO to prevent NO levels from reaching cytotoxic proportions. These other sources of NO are likely to be wild type NOS present in the cell line.

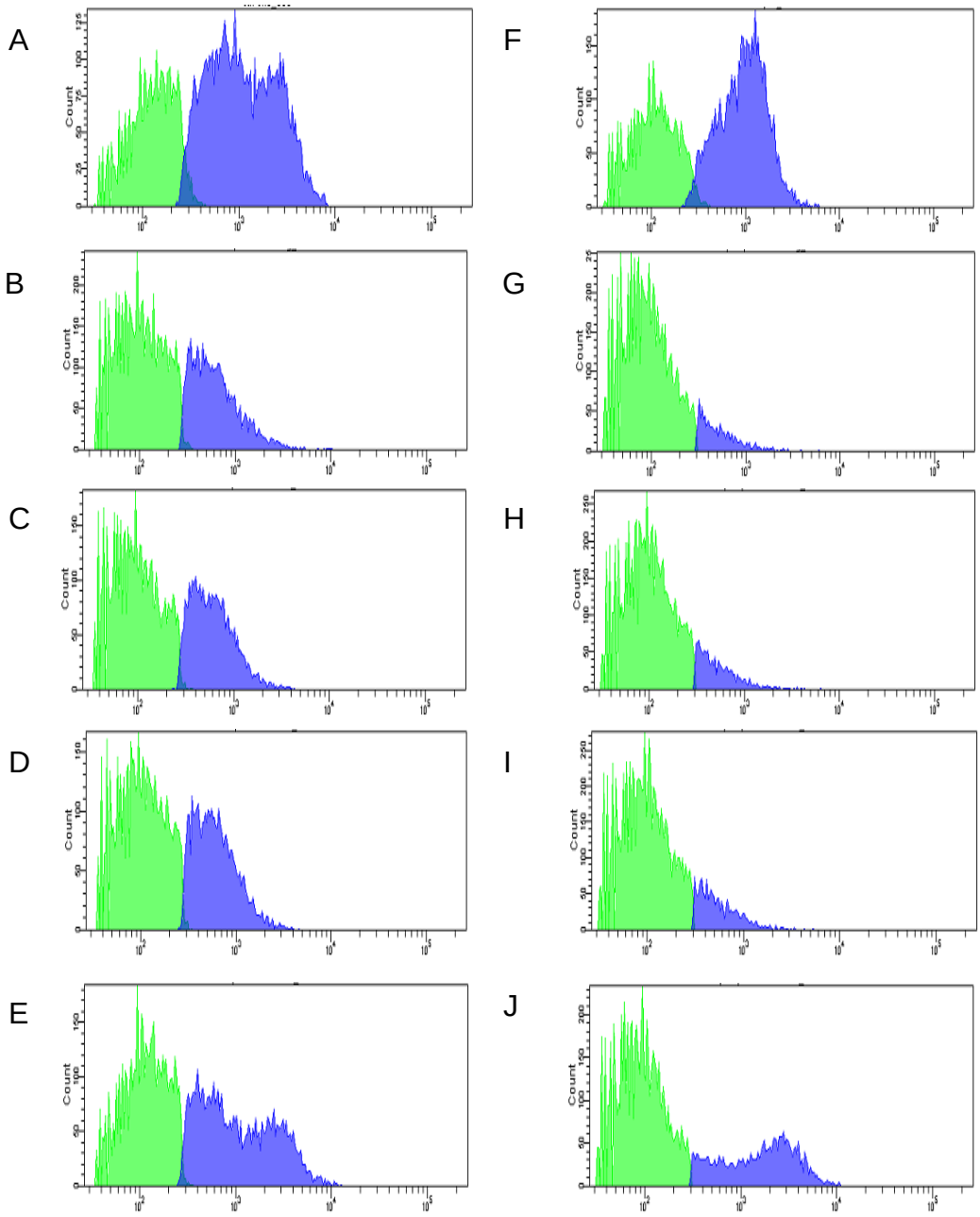

Figure 34 A) wild type Control B) wild type L-NMMA C) wild type L-NNA D) wild type 7N E) wild type inhibitor mix F) Mutant Control G) Mutant L-NMMA H) Mutant L-NNA I) Mutant 7N J) Mutant inhibitor mix. Green) Negative Population, Blue) Positive Population.

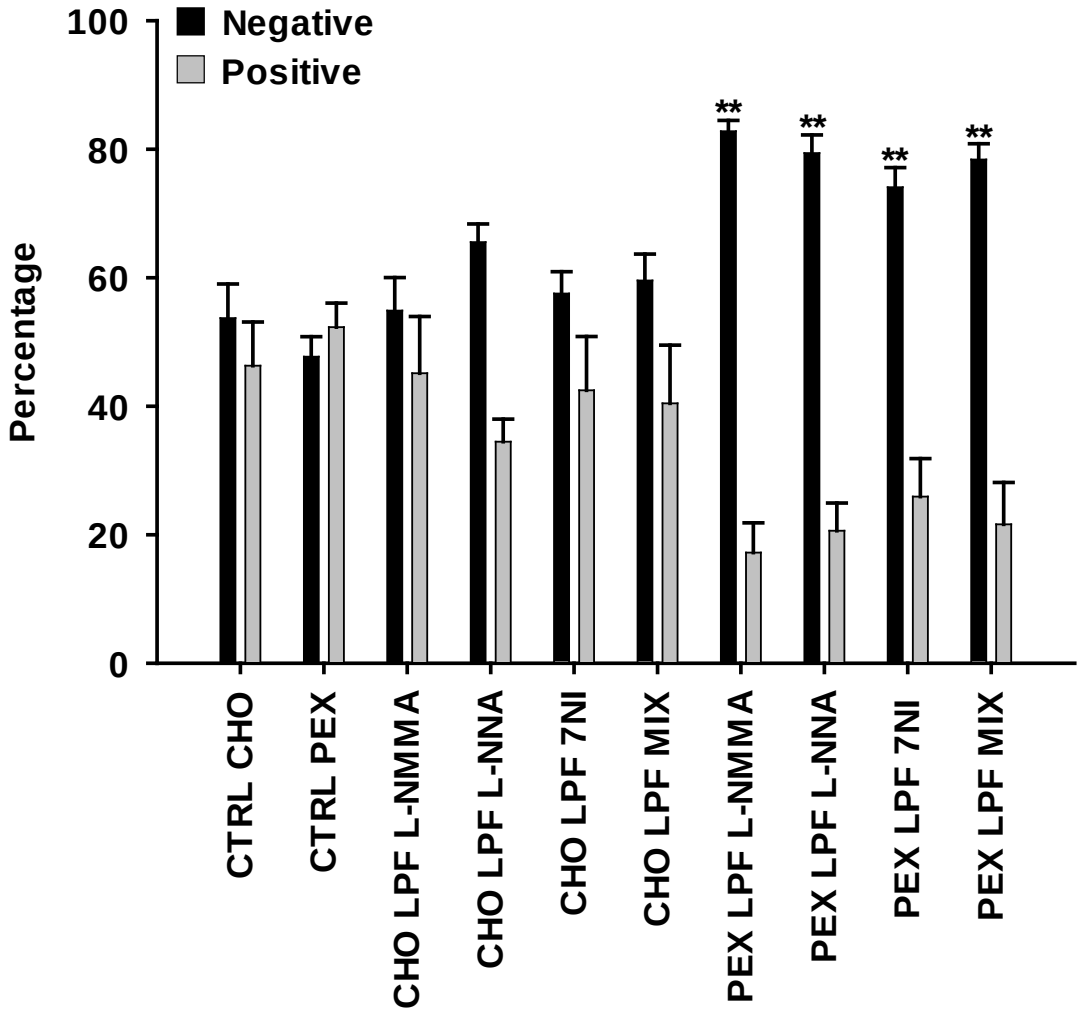

Figure 35 The percentage of positive and negative populations in all samples. For all samples N=6. Samples marked with ** have a *p* value of $p<0.01$.

It is also observed that inhibition is much more prevalent in the mutant than the wild type cell line (Figure 36) when the two are compared under identical experimental conditions. This is probably due to an alteration in the cell's NO production methods, which in turn would be a response to the inserted protein's activity. Although initial observations suggest that inhibitors that mimic L-arginine are slightly more effective in transfected cells than the heterocyclic 7-NI, there is no statistical difference between the four lipofectamine/inhibitor complexes employed. We suggest that in mutant cells the inhibitors initially suppress NO production *via* the e-NOS pathway. This may be compensated for *via* reactivation of the native cellular machinery however this is then also inhibited. As NO production is attenuated from two sources the reduction in the population of positive cells is much greater for mutant vs wild type cells, which only have a single means to produce NO.

A final observation is a slight reduction in cell volume in the positive versus negative populations for both mutant and wild type cells, as evidenced by histogram plots of forward scatter. However, upon further investigation the differences between the two populations were not shown to be statistically significant.

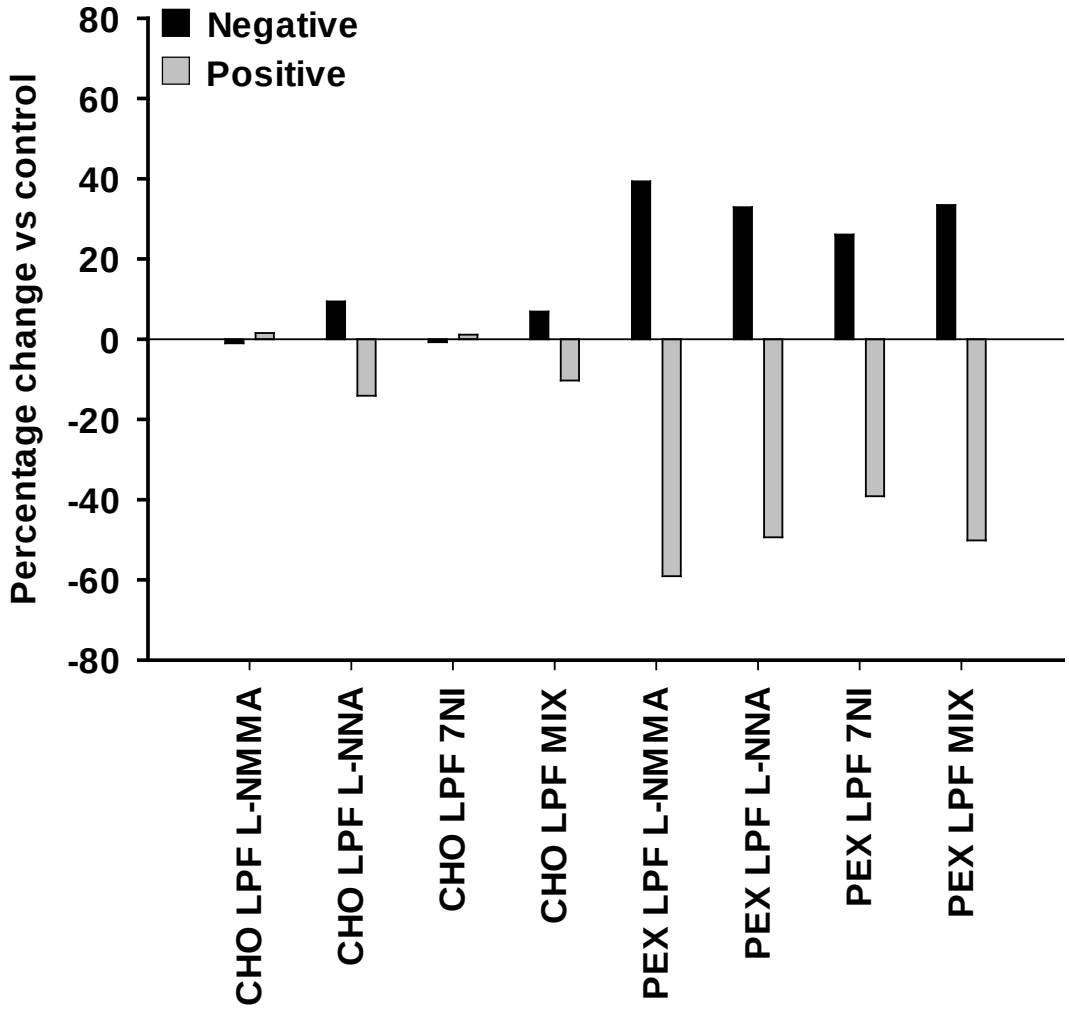

Figure 36 The Percentage change in populations vs the controls for each sample undergoing inhibition. It is quite clear that the changes in positive/negative ratio are significantly higher for the mutant cell line when compared to the wild type cell line.

3.4 Discussion

The use of liposomes as agents for drug delivery is widely reported.(Copland et al., 2003) The experiments conducted in this chapter demonstrate that liposomal delivery of inhibitory compounds into intracellular space is a more effective method than

conventional regular uptake for all inhibitors used. This is proven by the diminished positive population, cells that are actively producing NO. Lower concentrations of inhibitors than in some cases in the literature were used. This was to prevent saturation of the inhibitory effect; if the system is already saturated then the enhancing effect would not have been observable. The target concentration was determined using both literature values and IC50 values. We observed that in some cases, a concentration of up to 10 mM was used and that the IC50 values were smaller by multiple orders of magnitude.(Alderton et al., 2001) Therefore a value that was several times higher than IC50 values and several times lower than the methods used in some cases in the work of Kojima *et al* was adopted.(Hirotatsu Kojima, Naoki Nakatsubo, et al., 1998)

The data gathered also showed that the CHO-K1 cell line is actively expressing the mutant copy of eNOS. Although there was not a significant difference in the active population between the mutant and wild type controls, this is likely due to the cell regulating both its native NOS and the transfected eNOS. This is probably a mechanism of self-preservation as cells that are producing NO at high levels may cause cytotoxicity. The inhibitors chosen are partially selective towards eNOS when compared to nNOS or iNOS. The shift towards the negative population significantly larger in PEX mutants compared to wild type. This evidence suggests that cells are preferentially silencing their native genes as they are probably unable to suppress the mutant gene's promoter as effectively. As the mutant cell line therefore contains a larger percentage of its NO produced by eNOS, inhibition would therefore have a stronger effect. These findings support the case for the use of liposomal delivery of therapeutic agents.

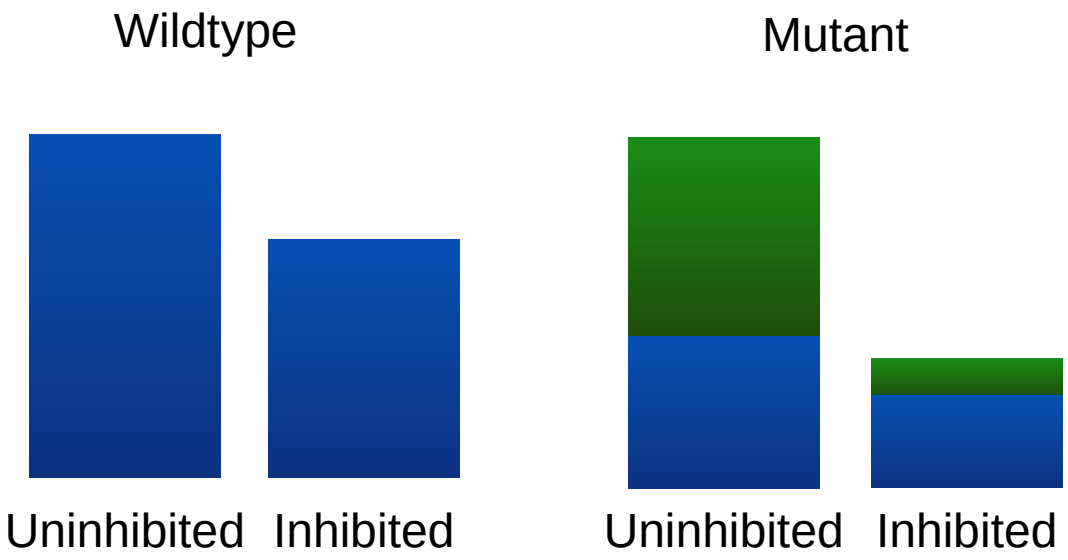

Figure 37 A model regarding the observed effects of inhibitors on both the mutant and wild type CHO cell lines. Blue: NO from wild type NOS machinery. Green: NO from inserted PEX plasmid. Uninhibited, both samples display a similar overall level of NO. Although both samples decrease in overall NO upon inhibition, the mutant cell line decreases substantially more than the wild type sample. The overall decrease in both samples suggests that the inhibitors are also targeting the wild type NOS machinery. The larger decrease in the mutant cell line would suggest that the function of inserted eNOS is severely debilitated in the presence of inhibitors. The similarity in the overall NO level between uninhibited samples suggests that NO levels are carefully regulated by the cells. The fact that the mutant cell line decreases more substantially suggests that the cell is unable to regulate the inserted gene as efficiently as it is capable of regulating its own internal wild type machinery. The larger decrease in the mutant cell line is also indicative of effective transfection with an NOS.

A possible area worth future investigation is the effect of L-arginine on the system. Increasing the amount of reaction substrate would allow for higher levels of protein activity and may make the observed differences/effects more distinct. As at the moment the cells are providing the substrate they can also limit its uptake and thereby inhibit some of the protein function. There is also the possibility that this regulatory effect is rescuing the cells from exposure to cytotoxic levels of NO.

Chapter 4 Chimeric eNOS

4.1 Chemosensitive eNOS

The work detailed in this chapter went towards the creation of novel chimeric constructs involving the eNOS gene for both chemical and optical signal detection.

Both the systems utilize the same NOS isoform, eNOS – obtained from the plasmid pEX_EF1_CFP-NOS3 acquired from ATCC. In order to preserve the machine-readable output and minimize electrode preparation/fabrication, both systems will use NO as the signal output molecule. Therefore, the eNOS gene is the best candidate for both systems.

In order to create a chemical signal dependent version of a nitric oxide synthase, cells were genetically modified to produce a mutant variant of eNOS (type III NOS). This protein is responsible for the catalytic conversion of L-arginine to L-citrulline, generating NO as by-product. The eNOS gene was selected for its constitutive expression and the fact that many of its properties, in particular the process of dimerization are relatively well understood and hence theoretically easier to manipulate.(Alderton et al., 2001)

Design of a chemically induced version of the protein aimed to bypass the disadvantageous time lag of promoter activation, therefore a chemical inducer of dimerization approach was taken. More information regarding CID's can be found in section 1.7

The genetic manipulation of eNOS has been designed to impede the production of NO so that the reaction will only occur in the presence of rapamycin. To this ends, the oxygenase and reductase domains of eNOS are separated. As the protein exists as a dimer, both domains are required in order for the protein to function and hence for NO to be produced. Subsequently each domain is fused to the fragments of the rapamycin targeting domains using serine linkers. FKBP12, part of the FK506 rapamycin binding protein, will be fused to the 3' of the oxygenase domain whilst FRAP will be attached to the 5' of the reductase domain. FKBP12 binds directly to rapamycin, and FRAP binds to the FBBP12/rapamycin complex. This results in sequential binding events leading to a FKBP12/rapamycin/FRAP complex in the presence of the chemical inducer of dimerization (Choi, J. Chen, S.L. Schreiber, & Clardy, 1996). In binding to rapamycin, the two domains of eNOS will be brought into close enough proximity to allow the

formation of stable dimers and restore the function of the protein, Figure 38. Although rapamycin has previously been used as a chemical inducer of dimerization, it has not been used to co-localise a split protein in order to retain functionality.

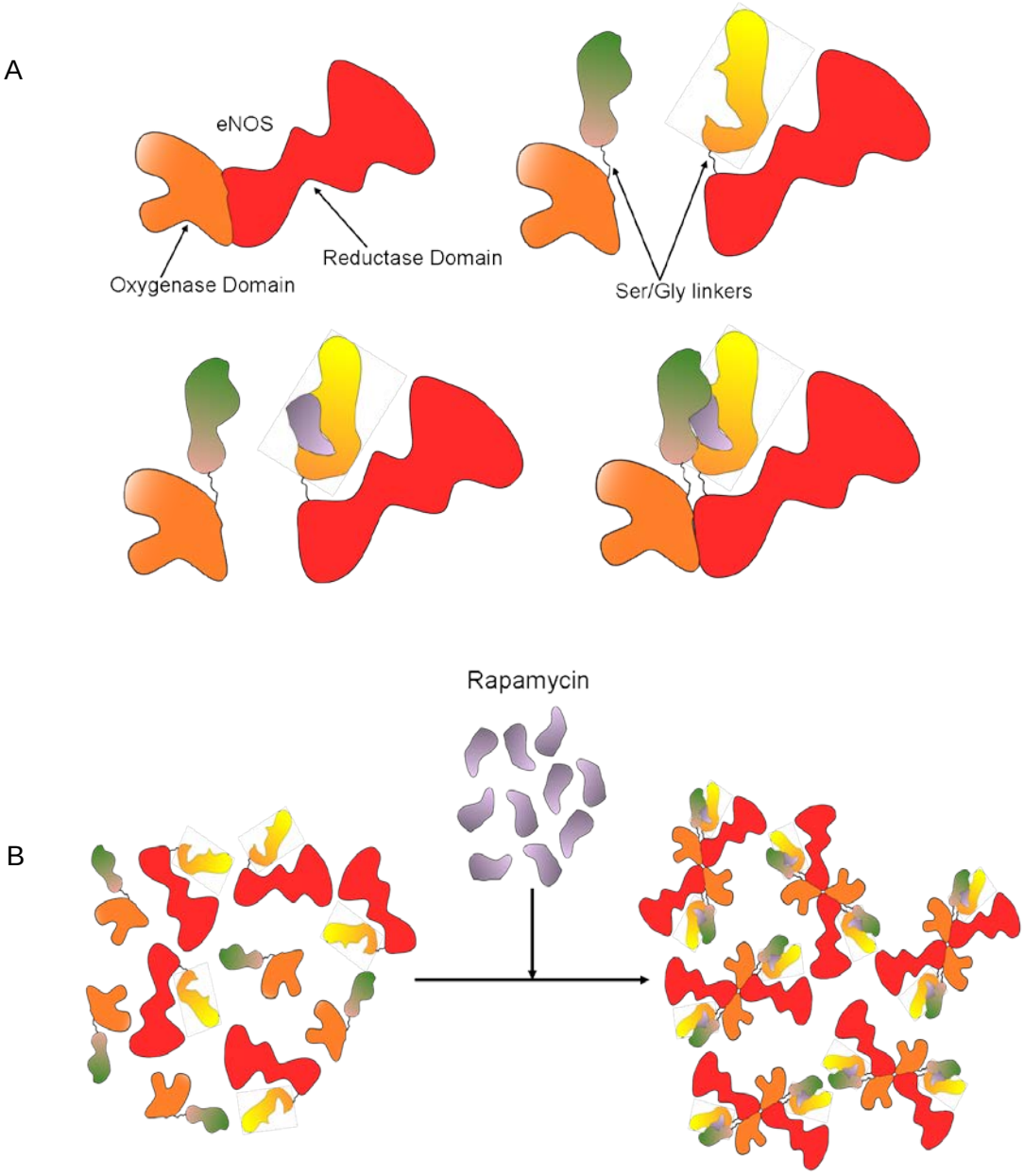

Figure 38 Diagram of the rapamycin dependent dimerization of eNOS. The concept depends upon the use of two domains known to interact with each other in the presence of rapamycin. This brings the two eNOS domains close enough together to allow dimer formation and subsequent protein activity. The FKBP12 fragment responsible for binding to rapamycin will be fused to the 3' end of the oxygenase domain of eNOS and FRAP fragment responsible for FKBP12/Rapamycin binding will be fused to the 5' end of the reductase domain of

eNOS. When rapamycin is present, the FKBP12/Rapamycin/FRAP complex formation will cause the two eNOS domains to come close enough together to form dimers with other full protein complements from other FKBP12/Rapamycin/Frap complexes. A) Three part system of the CID rapamycin system. Fragments of FKBP12 and FRAP are used so as to bind sequentially to rapamycin. B) eNOS is separated into its oxygenase and reductase domains. These are fused to a fragment of FKBP12 and the Frb region of FRAP together with Gly-Ser-Ser-Ser-Ser/ Gly-Ser-Ser-Ser-Ser linkers. When Rapamycin is introduced to the system the two domains of eNOS will come into sufficient proximity to allow protein function. C) eNOS domains become sufficiently co-localized to allow dimerization of eNOS and subsequent production of nitric oxide.

The creation of fusion proteins is not always successful as it may alter a protein's structure and consequently its function, diminishing, or even abolishing it. Therefore, the Rapamycin induction method is a good way to test whether this system can be manipulated in such a fashion and would lead to the construction of eNOS sequences with different active targets or the refinement of the Rapamycin induction. The latter would require the creation of a further step in the pathway to signalling where Rapamycin is released in response to the presence of a specific substance, consequently promoting NO production.

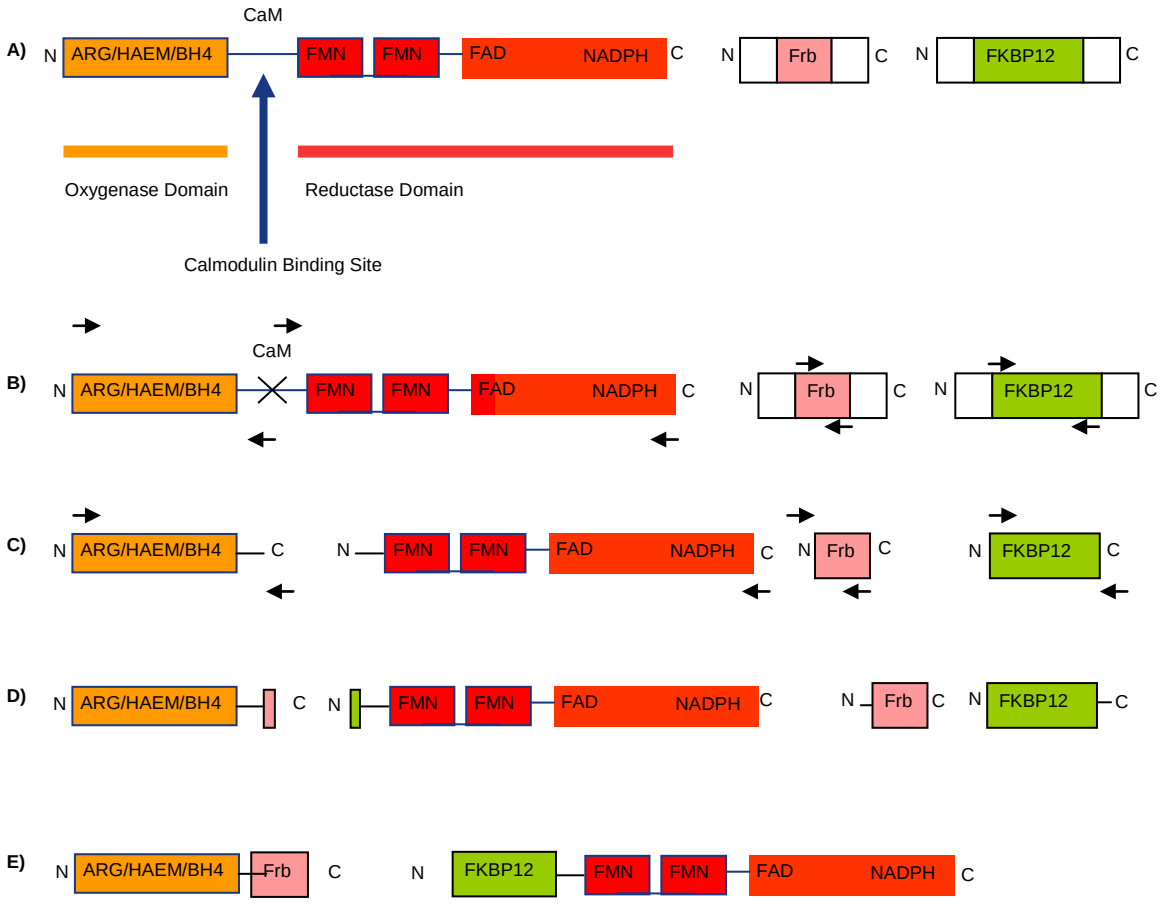

Figure 39 The strategy taken to create a rapamycin CID dependent eNOS. A) The eNOS gene and rapamycin CID system tags Frb and FKBP12 (within plasmid). B) Primer locations to clone out the Oxygenase and Reductase domains of eNOS separately as well as cloning of the CID tags. C) Amplification of the sequences created in B with extension primers complementary to gene fusion target. D) Resulting sequences from amplification shown in C; these sequences are now prepared for Gibson Assembly. E) Chimeric sequences created from Gibson assembly method for gene fusion. ARG: Arginine, HAEM (Iron Protoporphyrin IX Haem), FMN: Flavin Mononucleotide, FAD: Flavin Adenine Dinucleotide, NADPH: Nicotinamide Adenine Dinucleotide Phosphate. eNOS co-factor binding region data from Alderton *et al.* (Alderton et al., 2001)

The eNOS gene was obtained from the PEX_EF1-CFP_NOS3 plasmid purchased from ATCC and the plasmid Sequence is given in Sequence 9.

Sequence 9 The PEX_EF1-CFP_NOS3 plasmid sequence. Yellow: EF1 promoter. Orange: eNOS gene oxygenase domain. Burgundy: eNOS gene reductase domain. Green: CFP marker gene. Red: Kanamycin resistance gene.

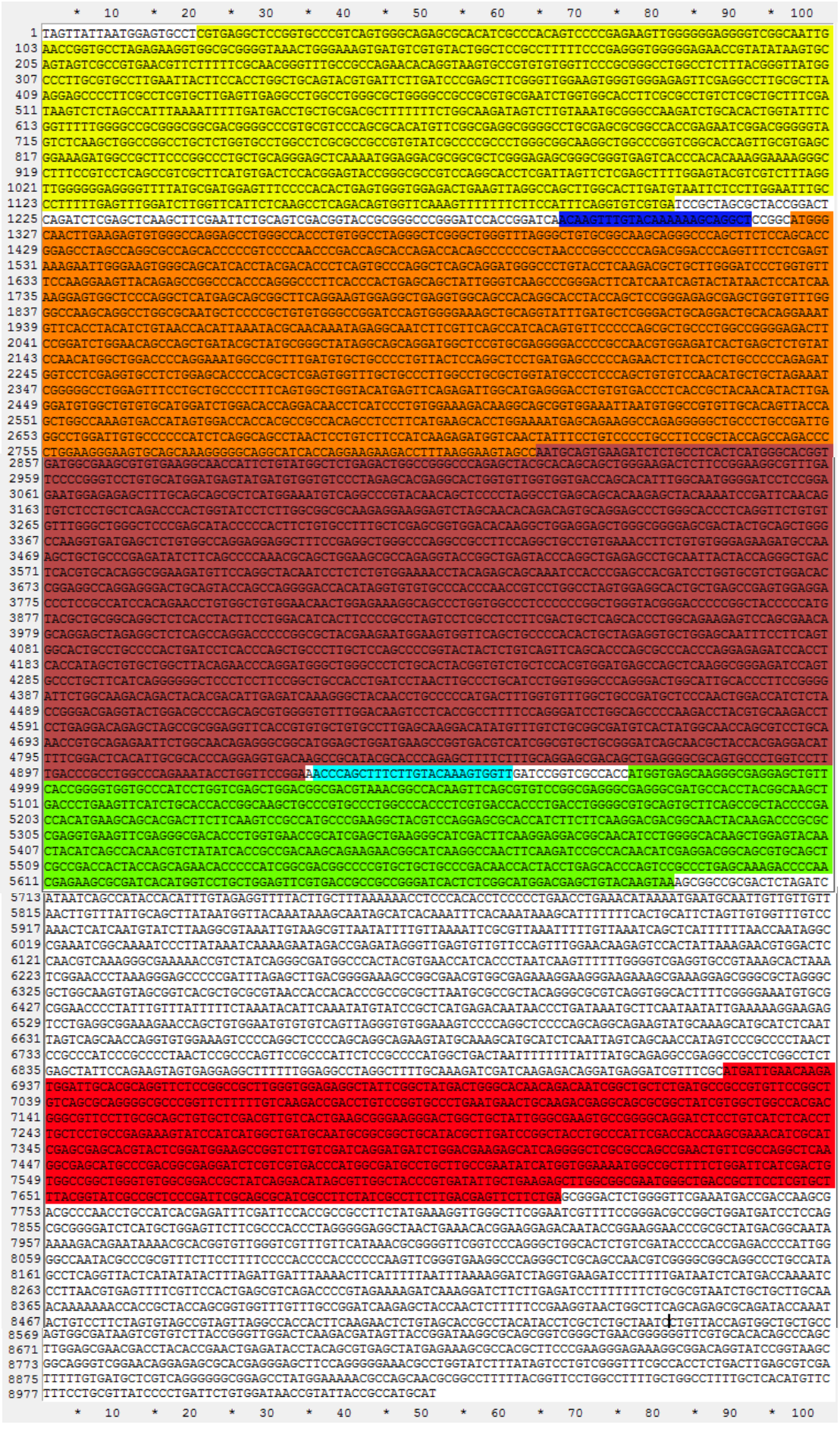

As shown in Figure 39, the strategy to form a chemo-sensitive eNOS involved splitting the eNOS gene into its oxygenase and reductase domains. This was done using the following primers:

DNA origin: PEX_EF1-CFP_NOS3

Oxygenase forward: CAACAAGTTTGTACAAAAAAGCAGGCTCCG

Oxygenase reverse: GAC CTT TAA GGA AGT AGC CAA TGC AGT GAA

Reductase forward: AAGGGGGCAGGCATCACCAGGAAG

Reductase reverse: GATCAACCACTTTGTACAAGAAAGCTGGGT

Following the splitting of eNOS, the two parts of the rapamycin CID system were amplified.

DNA origin: Frb-C-TEV plasmid.

Frb forward: GCCCACCATGGAGATGTGGCACGA

Frb reverse: GGTATCAGAGACCATGCTGCTCATGGA

Sequence 10 Frb Sequence from plasmid Frb-C-TEV. Blue: Frb DNA. Green: Linker

```
      *   10    *   20    *   30    *   40    *   50    *   60    *
  1 CCATGGAGATGTGGCACGAGGGACTCGAAGAGGCCAGCAGGCTGTACTTTGGCGAGAGGAACGTCA
 67 AGGGCATGTTCGAAGTGCTGGAGCCCCTCCATGCGATGATGGAAAGGGGCCCACAGACCCTGAAGG
133 AGACCAGCTTCAACCAGGCTTACGGCAGGGACCTGATGGAGGCACAGGAATGGTGCAGGAAGTACA
199 TGAAGAGCGGCAACGTGAAAGACCTGACCCAGGCGTGGGACCTCTACTACCACGTGTTCAGGAGGA
265 TCAGCAAGCAGGGAGGTGGCGGAAGCGGCGGTGGGGGAAGC
      *   10    *   20    *   30    *   40    *   50    *   60    *
```

DNA origin: FKBP-(GGGGS)x2-N-TEV

FKBP12 forward: GCCACCATGGGTGTGCAGGTAGAAACAATC

FKBP12 reverse: CCACCACCGTCGCCCCCTCCACCAAGGCCG

Sequence 11 FKBP12 Sequence from plasmid FKBP-(GGGGS)x2-N-TEV. Blue: Frb DNA. Green: Linker

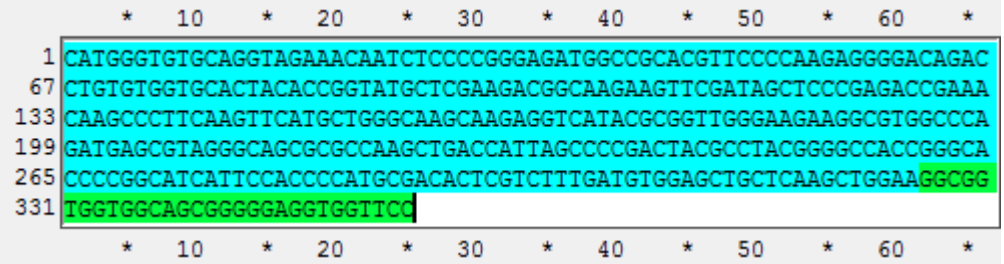

The purpose of these genetic amplifications is to create the following chimeras:

Sequence 12: The fused eNOS Oxygenase/Frb fragment. Orange: eNOS Oxygenase domain. Burgundy: eNOS reductase domain. Blue: Frb DNA. Green: Gly/Ser linker.

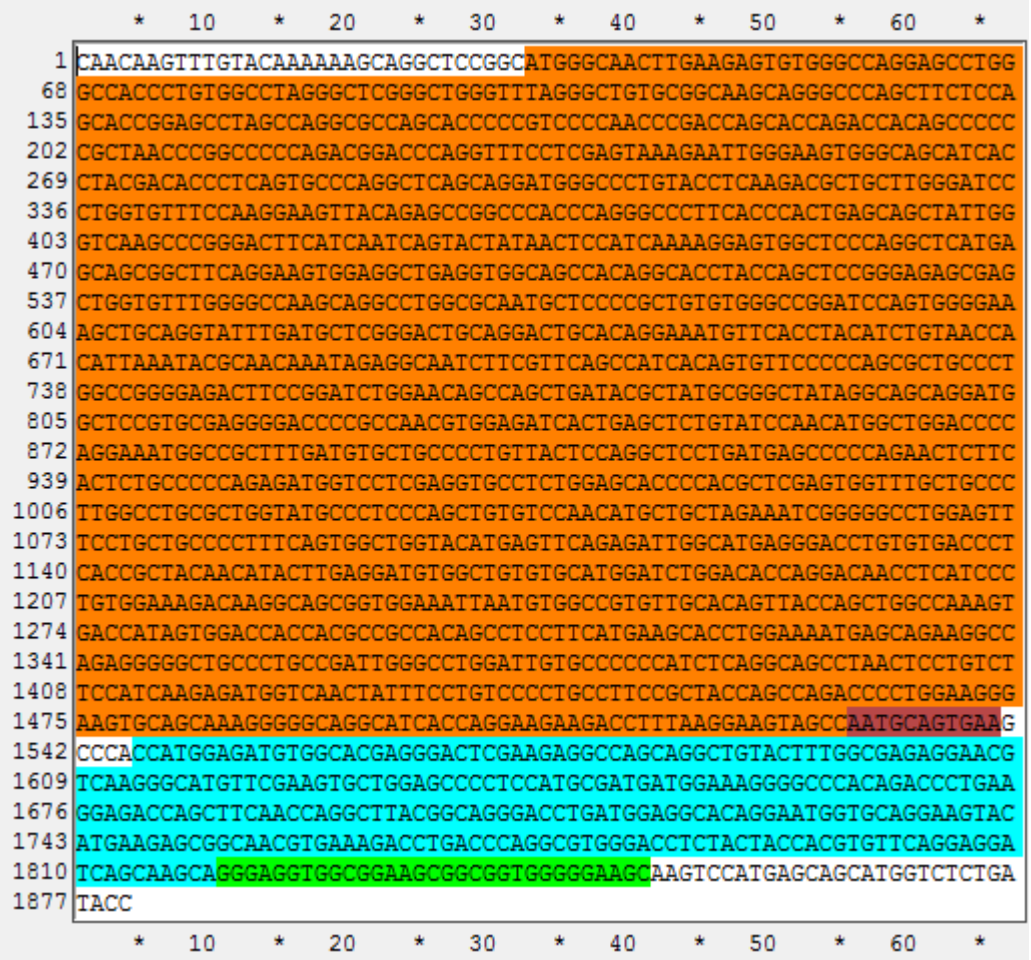

Sequence 13 eNOS Reductase/FKBP12 fragment. Orange: eNOS Oxygenase domain. Burgundy: eNOS reductase domain. Blue: FKBP12 DNA. Green: Gly/Ser linker.

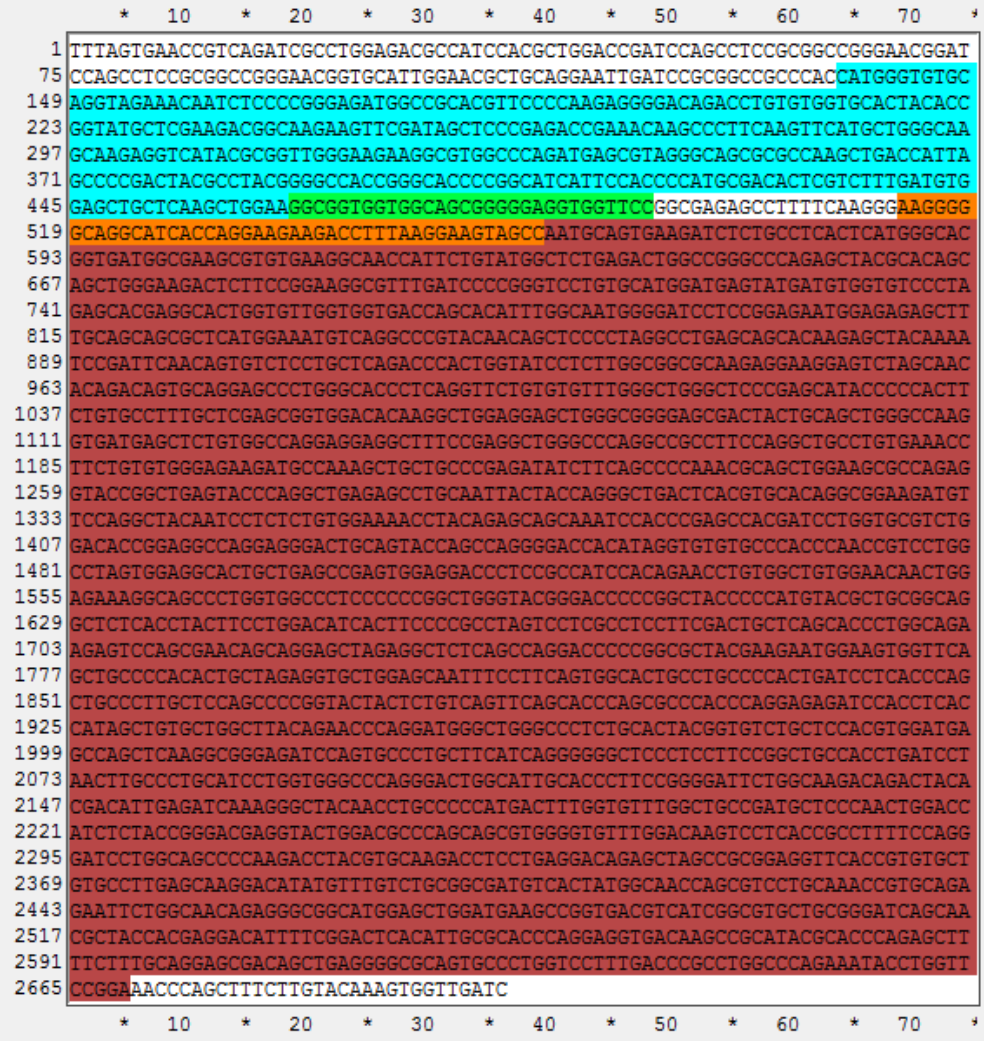

After successful cloning of all the target DNA fragments was proven *via* Gibson Assembly; PCR amplification using primers that target the flanking region of the assembled proto-chimeric DNA. The objective for this was to add Restriction Enzyme binding sites to permit ligation of the resulting chimeric DNA to a target plasmid multiple cloning site. The primers used to extend the sequences to allow plasmid integration (termed Ligation Primers with the abbreviation “Li”) were:

Forward Li Oxy: GGCCCGAGTCGACCAACAAGTTTGTACAAAAAAGCA
Reverse Li Oxy: AGCGGCCGCGGTATCAGAGACCAT
Forward Li Red: GCGGTCGACTTTAGTGAACCGTCAGATCGC
Reverse Li Red: AAGCGGCCGCACCACTTTGTACAAGAA

In order to produce the full target DNA sequences with the RE sites, the Oxygenase/FKBP12 chimera underwent PCR using the Forward Li Oxy and Reverse Li Oxy primers. The reductase domain was amplified using the Forward Li Red and Reverse Li Red primers. Upon completion of this further sequence extension, the

sequences were ready to undergo Restriction Enzyme digestion to render them complementary to the plasmid they will be inserted to.

The targeted plasmid for sequence ligation was PEX_EF1-CFP_NOS3 and the RE sites chosen permitted selection *via* fluorescence screening. The selected RE sites remove the CFP gene from the plasmid, whilst retaining Kanamycin resistance. Therefore colonies which survive on Kanamycin plates but do not fluoresce under 435 nm light will contain the desired mutation. In addition, the restriction sites targeted for plasmid integration are of two separate RE: AccI and HpaI. This is to circumvent the problem caused by the palindromic nature of RE sticky ends, a problem which leads to lack of control regarding the orientation of inserted DNA fragment. Therefore, different RE sites should be used and these should create dissimilar overhangs to prevent non-specific ligation.

4.2 Photo-inducible eNOS

In order to construct a light-induced mutant of eNOS, the LOV domain will be fused to the eNOS protein so as to produce NO upon light stimulus. By fusing LOV near FMN domains of eNOS it is expected that LOV's photo-dependent phosphorylation will lead to electron transfer from LOV to an FMN domain of eNOS. This electron would then travel along the eNOS natural electron transfer chain and reach the iron-haeme core where the catalytic activity takes place. Hence eNOS production of NO will be controlled by limiting it to a photoactive state. NO would only be produced when light at 385 nm wavelength is shone on the LOV domain of the chimeric eNOS, Figure 40.

As previously discussed in section 1.10 LOV domains have been shown to interact directly with FMN (flavin mononucleotides) by transferring an electron to FMN. This occurs when LOV is in an excited state and is in close enough proximity to the FMN molecule. As FMN is a constituent in the natural electron transfer chain of eNOS, the strategy in this thesis aims to hijack the ET chain and convert the system from dependence on a chemically active electron donor (NADPH) to a photoactivable electron donor (LOV). Genetic manipulation involved introducing an LOV domain in close proximity to the FMN domains of eNOS in one of three target sites, 3' from the FMN domains, 5' from the FMN domains and in between the two FMN domains. Multiple LOV introductions are also attempted. However there is a higher chance of failure as it will more extensively modify eNOS and therefore affect protein function in an unpredictable manner. The relationship between LOV and FMN has lead to the development of a family of FbFPs (FMN-based fluorescent proteins) which almost exclusively utilize blue light photoreceptors containing LOV domains.(Tielker, Eichhof, Jaeger, & Ernst, 2009) FbFPs are particularly useful as their fluorescence is oxygen independent allowing for the study of FMN even in anaerobic conditions, including anaerobic organisms.(Lobo, C. J. Smith, & E. R. Rocha, 2011)

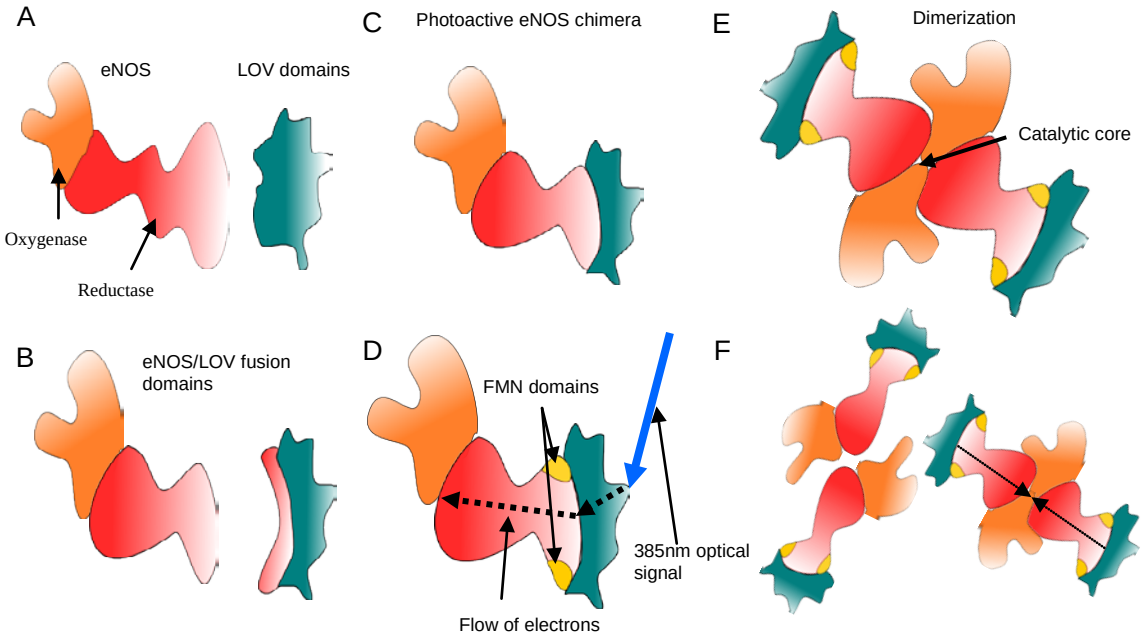

Figure 40 eNOS/LOV fusion strategy. A) The two proteins used to create the chimera - eNOS and LOV. eNOS oxygenase and reductase domains are represented by different colours. B) Fusion ready segments: eNOS with truncated reductase domain (removal of NADPH binding site) and LOV with eNOS matching overhang. C) After fusing the segments, a photoactive chimera of eNOS is created. D) Light at wavelength of 385nm drives autophosphorylation of the LOV domain. LOV can form a covalent bond with FMN in the phosphorylated state and therefore donate an electron to the FMN molecule. FMN is also a co-factor in the electron transfer (ET) eNOS enzyme. Due to its close proximity to the FMN domains of eNOS, it is postulated that the Light-activated LOV protein will donate electrons to the eNOS enzyme allowing for catalytic activity. E) eNOS works by forming dimer structures with a catalytic core. F) Using the novel eNOS/LOV chimera, it is proposed that NO production by eNOS will become completely NADPH independent and instead acquiring the ability to be Photo-activated due to the interaction of phosphorylated LOV with the eNOS reductase domain. Electron transfer direction illustrated with dotted arrow.

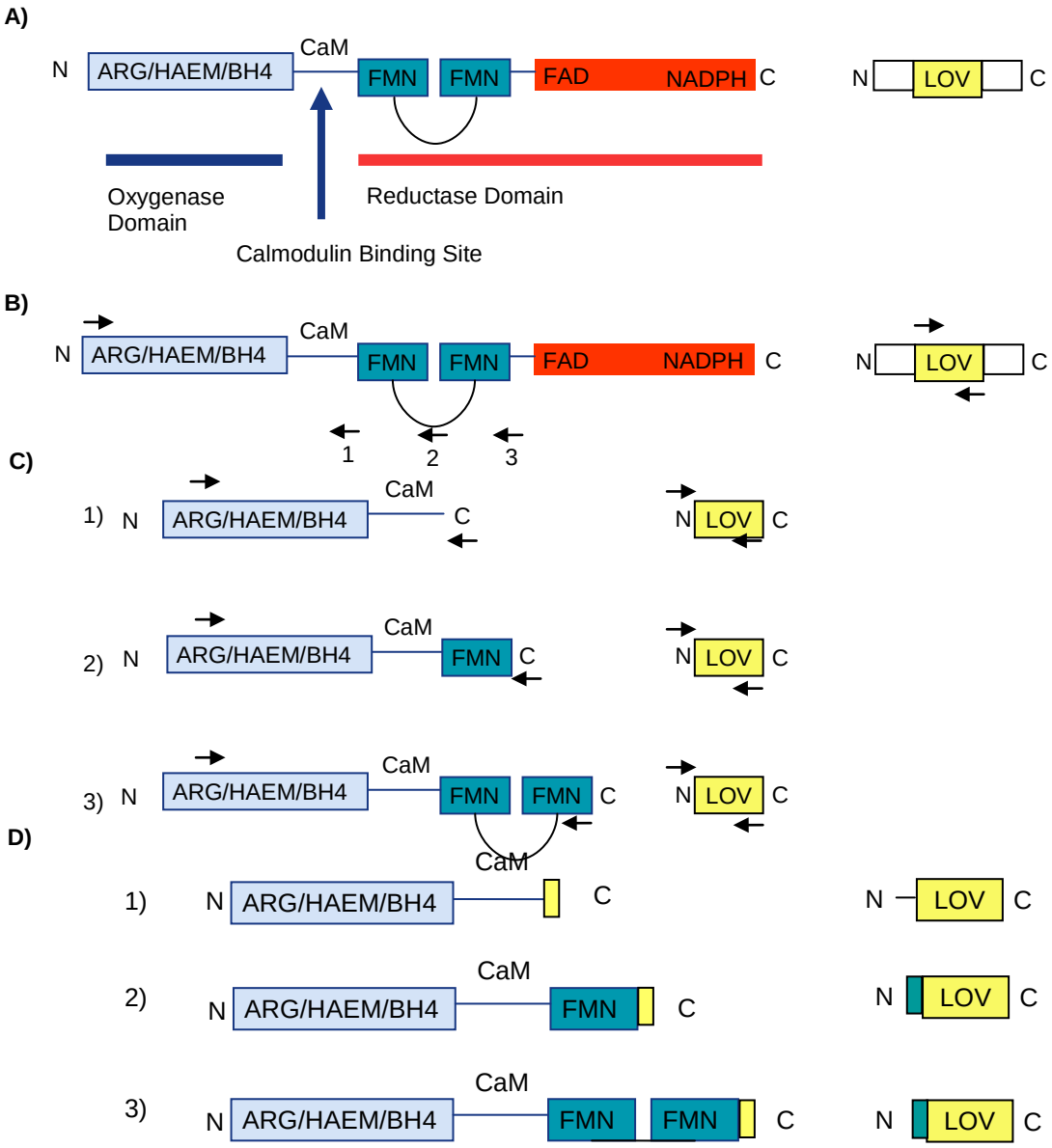
A)
N
ARG/HAEM/BH4
CaM
FMN
FMN
FAD
NADPH
C
N
LOV
C
Oxygenase Domain
Reductase Domain
Calmodulin Binding Site
B)
N
ARG/HAEM/BH4
CaM
FMN
FMN
FAD
NADPH
C
N
LOV
C
1
2
3
C)
1)
N
ARG/HAEM/BH4
CaM
C
N
LOV
C
2)
N
ARG/HAEM/BH4
CaM
FMN
C
N
LOV
C
3)
N
ARG/HAEM/BH4
CaM
FMN
FMN
C
N
LOV
C
D)
1)
N
ARG/HAEM/BH4
CaM
C
N
LOV
C
2)
N
ARG/HAEM/BH4
CaM
FMN
C
N
LOV
C
3)
N
ARG/HAEM/BH4
CaM
FMN
FMN
C
N
LOV
C

E)

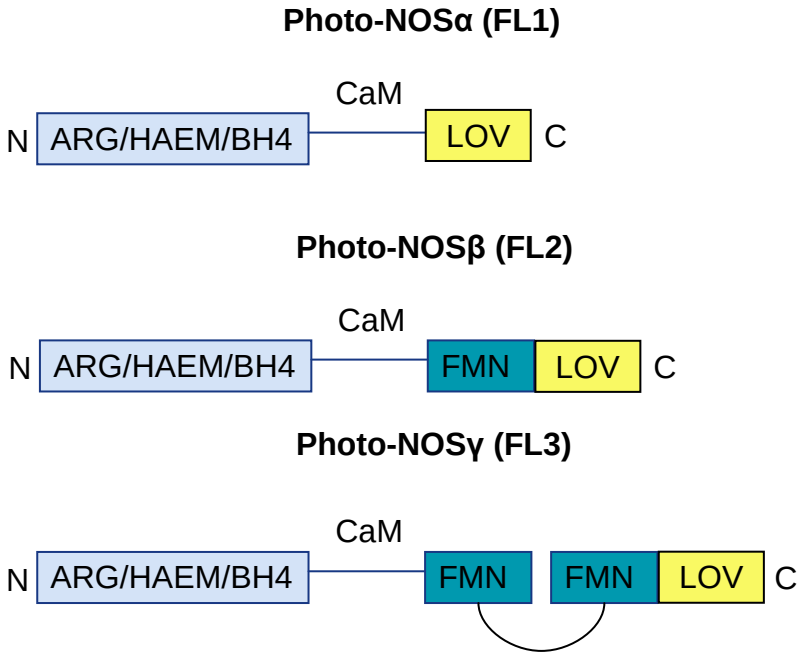

Figure 41 LOV insertion strategy for the formation of photoactivable eNOS. A) The eNOS gene with co-factor binding regions marked. B) Primer positions for PCR truncation of eNOS at proximal, distal and intermediate points of the FMN domains; Cloning out of LOV domains. C) The resulting truncations are then extended using primers to create a complementary region between the two fusion targets. D) The sequences created in C are prepared to undergo Gibson assembly. E) The resulting chimeric genes Photo-NOSα, β and γ (FL1, FL2, FL3). The expectation is that at one or more sites LOV excitation from photo stimulus will provide electron transfer to FMN thus allowing the protein to function independently of the presence of NADPH. ARG: Arginine, HAEM (Iron Protoporphyrin IX Haem), FMN: Flavin Mononucleotide, FAD: Flavin Adenine Dinucleotide, LOV: Light, Oxygen and Voltage, NADPH: Nicotinamide Adenine Dinucleotide Phosphate. eNOS co-factor binding region data from Alderton *et al.* (Alderton et al., 2001)

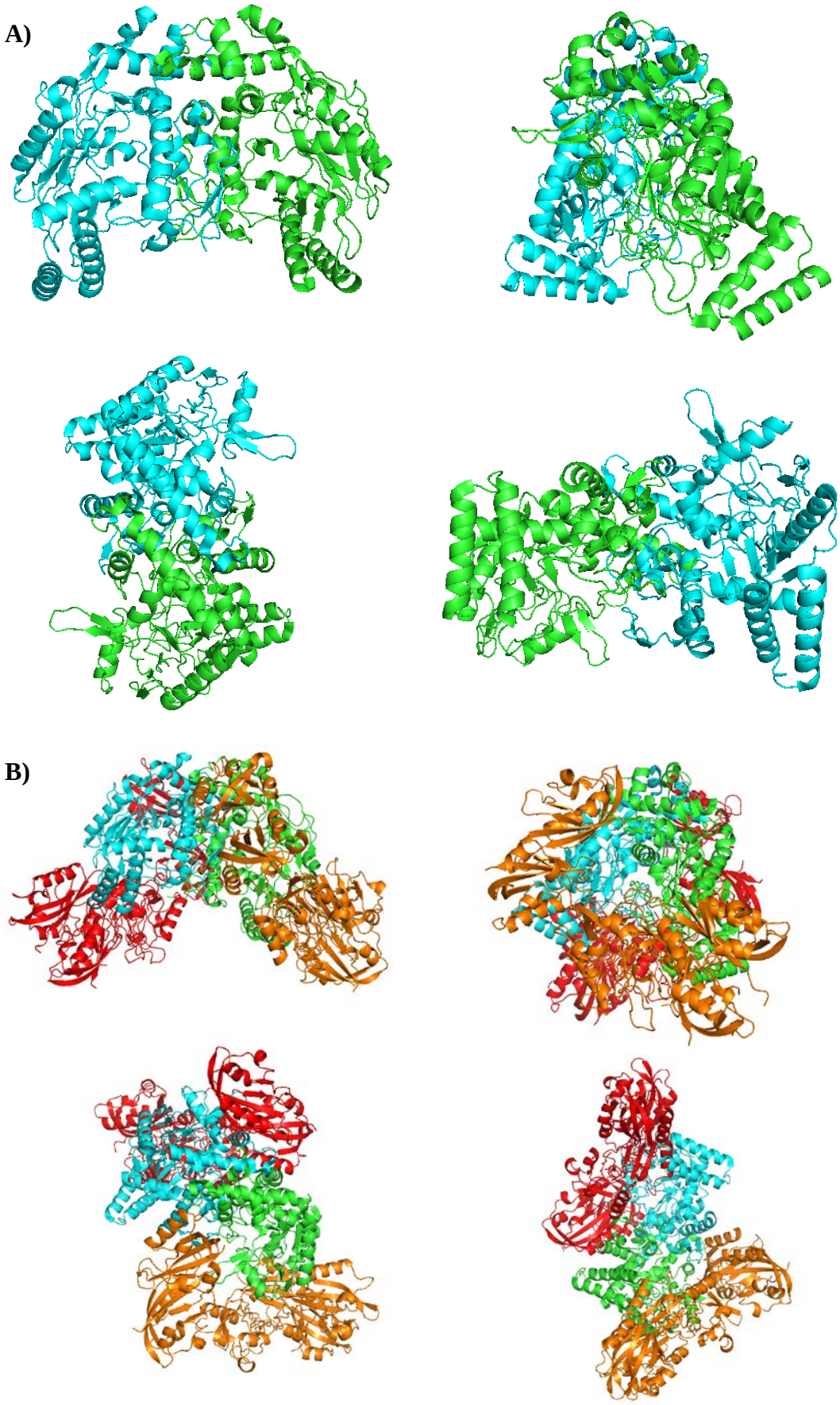

Figure 42 Multiple views of the hypothetical structure of the chimeric protein. A) An approximation of the truncation of eNOS into its oxygenase domain. B) The

addition of the LOV constructs and the most likely configuration of the resulting dimer. Green/Blue: individual chains of the eNOS dimer. Red/Orange: individual chains of LOV1/LOV2 as they form the dimer. Figure constructed using 1FOP, 2Z6D, 1JNU from PDB.

The aim of the proposed system is to hijack the natural eNOS electron transfer pathway and thereby drive NO production using electrons donated by excitation of LOV rather than NADPH binding. Figure 43 illustrates the proposed flow of electrons in the chimeric protein. The final electron donation creates the necessary charge to permit the conversion of L-arginine to citrulline.

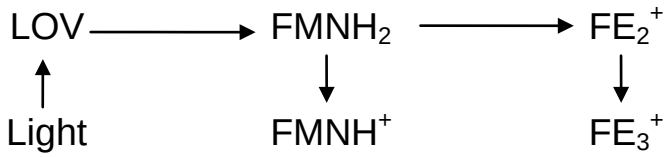

Figure 43 Expected flow of electrons in the eNOS/LOV chimera. LOV is phosphorylated by light at 385nm wavelength and in its excited state donates an electrode to $FMNH_2$. This is in turn donated to the Iron Haeme core where catalytic activity takes place and L-arginine is converted to L-citrulline.

By replacing the NADPH binding site of the eNOS protein with an upstream electron transfer chain electron donor the light activating strategy will effectively convert a chemically active protein into a photoactive analogue. The blue light receptor from *Avena sativa* contains two light oxygen voltage domains LOV1 and LOV2. These photoactive proteins are capable of transferring an electron to FMN domains upon excitation at a wavelength of 385 nm. Thus this design will remove the dependence of the eNOS protein on the chemical electron donor NADPH and substitute it for a photoactive electron donor, LOV1/2. FMN molecules are part of the natural electron transfer pathway of eNOS. In conjunction with other pathway co-factors they transfer the electron from the NADPH binding site through the FAD and tetrahydrobiopterin domains finally ending at the protoporphyrin IX core (where catalysis occurs). As the natural dimerization site of eNOS, the calmodullin binding region remains unaffected thus the expectation is that the protein will dimerize normally, with possible enhancement *via* induction of higher intracellular calcium levels.

The 3609bp eNOS gene was obtained from the PEX_EF1-CFP_NOS3 plasmid purchased from ATCC and originating from *Mus musculus*, sequence 15 LOV genes were obtained from the Nph1 gene contained in the pBABE-mpuro-CTET plasmid purchased from Addgene. Its origin is from the *Avena sativa* plant and its sequence is given in Sequence 16.

Sequence 15 The eNOS gene.

```
      *   10    *   20    *   30    *   40    *   50    *   60    *   70    *   80    *   90
    1 ATGGGCAACTTGAAGAGTGTGGGCCAGGAGCCTGGGCCACCCTGTGGCCTAGGGCTCGGGCTGGGTTTAGGGCTGTGCGGCAAGCAGGGCCCA
   94 GCCTCTCCAGCACCGGAGCCTAGCCAGGCGCCAGCACCCCCGTCCCCAACCCGACCAGCACCAGACCACAGCCCCCCGCTAACCCGGCCCCCA
  187 GACGGACCCAGGTTTCCTCGAGTAAAGAATTGGGAAGTGGGCAGCATCACCTACGACACCCTCAGTGCCCAGGCTCAGCAGGATGGGCCCTGT
  280 ACCTCAAGACGCTGCTTGGGATCCCTGGTGTTTCCAAGGAAGTTACAGAGCCGGCCCACCCAGGGCCCTTCACCCACTGAGCAGCTATTGGGT
  373 CAAGCCCGGGACTTCATCAATCAGTACTATAACTCCATCAAAAGGAGTGGCTCCCAGGCTCATGAGCAGCGGCTTCAGGAAGTGGAGGCTGAG
  466 GTGGCAGCCACAGGCACCTACCAGCTCCGGGAGAGCGAGCTGGTGTTTGGGGCCAAGCAGGCCTGGCGCAATGCTCCCCGCTGTGTGGGCCGG
  559 ATCCAGTGGGGAAAGCTGCAGGTATTTGATGCTCGGGACTGCAGGACTGCACAGGAAATGTTCACCTACATCTGTAACCACATTAAATACGCA
  652 ACAAATAGAGGCAATCTTCGTTCAGCCATCACAGTGTTCCCCCAGCGCTGCCCTGGCCGGGGAGACTTCCGGATCTGGAACAGCCAGCTGATA
  745 CGCTATGCGGGCTATAGGCAGCAGGATGGCTCCGTGCGAGGGGACCCCGCCAACGTGGAGATCACTGAGCTCTGTATCCAACATGGCTGGACC
  838 CCAGGAAATGGCCGCTTTGATGTGCTGCCCCTGTTACTCCAGGCTCCTGATGAGCCCCCAGAACTCTTCACTCTGCCCCCAGAGATGGTCCTC
  931 GAGGTGCCTCTGGAGCACCCCACGCTCGAGTGGTTTGCTGCCCTTGGCCTGCGCTGGTATGCCCTCCCAGCTGTGTCCAACATGCTGCTAGAA
 1024 ATCGGGGGCCTGGAGTTTCCTGCTGCCCCTTTCAGCGGCTGGTACATGAGTTCAGAGATTGGCATGAGGGACCTGTGTGACCCTCACCGCTAC
 1117 AACATACTTGAGGATGTGGCTGTGTGCATGGATCTGGACACCAGGACAACCTCATCCCTGTGGAAAGACAAGGCAGCGGTGGAAATTAATGTG
 1210 GCCGTGTTGCACAGTTACCAGCTGGCCAAAGTGACCATAGTGGACCACCACGCCGCCACAGCCTCCTTCATGAAGCACCTGGAAAATGAGCAG
 1303 AAGGCCAGAGGGGGCTGCCCTGCCGATTGGGCCTGGATTGTGCCCCCCATCTCAGGCAGCCTAACTCCTGTCTTCCATCAAGAGATGGTCAAC
 1396 TATTTCCTGTCCCCTGCCTTCCGCTACCAGCCAGACCCCTGGAAGGGAAGTGCAGCAAAGGGGGCAGGCATCACCAGGAAGAAGACCTTTAAG
 1489 GAAGTAGCCAATGCAGTGAAGATCTCTGCCTCACTCATGGGCACGGTGATGGCGAAGCGTGTGAAGGCAACCATTCTGTATGGCTCTGAGACT
 1582 GGCCGGGCCCAGAGCTACGCACAGCAGCTGGGAAGACTCTTCCGGAAGGCGTTTGATCCCCGGGTCCTGTGCATGGATGAGTATGATGTGGTG
 1675 TCCCTAGAGCACGAGGCACTGGTGTTGGTGGTGACCAGCACATTTGGCAATGGGGATCCTCCGGAGAATGGAGAGAGCTTTGCAGCAGCGCTC
 1768 ATGGAAATGTCAGGCCCGTACAACAGCTCCCCTAGGCCTGAGCAGCACAAGAGCTACAAAATCCGATTCAACAGTGTCTCCTGCTCAGACCCA
 1861 CTGGTATCCTCTTGGCGGCGCAAGAGGAAGGAGTCTAGCAACACAGACAGTGCAGGAGCCCTGGGCACCCTCAGGTTCTGTGTGTTTGGGCTG
 1954 GGCTCCCGAGCATACCCCCACTTCTGTGCCTTTGCTCGAGCGGTGGACACAAGGCTGGAGGAGCTGGGCGGGGAGCGACTACTGCAGCTGGGC
 2047 CAAGGTGATGAGCTCTGTGGCCAGGAGGAGGCTTTCCGAGGCTGGGCCCAGGCCGCCTTCCAGGCTGCCTGTGAAACCTTCTGTGTGGGAGAA
 2140 GATGCCAAAGCTGCTGCCCGAGATATCTTCAGCCCCAAACGCAGCTGGAAGCGCCAGAGGTACCGGCTGAGTACCCAGGCTGAGAGCCTGCAA
 2233 TTACTACCAGGGCTGACTCACGTGCACAGGCGGAAGATGTTCCAGGCTACAATCCTCTCTGTGGAAAACCTACAGAGCAGCAAATCCACCCGA
 2326 GCCACGATCCTGGTGCGTCTGGACACCGGAGGCCAGGAGGGACTGCAGTACCAGCCAGGGGACCACATAGGTGTGTGCCCACCCAACCGTCCT
 2419 GGCCTAGTGGAGGCACTGCTGAGCCGAGTGGAGGACCCTCCGCCATCCACAGAACCTGTGGCTGTGGAACAACTGGAGAAAGGCAGCCCTGGT
 2512 GGCCCTCCCCCCGGCTGGGTACGGGACCCCCGGCTACCCCCATGTACGCTGCGGCAGGCTCTCACCTACTTCCTGGACATCACTTCCCCGCCT
 2605 AGTCCTCGCCTCCTTCGACTGCTCAGCACCCTGGCAGAAGAGTCCAGCGAACAGCAGGAGCTAGAGGCTCTCAGCCAGGACCCCCGGCGCTAC
 2698 GAAGAATGGAAGTGGTTCAGCTGCCCCACACTGCTAGAGGTGCTGGAGCAATTTCCTTCAGTGGCACTGCCTGCCCCACTGATCCTCACCCAG
 2791 CTGCCCTTGCTCCAGCCCCGGTACTACTCTGTCAGTTCAGCACCCAGCGCCCACCCAGGAGAGATCCACCTCACCATAGCTGTGCTGGCTTAC
 2884 AGAACCCAGGATGGGCTGGGCCCTCTGCACTACGGTGTCTGCTCCACGTGGATGAGCCAGCTCAAGGCGGGAGATCCAGTGCCCTGCTTCATC
 2977 AGGGGGGCTCCCTCCTTCCGGCTGCCACCTGATCCTAACTTGCCCTGCATCCTGGTGGGCCCAGGGACTGGCATTGCACCCTTCCGGGGATTC
 3070 TGGCAAGACAGACTACACGACATTGAGATCAAAGGGCTACAACCTGCCCCCATGACTTTGGTGTTTGGCTGCCGATGCTCCCAACTGGACCAT
 3163 CTCTATCGGGACGAGGTACTGGACGCCCAGCAGCGTGGGGTGTTTGGACAAGTCCTCACCGCCTTTTCCAGGGATCCTGGCAGCCCCAAGACC
 3256 TACGTGCAAGACCTCCTGAGGACAGAGCTAGTCGCGGAGGTTCACCGTGTGCTGTGCCTTGAGCAAGGACATATGTTTGTCTGCGGCGATGTC
 3349 ACTATGGCAACCAGCGTCCTGCAAACCGTGCAGAGAATTCTGGCAACAGAGGGCGGCATGGAGCTGGATGAAGCCGGTGACGTCATCGGCGTG
 3442 CTGCGGGATCAGCAACGCTACCACGAGGACATTTTCGGACTCACATTGCGCACCCAGGAGGTGACAAGCCGCATACGCACCCAGAGCTTTTCT
 3535 TTGCAGGAGCGACAGCTGAGGGGCGCAGTGCCCTGGTCCTTTGACCCGCCTGGCCCAGAAATACCTGGTTCCTGA
      *   10    *   20    *   30    *   40    *   50    *   60    *   70    *   80    *   90
```

Sequence 16 The NhpI gene.

```
      *   10    *   20    *   30    *   40    *   50    *   60    *   70
    1 TTGGCTACTACACTTGAACGTATTGAGAAGAACTTTGTCATTACTGACCCAAGATTGCCAGATAATCCCA
   71 TTATATTCGCGTCCGATAGTTTCTTGCAGTTGACAGAATATAGCCGTGAAGAAATTTTGGGAAGAAACTG
  141 CAGGTTTCTACAAGGTCCTGAAACTGATCGCGCGACAGTGAGAAAAATTAGAGATGCCATAGATAACCAA
  211 ACAGAGGTCACTGTTCAGCTGATTAATTATACAAAGAGTGGTAAAAAGTTCTGGAACCTCTTTCACTTGC
  281 AGCCTATGCGAGATCAGAAGGGAGATGTCCAGTACTTTATTGGGGTTCAGTTGGATGGAACTGAGCATGT
  351 CCGAGATGCTGCCGAGAGAGAGGGAGTCATGCTGATTAAGAAAACTGCAGAAAATATTGATGAGGCGGCA
      *   10    *   20    *   30    *   40    *   50    *   60    *   70
```

Primers were initially designed to truncate the eNOS gene at three different points in the sequence. The strategy was planned so that the protein could be truncated at points proximal, intermediate and distal to the FMN binding domain, which allows for two separate experiments. The first of these relates to the possibility of eNOS photoactivation *via* the eNOS-LOV chimera. Secondly, the use of the eNOS protein truncated at the proximal region of the FMN binding domains which excludes these domains from the sequence will serve as a confirmation that LOV can photoactivate the eNOS protein only in the proximity of an FMN molecule to which it may donate an electron. FMN serves as an electron transfer co-factor in the electron transfer chain of native eNOS.

The FMN domain binding region of eNOS is given in Sequence 17. This Sequence is located 1536 bp downstream from the start site of the eNOS gene and runs until 2166 bp. Truncations to the eNOS protein will be centred around this region of DNA. The sequences created to serve the purposes discussed are given in sequences 18-20, where the oxygenase domain is depicted in orange and the reductase domain in purple.

Sequence 17 The FMN binding region of eNOS.

```
        *   10    *   20    *   30    *   40    *   50    *   60    *
  1 ATGGCGAAGCGTGTGAAGGCAACCATTCTGTATGGCTCTGAGACTGGCCGGGCCCAGAGCTACGCA
 67 CAGCAGCTGGGAAGACTCTTCCGGAAGGCGTTTGATCCCCGGGTCCTGTGCATGGATGAGTATGAT
133 GTGGTGTCCCTAGAGCACGAGGCACTGGTGTTGGTGGTGACCAGCACATTTGGCAATGGGGATCCT
199 CCGGAGAATGGAGAGAGCTTTGCAGCAGCGCTCATGGAAATGTCAGGCCCGTACAACAGCTCCCCT
265 AGGCCTGAGCAGCACAAGAGCTACAAAATCCGATTCAACAGTGTCTCCTGCTCAGACCCACTGGTA
331 TCCTCTTGGCGGCGCAAGAGGAAGGAGTCTAGCAACACAGACAGTGCAGGAGCCCTGGGCACCCTC
397 AGGTTCTGTGTGTTTGGGCTGGGCTCCCGAGCATACCCCCACTTCTGTGCCTTTGCTCGAGCGGTG
463 GACACAAGGCTGGAGGAGCTGGGCGGGGAGCGACTACTGCAGCTGGGCCAAGGTGATGAGCTCTGT
529 GGCCAGGAGGAGGCTTTCCGAGGCTGGGCCCAGGCCGCCTTCCAGGCTGCCTGTGAAACCTTCTGT
595 GTGGGAGAAGATGCCAAAGCTGCTGCCCGAGATATC
        *   10    *   20    *   30    *   40    *   50    *   60    *
```

Sequence 18 The first truncation of eNOS based on FMN domain location. Orange: eNOS Oxygenase domain. eNOS Burgundy: Reductase domain.

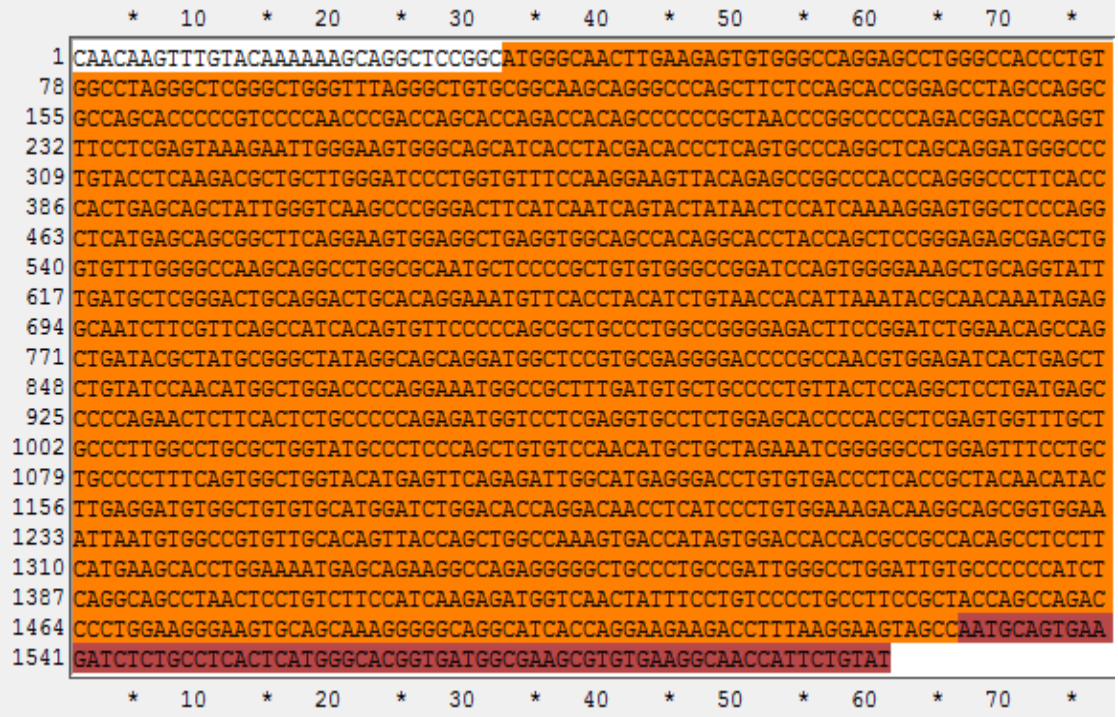

Sequence 19 The second truncation of eNOS based on FMN binding domain locations. Orange: eNOS Oxygenase domain. Burgundy: eNOS Reductase domain.

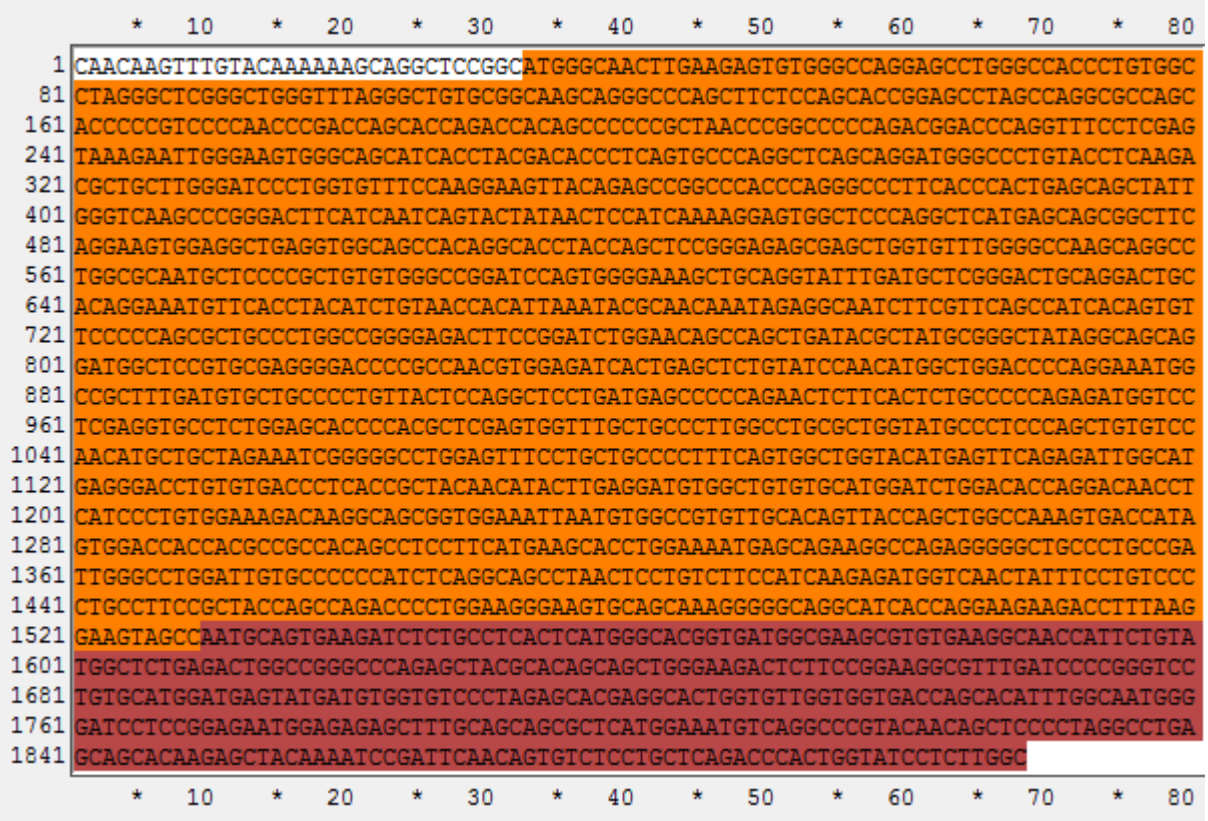

Sequence 20 The third truncation of eNOS based on FMN binding domain locations. Orange: eNOS Oxygenase domain. Burgundy: eNOS Reductase domain.

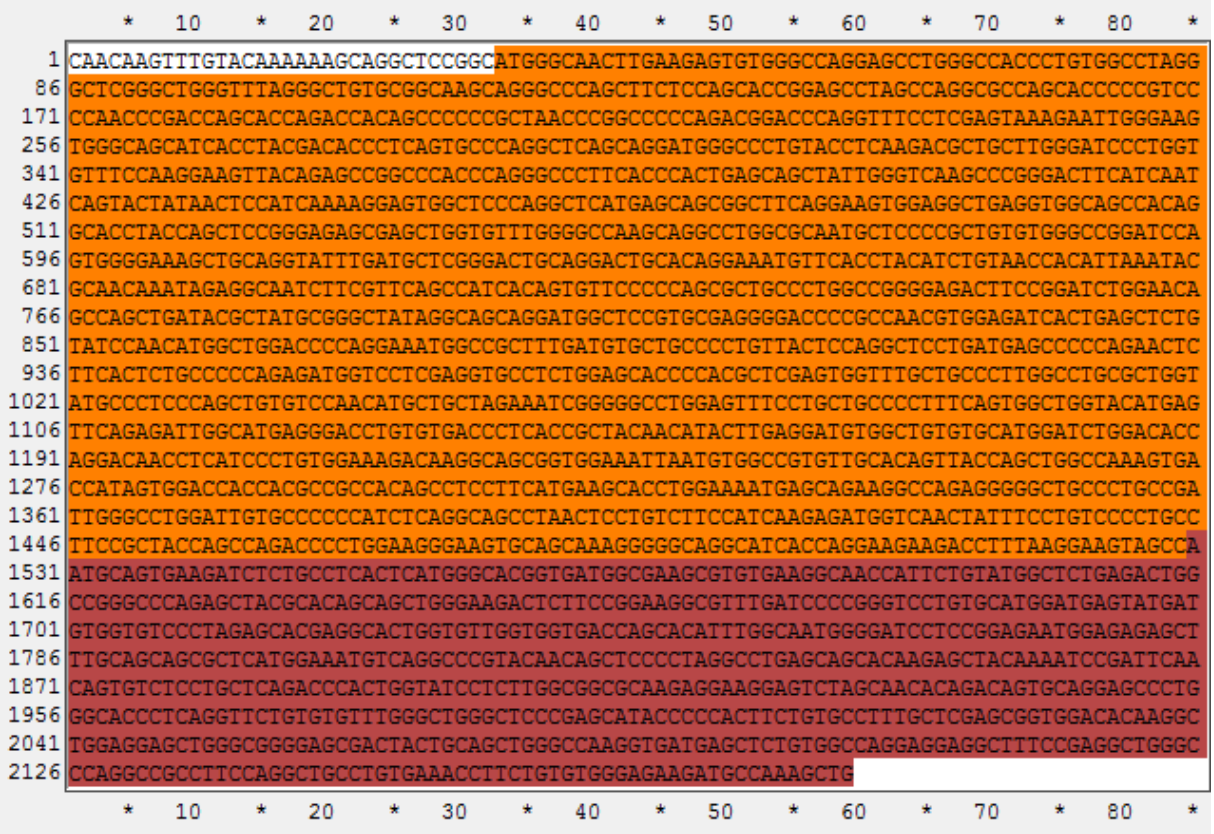

The forward primer for all eNOS sequences is identical as the truncation event occurs at a distance from the 5' region of the gene. The reverse primers (all eNOS FMN primers) are designed to truncate the gene at different points.

eNOS forward: CAACAAGTTTGTACAAAAAAGCAGGCTCCG

eNOS FMN 1: ATACAGAATGGTTGCCTTCACACGCTT
eNOS FMN 2: GCCAAGAGGATACCAGTGGGTCTGAGC
eNOS FMN 3: CAGCTTTGGCATCTTCTCCCACACAGA

LOV forward: AGGGTTCTGGAAGTGGATCTTTGGCTA

LOV reverse: CGGATCCAAGTTCTTTTGCCGCCTCAT

Sequence 21: LOV cloning. Blue: NhpI gene (containing LOV1-2 domains)

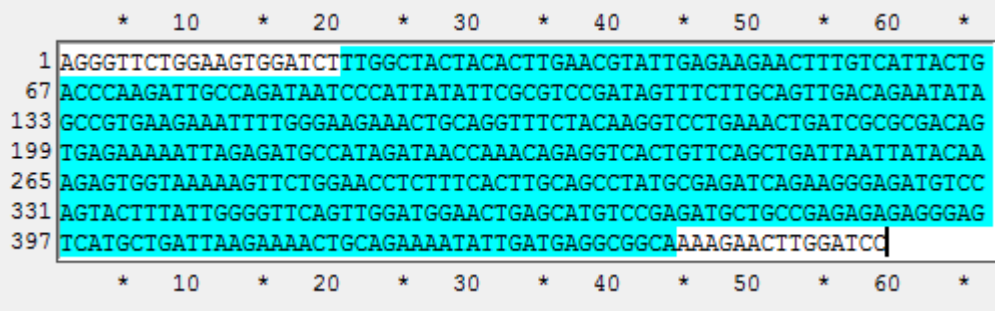

Following successful cloning of the truncated eNOS sequence, primers were designed to extend the fragments so as to allow Gibson ligation to occur and to insert a restriction enzyme binding site:

Forward Li Oxy: GGCCCGAGTCGACCAACAAGTTTGTACAAAAAAGCA

FMN1-LOV FUS: CACTTCCAGAACCCTATACAGAATGGTTGCCTT

FMN2-LOV FUS: TTCCAGAACCCTGCCAAGAGGATACCA

FMN3-LOV FUS: CACTTCCAGAACCCTCAGCTTTGGCATCTT

LOV-FMN1 FUS: GCAACCATTCTGTATAGGGTTCTGGAAGTGGATCTT

LOV-FMN2 FUS: TATCCTCTTGGCAGGGTTCTGGAAGTGGAT

LOV-FMN3 FUS: ATGCCAAAGCTGAGGGTTCTGGAAGTG

LOV Ligation: GTTAACATCCAAGTTCTTTTGCCGCCTCATCAA

Ligation primers contained a RE binding site which will be used to ligate the sequence to the plasmid multiple cloning site. FUS primers are used to extend the target sequences with a sequence complementary to that of the second fusion sequence. As an example, for truncated eNOS-LOV chimera 1, the oxygenase ligation primer was used as a forward primer for the truncated eNOS sequence with the FMN1-LOV FUS primer as its reverse. The LOV sequence used LOV-FMN1 FUS as its forward primer and the LOV ligation primer as its reverse. The same concept was used for all the chimeras

formed. The sequences generated by the truncated eNOS-LOV fusion are given in sequences 22-24.

Sequence 22 The first eNOS-LOV chimeric gene. Orange: eNOS Oxygenase domain. Burgundy: eNOS reductase domain. Blue: LOV domains.

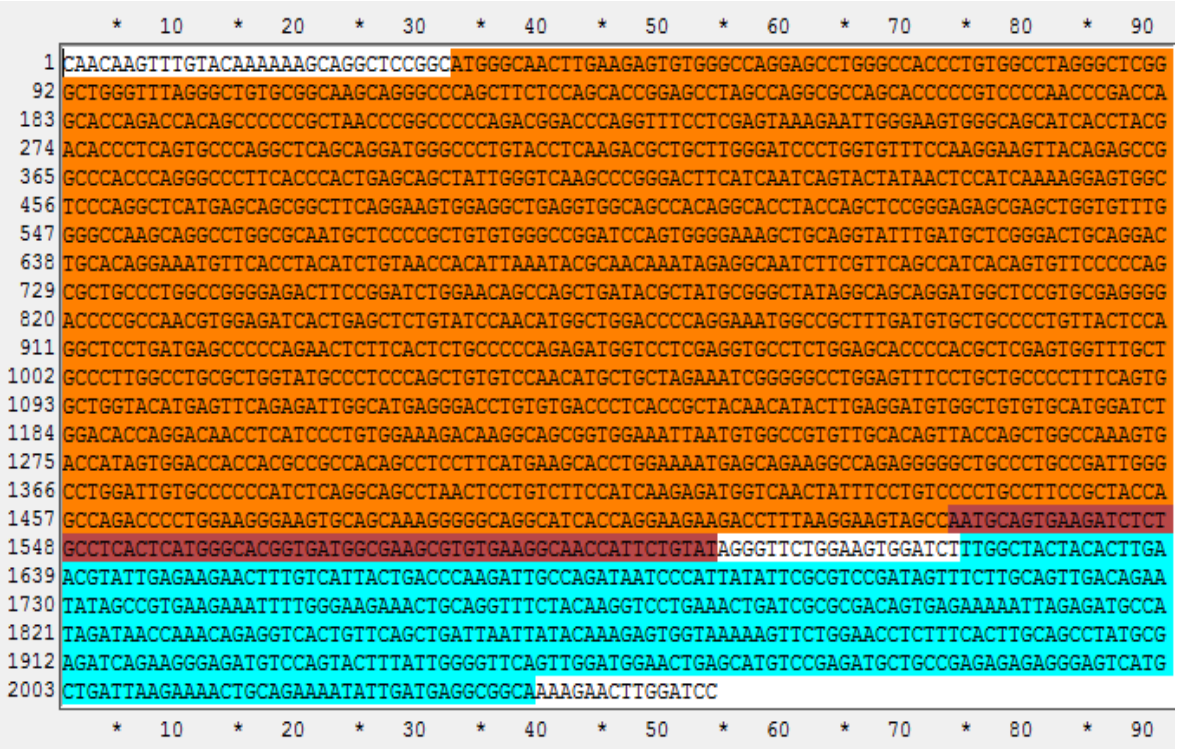

Sequence 23 The second eNOS-LOV chimeric gene. Orange: eNOS Oxygenase domain. Burgundy: eNOS reductase domain. Blue: LOV domains.

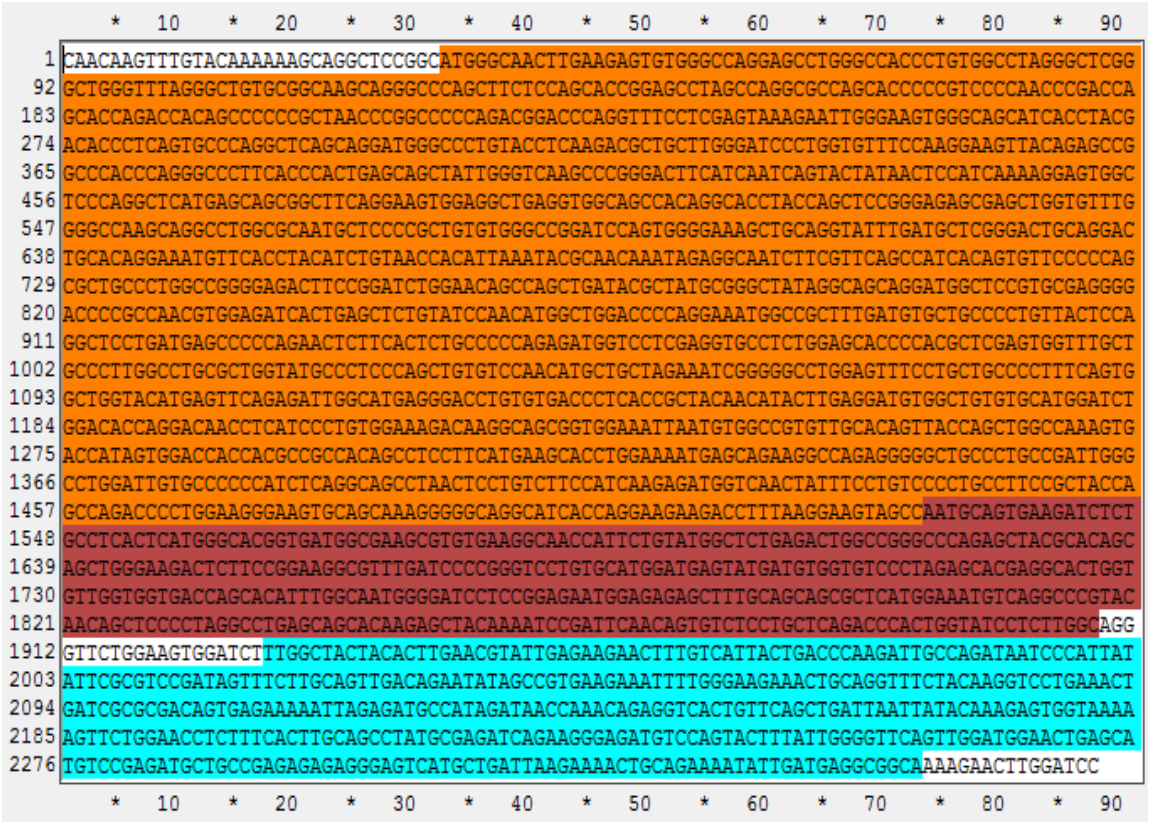

Sequence 24 The third eNOS-LOV chimeric gene. Orange: eNOS Oxygenase domain. Burgundy: eNOS reductase domain. Blue: LOV domains.

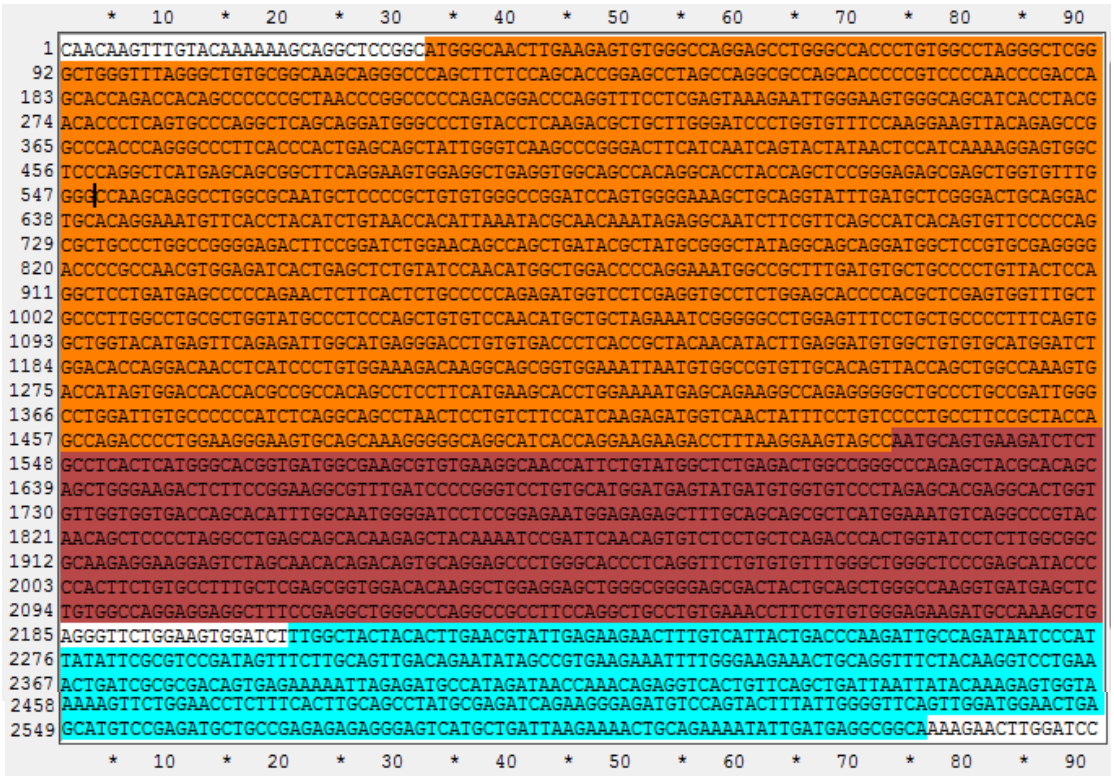

4.3 PCR Results

The ladder used to identify fragment size in kB throughout the results presented in this section was the NEB 1kb ladder, Figure 44. As can be seen in Figure 45, optimized PCR is highly efficient with samples 1-8 showing a product of the expected size. A slight shift is observed from left to right. However this is due to uneven gel morphology and is not reflective of the sequence size. Previous attempts using different settings, such as reduced final extension time or lower annealing temperature resulted in a less successful product with fewer or no samples yielding the desired product. Settings for the optimized PCR are as follows, with PCR cycles performed between steps two and step five for a total of thirty cycles.

1. 98 ºC - 30s
2. 98 ºC - 10s
3. 72 ºC - 60s
4. 62 ºC - 60s
5. 58 ºC - 60s
6. 72 ºC - 240s

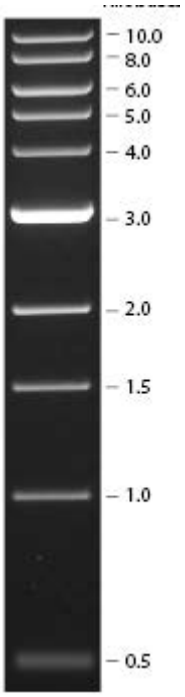

Figure 44 The NEB 1kB ladder. The bands result from the digestion of an especially designed plasmid digested with appropriate restriction enzymes. This provides a marker with known bp size. Sizes shown are in kB.

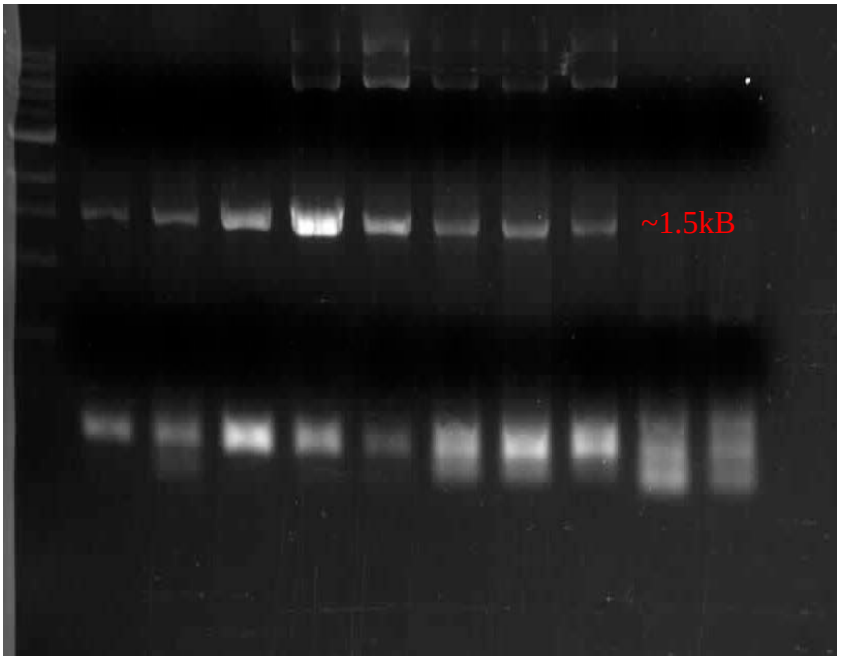

Figure 45 Result of optimized PCR for synthesis of the eNOS oxygenase domain sequence. The expected fragment size is 1540 bp and as can be seen in the image, the band is at the 1.5 kB marker. PCR was performed as described above the figure using the plasmid PEX_EF1-CFP_NOS3.

Different conditions were used to obtain the eNOS reductase domain. Although several conditions were used in the thermal cycles, none were found to be optimal and yield of target DNA was lower than in the case of the oxygenase domain.

1. 98 ºC - 30s
2. 98 ºC - 10s
3. 66 ºC - 60s
4. 64 ºC - 60s
5. 62 ºC - 60s
6. 58 ºC - 60s
7. 72 ºC - 240s

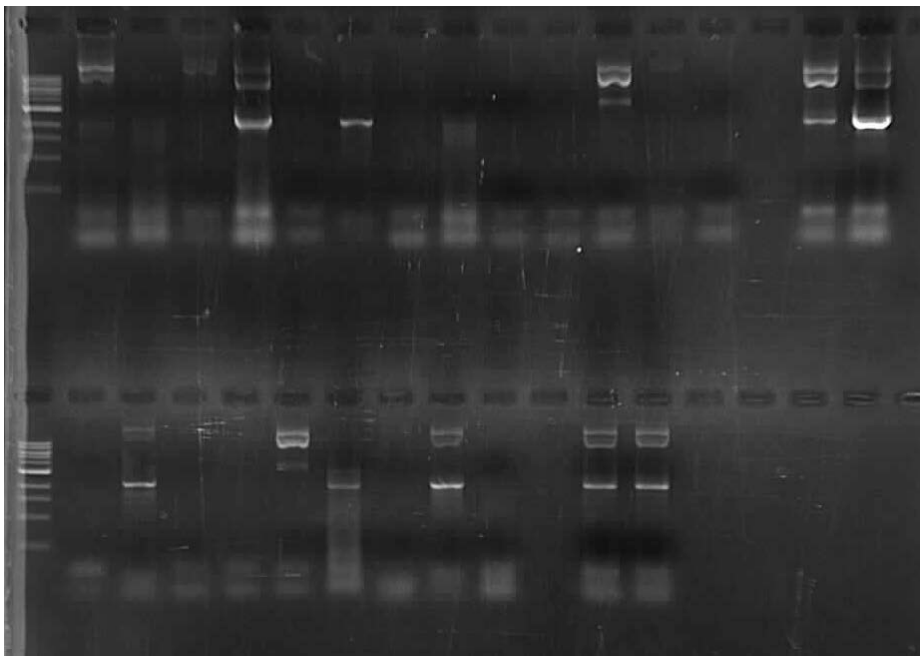

Figure 46 The result of several batches of PCR towards the amplification of the reductase domain of eNOS. Several miniprep products of transfected, grown *E. coli* were used. The target product at an approximate size of 2.2KB can be found through several lanes of the pictured gel. PCR was performed as described above the figure using the plasmid PEX_EF1-CFP_NOS3.

For the 355bp FKBP12 fragment, obtained from the plasmid FKBP-(GGGGS)x2-N-TEV, the following conditions were found to be optimal. PCR cycles were performed between steps two and step six for a total of thirty cycles.

1. 98 ºC - 30s
2. 98 ºC - 10s
3. 72 ºC - 30s
4. 70 ºC - 30s
5. 68 ºC - 30s
6. 64 ºC - 60s
7. 72 ºC - 420s

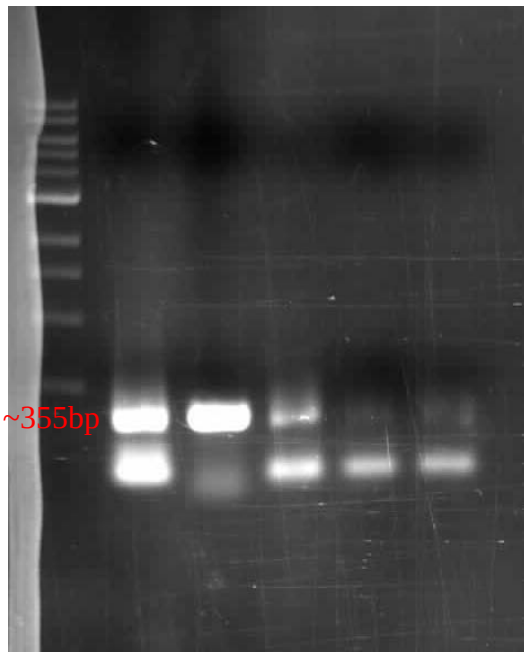

Figure 47 The 355bp fragment resulting from the PCR of the FKBP12. PCR was performed as described above the figure using the plasmid FKBP-(GGGGS)x2-N-TEV. The 304bp band can be seen in all samples, but stronger bands (higher concentration of DNA) are found in the first and second samples.

The 304bp fragment Frb was successfully amplified using the following PCR procedure. PCR cycles were performed between steps two and step six for a total of thirty cycles.

1. 98 ºC - 30s
2. 98 ºC - 10s
3. 64 ºC - 45s
4. 60 ºC - 45s
5. 72 ºC - 60s
6. 72 ºC - 420s

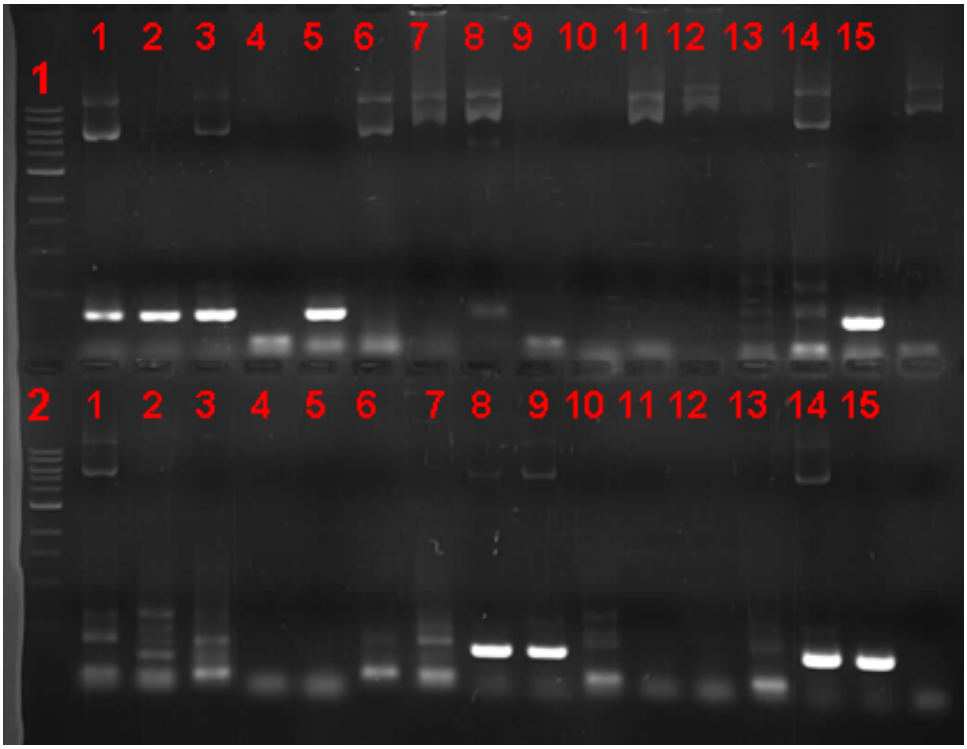

Figure 48 Results from several PCR batches to obtain the 304bp Frb fragment. Successfully amplified sequences can be found in: 1: 1-3, 5, 8, 15 2: 8, 9, 14-15. PCR was performed as described above the figure using the plasmid Frb-C-TEV.

Once all of the appropriate fragments had been obtained, Touchdown PCR was performed to amplify sequences with the appropriate extensions for Gibson Assembly. Cycles occur between steps two and ten for a total of thirty cycles.

Touchdown PCR:

1:

1. 98 ºC - 30s
2. 98 ºC - 10s
3. 70 ºC - 30s
4. 68 ºC - 30s
5. 66 ºC - 30s
6. 64 ºC - 30s
7. 62 ºC - 30s
8. 60 ºC - 30s
9. 58 ºC - 30s
10. 72 ºC - 30s

11. 72 ºC - 420s

2:

1. 98 ºC - 30s
2. 98 ºC - 10s
3. 72 ºC - 30s
4. 70 ºC - 30s
5. 68 ºC - 30s
6. 66 ºC - 30s
7. 64 ºC - 30s
8. 62 ºC - 30s
9. 60 ºC - 30s
10. 72 ºC - 420s

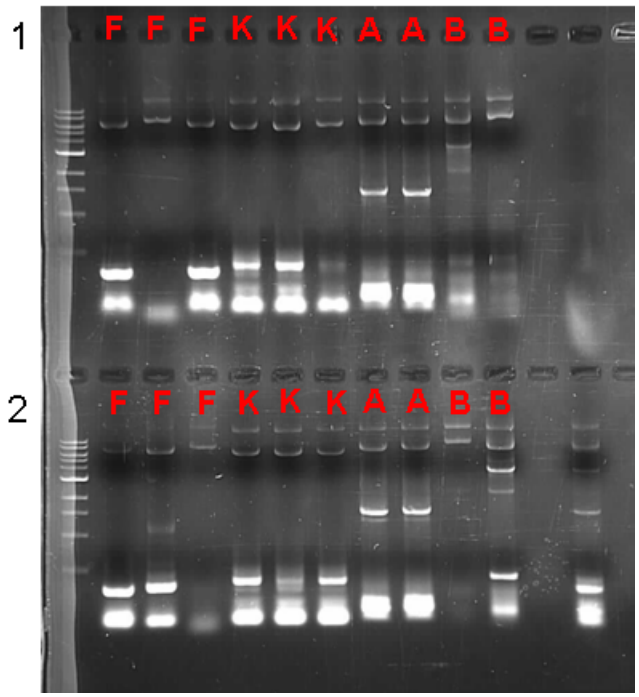

Figure 49 Results of Touchdown PCR to obtain extended fragments. A) eNOS oxygenase domain. B) eNOS reductase domain. F) Frb fragment K) FKBP12 fragment. PCR conditions are as those described above and the plasmids used for PCR are: A) PEX_EF1-CFP_NOS3 B) PEX_EF1-CFP_NOS3 F) Frb-C-TEV K) FKBP-(GGGGS)x2-N-TEV.

The fidelity of the produced fragments was verified using Gibson Assembly. Results of this experiment can be found in the appropriate section (4.4). Successful fusion verified the compatibility of the fragments. Following this step, the fragments were extended so as to include binding sites for the appropriate restriction enzymes, so as to allow plasmid integration.

4.4 Gibson Assembly.

Gibson assembly was used for two purposes, to verify whether extended sequences were correctly formed, and to fuse the sequences so as to create the chimeric gene. Gibson Assembly was performed as described in section 2.4.9.

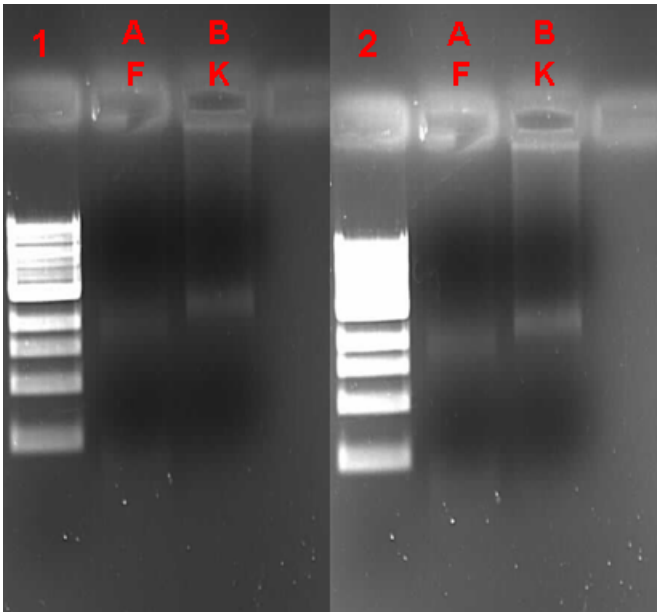

Figure 50 Gibson assembly results. 1 and 2 are images taken from the same gel with a different exposure time to UV. This is necessary due to the low concentrations of DNA used in Gibson assembly. AF) eNOS oxygenase domain fused to Frb fragment. BK) eNOS reductase domain fused to the FKBP12 fragment. A clear shift can be seen from the fragment sizes presented in Figure 49. The shifts correspond in size to the fusion of the 304bp fragment of Frb to the 1540bp fragment of the Oxygenase domain of eNOS (AF) and to the fusion of the 512bp FKBP12 fragment to the 2188bp Reductase domain of eNOS (BK).

4.5 Truncated eNOS PCR results

eNOS was truncated at three separate points near FMN domains. Touchdown PCR proved ineffective for the formation of truncated eNOS fragments. As a result, individual sets of conditions were used to obtain each of the three truncated eNOS fragments.

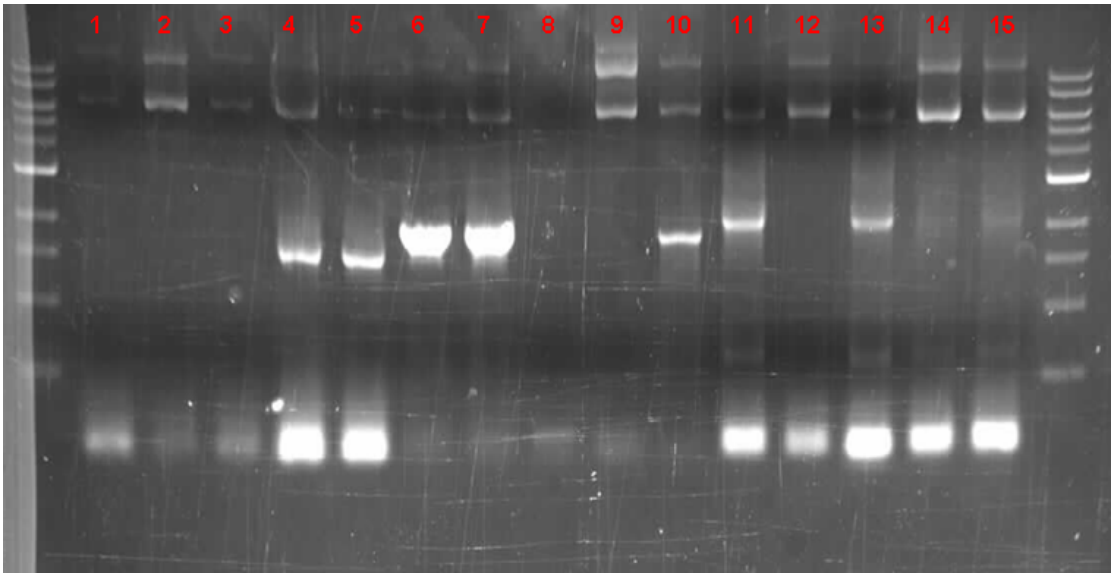

Figure 51 - Results of three different PCR reactions. 1-5) eNOS truncation 1. 6-10) eNOS truncation 2. 11-15) eNOS truncation 3. Three different PCR reactions were undertaken as described above. PCR1: 1,6,11. PCR2: 2-3, 7-8, 12-13. PCR3: 4-5, 9-10, 14-15. As shown, even with attempted optimization, efficiency was not increased and varying protocols achieved similar levels of product.

The PCR conditions to achieve the products shown in Figure 51 were different for each target sequence. The second truncation of eNOS was the first to be successfully amplified using the same PCR conditions as Touchdown PCR 1 described earlier.

Conditions were as follows:

Touchdown PCR 1:

1. 98ºC - 30s
2. 98ºC - 10s
3. 68ºC - 30s

4. 66ºC - 30s
5. 64ºC - 30s
6. 62ºC - 30s
7. 60ºC - 30s
8. 58ºC - 30s
9. 72ºC - 30s
10. 72ºC - 420s

Cycles occur between steps two and nine for a total of thirty cycles. The first and third truncations of eNOS were later successfully amplified using a different PCR protocol:

1. 98ºC - 30s
2. 98ºC - 10s
3. 60ºC - 30s
4. 58ºC - 30s
5. 72ºC - 30s
6. 72ºC - 420s

Cycles occur between steps two and five for a total of thirty cycles.

The LOV fragment was isolated separately. This was achieved by using the following temperature cycles. Cycles occur between steps two and five for a total of thirty cycles.

1. 98ºC - 30s
2. 98ºC - 10s
3. 62ºC - 30s
4. 60ºC - 30s
5. 72ºC - 30s
6. 72ºC - 420s

Following the successful amplification of all target sequences, the targets were extended with the extension primers. This was in preparation for fusion of the fragments and their subsequent integration into a plasmid. Towards this end, the LOV sequence was amplified using the forward primers LOV-FMN1 FUS, LOV-FMN2 FUS, LOV-FMN3 FUS and the reverse primer LOV LIGATION.

The eNOS sequence was amplified with the forward primer Forward Li Oxy and the reverse primers FMN1-LOV FUS, FMN2-LOV FUS, FMN3-LOV FUS. Doing this creates pre-fused fragments that contain a RE site at the 5' region of the eNOS gene and a second RE site at the 3' end of the LOV gene. Once the two fragments are then fused, there will be two separate and distinct RE sites, one at the 5' region and one at the 3' region. This will allow ligation of the sequence into a plasmid digested with the corresponding restriction enzymes.

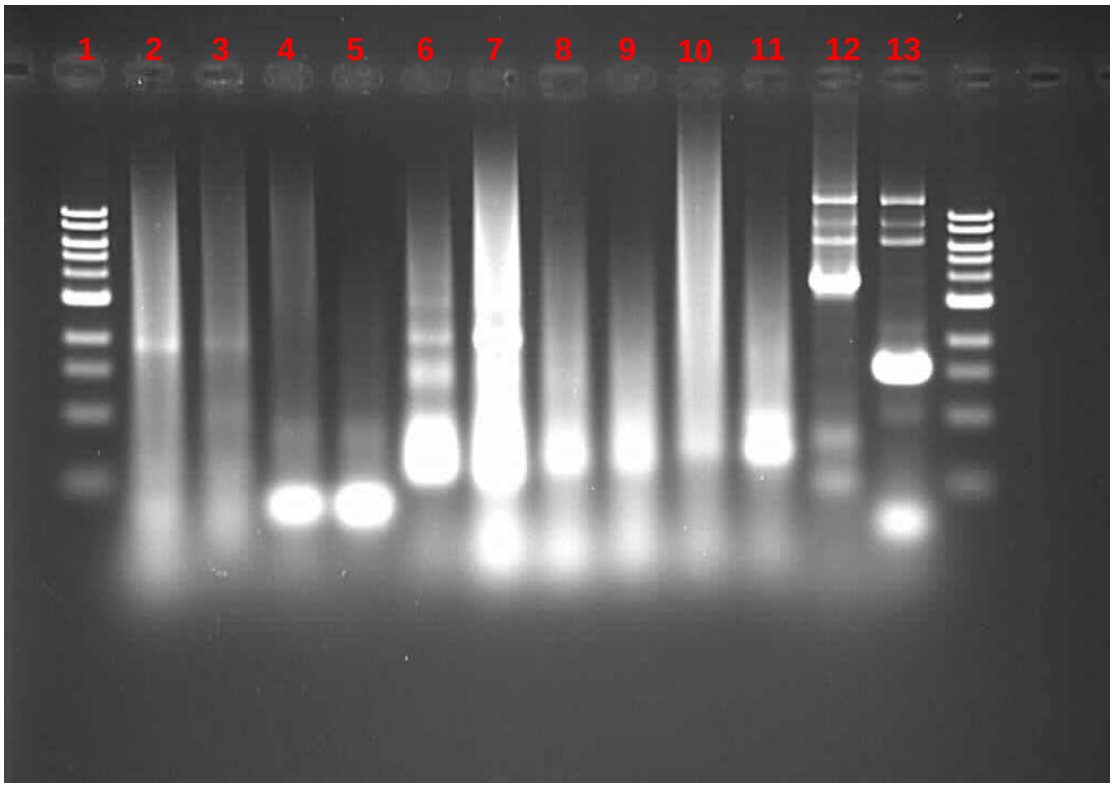

Figure 52 Gibson Assembly post-PCR. These are results of a Gibson Ligation which have been PCR amplified. 2-3: AF. 4-5: BK. 6-7 FMN1/LOV1. 8-9: FMN2/LOV2. 10-11: FMN3/LOV3. 12-13: Non-Gibson Ligated fragment A (to make a larger stock in case the fusion did not occur.)

The results depicted in Figure 52 show that only fusions of AF and FMN1/LOV1 were successful, yielding fragments of the expected sizes of approximately 1.9kb. Fragments that were successfully fused include: A-F, FMN1-LOV1, FMN2-LOV2, FMN3-LOV3. Although several attempts were made at achieving the B-K fusion, this fragment was, for unknown reasons, unobtainable.

4.6 Ligation

Ligation of the plasmid/insert pre-digested with AccI and HpaI was performed *via* electroporation as described in *2.4.2*. The following ligations were performed:

PEX_EF1-CFP/FMN1-LOV1
PEX_EF1-CFP/FMN2-LOV2
PEX_EF1-CFP/FMN3-LOV3

A different terminology represents the fact that the NOS3 gene had been cut from the plasmid prior to ligation using restriction digest. The following vector/insert DNA ratios were used for ligation:

1:1
1:3
1:6

4.7 *E.coli* Transformation

Wild type DH5α *E.coli* was transformed with the resulting ligations:

PEX_EF1-CFP/FMN1-LOV1
PEX_EF1-CFP/FMN2-LOV2
PEX_EF1-CFP/FMN3-LOV3

Transformations were performed with all vector/insert DNA ratios discussed in 5.4. A control using only vector DNA was also included to ensure that the plasmid was not simply re-ligating. Only the following transformations resulted in bacterial growth on Kanamycin plates:

1:3 ratio vector/insert DNA PEX_EF1-CFP/FMN1-LOV1

1:6 ratio vector/insert DNA PEX_EF1-CFP/FMN2-LOV2

1:3 ratio vector/insert DNA PEX_EF1-CFP/FMN3-LOV3

1:6 ratio vector/insert DNA PEX_EF1-CFP/FMN3-LOV3

All other plates exhibited no growth at 37 °C over a period of 48 hours on Kanamycin plates. Following successful transformation of *E.coli*, the new strains were grown for plasmid harvesting *via* miniprep. The extracted plasmid DNA was then sent for sequencing.

4.8 Sequencing results

Sequencing of the plasmid DNA proved inconclusive, therefore the following experiments were devised:

- Plasmid digestion with AccI and HpaI
- PCR of plasmid DNA with the appropriate primers for each strain (the primers used to create the mutant DNA). (Figures 49 and 51)

4.9 Mammalian Cell Transfection 1

Plasmid DNA harvested from the bacterial mutants was used to transfect the mammalian cell line CHO-K1. This cell line has been used by a number of groups to express eNOS for mechanistic studies. Transfection was performed using lipofection, as described in section 2.2.4 so as to exclude the need for viruses and still obtain a high ratio of successful transfection. The following transfections were attempted:

- Unmodified plasmid DNA (PEX_EF1-CFP_NOS3)
- FMN1-LOV1 mutant version of eNOS (PEX_EF1-CFP)
- FMN2-LOV2 mutant version of eNOS (PEX_EF1-CFP)

- FMN3-LOV3 mutant version of eNOS (PEX_EF1-CFP)
- Control: no plasmid
- Control: no transfection protocol administered, instead - media was added to replace the volumes used in protocol.

Following the transfection protocol, the cells were allowed to grow for 24 hours prior to introduction of the antibiotic for which the plasmid codes a resistance. In this case, G418, also known as Geneticin. A killing curve was constructed for all samples as it is necessary to confirm cell death in control samples and life in non-control samples. The killing curve was measured with cells grown in 5mg/mL of G418, 1 mg/mL G418, 0.75 mg/mL G418 and 0.5 mg/mL G418. Due to the method of antibiotic selectivity conferred by G418, cells were required to grow for one week at 37 °C, 5% CO2 prior to confirmation of resistance/non-resistance.

At the end of the first experiment, only the sample containing unmodified plasmid DNA (PEX_EF1-CFP_NOS3) exhibited resistance to G418 at all concentrations. All other samples exhibited cell death.

Following this experiment, a second round of transfection was carried out. In the second round of transfection, a replica of the initial transfection was carried out and the sample wrapped in sterilized aluminium foil. This was due to the fact that I had been unable to rule out a possible cause of cell death: uncontrollable activation of eNOS and therefore high levels of NO. As the wild type form of the protein is regulated by the availability of both L-arginine and NADPH, the cell would be able to thoroughly regulate eNOS activity (such in the case of the surviving sample.) However, if the mutant construct had been successful, NO production would only be dependent on L-arginine presence and light. As in the previous round of transfection this was not accounted for, cells may have been exposed to light for an overlong period of time, causing the accumulation of NO and possibly triggering cellular apoptosis on a mass scale.

The second round of transfection showed identical results to the first, in both light and dark samples, with the added observation that even the PEX_EF1-CFP_NOS3 sample showed reduced growth in darkenss. This may have occurred due to leftover ethanol on the surface of the aluminium foil. Due to the findings described in section 4.5, this series of experiments was scrapped and only the successful mutant line was kept so as to perform further experiments.

4.10 Troubleshooting

Plasmid digestion showed negative results, suggesting a non-integration event. PCR of the plasmid DNA, however, proved the presence of some individual fragments in the DNA. In order to understand what had happened, a review of all procedures to this point was performed. A second attempt at transforming *E.coli* was attempted which yielded the same results. An internet search was made to find the plasmid sequence in more databases, as this may have been a source of error. The search yielded a slightly different plasmid sequence, Sequence 25, from a different source. There were two critical differences, location of the CFP gene in the plasmid sequence and the RE site map of the plasmid.

Sequence 25 The second sequence obtained for the plasmid PEX_EF1-CFP_NOS3. Dark blue: EF1 promoter. Light blue: CFP marker gene. Orange: eNOS gene. Red: Kanamycin resistance gene.

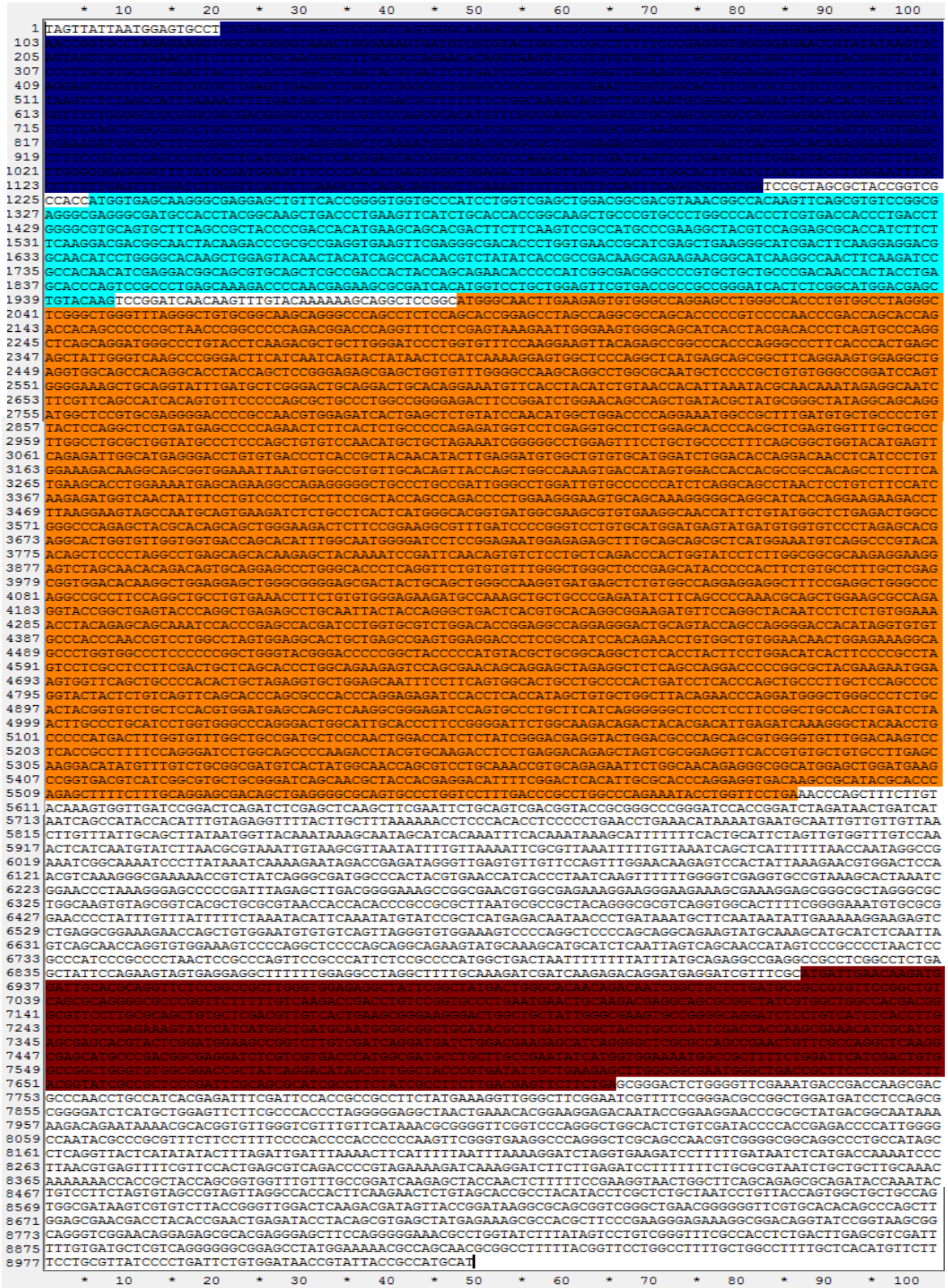

When comparing this plasmid sequence to the one originally obtained from the plasmid supplier, it can be seen that the CFP protein locus is now shifted to the anterior proximal region of the eNOS gene, rather than the originally though posterior proximal region. In addition, due to these changes, RE sites are no longer matching the initially proposed strategy. A hypothesis to explain the gain in resistance of the transformed bacteria is described in Figure 53.

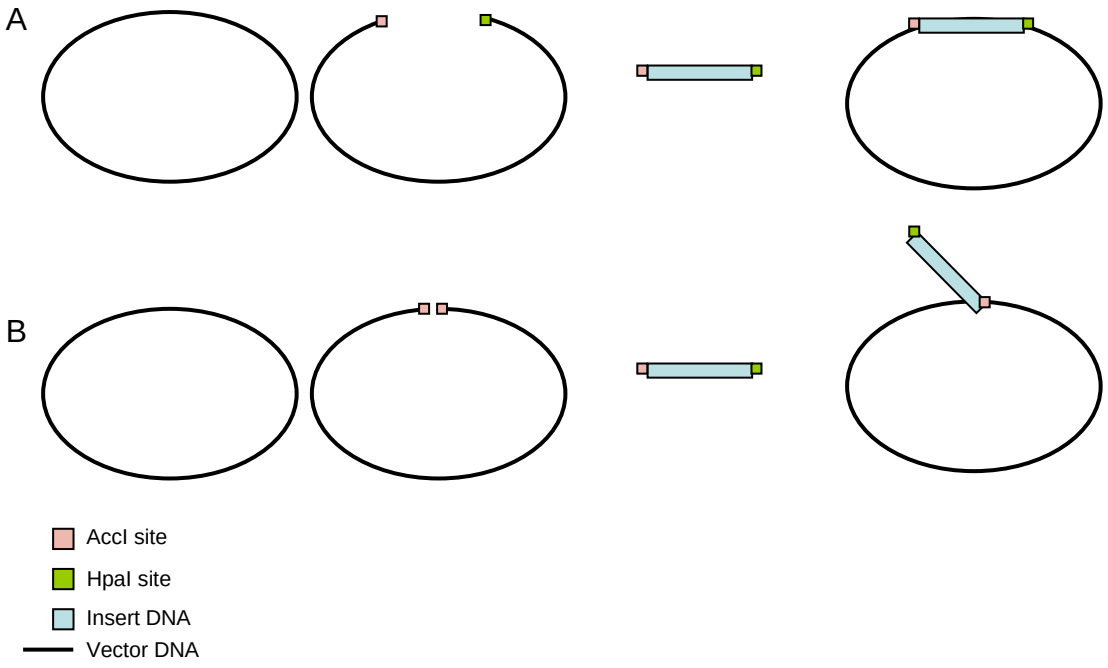

Figure 53 Hypothesis regarding the false positives obtained during transfection using improper RE sites. A) Depiction of how the ligation process would have worked if the plasmid sequence had been as originally thought. B) Depiction of how the ligation process probably occurred due to the RE site mismatch. As can be seen in B, due to the lack of an HpaI site, only a single cut was made in the plasmid. As one end of the insert fragment contained an AccI site, this may have bound and then been cut at any of several points due to processing within the bacteria.

Control ligation experiments involving only vector DNA did not show signs of self-ligation of plasmid DNA. In addition, PCR experiments confirmed the presence of the LOV DNA within the purified plasmid DNA. To confirm whether this was the case, the new plasmid map was analyzed and a restriction digest was planned based on its RE

sites. The enzymes selected were NheI and AccI, which flank the eNOS gene as given in the new sequence.

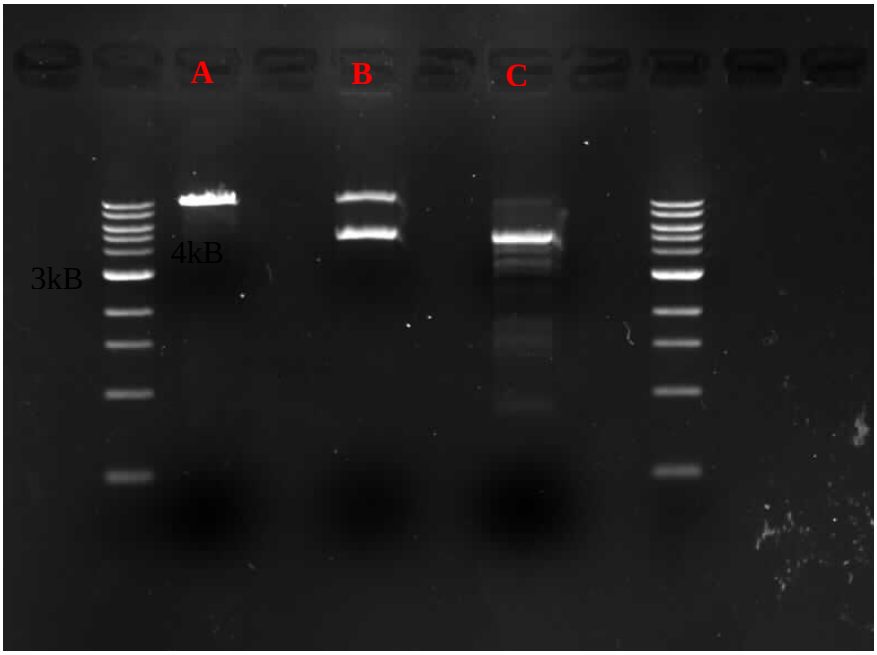

Figure 54 A restriction digest performed on the PEX_EF1-CFP_NOS3 plasmid using the following restriction enzymes: A) Nhe1, AccI. B) AccI, HpaI. C) AccI, NotI.

No restriction digest yielded the expected ~3.7kB fragment except the AccI-NotI digest, Figure 54, the result of which shows more bands than were expected. The newly found sequence does not contain a single NotI site contradicting the possibility that the original sequence data was incorrect. Compared to a restriction digest performed in earlier work, Figure 55.

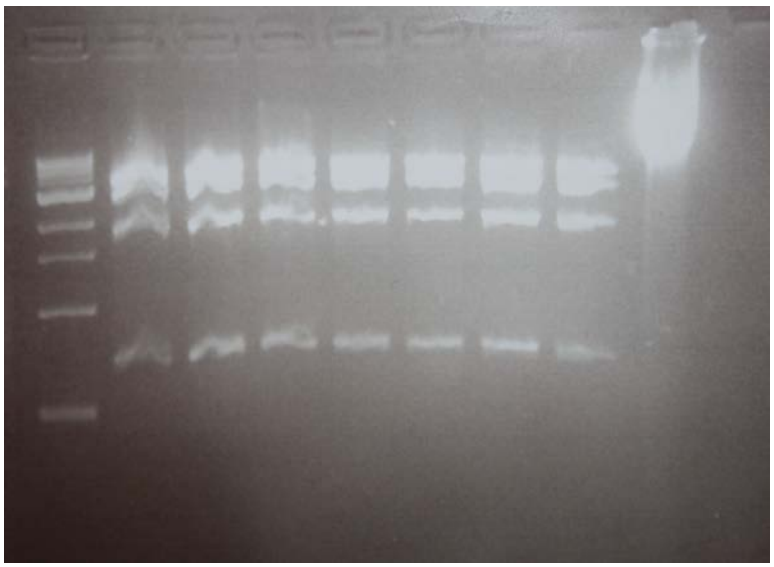

Figure 55 A previously performed restriction digest of PEX_EF1-CFP_NOS3 with AccI and NotI. All samples showed the same bands when digested. However, when compared to the AccI-NotI digestion described in Figure 54, one can observe the dissimilarities.

The difference in digest results between the two plasmids suggests that the plasmid had been mutated by the bacteria prior to harvesting. Although PCR had been successful, yielding bands of expected size, it is possible that some regions of the plasmid had been mutated. To verify this, frozen master colonies were thawed, plated and grown overnight for plasmid DNA extraction together. It would be expected that the master colonies would be closer to the original sequence as they are generationally closer to the original transformation point.

Restriction digest of the plasmid extracted from these colonies, however, proved identical to those demonstrated in Figure 54. Due to these findings, it was concluded that the strategy for plasmid integration required a full re-design. To this end, a new plasmid system was obtained. This system, the pTARGET^{TM} Mammalian Expression Vector System, was purchased from Promega and works in a completely different manner to the previously designed plasmid integration strategy. Rather than relying on restriction digests to create complementary regions for plasmid/insert ligation, this system provides pre-cut plasmid which contains a poly-T sequence at its 5' ends. The system requires insert amplification using a polymerase which does not create blunt end sequences, and instead creates 3' poly-A sequences - such as Taq polymerase.

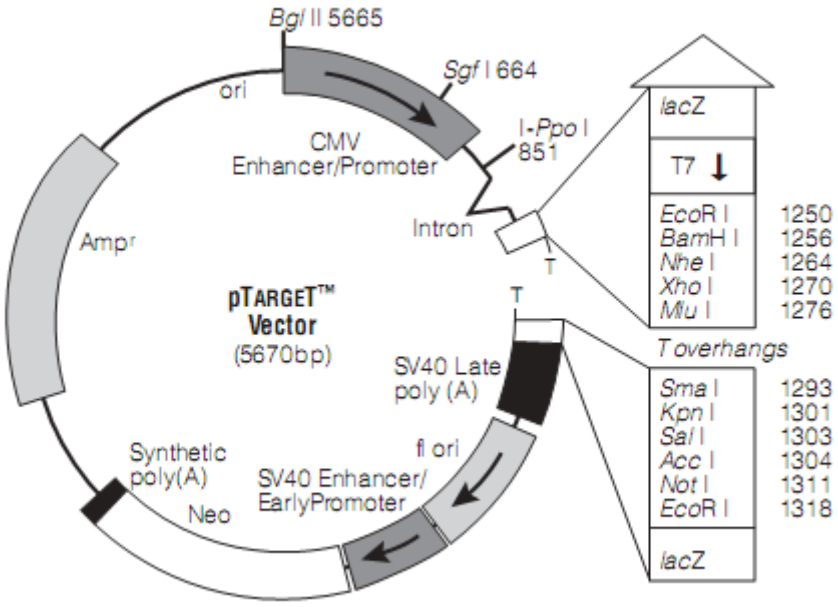

Figure 56 The 5.67kB pTarget mammalian expression vector. (Image from promega.com)

The pTARGET™ system contains a gene for Ampicillin resistance and also allows for blue/white colony screening by containing a LacZ gene which becomes interrupted upon successful insertion of constructs into the plasmid. Therefore, white colonies which grow on Ampicillin/IPTG/XGAL plates are likely to contain the construct of interest.

4.11 Employing the new strategy

In order to employ this new strategy, all fragments were re-amplified as per the original plasmid integration technique described in sections *4.3.*

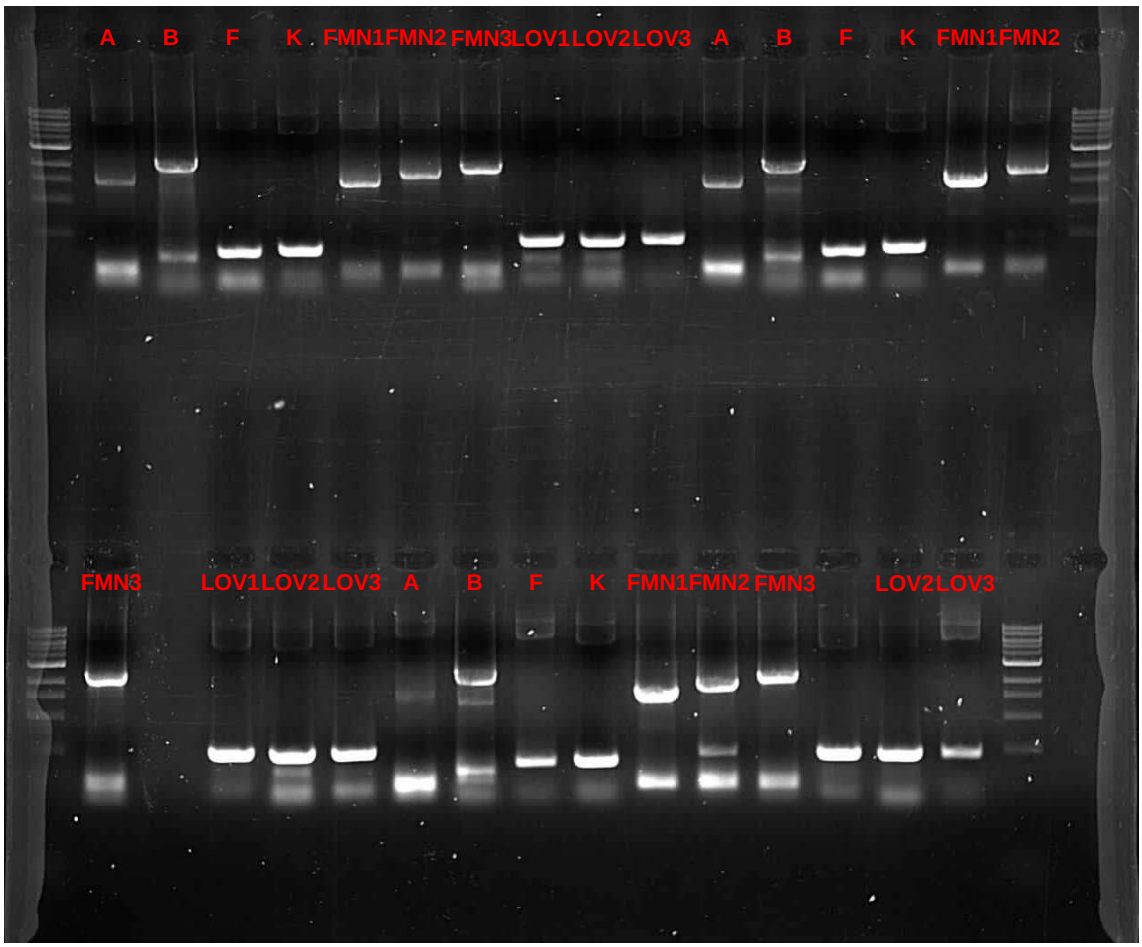

Figure 57 Amplification of all individual fragments using primers described in sections 4.3

Following this step, fragments underwent Gibson Ligation as described in 2.4.9. The resulting fused fragments then underwent PCR using Taq polymerase. It is noteworthy that this is the only amplification step which utilizes Taq polymerase due to its low amplification fidelity when compared to Phusion polymerase.

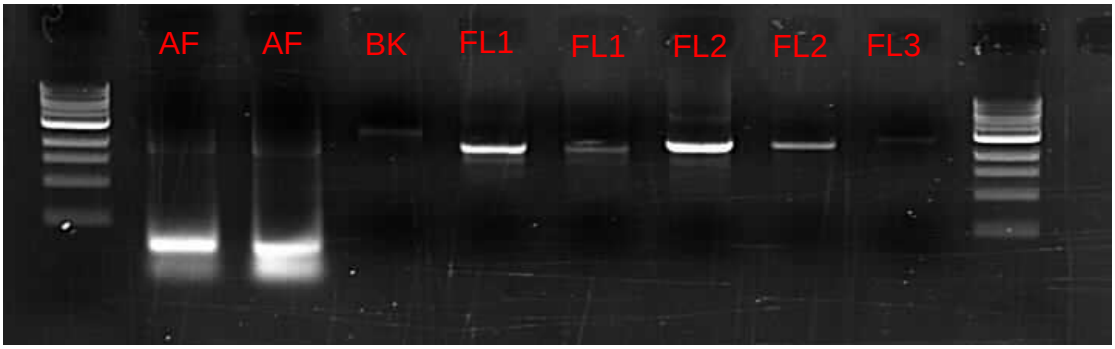

Figure 58 Amplification of Gibson Ligation results with Taq Polymerase, yielding constructs described in 4.3.

These constructs were then ligated to the pTARGET^{TM} vector, transformed into JM109 high efficiency competent cells, and plated on Ampicillin/IPTG/XGAL plates for blue/white screening of mutants. White colonies were selected and grown for the purpose of plasmid extraction *via* miniprep protocol. Amplification of the target sequences *via* PCR using the same primers which were used to originally amplify the fused constructs was used to verify plasmid integration. After a first round of transformation both AFand BK showed white colonies growing on plates, although very few colonies were observed. Of these, no white colonies from either mutant grew in a 100 μg/mL Ampicillin concentration.

Following this, a second round of ligation/transformation was performed. An additional step of gentle centrifugation at 1,000g was employed prior to plating the transformants. White colonies were observed for all transformants, however only AF mutants grew overnight in LB/Ampicillin. Plasmid extraction and subsequent PCR of these yielded the following results:

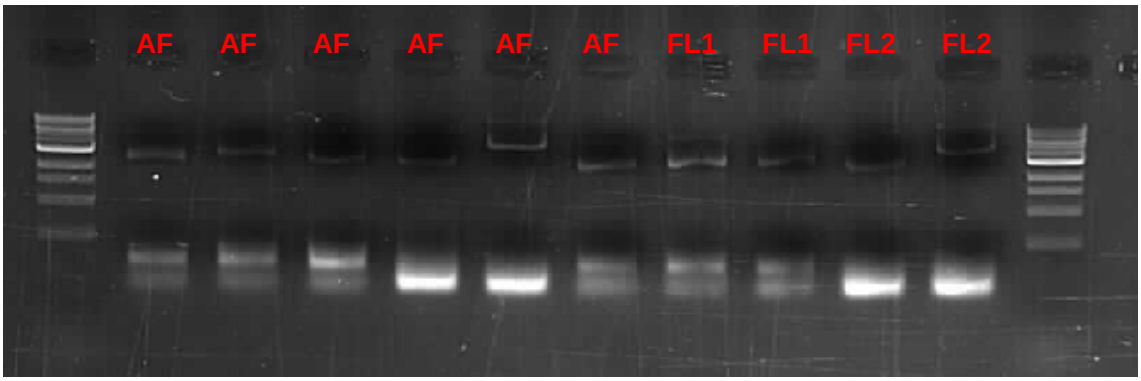

Figure 59 Results of PCR of plasmid extracted from AF, FL1 and FL2 white colonies. When compared to Figure 58, only the fourth AF construct and the first FL2 construct showed the expected size.

A final verification of the integrity of the construct was made *via* a restriction digest. Only the AF mutant from the rapamycin system was progressed sufficiently to reach this verification step.

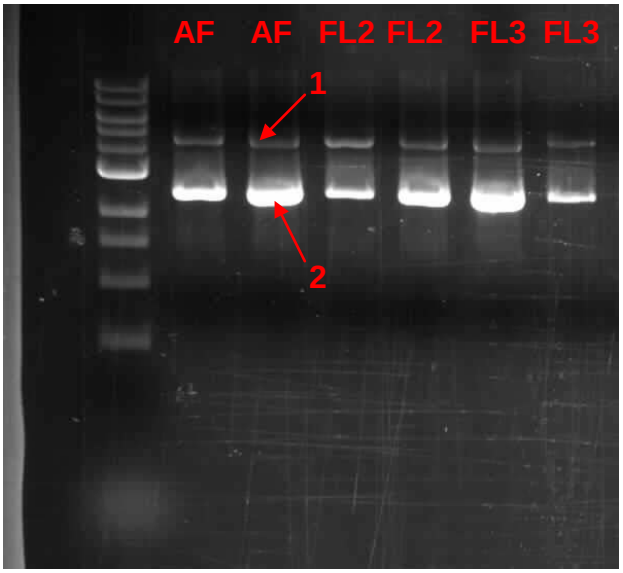

Figure 60 Results of Restriction digests of AF, FL2 and FL3 with EcoRI. 1: pTARGET empty vector. 2: Inserted fragment

Another attempt was made at creating the BK mutant, but was unsuccessful. Due to timeframe issues, the Rapamycin CID system remained incomplete. However, the obtained AF mutant was subsequently transfected into the CHO-K1 cell line successfully, Figure 61.

Wildtype

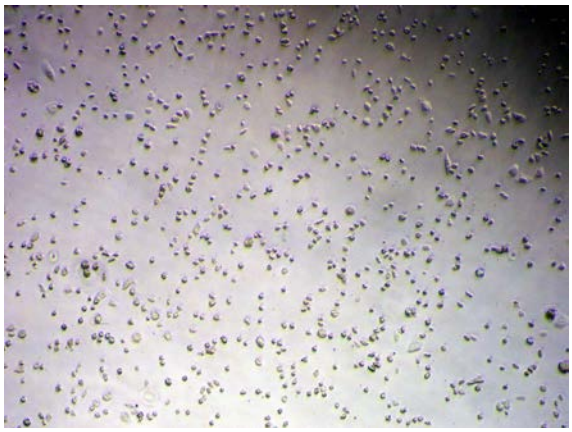

AF mutant

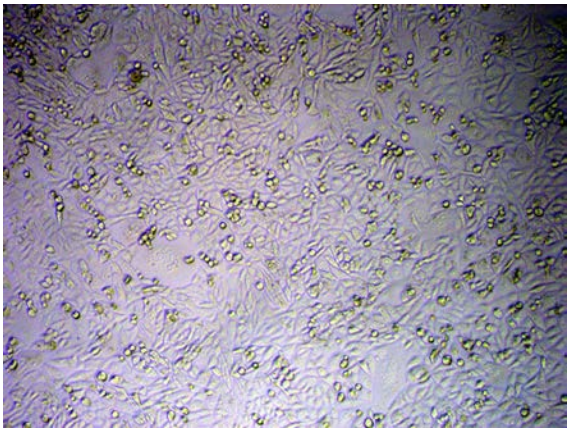

FL1 mutant

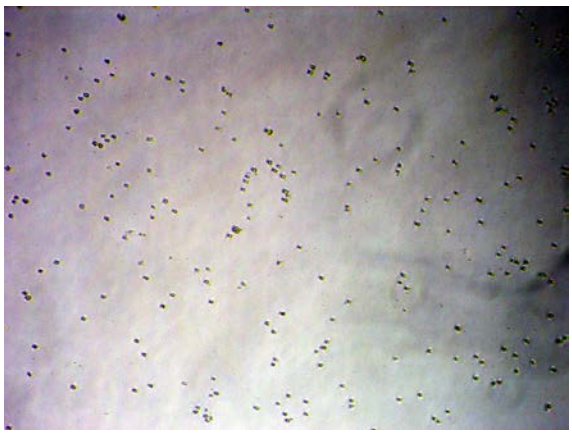

FL2 mutant

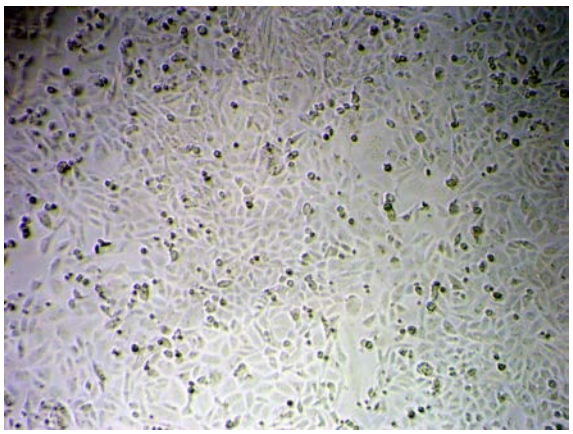

FL3 mutant

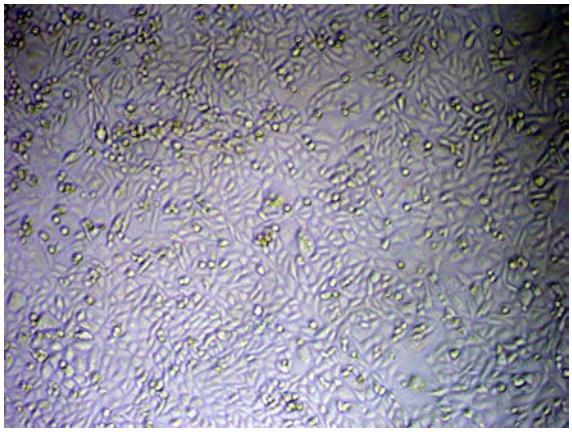

PEX mutant

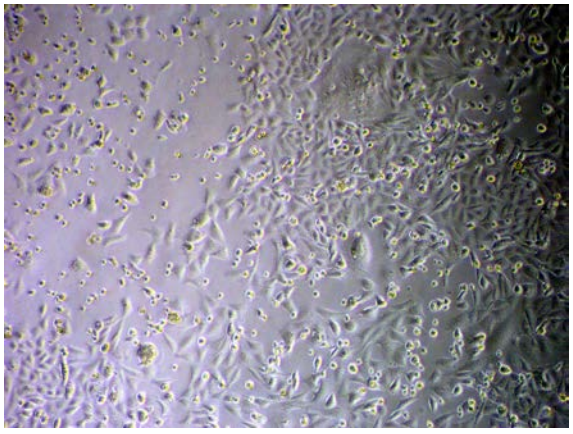

Figure 61 The results of a Geneticin killing curve. As can be observed, both the control cell line and the F1 mutant cell line show dead cells. All other samples showed living cells after a period of 7 days in Geneticin (G418)

4.12 Sensor Selection

Choice of electrochemical sensor to interface with the nitric oxide producing cells was based on rapid detection rate and the ability to detect nitric oxide at very low concentrations. The sensor used in this work has been demonstrated by McNeil *et al* for the detection of NO production levels in cultured cells.(Chang, Henderson, Cole, F. Bedioui, & Mcneil, 2005)

The sensor type chosen is amperometric, capable of detecting nanomolar concentrations of NO and producing a change in current showing a linear relationship with the concentration of NO. The electrode works by oxidation of NO resulting in a measurable change in the output signal, current in this instance.(Nazaré Pereira-Rodrigues et al., 2002) A platinum electrode is deposited with a NiTSPc (tetrasulphonated nickel phthalocyanine) layer which is then coated with a Nafion 117 film.

NiTSPc is deposited *via* electrodeposition in an alkaline NaOH aqueous solution of 2 mM NiTSPc at a constant potential of +1.2V versus an Ag/AgCl electrode for a period of ten minutes.(Pontie, Gobin, Pauporte, Fethi Bedioui, & Devynck, 2000) Subsequently 2 μL Nafion 117 is deposited from a 1.25% concentration in alcohol onto the modified electrode surface and left to dry at ambient temperature. The NiTSPc layer allows the necessary surface chemistry for the sensor to interact with NO and the Nafion 117 layer confers further selectivity to the electrode by limiting both the state and size range of molecules, thus selecting for gaseous NO.

4.13 Electrode preparation

The electrode was prepared as discussed in the methodology. Shown below are cyclic voltammogram curves depicting the electrodeposition of NiTSPc on to the platinum surface of the electrode.

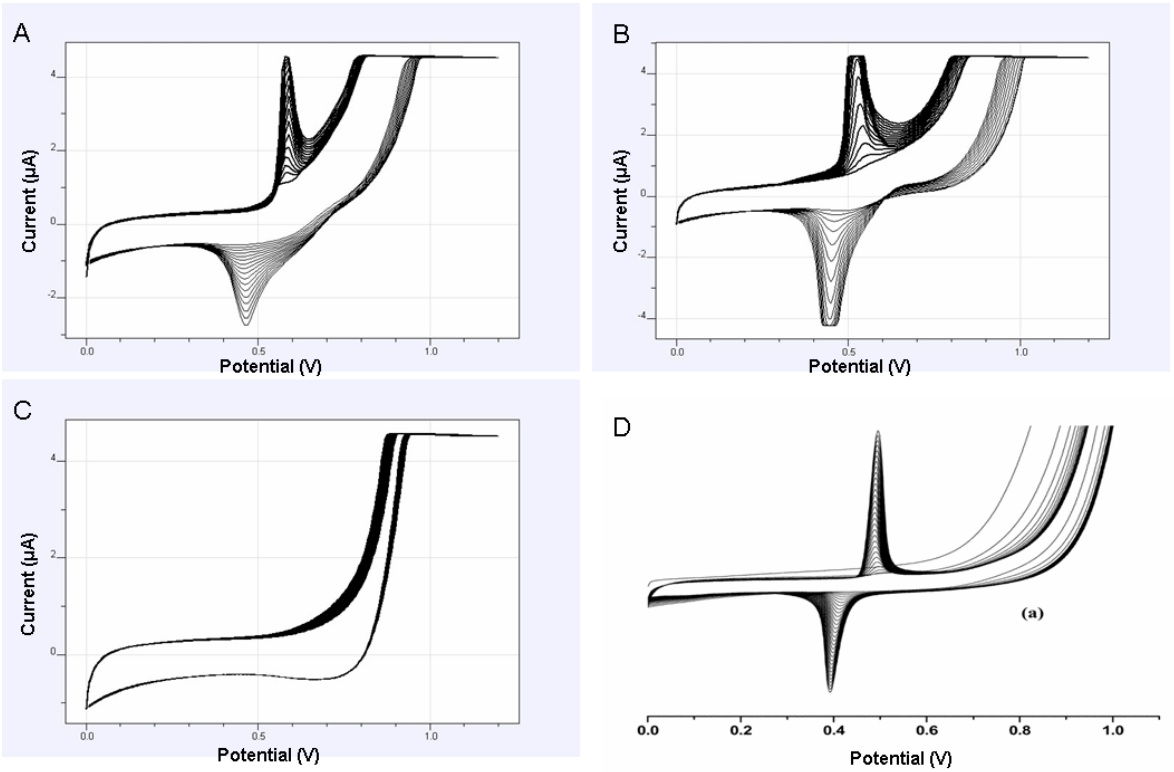

Figure 62 Cyclic voltammetry results for electrode functionalization. A) Fresh NiTSPc solution, 15 cycles. B) 2nd round of cyclic voltammetry performed on the electrode used in A, depicting cycles "16-30". C) Cyclic voltammetry using NiTSPc solution which had been left at room temperature overnight. D) Cyclic voltammetry curve taken from (Oni *et al*., 2004) **for the same functionalization procedure.**

As can be seen in Figure 62, subsequent scans between 0-1.2V(+) at 100mV/s show peaks representing gradual deposition of NiTSPc on the electrode surface. These curves concur with presented peaks in the literature shown in D. As a further experiment, a second round of cyclic voltammetry was applied to a functionalized electrode. This causes an increase in the amplitude of both peaks as shown in image B of Figure 62. The 2mM NiTSPc solution must be kept refrigerated. Failure to do so prevents correct electrodeposition. Image C from Figure 62 demonstrates a cyclic voltammogram of the electrode in un-refrigerated NiTSPc. This finding shows the importance of modifying the electrode surface *via* cyclic voltammetry as opposed to constant potential, another method of achieving the electrodeposition of NiTSPc. By using cyclic voltammetry, there is an added assurance to the quality of the prepared electrode.

4.14 Electrode Measurements

Various samples were subjected to the modified amperometric measurements. All measurements were performed on suspended cells in PBS using the same electrode preparation.

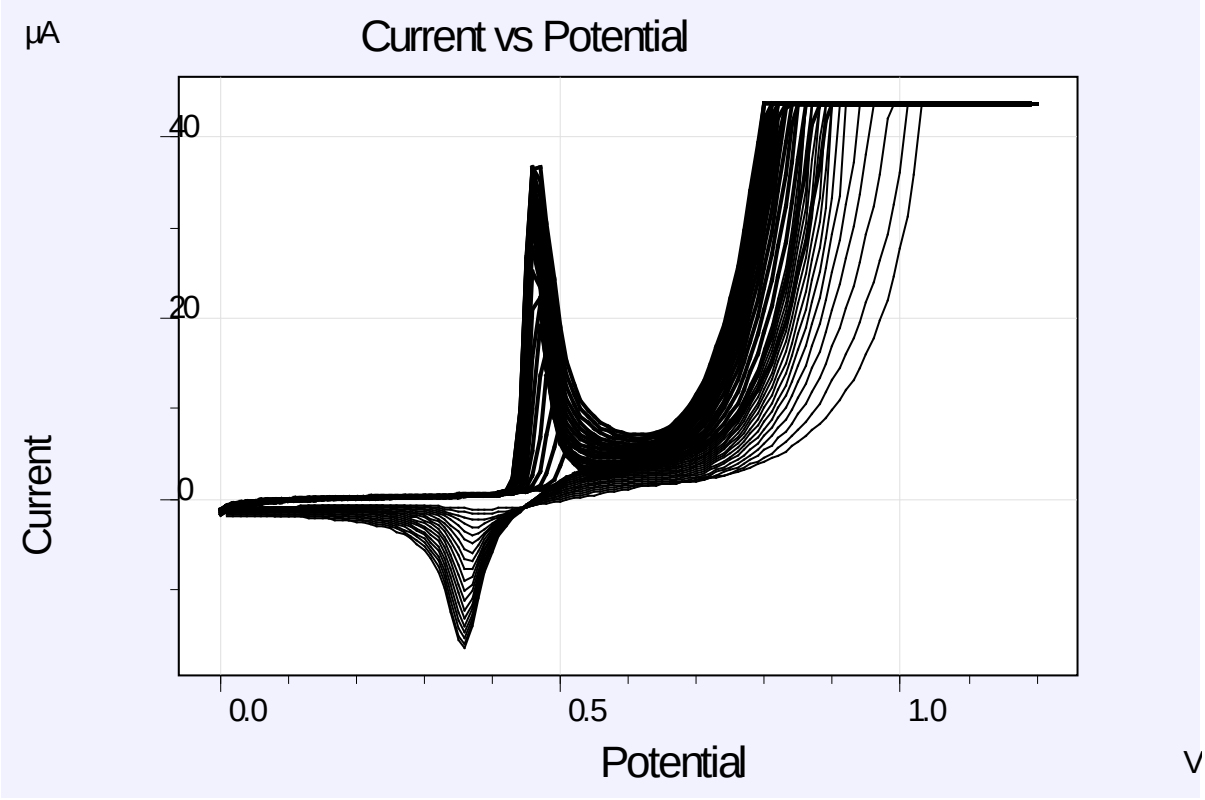

Figure 63 The Cyclic Voltammogram of the electrode used in the experiments described. A total of 20 sweeps were made at 0.1V/s, step 0.01V and vertices 0.0-1.2V. Cycles 2-20 shown.

Samples include:

- Control A - Untransformed Cells.
- Control B - Cells containing a transfected wild type eNOS gene (PEX_EF1_NOS3-CFP).
- Sample 2 - Truncated eNOS version 2 fused to LOV (FL2).
- Sample 3 - Truncated eNOS version 3 fused to LOV (FL3).
- PBS

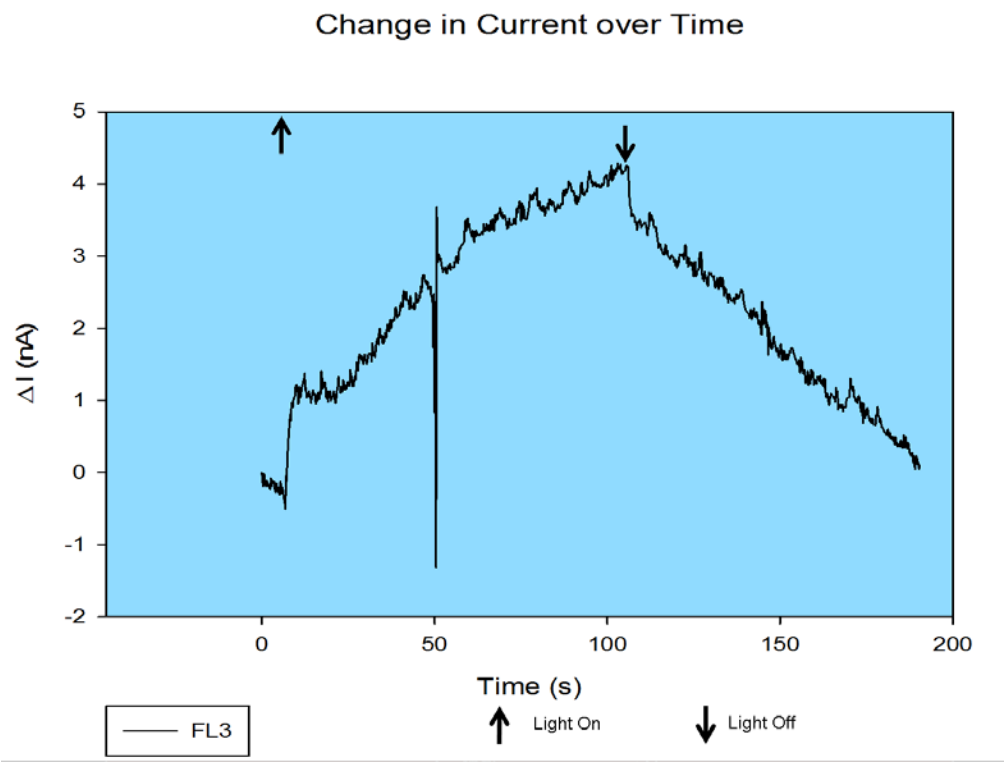

Figure 64 The effect of stimulus in the form of light on the FL3 eNOS mutant. Arrows indicate initiation and termination of stimulus. The curve not only shows a rapid change in current but also a gradual increase/decrease as more NO becomes generated from the mutant protein.

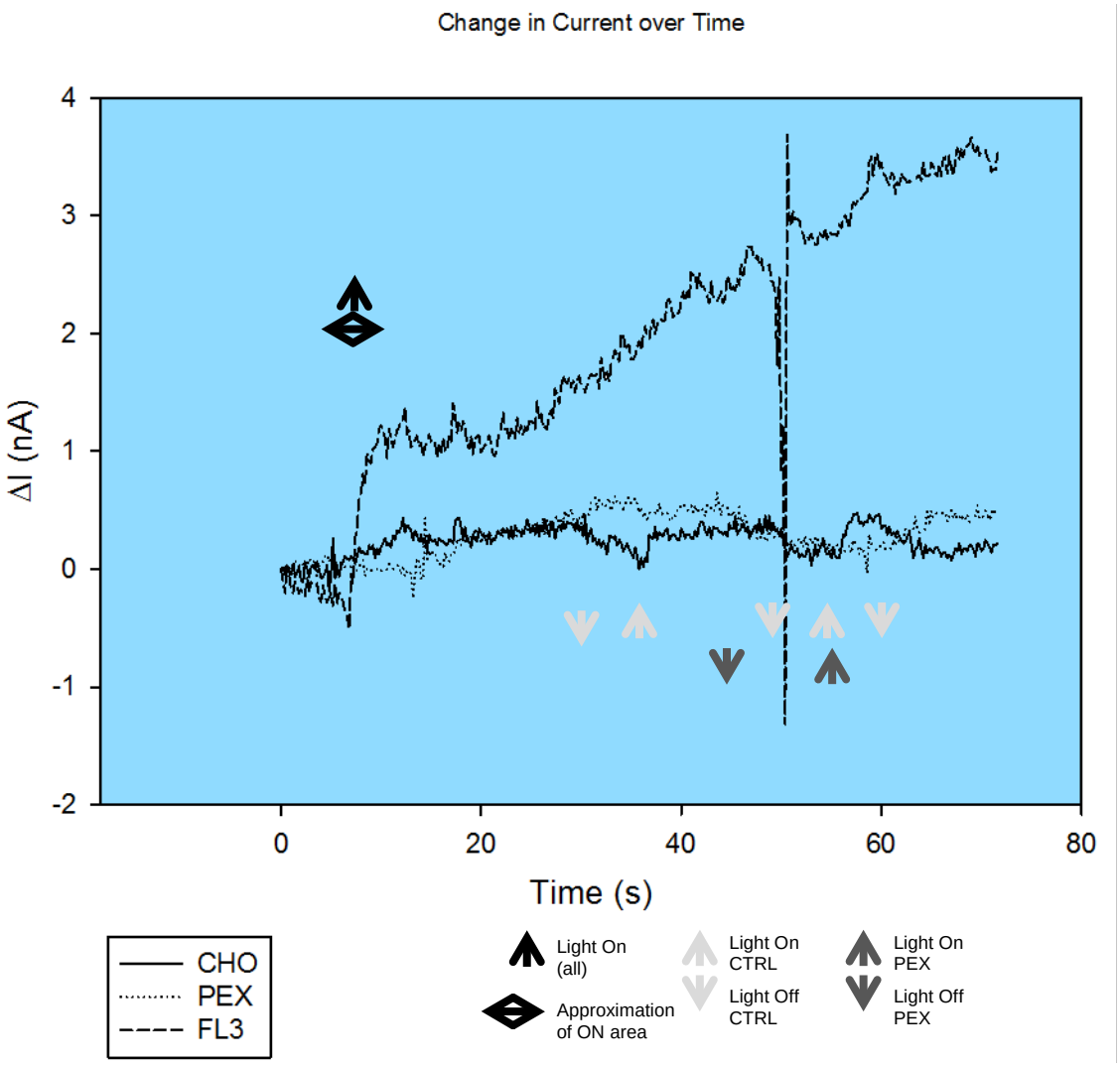

Figure 65 The change in current over time for the eNOS mutant FL3 vs the two controls: wild type CHO-K1 and CHO-K1 transfected with the PEX plasmid (wild type eNOS)

Evidence presented in Figure 65 strongly favours the conclusion that the FL3 eNOS mutant is capable of producing the desired effect, creating a signal transduction pathway which transduces an optical signal into a chemical signal.

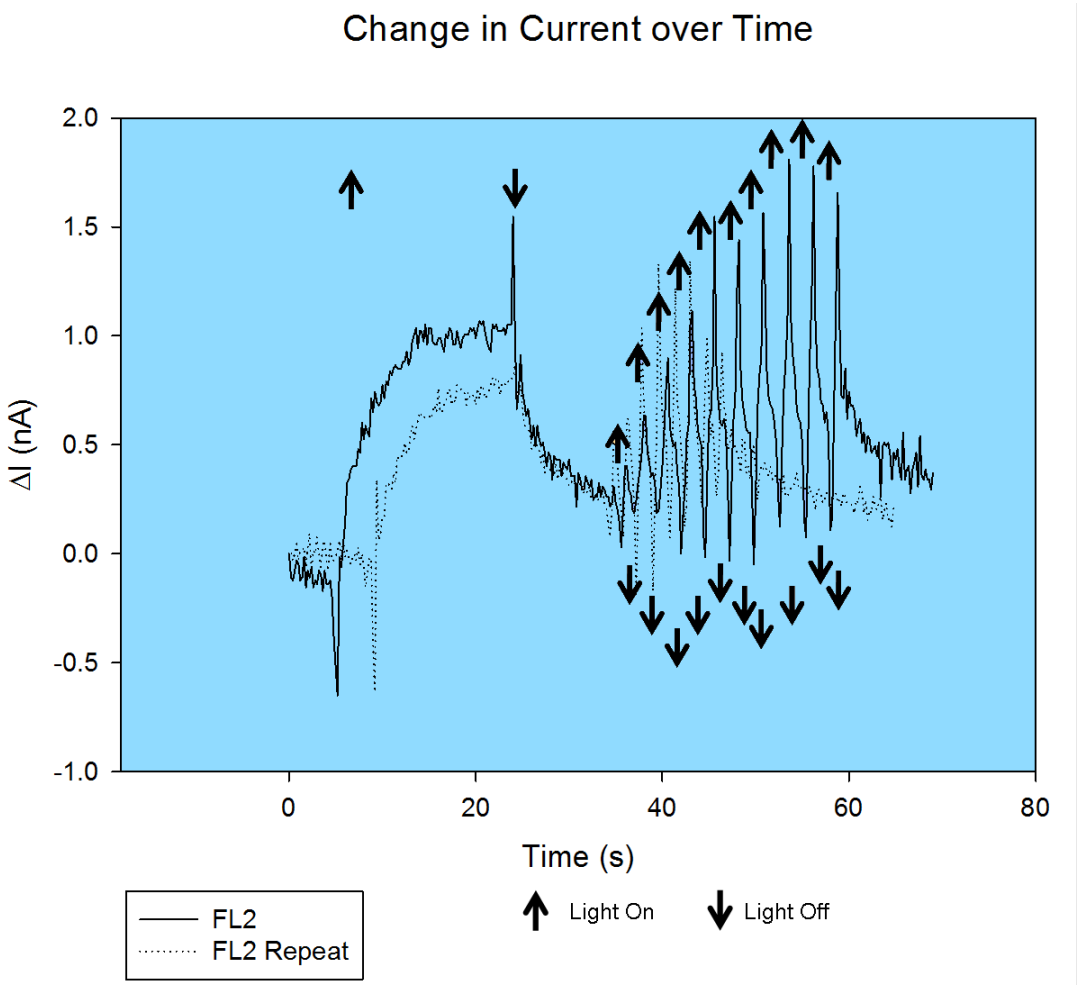

Figure 66 Two samples of FL2 undergoing approximately the same regime of light treatment. Although there is a slight decrease in current between runs, this may be due to cell number/protein expression levels.

Although an equal number of cells was placed in the 24 well plates, upon observation under brightfield microscopy it was noted that cell number was approximately the same but with some variation. This may affect the overall level of response.

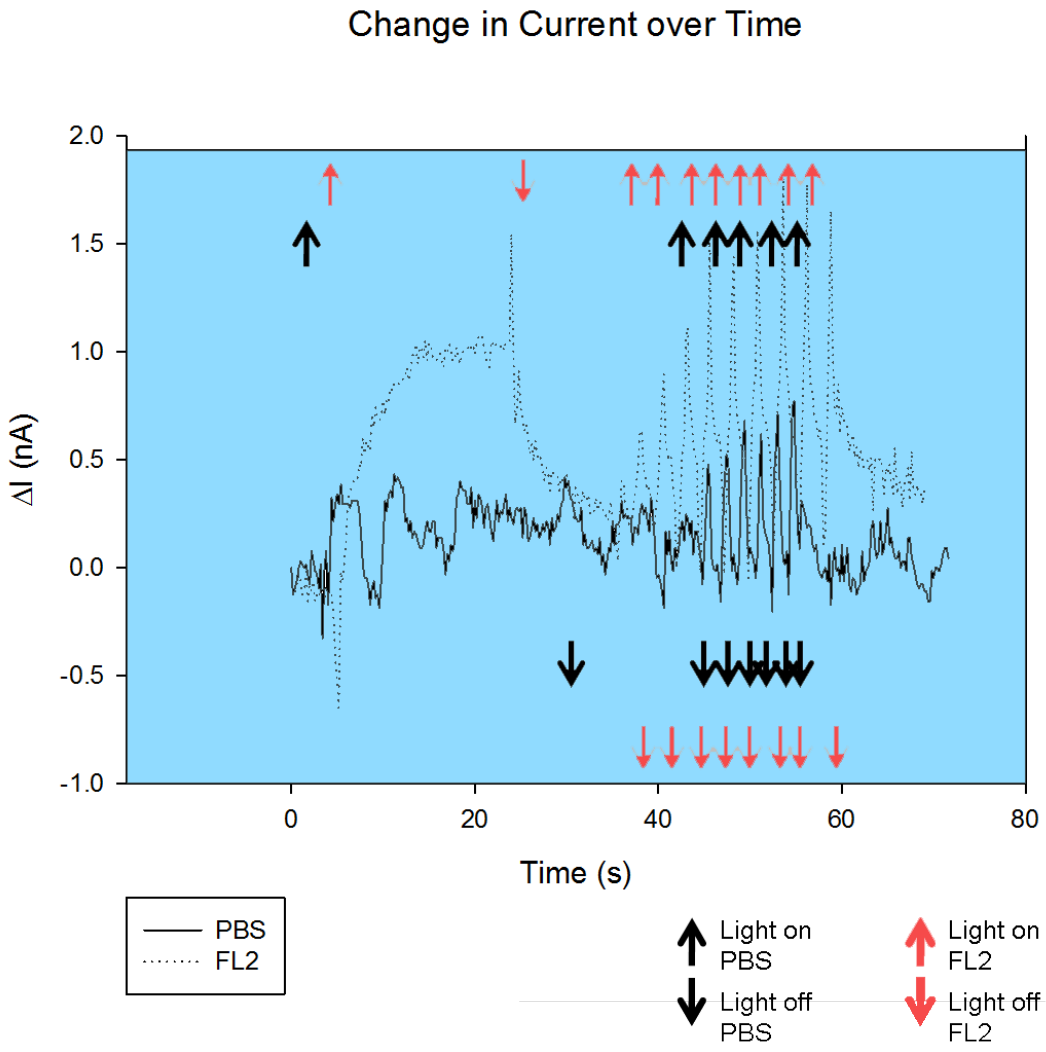

Figure 67 A comparison of the effect of light stimuli on a control phosphate buffered saline sample and on the FL2 mutant cell line. Although the electrode shows some photosensitivity and a similar trend in behaviour, it can be noted that the amplitude of change is at least double and that there is no increase over time for the PBS sample during the longer stimulus period. A large difference in the fast-response amplitude can also be seen between the two samples.

4.15 Discussion

The light inducible version of the eNOS mutants was successfully tested for NO production upon optical stimulation and the results confirmed that the designed system was functional. Upon the incidence of high intensity visible light an immediate response in the form of increased NO production was observed. In addition, the response time of the mutant proved activation/deactivation occurred on a sub-second timescale. It exhibited switching characteristics in response to on/off type stimuli, Figures 64-67.

Both Photo-NOSβ and Photo-NOSγ mutants showed the desired response. The implications of the finding that FL2 is photoactive are that either eNOS can function using a single FMN domain or that the LOV genes are recruiting their own FMN. As FMN is a critical co-factor in the electron transfer pathway of eNOS, knowledge regarding its ability to function with just one FMN co-factor is of interest. The Photo-NOSα version of the gene was designed to answer this question. Photo-NOSα was designed with no eNOS derived FMN binding domains and had the LOV genes attached to it at the distal end. If LOV recruits its own FMN then the maximum number of possible FMN binding domains is one. At this time, it is not know whether there are two or three FMN binding domains in FL3 and whether there are one or two FMN binding domains in FL2.

The fact that the electrode system itself proved to be somewhat photosensitive must be considered. This is likely due to the effect of the phthalocyanine moiety in NiTSPc and has been reported in the work of Xu *et al* (H. Xu *et al*., 1992). Although the group demonstrated the effect of light absorption of various phthalocyanines, NiTSPc was not investigated. However, they exemplified cases where a phthalocyanine derivative allowed for increased absorption of light.

The evidence towards system overcoming electrode photosensitivity is clear. Using the same electrode from the same preparation the difference in activity is very high between a sample with control CHO-K1 cells and the mutant cell line. Further evidence that the cells are the photoresponsive element stems from the curves depicted in Figure 67 which show a slower off response than the PBS control.

The use of inhibitors or L-arginine as well as tetrahydrobiopterin would provide relevant evidence of the experiments described in this body of work. Should the signal decrease upon use of inhibitor and increase when surplus substrate is present then the system can both be characterized further and more effectively.(Klatt et al., 1994)

A more standardized measurement regime would also be beneficial. The following two methods would most likely yield interesting results. Firstly, an experiment demonstrating the system's responsivity by applying a stimulus regimen with periods of 100 seconds on and 100 seconds off. It may be that the extra NO being generated is damaging cells and after several long cycles there will no longer be living cells producing NO. Secondly, the fast-response mechanism would be investigated using light pulses of varying duration. By testing the fast-response it may yield information regarding NO accumulation in cells. As the compound has a half life of a few seconds, it may be that repeated bursts of stimuli will slowly raise the background levels of NO

but keep the overall level lower than in the experimental methodology described previously.

Three attempts at sequencing the mutants failed. This was most likely due to a step in the protocol for sample preparation where the DNA sample is washed with a solution containing ethanol. However, plasmid digestion with EcoRI showed that there was a fragment of the expected size within the plasmid used for transfection. In addition, PCR of the extracted plasmid with the appropriate primers demonstrated successful amplification of the target area of DNA. Further evidence towards the success of the target DNA insertion includes the differences in sample photosensitivity between cell lines which were proven to be transfected with the modified pTARGET plasmids and wild type cells. Repeating these experiments with the wild type eNOS gene under a pTARGET vector would grant further robustness to the presented data. As all data generated *via* experiments pointed towards a working system, confirming the presence of both the plasmid and the fragments as well as the operation of the inserted system. A strong body of evidence supports the presence of the target gene. Sequencing using a different protocol for sample preparation should yield results.

Chapter 5 Conclusions

The experimental work performed in this thesis lead to novel findings regarding eNOS and its inhibition. Flow cytometry analysis of CHO-K1 samples found that the use of a liposomal delivery method for inhibitor/cell interaction was highly effective. The difference was found to be significant ($p<0.01$) and the protocol enhanced inhibitor activity. This difference is increased in the mutant cell line transfected with the PEX_EF1-CFP_NOS3 plasmid containing wild type eNOS protein. The statistical significance of this data was also found to be $p<0.01$. These findings served a double purpose: to investigate the properties of liposomal delivery of inhibitors and to confirm the suitability of the CHO-K1 cell line for expression of mutant constructs of an eNOS nature. Due to the difference found between the mutant and wild type NO production trends, a model regarding cellular regulation of NO in compensation for the inserted protein was created. The model states that the cell, in order to cope with the inserted mutation and limit overall NO will limit its own NOS machinery on a transcriptional level. This would explain the reason behind the bellow wild type cell baseline levels of NO observed in the mutant cell line when exposed to inhibitors. Repeating these experiments with the inserted gene under different promoters would be an ideal method to validate this hypothesis.

These findings also highlighted the possible use of CHO-K1 cells to create the cell-based biosensor for Cyberplasm. Two strategies were developed to create inducible eNOS chimeric variants. The designed constructs were to allow for a chemically induced NO response and an optically induced NO response respectively.

A chemically induced form of eNOS based on the rapamycin CID system was designed and all individual parts have been created *via* PCR. However, only half of the system was successfully introduced into mammalian cells. As the system absolutely requires both halves to function; the rapamycin system remains incomplete and untested. In order to reach testing stage of a chemically induced eNOS, the remaining fragment must be successfully integrated into plasmids, bacteria and then mammalian cells.

The light induced cell-based biosensor was found to be functional. When compared with suitable controls, levels of NO increased dramatically upon light incidence in both mutant cell lines Photo-NOSβ and Photo-NOSγ. The response time of the cell-based biosensor appears to be within seconds or subseconds. Both a fast response and a gradual, slow response were observed. The system also demonstrated a fast switching

ability, which is important for its end application. Further experimentation and characterization of the biosensor is necessary prior to integration into more complex systems such as Cyberplasm. However, the results presented suggest that a signal transduction pathway was created within the mutant cell line. This pathway was capable of translating an optical signal into a chemical signal which when combined with the appropriate electrode system, created a change in current in response to light incidence. These properties fit the requirements of Cyberplasm and it is proposed that with the right program development an array of cells combined with electrodes may serve as a navigation system for the bio-robotic hybrid.

Chapter 6 Future Work

Further characterization and standardization of the light-induced NO pathway is required. Should the sensor prove quantitative as well as qualitative through further investigation, which is likely, the usefulness of this designed system is increased manifold. In order to further develop the sensor, several methods are suggested. Firstly, a narrowing of the wavelength of light may elucidate the exact wavelengths of activation. This may even bypass electrode photosensitivity as the electrode may be stimulated by a different wavelength than the mutant construct. In addition, this opens the system to the use of bioluminescence. If a gene is tagged with a fluorophore capable of emitting light at the wavelength that causes FL2 or FL3 activation, it may be possible to appropriate the designed system for gene/protein detection purposes and thereby link gene/protein presence to NO. This may have profound implications in the study of gene regulation and protein activity.

In order to further develop the system, studies on adherent cells may be useful. By immobilizing cells in Cellagen© it will become possible to place cells at a fixed distance from the electrode, standardizing measurements further and preventing cellular exposure to high potentials.

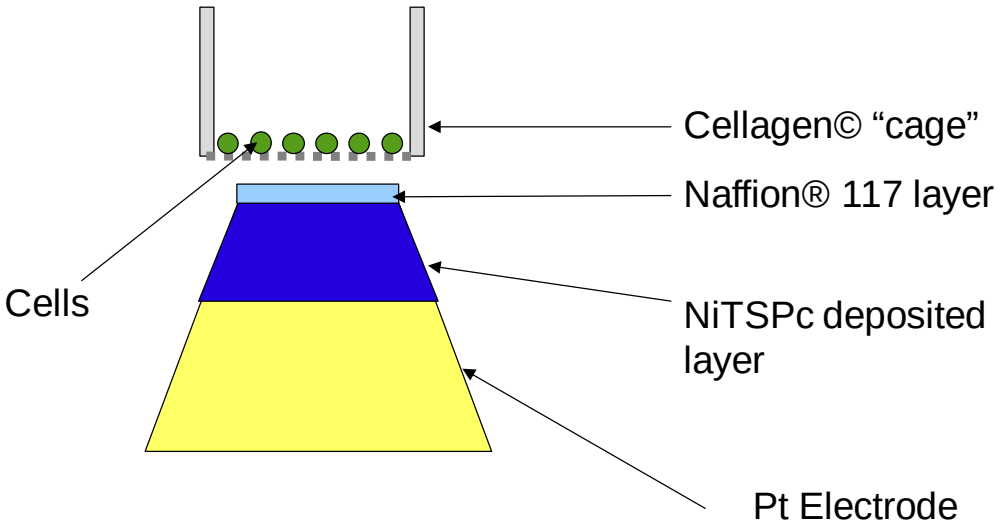

Figure 68 Schematic representation of the complete proposed sensor system.

The electrochemical sensor has the potential to be miniaturised and fabricated in electrode arrays allowing for use in a variety of applications. In order to increase the

signal/noise ratio, superoxide production can be inhibited in the cells by incubating cells with superoxide dismutase.(Chang, Henderson, Cole, F. Bedioui, & Mcneil, 2005) The presence of superoxide will also be further inhibited by the presence of H4 biopterin, a co-factor for the enzyme producing NO in the cells in question.

The work of Oni *et al* demonstrated the idea of using a Cellagen layer is proposed as a method of suspending the cells so that they are not in direct contact with the sensor.(Oni *et al*., 2004) By positioning the sensor a fixed distance away from the cells, the effect of the constant potential on the cells can be diminished. The importance of using Cellagen membranes is discussed in (Castillo *et al*., 2005). For many sensors this increased distance could prove crippling for detection, but the high diffusion rate of NO still allows for a fast response from the sensor and very little noise from background NO.

Another consideration in assessing the feasibility of measuring NO from the system is the optimum distance between electrode and cells. Due to its low half-life, availability of NO plateaus relatively quickly. As the electrode setup only requires a concentration of a few nM to recognize the signal, the system will work through a range of distances, but this would affect the timescale of detection. Placing cells in close proximity to the electrode will create conditions where cells are exposed to high potentials. In such environments, cells tend to agglomerate and clump as well as exhibiting unusual morphology (Oni *et al*., 2004).

One possible route for the appropriation of this sensor is to link NO production to GPCR activation. GPCRs (G-Protein Coupled Receptors) are a class of receptors responsible for the detection of a variety of signals and cause the release of a cascade of protein activation on several levels; from expression to phosphorylation, activating different pathways.(Hur & K.-tai Kim, 2002)(Selbie & Hill, 1998) If it will be possible to attach a fluorophore with an emission spectrum matching the absorption of the constructed mutants to a GPCR that will activate upon analyte detection, NO production would then be directly linked to GPCR activation in cells. This would allow the creation of a real-time machine readable signal confirming GPCR activation and thus the presence of the triggering chemical/odorant. The challenge with this approach lies in finding a place in the cascade of events related to GPCR signalling which influences NO production without interfering with other signalling events and without causing positive or negative feedback loops.

Chapter 7 Bibliography

Alderton, W. K., Cooper, C. E., & Knowles, R. G. (2001). Nitric oxide synthases : structure, function and inhibition. *Biochemical Journal*, *357*, 593-615.

Ali, M. F., Kirby, R., Goodey, A. P., Rodriguez, M. D., Ellington, A. D., Neikirk, D. P., & Mcdevitt, J. T. (2003). Dna hybridization and discrimination of single-nucleotide mismatches using chip-based microbead arrays. *Analytical Chemistry*, *75*, 4732-4739.

Amano, K. (2002). Enhancement of Ischemia-Induced Angiogenesis by eNOS Overexpression. *Hypertension*, *41*(1), 156-162.

Amatore, C., Holub, K., & Marecek, V., with K. Stulik. (2000). Microelectrodes. definitions, characterization, and applications. *Pure and Applied Chemistry*, *72*(8), 1483-1492.

Anderson, E. H. (1946). Growth Requirements of Virus-Resistant Mutants of Escherichia Coli Strain "B." *Proceedings of the National Academy of Sciences*, *32*, 120-128.

Ayers, J., & Rulkov, N. (2010). Controlling underwater robots with electronic nervous systems. *Applied Bionics and Biomechanics*, *7*(1), 57-67.

Ayers, J., & Witting, J. (2007). Biomimetic approaches to the control of underwater walking machines. *Philosophical transactions. Series A, Mathematical, physical, and engineering sciences*, *365*(1850), 273-95.

Babbedge, R. C., Bland-Ward, P. a, Hart, S. L., & Moore, P K. (1993). Inhibition of rat cerebellar nitric oxide synthase by 7-nitro indazole and related substituted indazoles. *British Journal of Pharmacology*, *110*(1), 225-8.

Bakker, E., & Telting-diaz, M. (2002). Electrochemical Sensors. *Analytical Chemistry*, *74*(12), 2781-2800.

Beaumont, E., Lambry, J.-C., Robin, A.-C., Martasek, Pavel, Blanchard-Desce, M., & Slama-Schwok, A. (2008). Two Photon-Induced Electron Injection From a Nanotrigger in Native Endothelial NO-Synthase. *Chem Phys Chem*, *9*(16), 2325-2331.

Beckman, J S, & Koppenol, W H. (1996). Nitric oxide, superoxide, and peroxynitrite: the good, the bad, and the ugly. *American Journal of Physiology*, *271*, 1424-1437.

Beckman, J.S., Beckman, T. W., Chen, J., Marshall, P. A., & Freeman, B. A. (1990). Apparent hydroxyl radical production by peroxynitrite: implications for endothelial injury from nitric oxide and superoxide. *Proceedings of the National Academy of Sciences*, *322*, 9-19.

Belshaw, P. J., Spencer, D. M., Crabtree, G. R., & Schreiber, S L. (1996). Controlling programmed cell death with a cyclophilin-cyclosporin-based chemical inducer of dimerization. *Chemistry & Biology*, *3*(9), 731-8.

Ben-Jacob, E., & Hanein, Y. (2008). Carbon nanotube micro-electrodes for neuronal interfacing. *Journal of Materials Chemistry*, *18*(43), 5181-5186.

Borutaite, V., & Brown, G. (2005). What else has to happen for nitric oxide to induce cell death? *Biochemical Society Transactions*, *33*, 1394-1396.

Boucher, J. L., Moali, C., & Tenu, J. P. (1999). Nitric oxide biosynthesis, nitric oxide synthase inhibitors and arginase competition for. *Cell and Molecular Life Science*, *55*, 1015-1028.

Bredt, D.S., & Snyder, S. H. (n.d.). Isolation of nitric oxide synthetase, a calmodulin-requiring enzyme. *Proceedings of the National Academy of Sciences*, *87*, 682.

Brenman, J. E., Chao, D. S., Gee, S. H., McGee, A. W., Craven, S. E., Santillano, D. R., Z. Wu, F. H., H. Xia, M. F. P., Froehner, S. C., & Bredt, D.S. (1996). Interaction of nitric oxide synthase with the postsynaptic density protein PSD-95 and alpha1-syntrophin mediated by PDZ domains. *Cell*, *84*, 757-767.

Briggs, Winslow R., Tseng, T.-S., Cho, H.-Y., Swartz, T. E., Sullivan, S., Bogomolni, R. A., Kaiserli, E., & Christie, John M. (2007). Phototropins and Their LOV Domains: Versatile Plant Blue-Light Receptors. *Journal of Integrative Plant Biology*, *49*(1), 4-10. Blackwell Publishing Asia.

Castillo, J., Isik, S., Blochl, A., Pereira-Rodrigues, Nazare, Bedioui, Fethi, Csoregi, E., Schuhmann, W., & Oni, J. (2005). Simultaneous detection of the release of glutamate and nitric oxide from adherently growing cells using an array of glutamate and nitric oxide selective electrodes. *Biosensors and Bioelectronics*, *20*(8), 1559-1565.

Chang, S., Henderson, J. R., Cole, A., Bedioui, F., & Mcneil, C. J. (2005). An electrochemical sensor array system for the direct, simultaneous in vitro monitoring of nitric oxide and superoxide production by cultured cells. *Biosensors and Bioelectronics*, *21*, 917-922.

Cho, H.-Y., Tseng, T.-S., Kaiserli, E., Sullivan, S., Christie, John M., & Briggs, Winslow R. (2007). Physiological Roles of the Light , Oxygen , or Voltage Domains of Phototropin 1 and Phototropin 2. *Plant Physiology*, *143*(January), 517-529.

Choi, J., Chen, J., Schreiber, S.L., & Clardy, J. (1996). Structure of the FKBP12-rapamycin complex interacting with the binding domain of human FRAP. *Science*, *273*(183), 5272.

Christie, J M, Salomon, M, Nozue, K., Wada, M, & Briggs, W R. (1999). LOV (light, oxygen, or voltage) domains of the blue-light photoreceptor phototropin (nph1): binding sites for the chromophore flavin mononucleotide. *Proceedings of the National Academy of Sciences*, *96*(15), 8779-83.

Clark, J. M., Gorman, C. L., & Cope, A. P. (2007). Nitric oxide, chronic inflammation and autoimmunity. *Immunology Letters*, *111*, 1-5.

Coddington, J. W., Hurst, J. K., & Lymar, S. V. (1999). Hydroxyl Radical Formation during Peroxynitrous Acid Decomposition. *Journal of the American Chemical Society*, *121*(11), 2438-2443. American Chemical Society.

Copland, M. J., Baird, M. A., Rades, T., McKenzie, J. L., Becker, B., Reck, F., Tyler, P. C., & Davies., N. M. (2003). Liposomal delivery of antigen to human dendritic cells. *Vaccine*, *21*(9-10), 883-90.

Crosson, S., Rajagopal, S., & Moffat, K. (2003). Current Topics The LOV Domain Family : Photoresponsive Signaling Modules Coupled to Diverse Output Domains †. *DNA Repair*, *42*, 2-10.

Deisseroth, K. (2011). Optogenetics. *Nature Methods*, *8*(1), 26-29.

Dimmeler, S., Fleming, I., Fisslthaler, B., Hermann, C., Busse, R., & Zeiher, A. M. (1999). Activation of nitric oxide synthase in endothelial cells by Akt-dependent phosphorylation. *Nature*, *399*(6736), 601-605. Molecular Cardiology, Department of Internal Medicine IV, University of Frankfurt, Germany.

Dimmeler, S., Hermann, C., Galle, J., & Zeiher, A. M. (1999). Upregulation of Superoxide Dismutase and Nitric Oxide Synthase Mediates the Apoptosis-Suppressive Effects of Shear Stress on Endothelial Cells. *Arteriosclerosis, Thrombosis, and Vascular Biology*, (March), 656-663.

Drenan, R. M., Liu, Xiangyu, Bertram, P. G., & Zheng, X. F. S. (2004). FKBP12-rapamycin-associated protein or mammalian target of rapamycin (FRAP/mTOR) localization in the endoplasmic reticulum and the Golgi apparatus. *The Journal of Biological Chemistry*, *279*(1), 772-8.

Egland, K. A., & Greenberg, E. P. (1999). Quorum sensing in Vibrio fischeri : elements of the luxI promoter. *Molecular Microbiology*, *31*, 1197-1204.

Estevez, A. Y., & Phillis, J. W. (1997). Hypercapnia-induced increases in cerebral blood flow: roles of adenosine, nitric oxide and cortical arousal. *Brain Research*, *758*(1-2), 1-8.

Fan, Y. W. (2001). *Study on recovery tissue engineering of cerebral central nerves and blood vessels.* Tinghua University.

Fang, F. C. (1997). Mechanisms of Nitric Oxide-Related Antimicrobial Activity. *Journal of Clinical Investigation*, *99*(12), 2818-2825.

Feron, O., & Balligand, J.-L. (2006). Caveolins and the regulation of endothelial nitric oxide synthase in the heart. *Cardiovascular Research*, *69*(4), 788-97.

Florio, T., Arena, S., Pattarozzi, A., Thellung, S., Corsaro, A., Villa, V., Massa, A., Diana, F., Spoto, G., Forcella, S., Damonte, G., Filocamo, M., Benatti, U., & Schettini, G. (2003). Basic fibroblast growth factor activates endothelial nitric-oxide synthase in CHO-K1 cells via the activation of ceramide synthesis. *Molecular Pharmacology*, *63*(2), 297-310.

Frost, M. C., Rudich, S. M., Zhang, H., Maraschio, M. A., & Meyerhoff, M. E. (2002). In Vivo Biocompatibility and Analytical Performance of Intravascular Amperometric Oxygen Sensors Prepared with Improved Nitric Oxide-Releasing Silicone Rubber Coating. *Analytical Chemistry*, *74*(23), 5942-5947. American Chemical Society.

Furchgott, R. F., & Zawadzki, J. V. (1980). The obligatory role of endothelial cells in the relaxation of arterial smooth muscle by acetylcholine. *Nature*, *288*(5789), 373-376.

Furfine, E. S., Harmon, M. F., Paith, J. E., & Garvey, E. P. (1993). Selective inhibition of constitutive nitric oxide synthase by L-NG-nitroarginine. *Biochemistry*, *32*(33), 8512-7.

Gachhui, R., Presta, A., Bentley, D. F., Abu-Soud, H. M., McArthur, R., Brudvig, G., Ghosh, D. K., & Stuehr, D. J. (1996). Characterization of the reductase domain of rat neuronal nitric oxide synthase generated in the methylotrophic yeast Pichia pastoris. Calmodulin response is complete within the reductase domain itself. *The Journal of Biological Chemistry*, *271*, 20594-20602.

Geller, D. A., Lowenstein, C. J., Shapiro, R. A., Nussler, A. K., Di Silvio, M., Wang, S. C., Nakayama, D. K., Simmons, R. L., Snyder, S. H., & Billiar, T. R. (n.d.). Molecular cloning and expresion of inducible nitric oxide synthase from human hepatocytes. *Proceedings of the National Academy of Sciences*, *90*(1993), 3491-3495.

George, M., Parak, W. J., & Gaub, H. E. (2000). Highly integrated surface potential sensors. *Sensors And Actuators*, *69*, 266-275.

Gibson, D. G., Young, L., Chuang, R.-Y., Venter, J. C., Hutchison, C. A., & Smith, H. O. (2009). Enzymatic assembly of DNA molecules up to several hundred kilobases. *Nature Methods*, *6*(5), 12-16.

Gorokhovatsky, A. Y., Marchenkov, V. V., Rudenko, N. V., Ivashina, T. V., Ksenzenko, V. N., Burkhardt, N., Semisotnov, G. V., Vinokurov, L. M., & Alakhov, Y. B. (2004). Fusion of Aequorea victoria GFP and aequorin provides their Ca (2+)-induced interaction that results in red shift of GFP absorption and efficient bioluminescence energy transfer. *In Vitro*, *320*, 703-711.

Gosh, D. K., & Salerno, J. C. (2003). Nitric Oxide Synthases: Domain Structure and Alignment in Enzyme Function and Control. *Frontiers in BioScience*, *8*(24), 193-209.

Gross, A., Spiesser, S., Terraza, A., Rouot, B., Caron, E., & Dornand, J. (1998). Expression and Bactericidal Activity of Nitric Oxide Synthase in Brucella-suis infected murine macrophages. *Infection and Immunity*, *66*(4), 1309-1316.

Guo, J.-P., Murohara, T., Buerke, M., Scalia, R., & Lefer, A. M. (1996). Direct measurement of nitric oxide release from vascular endothelial cells. *Journal of Applied Physiology*, *81*(2), 774-779.

Gurjar, M. V., Sharma, R. V., & Bhalla, R. C. (1999). eNOS gene transfer inhibits smooth muscle cell migration and MMP-2 and MMP-9 activity. *Arteriosclerosis, Thrombosis, and Vascular Biology*, *19*(12), 2871-7.

Handy, R. L. C., Harb, H. L., Wallace, P., Gaffen, Z., Whitehead, K. J., & Moore, P.K. (1996). Inhibition of nitric oxide synthase by 1-(2-trifluoromethylphenyl) imidazole (TRIM) in vitro: antinociceptive and cardiovascular effects. *British Journal of Pharmacology*, *119*(2), 423-31.

Hanrahan, G., Patil, D. G., & Wang, Joseph. (2004). Electrochemical sensors for environmental monitoring: design, development and applications. *Journal of Environmental Monitoring*, *6*, 657-664.

Heitman, J., Movva, N. R., & Hall, M. N. (1991). Targets for cell cycle arrest by the immunosuppressant rapamycin in yeast. *Science*, *253*(5022), 905-909.

Helling, R. B., Goodman, H. M., & Boyer, H. W. (1974). Analysis of Endonuclease R-EcoRI Fragments of DNA from Lambdoid Bacteriophages and Other Viruses by Agarose-Gel Electrophoresis. *Journal of Virology*, *14*(5), 1235-1244.

Herrera, M., Hong, N. J., & Garvin, J. L. (2006). Aquaporin-1 transports NO across cell membranes. *Hypertension*, *48*(1), 157-64.

Hur, E.-mi, & Kim, K.-tai. (2002). G protein-coupled receptor signalling and cross-talk Achieving rapidity and specificity. *Cellular Signalling*, *14*, 397 - 405.

Iadecola, C., Zhang, F., & Xu, X. (1993). Role of nitric oxide synthase-containing vascular nerves in cerebrovasodilation elicited from cerebellum. *American Journal of Physiology Integrative and Comparative Physiology*, *264*(4), 738-746.

Iino, M. (2006). Toward understanding the ecological functions of tropisms : interactions among and effects of light on tropisms Commentary. *Current Opinion in Plant Biology*, *9*, 89-93.

Inoue, S., Kinoshita, T., Takemiya, A., Doi, M., & Shimazaki, K. (2008). Leaf positioning of Arabidopsis in response to blue light. *Molecular Plant*, *1*(1), 15-26.

Kader, K. N., Akella, R., Ziats, N. P., Lakey, L. a, Harasaki, H., Ranieri, J. P., & Bellamkonda, R. V. (2000). eNOS-overexpressing endothelial cells inhibit platelet aggregation and smooth muscle cell proliferation in vitro. *Tissue Engineering*, *6*(3), 241-51.

Katz, H. E., & Bao, Z. (2000). The Physical Chemistry of Organic Field-Effect Transistors. *Journal of Physical Chemistry B*, *104*, 671-678.

Kaur, S., Kumar, T. R. S., Uruno, A., Sugawara, A., Jayakumar, K., & Kartha, C. C. (2009). Genetic engineering with endothelial nitric oxide synthase improves functional properties of endothelial progenitor cells from patients with coronary artery disease : an in vitro study. *Basic Research in Cardiology*, *104*, 739-749.

Kinoshita, Toshinori, Doi, Michio, Suetsugu, N., Kagawa, T., Wada, Masamitsu, & Shimazaki, K.-ichiro. (2001). phot1 and phot2 mediate blue light regulation of stomatal opening. *Nature*, *414*(6864), 656-660.

Klatt, P., Schmid, M., Leopold, E., Schmidt, K., Werner, E. R., & Mayer, B. (1994). The pteridine binding site of brain nitric oxide synthase. Tetrahydrobiopterin binding kinetics, specificity, and allosteric interaction with the substrate domain. *The Journal of Biological Chemistry*, *269*(19), 13861-6.

Klatt, P., Schmidt, K., Lehner, D., Glatter, O., Bachinger, H. P., & Mayer, B. (1995). Structural analysis of porcine brain nitric oxide synthase reveals a role for tetrahydrobiopterin and L-arginine in the formation of an SDS-resistant dimer. *European Molecular Biology Organization Journal*, *14*(15), 3687-3695.

Kojima, H, Sakurai, K, Kikuchi, K., Kawahara, S., Kirino, Y., Nagoshi, H., Hirata, Y., & Nagano, T. (1998). Development of a Fluorescent Indicator for Nitric Oxide Based on the Fluorescein Chromophore. *Chemical and Pharmaceutical Bulletin*, *46*(2), 373-375. WILEY-VCH Verlag.

Kojima, Hirotatsu, Nakatsubo, Naoki, Kikuchi, Kazuya, Nagoshi, Hiroshi, Hirata, Yasunou, & Nagano, Tetsuo. (1998). Detection and imaging of nitric oxide with novel fluorescent indicators: diaminofluoresceins. *Analytical Chemistry*, *70*(13), 2446-53.

Kojima, Hirotatsu, Sakurai, Kuniko, Kikuchi, Kazuya, Kawahara, Shigenori, Kirino, Yukata, Nagoshi, Hiroshi, Hirata, Yasunobu, & Nagano, Tetsuo. (1998). Development of a fluorescent indicator for nitric oxide based on the fluorescein chromophore. *Chemical and Pharmaceutical Bulletin*, *46*(February), 373-375.

Kopec, K. K., & Carroll, R. T. (2000). Phagocytosis is Regulated by Nitric Oxide in Murine Microglia. *Nitric Oxide*, *4*(2), 103-111.

Koppenol, W.H., Moreno, J. J., Pryor, W. A., Ischiropoulos, H., & Beckman, J.S. (1992). Peroxynitrite, a cloaked oxidant formed by nitric oxide and superoxide. *Chemical Research in Toxicology*, *5*, 834-842.

Kopytek, S. J., Standaert, R. F., Dyer, J. C., & Hu, J. C. (2000). Chemically induced dimerization of dihydrofolate reductase by a homobifunctional dimer of methotrexate. *Chemistry & biology*, *7*(5), 313-21.

Lamas, S, Marsden, P. a, Li, G. K., Tempst, P., & Michel, T. (1992). Endothelial nitric oxide synthase: molecular cloning and characterization of a distinct constitutive enzyme isoform. *Proceedings of the National Academy of Sciences*, *89*(14), 6348-52.

Lambry, J.-C., Beaumont, E., Tarus, B., Blanchard-Desce, M., & Slama-Schwok, A. (2009). Selective probing of a NADPH site controlled light-induced enzymatic catalysis. *Journal of Molecular Recognition*.

Lee, S. J., Lee, Jong Hee, Jin, H. J., Lee, Jeong Ho, Ryu, H. Y., Kim, Y., Kong, I. S., & Kim, K. W. (2000). A Novel Technique for the Effective Production of Short

Peptide Analogs from Concatameric Short Peptide Multimers. *Molecules and Cells*, *10*(2), 236-240.

Levskaya, A., Chevalier, A. A., Tabor, J. J., Simpson, Z. B., Lavery, L. A., Levy, M., Davidson, E. A., Scouras, A., Ellington, A. D., Marcotte, E. M., & Voigt, C. A. (2005). Synthetic biology: Engineering Escherichia coli to see light. *Nature*, *438*(7067), 441-442.

Li, H., Raman, C. S., Glaser, C. B., Blasko, E., Young, T. A., Parkinson, J. F., Whitlow, M., & Poulos, T. L. (1999). Crystal structures of zinc-free and bound heme domain of human inducible nitric-oxide synthase. Implications for dimer stability and comparison with endothelial nitric-oxide synthase. *The Journal of Biological Chemistry*, *274*, 21276-21284.

Liu, Xiaoping, Srinivasan, P., Collard, E., Grajdeanu, P., Zweier, Jay L., & Friedman, A. (2008). Nitric Oxide Diffusion Rate is Reduced in the Aortic Wall. *Biophysical Journal*, *94*(5), 1880-1889.

Llorens, S., Jordán, J., & Nava, E. (2002). The nitric oxide pathway in the cardiovascular system. *Journal of Physiology and Biochemistry*, *58*(3), 179-88.

Lobo, L. a, Smith, C. J., & Rocha, E. R. (2011). Flavin mononucleotide (FMN)-based fluorescent protein (FbFP) as reporter for gene expression in the anaerobe Bacteroides fragilis. *Federation of European Microbiological Societies Microbiology Letters*, 1-8.

Lowe, P. N., Smith, D., Stammers, D. K., Riveros-Moreno, V., Moncada, S., Charles, I., & Boyhan, A. (1996). Identification of the domains of neural nitric oxide synthase by limited proteolysis. *Biochemical Journal*, *315*, 55-62.

Lue, T. F. (2000). Erectile Dysfunction. *The New england Journal of Medicine*, *342*(24), 1802-1813.

Markas, A., Gilmartin, T., & Hart, J. P. (1994). Novel, reagentless, amperometric biosensor for uric acid based on a chemically modified screen-printed carbon electrode coated with cellulose acetate and uricase. *The Analyst*, *119*, 833-840.

Marsden, P. A., Schappert, K. T., Chen, H. S., Flowers, M., Sundell, C. L., Wilcox, J. N., Lamas, S., & Michel, T. (1992). Molecular cloning and charaterization of human endothelial nitric oxide synthase. *Federation of the Societies of Biochemistry and Molecular Biology Letters*, *307*, 287-293.

Matsuoka, D., Iwata, T., Zikihara, K., Kandori, H., & Tokutomi, S. (2007). Primary Processes During the Light-signal Transduction of Phototropin. *Journal of Photochemistry and Photobiology*, *8*(16), 122-130.

Mayer, B., & Hernmens, B. (1997). Biosynthesis and Action of Nitric Oxide in Mammalian Cells. *Trends in Biochemical Sciences*, *22*(12), 477-481.

Michel, Thomas. (1999). Targeting and translocation of endothelial nitric oxide synthase. *Brazilian Journal of Medical and Biological Research*, *32*, 1361-1366.

Moncada, S., & Higgs, E. A. (2006). The discovery of nitric oxide and its role in vascular biology. *British Journal of Pharmacology*, *147*, 193-201.

Moore, P K, & Handy, R. L. (1997). Selective inhibitors of neuronal nitric oxide synthase--is no NOS really good NOS for the nervous system? *Trends in Pharmacological Sciences*, *18*(6), 204-11.

Motoike, T., Loughna, S., Perens, E., Roman, B. L., Liao, W., Chau, T. C., Richardson, C. D., Kawate, T., Kuno, J., Weinstein, B. M., Stainier, D. Y. R., & Sato, T. N. (2000). Universal GFP Reporter for the Study of Vascular Development. *Genesis*, *28*, 75- 81.

Mungrue, I. N., Bredt, D S, Stewart, D. J., & Husain, M. (2003). From molecules to mammals: what's NOS got to do with it? *Acta Physiologica Scandinavica*, *179*, 123-135.

Murad, F. (2005). Discovery of some of the biological effects of nitric oxide and its role in cell signaling. *Bioscience Reports*, *24*(4-5), 452-74.

Murray, R. W., Ewing, A. G., & Durst, R. A. (1987). Chemically modified electrodes. Molecular design for electroanalysis. *Analytical Chemistry*, *59*(5), 379-390.

Möglich, A., Ayers, R., & Moffat, K. (2009). Design and signaling mechanism of light-regulated histidine kinases. *Journal of Molecular Biology*, *385*(5), 1433-44. Elsevier B.V.

Nag, B., Wada, H. G., Deshpande, S. V., Passmore, D., & Kendrick, T. (1993). Stimulation of T cells by antigenic peptide complexed with isolated chains of major histocompatibility complex class II molecules. *Proceedings of the National Academy of Sciences*, *90*, 1604-1648.

Nag, B., Wada, H. G., Fok, K. S., Green, D. J., & Sharma, S. D. (1992). Antigen-specific stimulation of T cell extracellular acidification by MHC class II-peptide complexes. *Journal of Immunology*, *148*, 2040-2044.

Nakatsubo, N. (1998). Direct evidence of nitric oxide production from bovine aortic endothelial cells using new fluorescence indicators: diaminofluoresceins. *Federation of the Societies of Biochemistry and Molecular Biology Letters*, *427*(2), 263-266.

Nascimento, F. R. F., Ribeiro-Dias, F., & Russo, M. (1998). Cytotoxic activity of BCG-activated macrophages against L929 tumor cells is nitric oxide-dependent. *Brazilian Journal of Medical and Biological Research*, *31*(12), 1593-1596.

Navarro-antolin, J., & Lamas, Santiago. (2001). Nitrosative stress by cyclosporin A in the endothelium : studies with the NO-sensitive probe diaminofluorescein-2 diacetate using flow cytometry, 7-10.

Neher, E. (2001). Molecular biology meets microelectronics. *Nature Biotechnology*, *19*(February), 114.

Neill, S. J., Desikan, R., & Hancock, J. T. (2003). Nitric Oxide Signalling in Plants. *New Phytologist*, *159*(1), 11-35.

Nishizawa, M., Matsue, T., & Uchida, I. (1992). Penicillin sensor based on a microarray electrode coated with pH-responsive polypyrrole. *Analytical Chemistry*, *64*(21), 2642-2644. American Chemical Society.

Noiri, E. (2002). Association of eNOS Glu298Asp Polymorphism With End-Stage Renal Disease. *Hypertension*, *40*(4), 535-540.

Olken, N. M., & Marletta, M. a. (1993). NG-methyl-L-arginine functions as an alternate substrate and mechanism-based inhibitor of nitric oxide synthase. *Biochemistry*, *32*(37), 9677-85.

Oni, J., Pailleret, A., Isik, S., Diab, N., Radtke, I., Blöchl, A., Jackson, M., Bedioui, Fethi, & Schuhmann, W. (2004). Functionalised electrode array for the detection of nitric oxide released by endothelial cells using different NO-sensing chemistries. *Analytical and Bioanalytical Chemistry*, *378*, 1594-1600.

Owicki, J.C., Parce, J. W., Kercso, K. M., Sigal, G. B., & Muir, V. C. (1992). Biosensors based on the energy metabolism of living cells: the physical chemistry and cell biology of extracellular acidification. *Biosensors and Bioelectronics*, *7*, 255-272.

Owicki, John C, Bousse, L. J., Hafeman, D. G., Kirk, G. L., Olson, J. D., Garrett, W. H., & Parce, W. J. (1994). The light-addressable potentiometric sensor: Principles and Biological Applications. *Annual Review of Biophysics and Biomolecular Structure*, *23*, 87-113.

Palmer, R. M. J., Ferrige, A. G., & Moncada, S. (1987). Nitric oxide release accounts for the biological activity of endothelium-derived relaxing factor. *Nature*, *327*(June), 524-526.

Pastrana, E. (2010). Optogenetics: controlling cell function with light. *Nature Methods*, *8*(1), 24-25.

Pereira-Rodrigues, Nazaré, Albin, V., Koudelka-Hep, M., Auger, V., Pailleret, A., & Bedioui, Fethi. (2002). Nickel tetrasulfonated phthalocyanine based platinum microelectrode array for nitric oxide oxidation. *Electrochemistry Communications*, *4*(11), 922-927.

Pontie, M., Gobin, C., Pauporte, T., Bedioui, Fethi, & Devynck, J. (2000). Electrochemical nitric oxide microsensors: sensitivity and selectivity characterisation. *Analytica Chimica Acta*, *411*(1-2), 175-185.

Rainina, E. I., Efremenco, E. N., & Varfolomeyev, S. D. (1996). The development of a new biosensor based on recombinant E. coli for the direct detection of organophosphorus neurotoxins. *Biosensors and Bioelectronics*, *11*(10), 991-1000.

Raley-Susman, K. M., Miller, K. R., Owicki, J.C., & Sapolsky, R. M. (1992). Effects of excitotoxin exposure on metabolic rate of primary hippocampal cultures:

application of silicon microphysiometry to neurobiology. *Journal of Neuroscience, 12*, 773-780.

Raman, C. S., Li, H., Martasek, P., Kral, V., Masters, B. S., & Poulos, T. L. (1998). Crystal structure of constitutive endothelial nitric oxide synthase: a paradigm for pterin function involving a novel metal center. *Cell, 95*, 939-950.

Rider, T. H., Petrovick, M. S., Nargi, F. E., Harper, J. D., Schwoebel, E. D., Mathews, R. H., David, J. B., Bortolin, L. T., Young, A. M., Chen, Jianzhu, & Hollis, M. A. (2003). A B Cell-Based Sensor for Rapid Identification of Pathogens. *Science, 301*(July), 213-215.

Robinson, L. J., & Michel, T. (1995). Mutagenesis of palmitoylation sites in endothelial nitric oxide synthase identifies a novel motif for dual acylation and subcellular targeting. *Proceedings of the National Academy of Sciences*, *92*(25), 11776-80.

Rocha, J. R. C., Angnes, L., Bertotti, M., Araki, K., & Toma, H. E. (2002). Amperometric detection of nitrite and nitrate at tetraruthenated porphyrin-modified electrodes in a continuous-flow assembly. *Analytica Chimica Acta*, *452*(1), 23-28.

Salomon, Michael, Christie, John M, Knieb, E., Lempert, U., & Briggs, Winslow R. (2000). Photochemical and Mutational Analysis of the FMN-Binding Domains of the Plant Blue Light Receptor, Phototropin. *Biochemistry*, *39*(31), 9401-9410. American Chemical Society.

Salomon, Michael, Eisenreich, W., Dürr, H., Schleicher, E., Knieb, E., Massey, V., Rüdiger, W., Müller, F., Bacher, A., & Richter, G. (2001). An optomechanical transducer in the blue light receptor phototropin from Avena sativa. *Proceedings of the National Academy of Sciences*, *98*(22), 12357-61.

Sato, J., Nair, K., Hiddinga, J., L.Eberhardt, N., Fitzpatrick, L. A., Katusic, Z. S., & O'Brien, T. (2000). eNOS gene transfer to vascular smooth muscle cells inhibits cell proliferation via upregulation of p27 and p21 and not apoptosis. *Cardiovascular Research*, *47*(4), 697-706.

Sato, N., & Okuma, H. (2006). Amperometric simultaneous sensing system for D - glucose and L -lactate based on enzyme-modified bilayer electrodes. *Analytica Chimica Acta*, *565*, 250-254.

Schmidt, H. H., & Walter, U. (1994). NO at Work. *Cell, 78*(6), 919-925.

Schoning, M. J., & Poghossian, A. (2002). Recent advances in biologically sensitive field-effect transistors (BioFETs). *The Analyst*, *127*, 1137-1151.

Selbie, L. A., & Hill, S. J. (1998). G protein-coupled- receptor cross-talk : the fine-tuning of multiple pathways. *Development*, *19*(March), 87-93.

Shin, J. H., & Schoenfisch, M. H. (2006). Improving the biocompatibility of in vivo sensors via nitric oxide release. *The Analyst*, *131*, 609-615.

Sigal, G. B., Hafeman, D. H., Parce, J. W., & McConnel, H. M. (1989). *Electrical properties of phospholipid bilayer membranes measured with a light-addressable*

potentiometric sensor. (W. R. S. R.W. Murray, D.E. Dessy, W.R. Heineman, J. Janata, Ed.) (ACS sympos., pp. 46-64). Washington D.C.

Sroes, E., Hijmering, M., Van Zandvoort, M., Wever, R., Rabelink, T. J., & Van Fraassen, E. E. (1998). Origin of superoxide production by endothelial nitric oxide synthase. *Federation of the Societies of Biochemistry and Molecular Biology Letters*, *438*, 161-164.

Stauss, H. M., Nafz, B., Mrowka, R., & Persson, P. B. (2000). Blood pressure control in eNOS knock-out mice: comparison with other species under NO blockade. *Acta Physiologica Scandinavica*, *168*(1), 155-60.

Stocks, J., Thorn, J. A., & Galton, D. J. (1992). Lipoprotein lipase genotypes for a common premature termination codon mutation detected by PCR-mediated site-directed mutagenesis and restriction digestion. *Journal Of Lipid Research*, *33*(3), 853-857.

Stone, J. R., Sands, R. H., Dunham, W. R., & Marletta, M. A. (1995). Electron Paramagnetic Resonance Spectral Evidence for the Formation of a Pentacoordinate Nitrosyl-Heme Complex on Soluble Guanylate Cyclase. *Biochemical and Biophysical Research Communications*, *207*(2), 572-577.

Stradiotto, N. R., Yamanaka, H., & Zanoni, M. V. B. (2003). Electrochemical Sensors: A Powerful Tool in Analytical Chemistry. *Journal of The Brazilian Chemical Society*, *14*(2), 159-173.

Tabor, J. J., Salis, H. M., Simpson, Z. B., Chevalier, A. A., Levskaya, A., Marcotte, E. M., Voigt, C. A., & Ellington, A. D. (2009). A Synthetic Genetic Edge Detection Program. *Cell*, *137*(7), 1272-1281. Elsevier Ltd.

Thomassen, M. J., Buhrow, L. T., Connors, M. J., Kaneko, F. T., Erzurum, S. C., & Kavuru, M. S. (1997). Nitric Oxide Inhibits Inflammatory Cytokine Production by Human Alveolar Macrophages. *American Journal of Respiratory Cell and Molecular Biology*, *17*, 279-283.

Tielker, D., Eichhof, I., Jaeger, K.-E., & Ernst, J. F. (2009). Flavin mononucleotide-based fluorescent protein as an oxygen-independent reporter in Candida albicans and Saccharomyces cerevisiae. *Eukaryotic Cell*, *8*(6), 913-5.

Tsai, W. C., Strieter, R. M., Zisman, D. A., Wilkowski, J. M., Bucknell, K. A., Chen, G.-H., & Standiford, T. J. (1997). Nitric Oxide Is Required for Effective Innate Immunity against Klebsiella pneumoniae. *Infection and Immunity*, *65*(5), 1870-1875.

Valderrama, E., Garrido, P., Cabruja, E., Heiduschka, P., Harsch, A., & Göpel, W. (1995). Microfabrication and Characterisation of Microelectrode Arrays for In Vivo Nerve Signal Recording. *Solid State Signals*.

Venema, R. C., Hong Ju, R. Z., Ryan, J. W., & Venema, V. J. (1997). Subunit Interactions of Endothelial Nitric-oxide Synthase: Comparisons to the Neuronal and Inducible Nitric-Oxide Synthase Isoforms. *The Journal of Biological Chemistry*, *272*(2), 1276 -1282.

Volkov, A. G., & Ranatunga, D. R. a. (2006). Plants as environmental biosensors. *Plant Signaling & Behavior*, *1*(3), 105-15.

Wada, H. G., Indelicato, S. R., Meyer, L., Kitamura, T., & Miyajima, A. (1993). GM-CSF triggers a rapid, glucose dependent extracellular acidification by TF-1 cells: evidence for sodium/proton antiporter and PKC mediated activation of acid production. *Journal of Cell Physiology*, *154*, 129-138.

Wang, Joseph. (1999). Amperometric biosensors for clinical and therapeutic drug monitoring : a review. *Journal of Pharmaceutical and Biomedical Analysis*, *19*, 47 - 53.

Wang, Joseph, Lu, J., Luo, D., Wang, Jianyan, Jiang, M., & Tian, B. (1997). Renewable-reagent electrochemical sensor for monitoring trace metal contaminants. *Analytical Chemistry*, *69*, 2640-2645.

Weigum, S. E., Floriano, P. N., Christodoulides, N., & Mcdevitt, J. T. (2007). Cell-based sensor for analysis of EGFR biomarker expression in oral Cancer. *Lab on a Chip*, *7*(8), 941-1080.

Weikert, L. F., Lopez, J. P., Abdolrasulnia, R., Chroneos, Z. C., & Shepherd, V. L. (2000). Surfactant protein A enhances mycobacterial killing by rat macrophages through a nitric oxide-dependent pathway. *American Journal of Physiology Lung Cell Molecular Physiology*, *279*, 216-223.

Wendehenne, D., Pugin, A., & Klessig, D. F. (2001). Nitric oxide: comparative synthesis and signaling in animal and plant cells. *Trends in Plant Science*, *6*(4), 177-183.

Willner, I., Katz, E., & Willner, B. (2005). Electrical contact of redox enzyme layers associated with electrodes: Routes to amperometric biosensors. *Electroanalysis*, *9*(13), 965-977.

Wisniewski, N., & Reichert, M. (2000). Methods for reducing biosensor membrane biofouling. *Colloids and Surfaces B: Biointerfaces*, *18*, 197 - 219.

Xia, Y., Roman, L. J., Masters, B. S., & Zweier, J.L. (1998). Inducible nitric-oxide synthase generates superoxide from the reductase domain. *The Journal of Biological Chemistry*, *273*, 22635-22639.

Xu, G., Ye, X., Qin, L., Xu, Y., Yan Li, R. L., & Wang, P. (2005). Cell-based biosensors based on light-addressable potentiometric sensors for single cell monitoring. *Biosensors and Bioelectronics*, *20*, 1757-1763.

Xu, H., Shen, T., Zhou, Q., Shen, S., Liu, J., Li, L., Zhou, S., Zhang, X., Yu, Q., Bi, Z., & Xiao, X. (1992). Aspects of metal phthalocyanine photosensitization systems for light energy conversion. *Journal of Photochemistry and Photobiology A: Chemistry*, *65*(1-2), 267-276.

Ye, H., Daoud-El Baba, M., Peng, R.-W., & Fussenegger, M. (2011). A synthetic optogenetic transcription device enhances blood-glucose homeostasis in mice. *Science*, *332*(6037), 1565-8.

Young, C. K., Ingebrandt, S., Krause, M., Offenhauser, A., & Knoll, W. (2001). Validation of the use of field effect transistors for extracellular signal recording in pharmacological bioassays. *Journal of Pharmacological Toxicology Methods*, *45*, 207-214.

Zenichowski, K., Gothe, M., & Saalfrank, P. (2007). Exciting flavins : Absorption spectra and spin – orbit coupling in light – oxygen – voltage (LOV) domains. *Journal of Photochemistry and Photobiology*, *190*, 290-300.

Zhan, X., Li, D., & Johns, R. a. (2003). Expression of Endothelial Nitric Oxide Synthase in Ciliated Epithelia of Rats. *Journal of Histochemistry & Cytochemistry*, *51*(1), 81-87.

Zhang, B., Cao, G. L., Cross, A., Domachowske, J. B., & Rosen, G. M. (2002). Differential antibacterial activity of nitric oxide from the immunological isozyme of nitric oxide synthase transduced into endothelial cells. *Nitric Oxide*, *7*, 42-49.